NICKEL AMINE/IMINE AND AMINE/AMIDE BISTHIOLATE COMPLEXES AS MODELS FOR THE ACTIVE SITE OF NICKEL SUPEROXIDE DISMUTASE

A Dissertation by

Senaratnelage Nilmini Kumari Senaratne

Master of Science, Wichita State University, 2016

Bachelor of Science, University of Peradeniya, 2007

Submitted to the Department of Chemistry
and the faculty of the Graduate School of
Wichita State University
in partial fulfillment of
the requirements for the degree of
Doctor of Philosophy

July 2017

NICKEL AMINE/IMINE AND AMINE/AMIDE BISTHIOLATE COMPLEXES AS MODELS FOR THE ACTIVE SITE OF NICKEL SUPEROXIDE DISMUTASE

The following faculty members have examined the final copy of this dissertation for form and content and recommend that it be accepted in partial fulfillment of the requirement for the degree of Doctor of Philosophy with a major in Chemistry.

_____
David M. Eichhorn, Committee Chair

_____
D. Paul Rillema, Committee Member

_____
Kandatage Wimalasena, Committee Member

_____
William C. Groutas, Committee Member

_____
George Bousfield, Committee Member

Accepted for the Fairmount College of Liberal Arts & Sciences

_____
Ron Matson, Dean

Accepted for the Graduate School

_____
Dennis Livesay, Dean

DEDICATION

To my Family

ACKNOWLEDGEMENTS

First of all, I would like to convey my deep gratitude and respect for my advisor Prof. David Eichhorn for his continuous support throughout my PhD study. Without his guidance and persistent help this dissertation would not have been possible. He was always willing to help. His immense knowledge of the subject and intelligence have been a true inspiration for me to gain the success of my research. I deeply appreciate his great humane qualities, kindness, helpfulness and understanding.

My sincere thanks must also go to the members of my graduate committee; Prof. Kandatage Wimalasena, Prof. William Groutas, Prof. Paul Rillema and Prof. George Bousfield for their help, valuable advice and encouragement. I would also like to thank the faculty, the staff in the office and in the stock room of the department of chemistry for all their kind support during my stay in the department.

I would also like to thank my past and present lab mates, Tom, Lava, John and Alan. They always shared their fruitful ideas with me for my research work and assisted me in numerous ways. My thanks also go to all the graduate and undergraduate students in the department for being nice friends. I would like to thank Dr. Kevin Langenwalter for fixing our X-ray diffractometer in countless times during past few years. I would also like to thank Ali Jehan, Matt Baird and Dr. Tod Williams (KU) for performing mass spectrometry on my samples.

I am very much grateful to my parents for their tremendous sacrifices made to give me a good education. I am blessed to have their unconditional love and caring throughout my life. My special thanks goes to my loving sister Renuka for her love and support.

Finally, I would like to thank my beloved husband, Anushka for his endless love and encouragement throughout this entire journey. To my beloved little son Viduna, I would like to express my thanks for being such a cute boy always cheering me up.

ABSTRACT

Nickel Superoxide Dismutase (NiSOD) catalyzes disproportionation of cytotoxic superoxide radical to H_2O_2 and molecular O_2. The mononuclear nickel center in the active site undergoes alternate oxidation and reduction during the catalytic cycle and, the coordination geometry around the Ni changes accordingly. The four-coordinate reduced state of the NiSOD is coordinated by the N-terminal amine of His1, carboxamido N of Cys2 and, two thiolato S atoms from Cys2 and Cys6 in a square-planar geometry. The oxidized state contains an additional N donor arise from the imidazole of His1 giving a five-coordinate square-pyramidal geometry. The highly unusual coordination environment of the NiSOD makes it distinct among other known SODs and motivates researchers to study about it.

This research is mainly focused on to understand the role of the amide N coordination in the NiSOD which is only found in very few metalloenzymes. Through a synthetic model approach we have synthesized two types of model systems which contain amine/amide and amine/imine bisthiolate coordination. The imidazole N from His is the common N donor found in metalloenzymes and we made imine N containing models to represent the normal His imidazole N. The imine containing complexes, [Ni($NN^{im}S$]SR] were compared with the amide containing complexes, [Ni($NN^{am}S$)SR] utilizing X-ray crystallography, spectroscopic techniques, electrochemical measurements, and reactivity studies. Different thiolates with varying electron donating ability were used to study the effect of nature of the thiolates on the properties of the Ni center. This comparison allows us to understand the effective role of the amide N donation in NiSOD. In addition to our attempts at synthesizing four-coordinate NiN_2S_2 model complexes, this work describes our attempts at synthesizing NiN_3S_2 complexes as models for the oxidized state of the NiSOD.

TABLE OF CONTENTS

TABLE OF CONTENTS (continued)

TABLE OF CONTENTS (continued)

TABLE OF CONTENTS (continued)

LIST OF FIGURES

LIST OF FIGURES (continued)

LIST OF FIGURES (continued)

LIST OF TABLES

LIST OF ABBREVIATIONS

SOD	Superoxide Dismutase
NHE	Normal Hydrogen Electrode
PDB	Protein Data Base
His	Histidine
CODH	Carbon Monoxide Dehydrogenase
ACS	Acetyl Co-enzyme A Synthase
MCR	Methyl-Coenzyme M Reductase
NiSOD	Nickel Superoxide Dismutase
ARD	Acireductone Dioxygenase
CFeSP	Corrinoid Iron-Sulfur Protein
Cys	Cystine
ROS	Reactive Oxygen Species
LMCT	Ligand to Metal Charge Transfer
Tyr	Tyrosine
Me	Methyl
Tos	Tosyl
DNP	2,4-dinitrophenyl
XAS	X-ray Absorption Spectroscopy
NMR	Nuclear Magnetic Resonance
NBT	Nitro Blue Tetrazolium
ORTEP	Oarridge Thermal Ellipsois Program
Tp	Trispyrazolylborate
nmp	N-(2-mercaptoethyl)picolinamide
DTDB	2, 2’-dithiodibenzaldehyde
CH_2Cl_2	Dichloromethane
MeOH	Methanol

LIST OF ABBREVIATIONS (continued)

MeCN	Acetonitrile
DMF	Dimethylformamide
IR	Infrared
THF	Tetrahydrofuran
Et_2O	Diethylether
ESI-MS	Electrospray Ionization Mass Spectrometry
Vis	Visible
DTSACl	2,2'-dithiodisalicylic acid chloride
DTSA	2,2'-dithiodisalicylic acid
TEA	Triethylamine
RT	Room Temperature
OAc	Acetate
RS^-	Thiolate
dmen	N,N-dimethylethylenediamine
dmpd	N,N-dimethylpropylenediamine
BOC	Di-tert-butyl dicarbonate
DMSO	Dimethyl sulfoxide

CHAPTER 1: INTRODUCTION

1.1. Superoxide Dismutases

With the rise of O_2 levels on Earth superoxide dismutase enzymes emerged as important components in oxygen-utilizing living systems to protect biological molecules from oxidative damage by superoxide or reactive oxygen species (ROS) generated from superoxide associated with oxygen metabolism, including respiration and oxidative stress events.[1,2] Elevated levels of superoxide have been linked to the aging process and various disorders and diseases, including cancer, atherosclerosis, neurodegenerative disorders like Parkinson's and Alzheimer's, diabetes, and cardiovascular disease and post ischemic issue injury.[3,4,5]

SOD enzymes catalyze the disproportionation of the cytotoxic superoxide radical into hydrogen peroxide and molecular oxygen (Scheme 1) near the diffusion control limit[6] (10^9 M^{-1} s^{-1}) and protect the living systems.

$$O_2^{\bullet-} + M^{n+1} \longrightarrow O_2 + M^{n+} \qquad (1)$$

$$O_2^{\bullet-} + M^{n+} \longrightarrow H_2O_2 + M^{n+1} \qquad (2)$$

$$2H^+ + 2O_2^{\bullet-} \longrightarrow O_2 + H_2O_2$$

Scheme 1: SOD catalysis in two steps

All known SODs are metalloenzymes and utilize metal-centered one-electron redox chemistry tuned by the coordination environment and the overall protein fold to achieve the required redox potential between the redox potentials for oxidation and reduction of superoxide; 870 mV and -160 mV vs NHE respectively,[6] to perform the superoxide dismutation. The mid-point potential of

equations 1 and 2 are around 360 mV in aqueous solutions at pH 7 and all SODs have measured redox potentials that are essentially centered at 300 mV±100 mV.[6]

Depending on the metal cofactor, SODs can be classified into four groups Mn, Fe and CuZn SODs and the more recently discovered Ni containing SOD. Mn and Fe SODs are structurally similar, follow the same catalytic mechanism, and are found in both prokaryotes and eukaryotes. They are uniformly distributed in the cytosol of prokaryotes and in the mitochondrial matrix of the eukaryotes.[7]

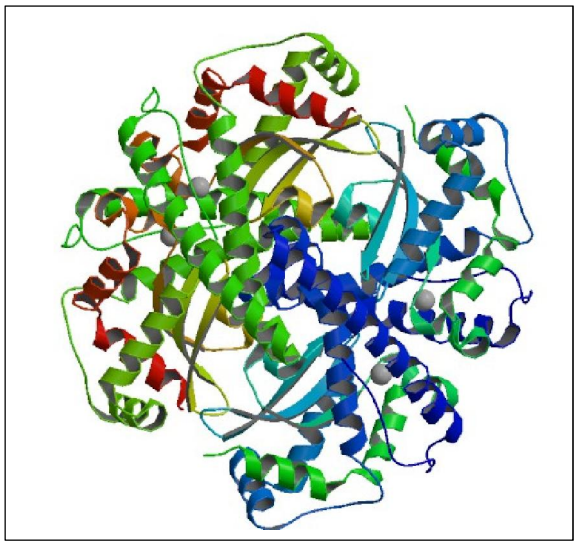

Figure 1.1.1. Crystal structure of human MnSOD (PDB: 1LUV)

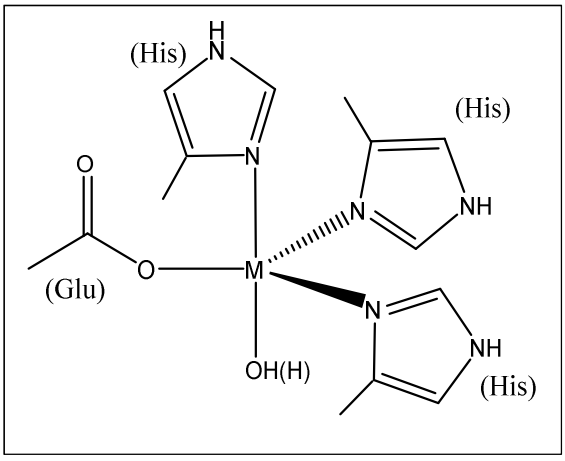

Figure 1.1.2. Structure of the active site of Mn and FeSOD[8]

Mn/Fe SODs are often found as a homodimer or homotetramer[9,10,11] with one Mn/Fe per monomer subunit (Figure 1.1.1).[12] Each subunit consists of two domains-an α-helical N-terminal domain and a mixed α/β C-terminal domain. The active site lies on the interface between these domains.[10,13,14] The active site metal center is bound to three histidines, one aspartate and either a water or hydroxide, giving a trigonal bipyramidal geometry (Figure 1.1.2). Two histidines and the aspartate lie in the equatorial plane and the third histidine and hydroxide/water occupy the two axial positions.[10,8] The Mn/Fe oxidation state is cycled between +2 and +3 in the catalytic cycle [7,15,16] and, depending on the oxidation state, the bound solvent molecule is interpreted as either water or hydroxide.[10] It has been reported that this water molecule plays a crucial role in making an extended hydrogen bonding network at the interface between subunits to support the proton transfer with outer-sphere residues during catalysis.[17,18]

Cu-Zn SOD is found in all eukaryotes and in some prokaryotes[17] and it is distributed throughout the cell, including cytosol, mitochondrial intermembrane space and nucleus.[19] It has been found that mutations of this enzyme are linked to the fatal neurodegenerative disease amyotrophic lateral sclerosis (ALS) and scientists started to pay attention to this enzyme after Mann and Keilin isolated this blue colored protein.[17] In 1969 McCord and Fridovich named this enzyme and the complete three dimensional structure of Cu-Zn SOD was established in 1982.[17,20]

Cu-Zn SOD is a homodimer (Figure 1.1.3) and each subunit consists of eight antiparallel β-strands which are connected and stabilized by disulfide bonds.[17,19,21] Each subunit contains a bimetallic active site containing one Zn(II) and one Cu(II) ion. Cu(II) is coordinated to three histidines in the reduced state and Zn(II) is coordinated to one aspartic acid and three histidines. One of these histidines connected to the Zn can act as a bridging ligand and also coordinates with Cu via the deprotonated imidazole ring in the oxidized state.[17,22] According to the most accepted catalytic

mechanism, in the first step, Cu(II) undergoes reduction to Cu(I) by oxidizing superoxide to molecular O_2 and simultaneously breaking the Cu-His-Zn bridge. In the second step the Cu(I) is reoxidized to Cu(II) by another superoxide, forming H_2O_2 and reforming the Cu-His-Zn bridge. The surrounding water molecules act as the proton source for the bridging histidine during catalysis.[21,22]

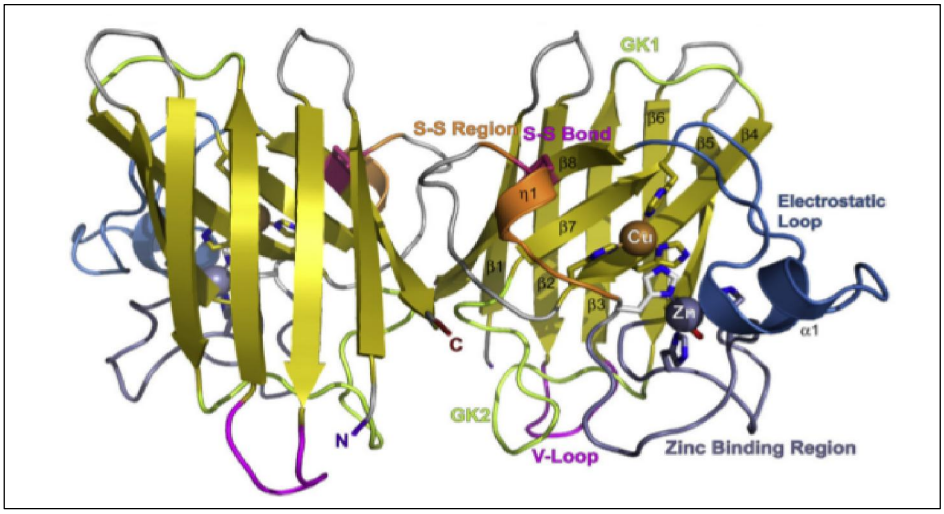

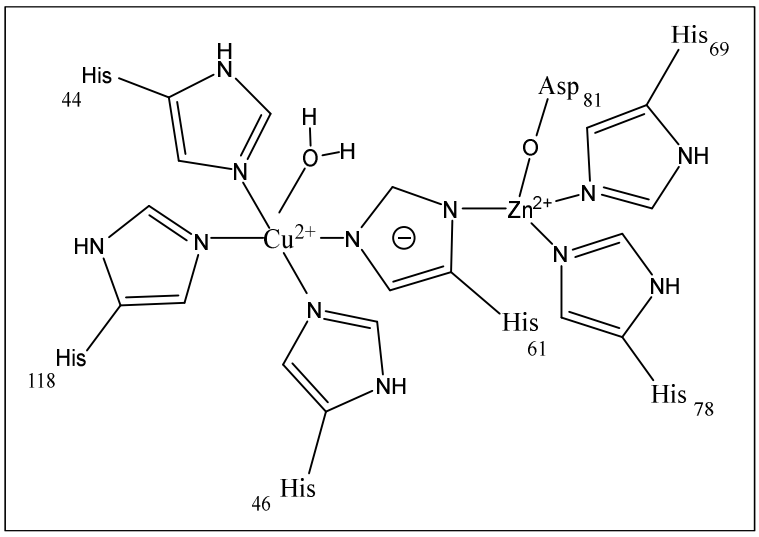

Figure 1.1.3: Structure of Cu-Zn SOD protein (top).[17] Active site of Cu-Zn SOD in the oxidized Cu(II) state (bottom).

Zn(II) in Cu-Zn SOD is noncatalytic and is not directly involved in the catalytic mechanism, but plays an important role in the stability and the proper geometry of the Cu site.[18,19,22]

1.2. Nickel in biological systems

Nickel is an important element for life on Earth and it was discovered in 1751 by the Swedish chemist A.F. Cronstedt.[1,23] It is in the d block of the periodic table with the atomic number 28, electronic configuration $[Ar]3d^8 4s^2$ and abundance nearly 80 $\mu g g^{-1}$ in the Earth's crust.[1] The most common oxidation state of nickel in aqueous environment at all pH levels is Ni^{+2}, commonly associated with octahedral, square planar and tetrahedral geometries; square pyramidal and trigonal bipyramidal geometries have also been observed. Less common oxidation states Ni^{+1} and Ni^{+3} are also found in biology. Ni^{+1} is associated with distorted octahedral or square planar geometries and Ni^{+3} is associated with distorted octahedral and trigonal bipyramidal geometries. The Ni^{+4} oxidation state is rarely observed, but has been seen under certain conditions. Four-coordinate square planar Ni^{+2} and six-coordinate octahedral Ni^{+2} are more common in proteins and their magnetic properties are different as square planar Ni^{+2} is diamagnetic and octahedral Ni^{+2} is paramagnetic.[24,25]

Nickel plays an essential role in the life of plants, cyanobacteria, and for certain bacteria in several catalytic functions including conversion of urea into ammonia and carbon dioxide by plants, nitrogen fixation, hydrogen oxidation, hydrogen production and superoxide dismutation by cyanobacteria and bacteria.[1,26,27] The coordination geometry around Ni is changed during catalysis when Ni^{+2} undergoes oxidation depending on the flexibility and the type of biological ligands. The stabilization of high oxidation states requires ligands with high electron density or more negative charges in order to allow for some charge delocalization from the metal to the ligand. Nickel forms

complexes with peptides by coordinating with oxygen, nitrogen or sulfur donor atoms in the side chains of amino acids and, less commonly with the amine or amide N atoms of the peptide backbone.[28,29] Among them, imidazolyl nitrogen atoms of histidines and thiol sulfur atoms of cysteine residues are the most common and efficient metal binding sites. Nickel has the second highest ability to make complexes (log K_f = 6-7) with acidic amino acids, behind only Cu (II).[24]

1.3.Nickel containing enzymes

Eight nickel containing enzymes have been identified, which catalyze very important biological processes. Of these eight enzymes seven either use or produce gases like CO_2, H_2, NH_3, O_2 and CO and are involved with global carbon, hydrogen, and oxygen cycles.[30] Among these enzymes, carbon monoxide dehydrogenase (CODH), acetyl-Coenzyme A synthase (ACS), NiFe hydrogenase, methyl-Coenzyme M reductase (MCR) and nickel superoxide dismutase (NiSOD) are redox enzymes.[30,31,32] Glyoxalase-I, acireductone dioxygenase (ARD) and urease are non-redox enzymes.[24,30,33] The following discussion is limited to redox enzymes which are close to NiSOD.

1.3.1. CO dehydrogenase (CODH) / Acetyl Co-enzyme A synthase (ACS)

CODH/ACS is an enzyme system and plays an important role in the global carbon cycle, allowing anaerobic microorganisms to live with CO and CO_2 and to fix cellular carbon.[31,34,35] CODH catalyzes the reversible oxidation of CO to CO_2 while ACS catalyzes the formation of acetyl-CoA from CO, coenzyme A and a methyl group derived from a corrinoid iron-sulfur protein (CFeSP).[36] Crystallographic studies reveal that the active site of CODH, which is denoted as the C-cluster consists of an [Fe_3S_4] unit bridged to a binuclear NiFe unit buried 18 Å below the protein surface (Figure 1.3.1.1 (a)). [24,37] The active site of ACS is known as the A-cluster and it consists of a [4Fe-

4S] cluster bridged to a Ni site which is bridged via two thiolates to another Ni ion in a N_2S_2 coordination environment composed of two thiolato S and two carboxamido N ligands. Therefore the A-cluster is a binuclear Ni-Ni unit bridged by a cysteine residue to a [4Fe-4S] cluster (Figure 1.3.1.1(b)).[30,37] Several mechanisms have been proposed[31,34,38] for the CODH/ACS function and the precise mechanism is yet to be established. A more likely mechanism of CO oxidation in the C-cluster involves 4 steps (Figure 1.3.1.2).[30,37] In the first step CO and H_2O bind to the C-cluster and form a Ni^{+2}-CO intermediate.

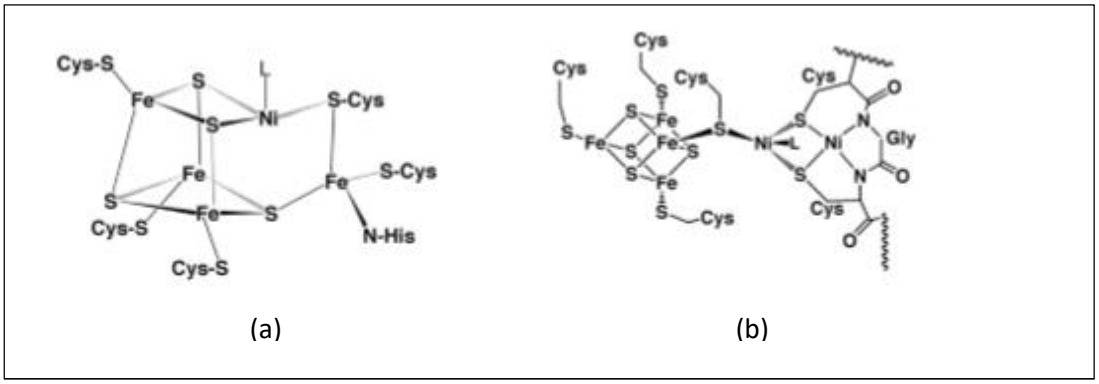

Figure 1.3.1.1. (a) active site of CODH and (b) active site of ACS[30,37]

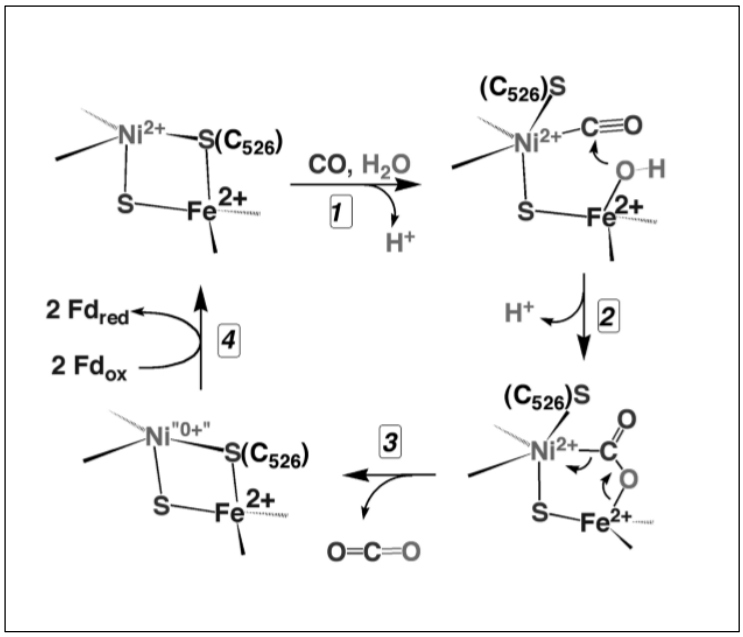

Figure 1.3.1.2. Proposed mechanism of CODH[30,37]

In the second step, the Ni-bound CO is attacked by the Fe-bound OH to form a complex with a formate ion bridging the Ni^{+2}-Fe^{+2} centers. Then Ni^{+2} undergoes a two-electron reduction by releasing CO_2 and, in the fourth step, Ni(0) is oxidized back to Ni^{+2} by transferring electrons to ferredoxin or another electron carrier. Figure 1.3.1.3 shows a proposed mechanism[37] for ACS which involves Ni(0) and Ni^{+2} oxidation states. The oxidation state of the distal Ni which is in the N_2S_2 environment remains unchanged throughout the catalytic cycle. As shown in Figure 1.3.1.3, CO produced in the C-cluster migrates to the A-cluster and binds with Ni in the zero-valent state. A methyl group is then transferred from a methylated cobalt corrinoid-iron sulfur protein (CoFeSP) to the Ni-CO complex binding to Ni, and forming a methylated Ni^{+2}-CO unit. In the next step C-C bond formation occurs by condensation of methyl and carbonyl groups to make a Ni^{+2}-acetyl species. Finally CoA triggers the reductive thiolysis of the Ni^{+2}-C bond, producing acetyl CoA and regenerating the active enzyme.[30]

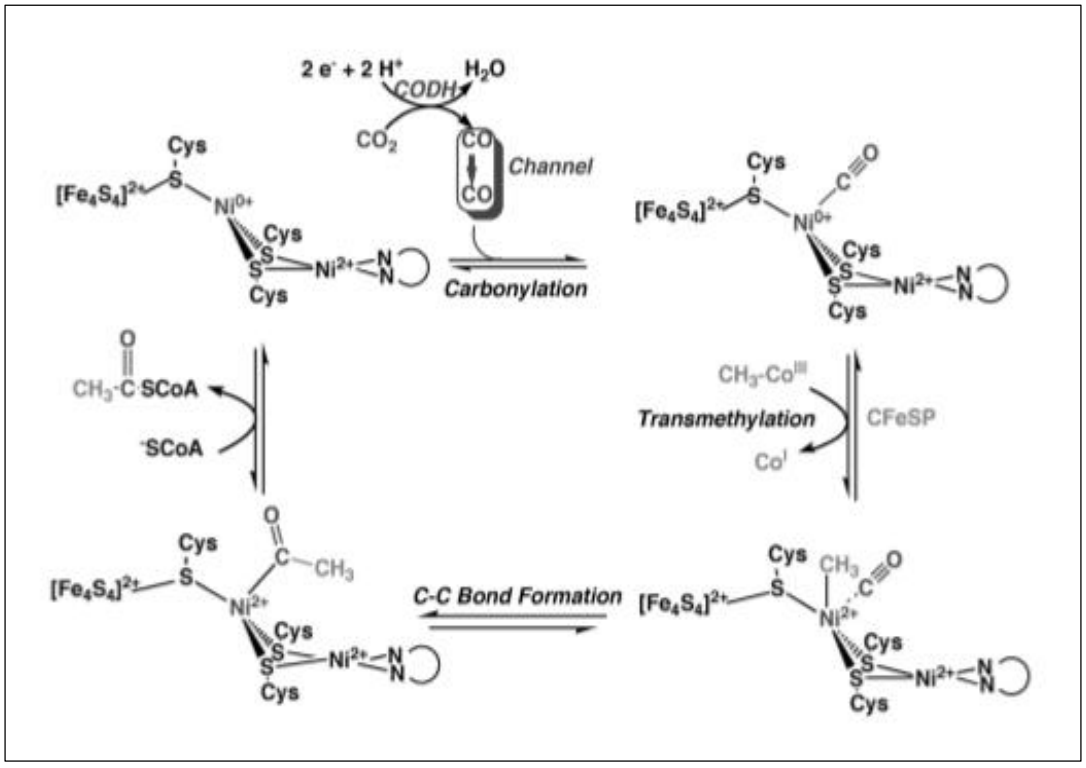

Figure 1.3.1.3: Proposed mechanism of ACS[37]

1.3.2. NiFe hydrogenase

Hydrogenase enzymes catalyze the interconversion between H_2 gas and protons and electrons. H_2-utilizing microbes couple the oxidation of H_2 with the reduction of various electron accepters like O_2, SO_4^{-2}, CO_2 and NO_3^- and H_2-evolving microbes reduce protons to H_2 in order to remove excess cellular reducing equivalents.[30,39,40] NiFe hydrogenase is found in variety of microorganisms and plays a vital role in metabolism via consumption as well as production of H_2 gas.[40] This enzyme consists of two subunits of around 60 and 30 kDa and the Ni-Fe active site resides in the large subunit coupled to the small unit which contains at least one [4Fe-4S] cluster that are involved in elctron transfer between the active site and the protein surface.[41,42] The heterodinuclear Ni-Fe metal centers are bridged by two cysteine residues. In addition, the Ni center is coordinated to two terminal cysteine residues, forming a distorted tetrahedral geometry. Fe is in the low-spin divalent state and is coordinated by two biologically unusual CN^- ligands and one CO ligand, giving a square pyramidal geometry.[42,43,44]

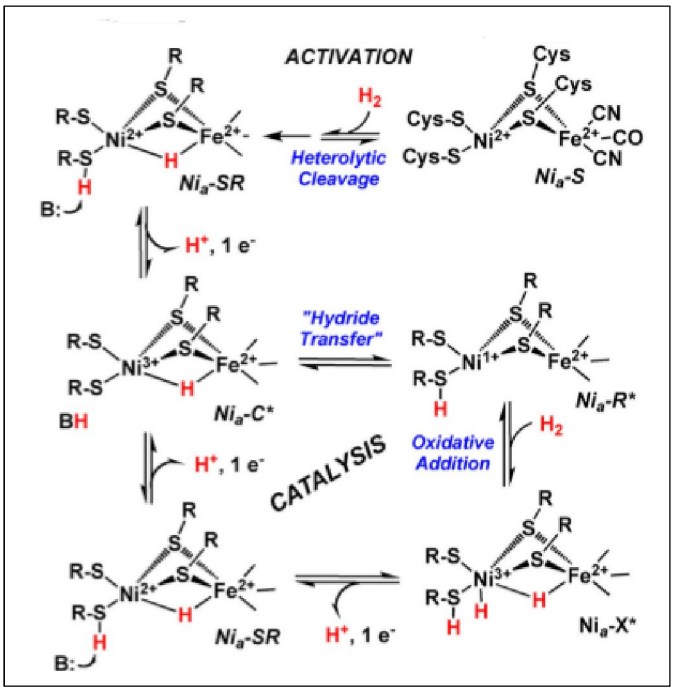

Figure 1.3.2.1. Structure and proposed mechanism of NiFe hydrogenase[42]

Much research has been done to understand the precise mechanism of NiFe hydrogenase and still some details are unresolved. According to the mechanism proposed by Lill and Siegbahn (Figure 1.3.2.1) four states are involved in the catalytic cycle, which are termed as Ni-SR, Ni-C, Ni-R and Ni-X. The first step involves activation by H_2 and heterolytic cleavage of the H-H bond takes place to make the Ni-C state where Ni is in the +3 state. The Ni-C state is converted to the Ni-R state where the oxidation state of Ni goes to Ni^{+1} by a hydride transfer or proton coupled electron transfer reaction, allowing productive binding of H_2. Finally, the Ni-X state is generated by H-H cleavage by an oxidative addition mechanism which undergoes two successive proton coupled electron transfer steps to produce the Ni-C state again.[42]

1.3.3. Methyl-Coenzyme M reductase (MCR)

MCR is an important enzyme in the energy metabolism of all methanogenic microorganisms. It catalyzes the formation of methane and the heterodisulfide (CoBSSCoM) by reduction of methyl-coenzyme M with coenzyme B[45,46,47](Figure 1.3.3.1).[1]

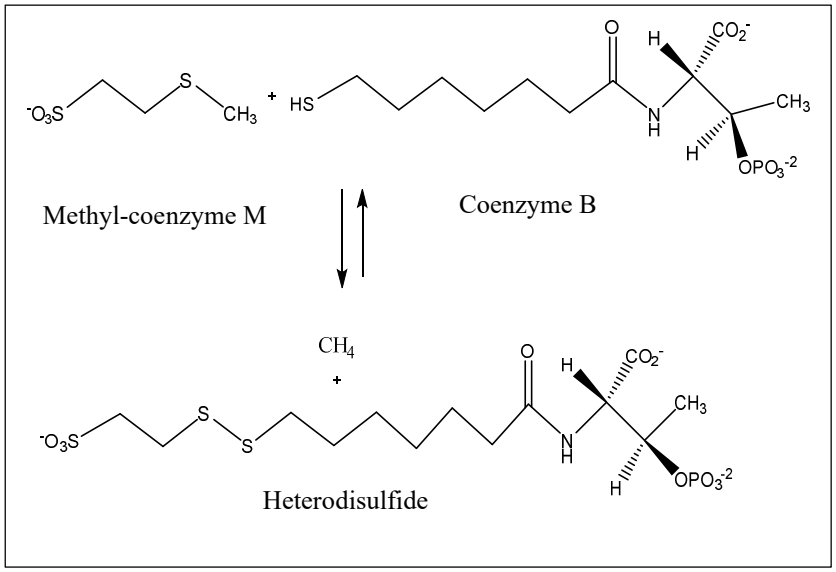

Figure 1.3.3.1. Reaction catalyzed by methyl-coenzyme M reductase from methanogenic bacteria.[1]

In the active site of MCR, a nickel ion is coordinated to a tetrahydrocorphinoid complex called coenzyme F-430 via four pyrrolic nitrogens in the basal plane of a square-pyramidal coordination sphere (Figure: 1.3.3.2).[46,47]

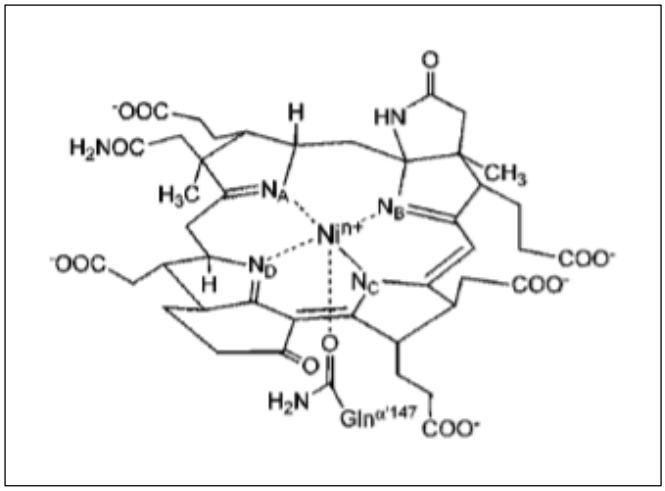

Figure 1.3.3.2. Coenzyme F-430 in MCR[48]

The carbonyl oxygen of a glutamine residue is bound to nickel in the axial position. The Ni center in the active site is redox active and shuttles between the +1, +2 and +3 oxidation states. Two possible mechanisms for MCR-catalyzed methane formation have been proposed (Figure 1.3.3.3),[30,49] mainly differing in the type of C-S bond cleavage of CH_3-S-CoM.

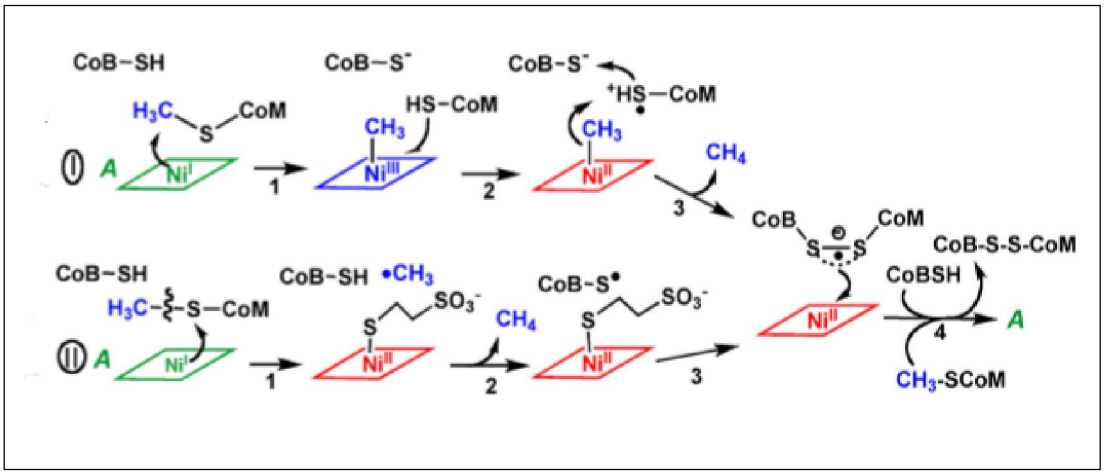

Figure 1.3.3.3. Two proposed mechanisms for methane formation by MCR[49]

In the first step of mechanism 1, methyl-CoM undergoes nucleophilic attack by Ni^{+1} to form a methyl-bound Ni^{+3} intermediate and release CoM. Then a methyl-Ni^{+2} species and CoM radical are generated by electron transfer from CoM to the methyl-Ni^{+3} species in the second step. After that, the bound methyl group abstracts a proton from the CoM radical and generates methane while the CoM radical reacts with $CoBS^-$ to form a disulfide radical anion. In step four, the radical anion reduces Ni^{+2} generating the CoB-SS-CoM heterodisulfide and regenerating the active Ni^{+1} enzyme. In mechanism 2, the first step involves formation of a methyl radical. Reaction of Ni^{+1} with methyl-SCoM supports homolytic cleavage of the C-S bond by forming a coordination complex with the sulfur of CoM, forming a methyl radical and Ni^{+2}-thiol bond. In step two, methane and a thiyl radical on CoB are formed as the methyl radical abstracts a hydrogen atom from CoBSH. After that the third step involves formation of the same disulfide anion radical resulting from mechanism 1. Finally the disulfide anion radical offers an electron to Ni^{+2} and forms the active Ni^{+1} state and the heterodisulfide.[30,46,47]

All three enzymes discussed above utilize redox-active Ni centers for catalysis. NiSOD is another enzyme with a redox active Ni center in the active site with unique properties. By studying the mechanisms of these three enzymes, the uniqueness of NiSOD can be very well recognized.

1.4. Nickel Superoxide Dismutase (NiSOD)

Similar to other SODs, NiSOD catalyzes the disproportionation of superoxide anion radical to H_2O_2 and molecular O_2. It was discovered in 1996 by Youn and Kang, ital, from *Streptomyces* species.[50] It can also be found in marine cyanobacteria.[1,16,50,51] NiSOD has very few features in common with other SOD types and shows distinct properties. It is a product of the sodN gene and is a small protein with 117 amino acids. The primary amino acid sequence of NiSOD shares no sequence or structural homology with other SODs.[3,52,53] Two crystal structures of NiSOD have

been solved with protein isolated from *Streptomyces seolensis*[1] and *Streptomyces coelicolor*[1] and they show NiSOD forms a homohexamer comprised of four-helix bundle monomers, stabilized by hydrophobic, salt bridge and hydrogen-bonding interactions.[1,54] Each monomer has a mononuclear nickel active site at the N-terminus, which are spaced 20 Å apart.[1] The nickel binding domain, known as the nickel hook in each unit, consists of nine amino acid residues giving a hook-like shape. This nickel hook protrudes out of the bundle in NiSOD, making a characteristic metal binding site unique among other metalloenzymes[1,52,55] (Figure 1.4.1).

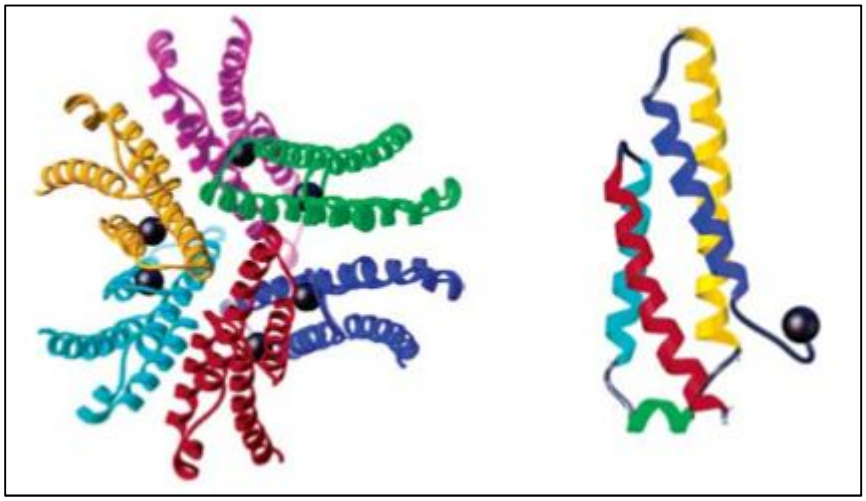

Figure 1.4.1. (Left) Crystal structure of NiSOD from *Streptomyces coelicolor*[3] showing hexameric assembly of four helix bundles. (right) subunit with the Ni binding hook.

In both crystal structures of NiSOD, two states of nickel have been identified in two different coordination environments. The nickel center in half of the structure is in the +2 oxidation state and the other half is in the +3 state. Based on these observations, it has been identified that the mononuclear nickel center in the active site undergoes alternate oxidation and reduction during catalysis[52,56,57] (Figure 1.4.2).[58] In the reduced state, Ni^{+2} ion forms a N_2S_2 square planar coordination environment composed of two thiolato-S atoms from Cys2 and Cys6 and two N atoms from the N-terminal amine of His1 and carboxamido N from Cys2. In the oxidized state

nickel is in the +3 state and forms a fifth Ni-N coordination bound with the imidazole-N of His1 giving a N_3S_2 square pyramidal geometry around Ni.[59,60,61] Bond distances for NiSOD from *Streptomyces coelicolor* are given in Table 1.4.1.[3] NiSOD is the only SOD which shows oxidation state dependent changing coordination environment in the catalytic mechanism.

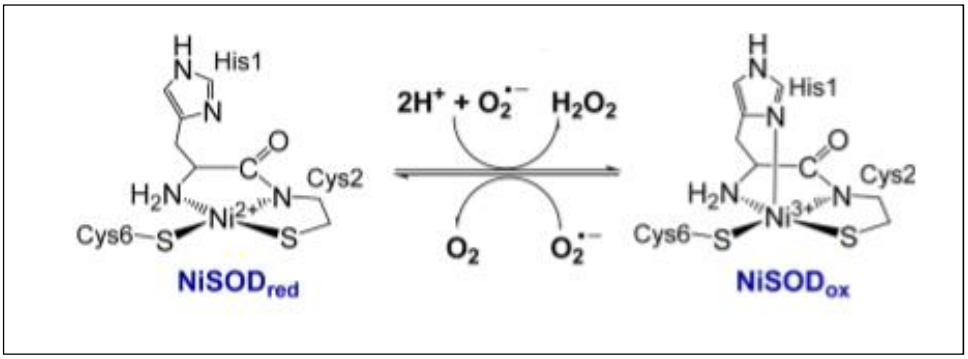

Figure 1.4.2. Catalytic reaction of NiSOD involving reduced state and oxidized state of the active site [58]

The NiSOD active site has unique properties. Carboxamido N coordination to the metal is rare in metalloenzymes; the distal Ni site of ACS/CODH, nitrile hydratase and the oxidized P-cluster of nitrogenase are exceptions.[52] Coordination of the N-terminal amine is also reported in very few cases. The presence of both amide and amine coordination together in NiSOD is one of the distinct properties of the NiSOD active site compared to other metalloenzymes.[62,63] Furthermore, the two cysteine-S coordination is also fascinating, they help to maintain the Ni^{+2}/Ni^{+3} redox potential to perform the superoxide dismutation without being oxidized although they are highly susceptible for S-based oxidation in the presence of ROS.[3,52,61]

Table 1.4.1. Bond distances for NiSOD from *Streptomyces coelicolor*[3]

Bond	**Distance Å**
$Ni^{+2/+3}$ -S_{Cys2}	2.16 ± 0.02
$Ni^{+2/+3}$ -S_{Cys6}	2.19 ± 0.02
$Ni^{+2/+3}$ -N_{Cys2}	1.91 ± 0.03
Ni^{+2} -N_{His1}	1.87 ± 0.06
Ni^{+3} -N_{His1}	2.02 ± 0.10
Ni^{+3} -$N_{ax\ His1}$	2.35 ± 0.05

Unlike other SODs, all of which contain metal ions whose aqueous redox potential are close to that required for SOD activity, the aquated Ni ion is not capable of SOD catalysis, as the redox potential of aqueous Ni (2.29V)[30] lies outside the range of the potential for superoxide dismutation, between -0.16V and 0.87V.[30] Therefore, this unique coordination and the protein fold of NiSOD regulate the redox potential of the Ni center and bring it to a suitable range (0.286V)[30] to perform the disproportionation of superoxide, provide a proton source for the reduction of superoxide and control the access of superoxide to the active site.

Several spectroscopic techniques have been used to reveal electronic and structural properties of NiSOD, including EPR, UV-Vis and resonance Raman spectroscopy.[29,64] EPR spectra of NiSOD confirm the cycling between diamagnetic Ni^{+2} and paramagnetic Ni^{+3} and the axial N coordination in the oxidized state.[65,66] The UV/Vis spectrum of the wildtype oxidized state of NiSOD shows two absorption maxima. The peak at 378 nm arises from S to Ni^{+3} LMCT transition and the peak at 540 nm is assigned to a d-d transition.[1]

Kinetic studies of the NiSOD reaction reveal that the enzyme operates at a rate near the diffusion limit and is pH independent near physiological pH.[1,50,67] Several model studies have been done to

understand the exact mechanism of NiSOD and both inner-sphere and outer-sphere mechanisms have been presented; the topic is still to be resolved. Getzoff and coworkers reported an inner-sphere mechanism (Figure 1.4.3)[1-3] that involves formation of a Ni-O_2^- bond. NiSOD does not have any hydroxyl or aqua ligands to serve as a proton source during catalysis. Tyr9 residue located 5 Å from the Ni center makes a H-bonding network with water molecules and other residues and acts as the proton source.

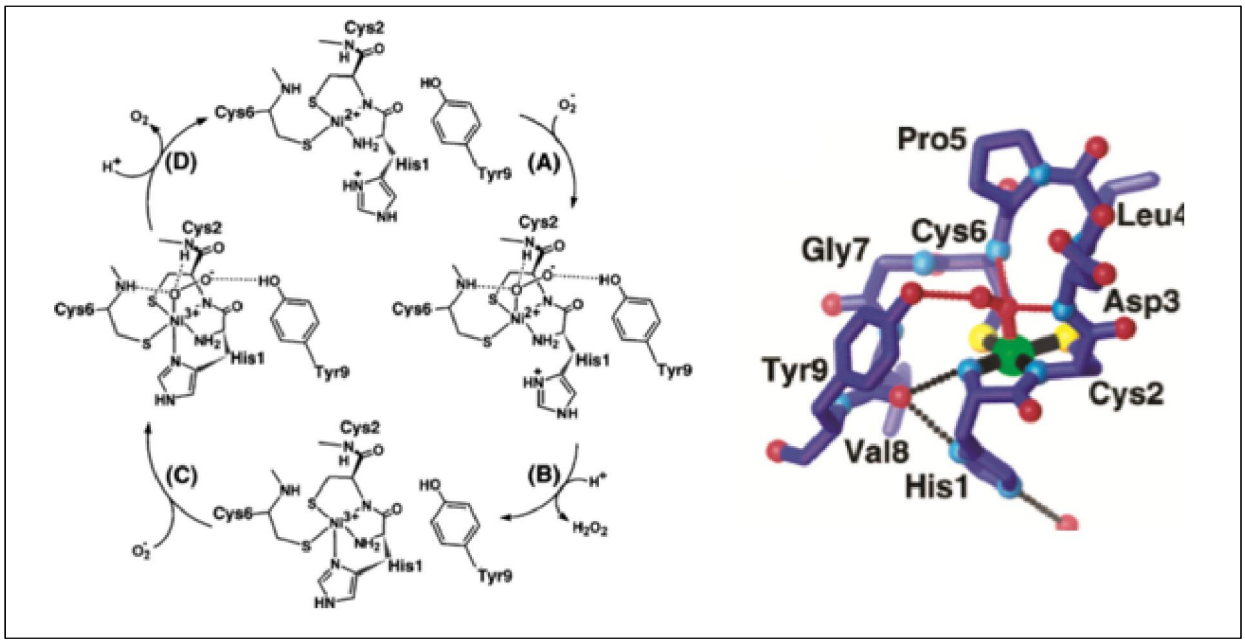

Figure 1.4.3. (Left) Catalytic mechanism of NiSOD as proposed by Getzoff ,[3] (right) NiSOD reduced active site with the superoxide bound to Ni^{+2}

Superoxide binds to the reduced active site opposite the His1 side chain. Electron transfer from the Ni center to superoxide occurs through an inner sphere mechanism and it is coupled to proton transfer to generate H_2O_2. It has been suggested that the side chain hydroxyl of Tyr9 or backbone amides of Asp3 or Cys6 act as a proton donor during reduction of superoxide. This is similar to Tyr34 in MnSOD, which is located at the same distance, and in the same orientation as Tyr9 in NiSOD, acting as the proton donor in the catalysis. Upon electron transfer from Ni^{+2} to superoxide

His imidazole-N binds with the Ni^{+3} center axially and converts four-coordinate square planar geometry to five- coordinate square pyramidal geometry. Then another superoxide binds with the oxidized Ni^{+3} center and electron transfer from superoxide reduces Ni^{+3} to Ni^{+2} producing molecular O_2 to complete the cycle.[3,50,55] Buntkowsky and coworkers have also presented a mechanism supporting an inner-sphere electron transfer.[68]

Anion binding studies have found that NiSOD has low affinity towards the azide (N_3^-) anion[52,59] which is a common substitute for O_2^-, and therefore an outer-sphere mechanism is probable. Cabelli and coworkers proposed an outer-sphere mechanism where no Ni-O_2^- bond formation occurs during catalysis[59] (Figure 1.4.4). According to the mechanism, superoxide displaces the two water molecules in the binding pocket and sits between Asp3 and Cys6 amide backbones. Electron transfer occurs, associated with proton transfer forming Ni^{+2} and O_2, in the substrate oxidation cycle. In the reduction cycle, electron and proton transfer with O_2^- in the substrate binding pocket forms Ni^{+2} and H_2O_2.

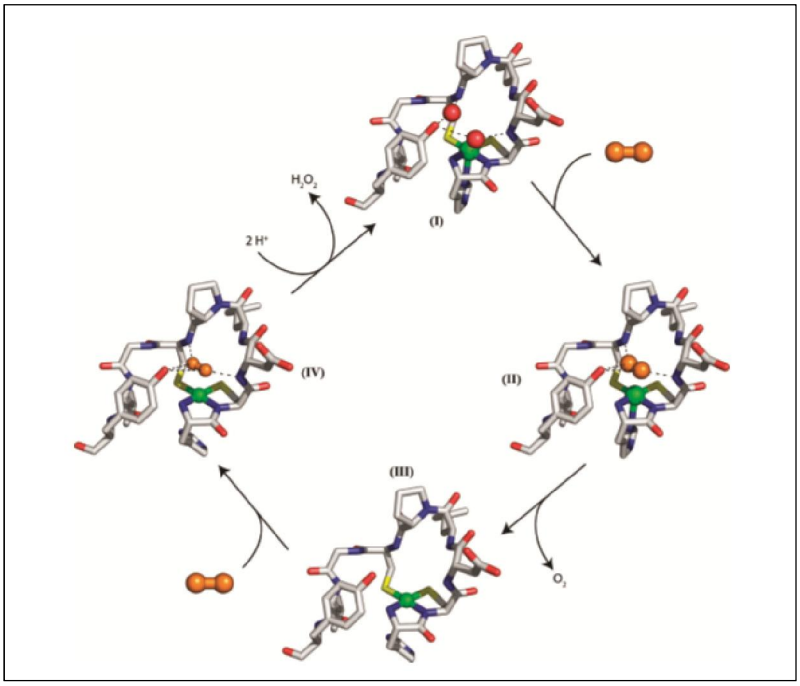

Figure 1.4.4. Catalytic mechanism of NiSOD as proposed by Cabelli and coworkers[59]

All of the proposed mechanisms involve stabilization of the O_2^- in the active site by H-bonding and the source of H is not yet clear. As per suggestions Tyr9, the protonated imidazole-N of His-1, and Cys2 or Cys6 involve with H-bonding and H^+-donor to form H_2O_2 in the reductive cycle.[52,69]

1.5. Models for NiSOD

The unique structure and properties of NiSOD compared to other Ni containing enzymes generate questions regarding its structure-function relationship. Making careful synthetic models representing the coordination environment for NiSOD is beneficial to understand the importance of the presence of amine/amide and two cysteine-S coordination and what properties are imparted to the Ni center by these ligands, how it regulates the redox potential without oxidizing the Cys-S and what the typical reaction mechanism is. In this synthetic analogue approach creating the N_2S_2 ligand frame as in the primary coordination sphere of the enzyme which shows special and electronic features of the enzyme is an important factor.

1.5.1. Models with short polypeptides

Out of all the approaches that have been taken in modeling NiSOD so far, models with peptides have been the most successful ones. The first peptide model [labeled as $Ni^{II}(SOD^{M1}$-Im-H) where SOD^{M1} is HCDLPCGVYDPA] was synthesized by Shearer and coworkers (Figure 1.5.1.1).[52,70-71] This model is comprised of the first 12 amino acids in the N-terminus of the active site of *Streptomyces Coelicolor* NiSOD and it coordinates with Ni in a1:1 ratio in a slightly basic medium. Derivatives of this model were also synthesized to modify the His1residue, named $Ni^{II}(SOD^{M1}$-Im-X) where X= Methyl (Me), 2,4-dinitrophenyl (DNP) and tosyl (Tos) (Figure 1.5.1.1).[52,71] All these models have been characterized by UV-Vis, X-ray absorption spectroscopy (XAS) and electrochemistry. The results reveal that these models nearly resemble $NiSOD_{red}$. UV-Vis spectra

indicate two low intensity ligand field bands at 461 nm and 553 nm which are consistent with Ni(II) square planar N_2S_2 coordination complexes.[52]

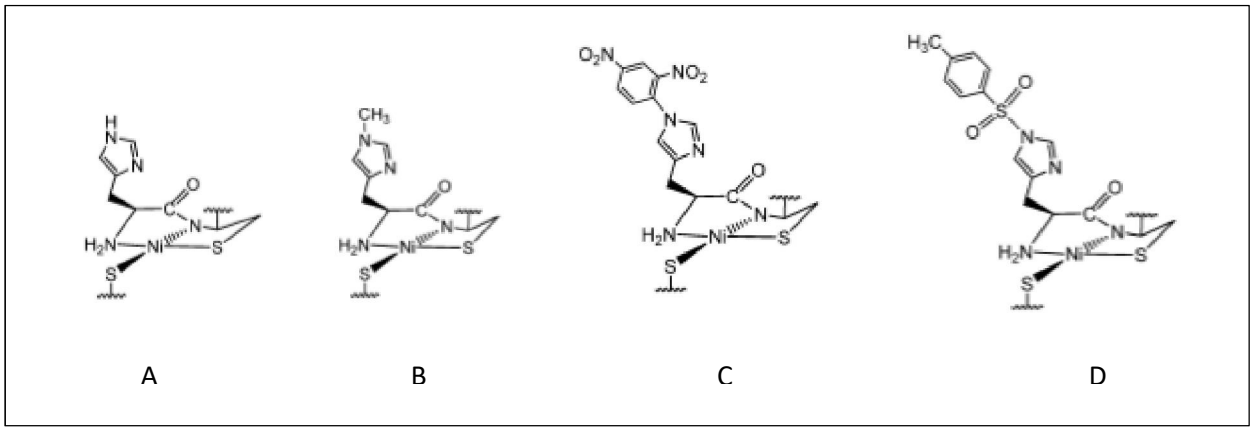

Figure 1.5.1.1. First reported peptide models of NiSOD, A: $Ni^{II}(SOD^{M1}$-Im-H) and its derivatives B: $Ni^{II}(SOD^{M1}$-Im-Me) C: $Ni^{II}(SOD^{M1}$-Im-DNP) D: $Ni^{II}(SOD^{M1}$-Im-Tos) [52]

Electrochemistry studies via cyclic voltammetry revealed quasi-reversible redox couples with potentials for Ni(III/II) ranging from 0.280-0.600 V. These lie within the superoxide dismutation window, suggesting these models could perform superoxide dismutation. SOD activity has been investigated by stopped- flow kinetics[71] by monitoring the disappearance of O_2^- at 245 nm and all four models have displayed activity. Models with electron withdrawing substituents, DNP and Tos on the imidazole-N showed more efficient catalysis on the order of 10^8 $M^{-1}s^{-1}$, one order of magnitude slower than NiSOD catalysis at pH 8.00. The $Ni(SOD^{M1}$-Im-H) metallopeptide afforded a slower reaction rate (on the order of 10^7) compared to the other two imidazole-N-DNP and imidazole-N-Tos containing metallopeptides. The most electron rich Ni^{III} center containing an imidazole-N-methyl substituted model, $Ni(SOD^{M1}$-Im-Me), has shown the slowest reaction rate with O_2^- (on the order of 10^6) out of all four models. This analysis reveals that the axial Ni-N bond strength has a big impact on the efficiency of SOD catalysis and it is expected that the H-bonding

network of NiSOD effectively reduces the Lewis basicity of the imidazole N to optimize the electron transfer properties.[52,71]

Shearer and co-workers have reported another peptide-based model known as $Ni^{II}(SOD^{M2})$, (where SOD^{M2} = HCDLPCG) composed of seven amino acid residues found in the Ni binding hook in NiSOD.[72] Two derivatives of $Ni^{II}(SOD^{M2})$ have been made by replacing His1 with Ala (A) and Asp(D) residues (Figure 1.5.1.2).[72]

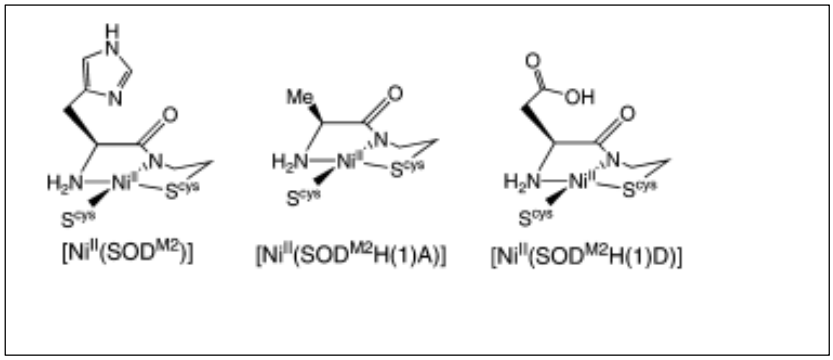

Figure 1.5.1.2. $Ni^{II}(SOD^{M2})$ peptide-based model of NiSOD and its derivatives [72]

Spectroscopic characterization of $Ni^{II}(SOD^{M2})$ similar to $Ni^{II}(SOD^{M1})$, resembles $NiSOD_{red}$. SOD activity revealed that the mutants have significantly lower activity compared to the parent metallopeptide. Two findings have been suggested based on the results; axial ligation is important to optimize the active site of NiSOD for catalysis and lack of axial ligation by the metallopeptides reduces the activity of NiSOD significantly but does not completely disable it.

Another functional biomimetic for NiSOD which is comprised of nine residues from the N-terminal of the "Ni Hook" labeled as [Ni(mSOD)] where mSOD = HCDLPCGVY was synthesized by the Weston and Buntkowsky groups [52,55,68] They have been able to make [Ni(CN)(mSOD)] with CN bound as a substrate analogous to O_2^- for the first time. UV-Vis spectroscopy, IR, and solid and solution NMR techniques have been used to confirm the single CN anion bound structure

and this suggests a possible inner-sphere mechanism for NiSOD catalysis. Quantitative SOD activity analysis of this nonapeptide model showed 1250 units of activity compared to 75,000 units of NiSOD enzyme activity.[55]

1.5.2. Low molecular weight models of NiSOD

Several low molecular weight models containing approximate features of NiSOD have been reported. The first functional model synthesized by Darensbourg and co-workers[73,52] (Figure 1.5.2.1 left) features N_3S coordination which differs from the N_2S_2 coordination in $NiSOD_{red}$. Even though this complex behaves differently in UV-Vis and cyclic voltammetry from Ni(II)-N_2S_2 complexes, it shows 40% decrease in the intensity of the absorption band centered at 580 nm when treated with 100 eq. of O_2^- by NBT/Formazan assay reflecting the O_2^- scavenging ability, but the role of the Ni center during activity is not clear. This complex has been modified to get a N_3S_2 coordinated complex and it does not show any SOD activity (Figure 1.5.2.1 right).[73]

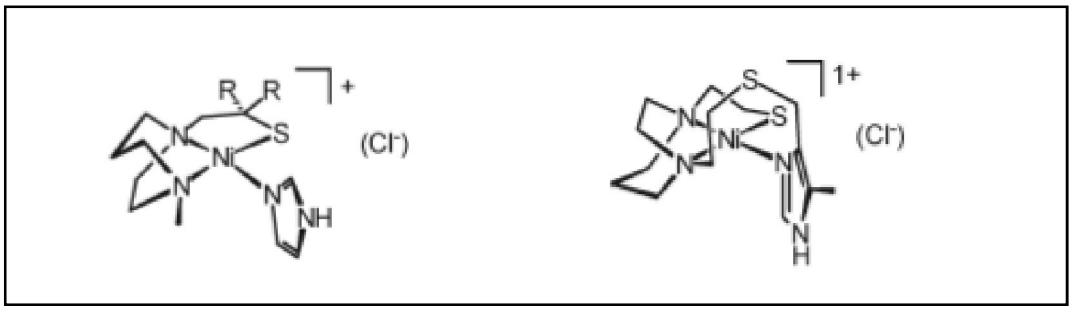

Figure 1.5.2.1. Structures of NiSOD model complexes as synthesized by Darensbourg and co-workers.[73]

Square planar Ni-N_2S_2 type model complexes containing different ligand environments have been synthesized by different research groups. Some Ni(III)-N_2S_2 type models with diamide/dithiolate coordination were synthesized by Holm and Kruger (Figure 1.5.2.2) and the importance of Ni^{+3}-S

interaction relevant to NiSOD using those complexes has been studied by Brunold and co-workers.[74]

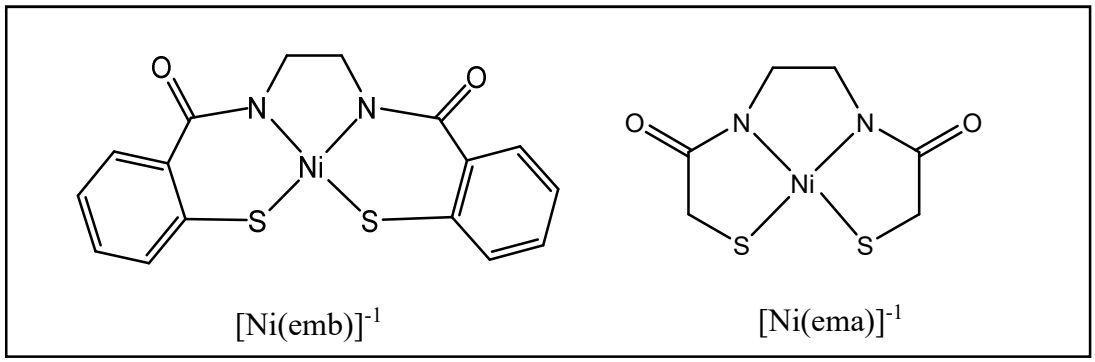

Figure 1.5.2.2. Ni(III)-N_2S_2 models as synthesized by Holm and Kruger[74]

Ni^{+3}-S stretching force constants of these diamide complexes were calculated and they reveal that the Ni^{+3} center is more stabilized in these complexes as compared to amine coordinated complexes. Bond strengths were compared with $NiSOD_{ox}$ as shown in Table 1.5.2.1.[74] The comparison indicates that the Ni^{+3}- S/N_{amide} bond strengths in $NiSOD_{ox\ are}$ considerably higher than these model complexes and the reason could be the unique coordination environment of NiSOD.

Table 1.5.2.1. Comparison of metal-ligand force constants

System	**Metal-Ligand bond**	**Force constant**
		(mdyn $Å^{-1}$)
$NiSOD_{ox}$	Ni^{+3}-S_2	1.79
	Ni^{+3}-S_6	1.68
	Ni^{+3}-N_{Cys2}	1.34
[Ni(emb)]$^{-1}$	Ni^{+3}-S	1.59
	Ni^{+3}-N_{amide}	1.21
[Ni(ema)]$^{-1}$	Ni^{+3}-S	1.51
	Ni^{+3}-N_{amide}	1.28

The first small molecule model, $(Me_4N)[Ni^{II}(BEAAM)]$ with amine/amide/bisthiolate coordination was synthesized by Shearer and Zhao[75] (Figure 1.5.2.3).

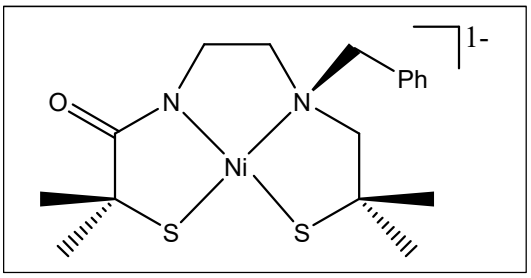

Figure 1.5.2.3. The structure of $[Ni^{II}(BEAAM)]^{-1}$ as synthesized by Shearer and Zhao

Bond distances for Ni-N_{amine}, Ni-N_{amide}, Ni-S(trans to amide N) and Ni-S(trans to amine N) in this model complex are 1.987, 1.858, 2.137, 2.177 Å, respectively, which compare well with those in NiSOD, which are 1.87, 1.91, 2.19, 2.16 Å, respectively. The reason suggested for the small difference in bond lengths is the induced chelate ring strain present in $[Ni^{II}(BEAAM)]^{-1}$ which is not present in NiSOD. $[Ni^{II}(BEAAM)]^{-1}$ has a $Ni^{+2/+3}$ redox potential of 0.12 V but does not show any SOD activity using the xanthine/xanthine oxidase assay.[75]

With the idea of understanding the effect of the unique NiN_2S_2 coordination of NiSOD on the properties of the Ni center, Shearer, Hegg, and co-workers have synthesized and compared a NiN_2S_2 complex, $(Ni^{II}(HL2))^-$ with amine/amide/bisthiolate coordination and the analogous diamide complex $(Ni^{II}(L1))^{-2}$ (Figure 1.5.2.4).[76]

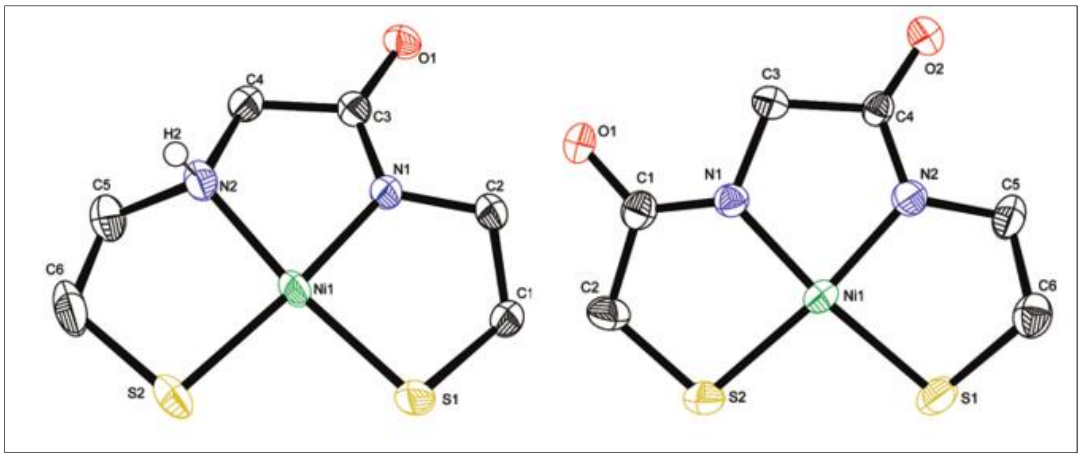

Figure 1.5.2.4. ORTEP diagrams of $(Ni^{II}(HL2))^{-}$ (left) and $(Ni^{II}(L1))^{-2}$ (right) complexes as synthesized by Shearer, Hegg and co-workers.[76]

These studies revealed that the diamide complex is highly reactive towards O_2 and shows a more negative Ni^{+3}/Ni^{+2} oxidation potential than the mixed amine/amide complex and thereby stabilizes Ni^{+3} more. Previous studies have shown that the diamine complexes are stable towards O_2 compared to analogous diamide complexes[77] and by utilizing mixed amine/amide coordination NiSOD gains both stability in oxidative environment and lower oxidation potential. The results also suggest that a slight difference in the coordination environment of NiSOD can have a significant impact on the Ni center.

Harrop and co-workers synthesized four NiN_2S_2 complexes containing amide/pyridine/bisthiolate coordination, (Et_4N)[Ni(nmp)(SC_6H_4-p-Cl)], (Et_4N)[Ni(nmp)(S^tBu)],(Et_4N)[Ni(nmp)(S-o-babt)] and (Et_4N)[Ni(nmp)(S-meb)], that successfully resemble the electronic and spatial characteristics of the primary coordination sphere of NiSOD[78,79] (Figure 1.5.2.5).

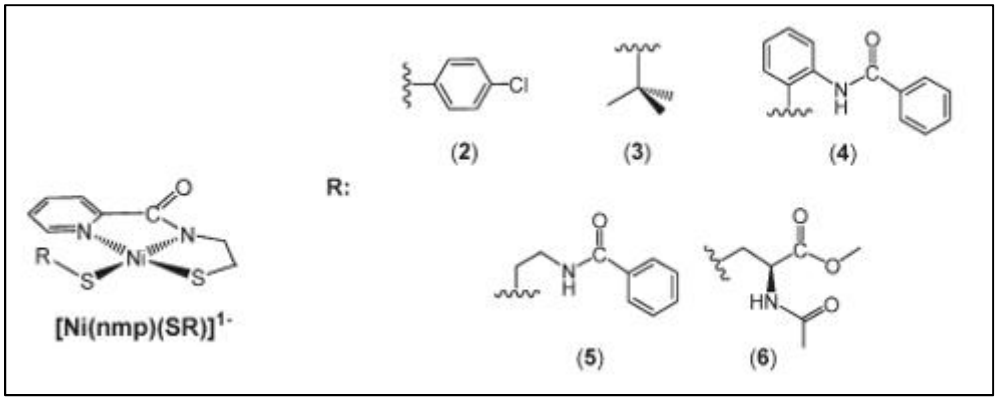

Figure 1.5.2.5. Basic structure of $[Ni(nmp)(SR)]^{-1}$ model systems (left) and R groups used (right) as synthesized by Harrop and co-workers.[78,79]

Ni-N/S bond distances of these complexes compare well with those in $NiSOD_{red}$. All these complexes show irreversible oxidation events and none of them display any SOD activity, likely demonstrating again the necessity of these complexes to stabilize the Ni^{+3} state and the importance of the presence of the fifth N coordination for enzymatic activity. Another series of Ni(II)-N_2S_2 complexes has also been synthesized by Harrop's group by employing the same Ni(nmp) ligand frame with different thiolates with and without an additional N donor to support the formation of N_3S_2 coordination (Figure 1.5.2.6).[58] The impact of the electron deficient nature of S_{exo} (exogenous second thiolate coordination) group and N_{axial} bound S_{exo} groups on redox properties of these model complexes has also been studied. As with the above discussed Ni(II)N_2S_2 complexes, these models were unable to stabilize the oxidized Ni^{+3} state and no spectroscopic or crystallographic evidence was obtained for the formation of a Ni^{+2}-NH_2Ph bond.

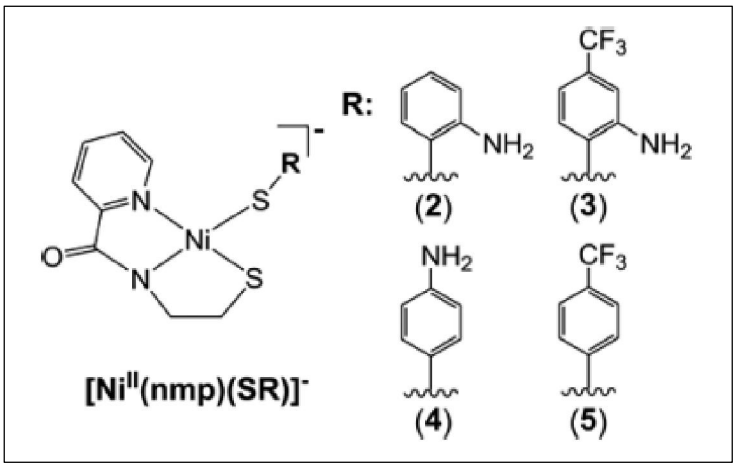

Figure 1.5.2.6. Basic structure of $[Ni(nmp)(SR)]^{-1}$ model systems (left) and R groups used (right) as synthesized by Harrop and co-workers.[58]

Cyclic voltammetric studies of complexes 4 and 5 showed irreversible waves with E_{ox} values of 0.51V and -0.47 V respectively. Complexes 2 and 3 showed Ni^{+2}/Ni^{+3} based quasi reversible waves at $E_{1/2}$ = -0.69 V and -0.43 V. Oxidation of 2 and 4 is easier than 3 and 5 due to the inclusion in the latter of electron-withdrawing CF_3 groups. Chemically oxidized complexes 2 and 3 generated reversible waves in cyclic voltammetry and this could arise from $[Ni^{II}(nmp)(SR)]^{-}$ /$[Ni^{III}(nmp)(SR)]$ couple or $[Ni^{II}(nmp)(SR)]^{-}$/$[Ni^{II}(nmp)(\cdot SR)]$ couple. It is confirmed that the oxidized species of the redox couple is a hybrid resonance of $[Ni^{III}(nmp)(SR)]$ and $[Ni^{II}(nmp)(\cdot SR)]$ from experimental and theoretical studies. This result suggests that the NiSOD catalytic mechanism may involve a Ni-coordinated ·S(Cys) during the transition from $NiSOD_{red}$ to the five-coordinate oxidized state of NiSOD ($NiSOD_{ox}$).[58]

Jensen and co-workers have come up with a new approach to mimic NiSOD by utilizing "scorpionate" ligands which are capable of chelating in κ^2 and κ^3 fashion with Ni. In their three model complexes, hydrotris(3-phenyl-5-methylpyrazolyl)borate ($Tp^{Ph,Me}$), a scorpionate ligand, has been used to mimic the monoanionic facial array of nitrogen donors (Figure 1.5.2.7).[80]

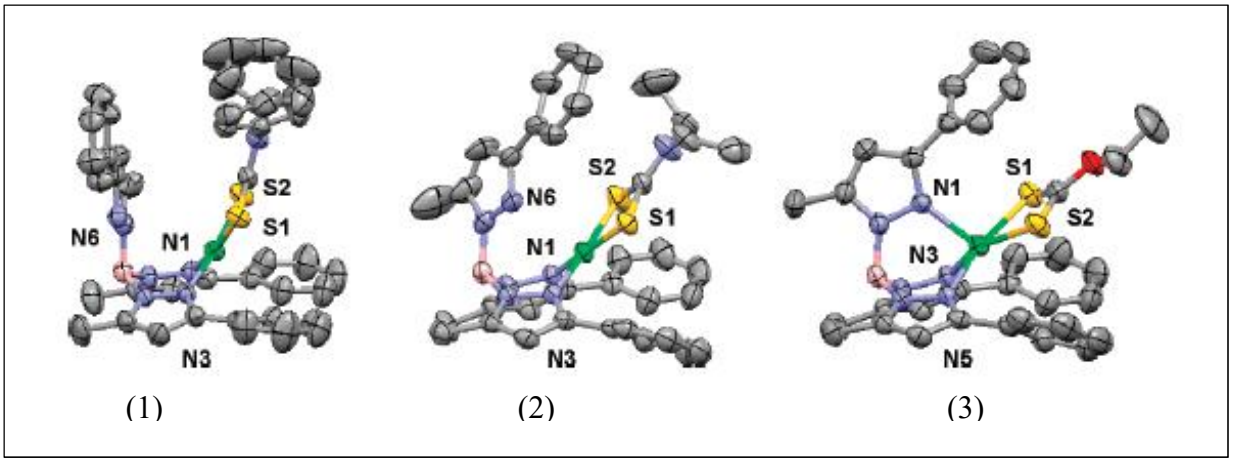

(1) (2) (3)

Figure 1.5.2.7. X-ray crystal structures of $Tp^{Ph,Me}NiS_2CNPh_2$ (1), $Tp^{Ph,Me}NiS_2CNEt_2$ (2) and $Tp^{Ph,Me}NiS_2COEt$ (3) as synthesized by Jensen and co-workers.[80]

1,1-S,S'-chelating dithiocarbamates (R_2NCS_2) R=Et and Ph for complexes 1 and 2 and organoxanthate ($EtOCS_2$) for complex 3 have been used as coligands to mimic the dithiolate unit.

X-ray crystallographic studies have confirmed the formation of square planar Ni^{II}-N_2S_2 complexes with dithiocarbomates and Ni^{II}-N_3S_2 complex with xanthate. The S,S'chelates occupy cis positions in the N_2S_2 square plane and two arms of the Tp ligand occupy the other two positions. The third arm of the Tp ligand is positioned in a way that would enable it to bind axially with Ni. In complex 3 the third arm of the Tp ligand has moved within bonding distance of the Ni, producing a square-pyramidal geometry. Complex 3 has elongated coordinate bonding compared to 1 and 2 due to high spin paramagnetic Ni^{II} and still Ni-N/S bond lengths are comparable to $NiSOD_{red}$. These three complexes show quasi reversible Ni^{+3}/Ni^{+2} couples at -0.08 V, +0.05 V, and +0.26 V respectively. These potentials lie in a suitable range for superoxide dismutation and it is suggested that they may display enzyme activity under suitable solvent conditions.[80]

It has been found that, the second-sphere H-bonds in NiSOD play a key role in catalysis by facilitating communication between subunits, controlling access to the active site and tuning active

site geometry and electronics.[3] Also, the secondary interactions protect M-SCys bonds and peptide NH-Scys H-bonds from potential oxidation.[81] Harrop and co-workers have synthesized the trimetallic compound $Na_3[\{Ni(nmp)\}_3(S_3BTA^{alk})]$, ($nmp^{2-}$ = deprotonated form of N-(2-mercaptoethyl)-picolinamide; $H_3S_3BTAalk$ = N1,N3,N5-tris(2-mercaptoethyl)benzene-1,3,5-tricarboxamide, where H-dissociable protons) in order to model the H-bonding environment around multiple Ni sites in NiSOD.[81] This complex showed condition-dependent speciation named as 1^A and 1^M and both species were stable in protic solvents compared to their monomeric units; and this indicates prevention of the protonation of the Ni-S-BTA bond due to H-bonding from BTA-carboxamide (Figure 1.5.2.8).[81] The intramolecular NH-S bonding in 1^M stabilize S-based orbitals and, thereby provides thiolate protection against O_2. The Ni-S bond in 1^A form is not involved in H-bonding and therefore thiolate-P(π) orbitals are exposed and susceptible to undergo oxidation. However due to lack of supramolecular structure, 1^M is vulnerable to ligand exchange. Therefore, this study reveals that the steric protection as in 1^A and electronic protection as in 1^M are necessary to protect the thiolates against ROS.

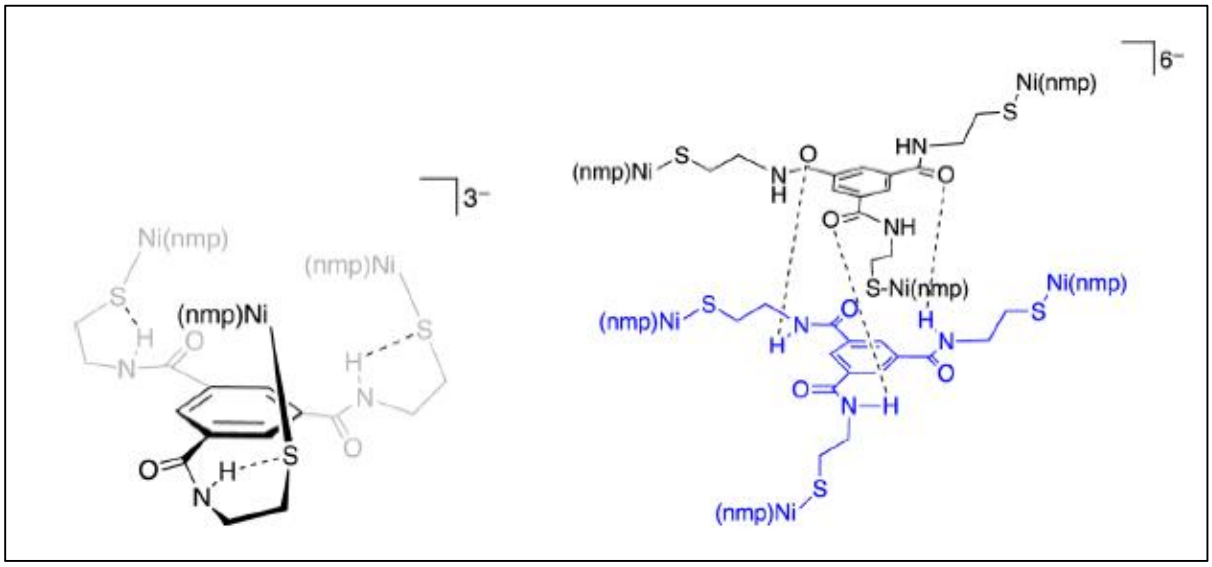

Figure 1.5.2.8. Proposed models 1^M (left) and 1^A (right) as per Harrop and co-workers.

1.6. DTDB (2, 2'-dithiodibenzaldehyde) as a reagent

1.6.1. Formation of metal complexes with mixed imine/thiolate coordination

Our research group has been using DTDB for years as an interesting starting material in order to synthesize metal complexes with mixed N/S coordination. It has been successfully utilized to make Ni(II), Cu(II), Fe(III), In(III) and Co(III) complexes containing NS_2, N_2S, N_3S and N_2S_2 coordination.[82] DTDB is an air stable S-containing compound. Reaction of the appropriate primary amines with DTDB produces imine-containing thiolate ligands via Schiff-base condensation and reductive cleavage of the S-S bond without the need to protect/deprotect the S group. Applications of DTDB in our past research work are summarized in Figure 1.6.1.1 and Figure 1.6.1.2.[82,83,84,85,86]

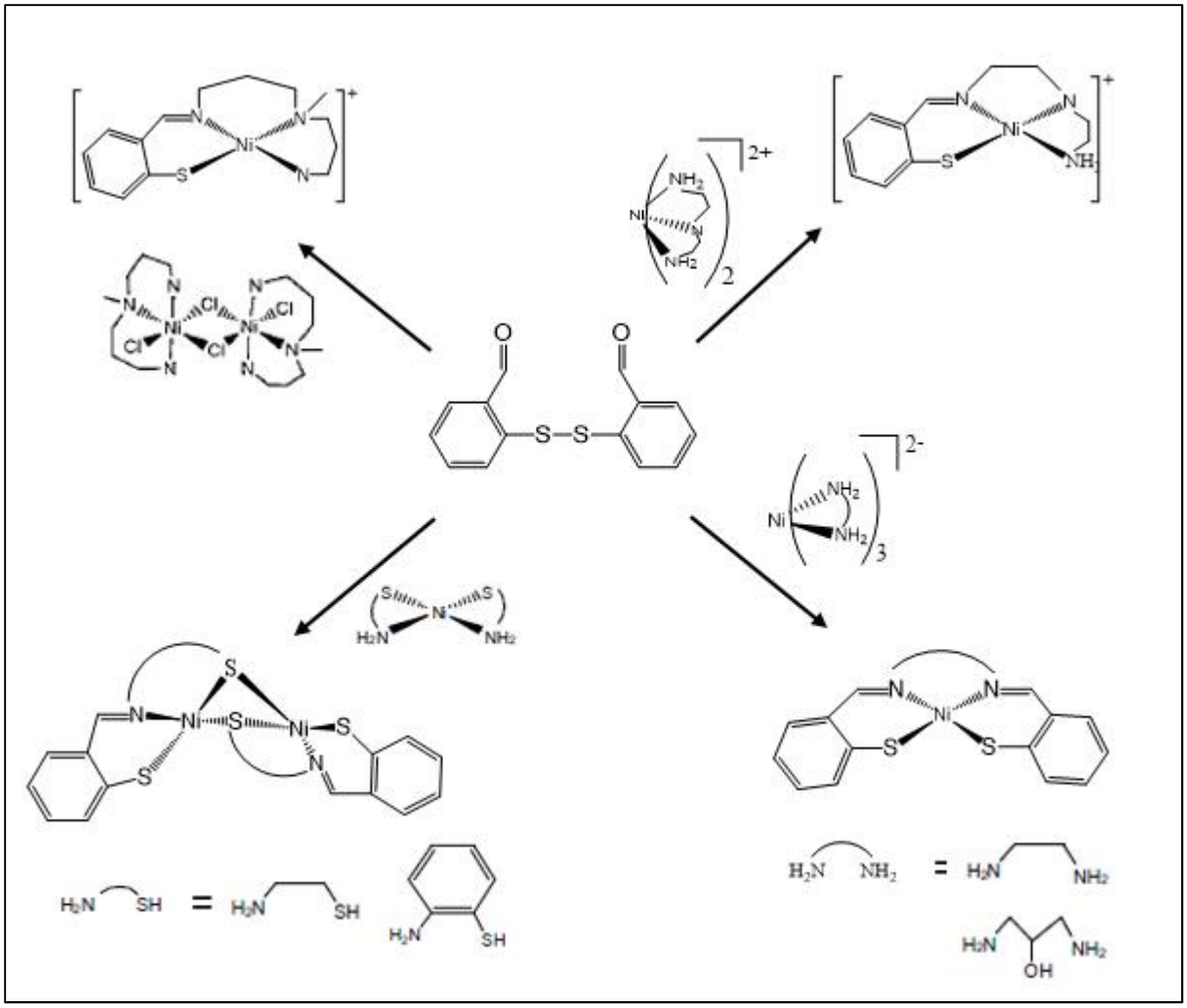

Figure 1.6.1.1. Previous Ni-S/N complexes prepared using DTDB in our research group

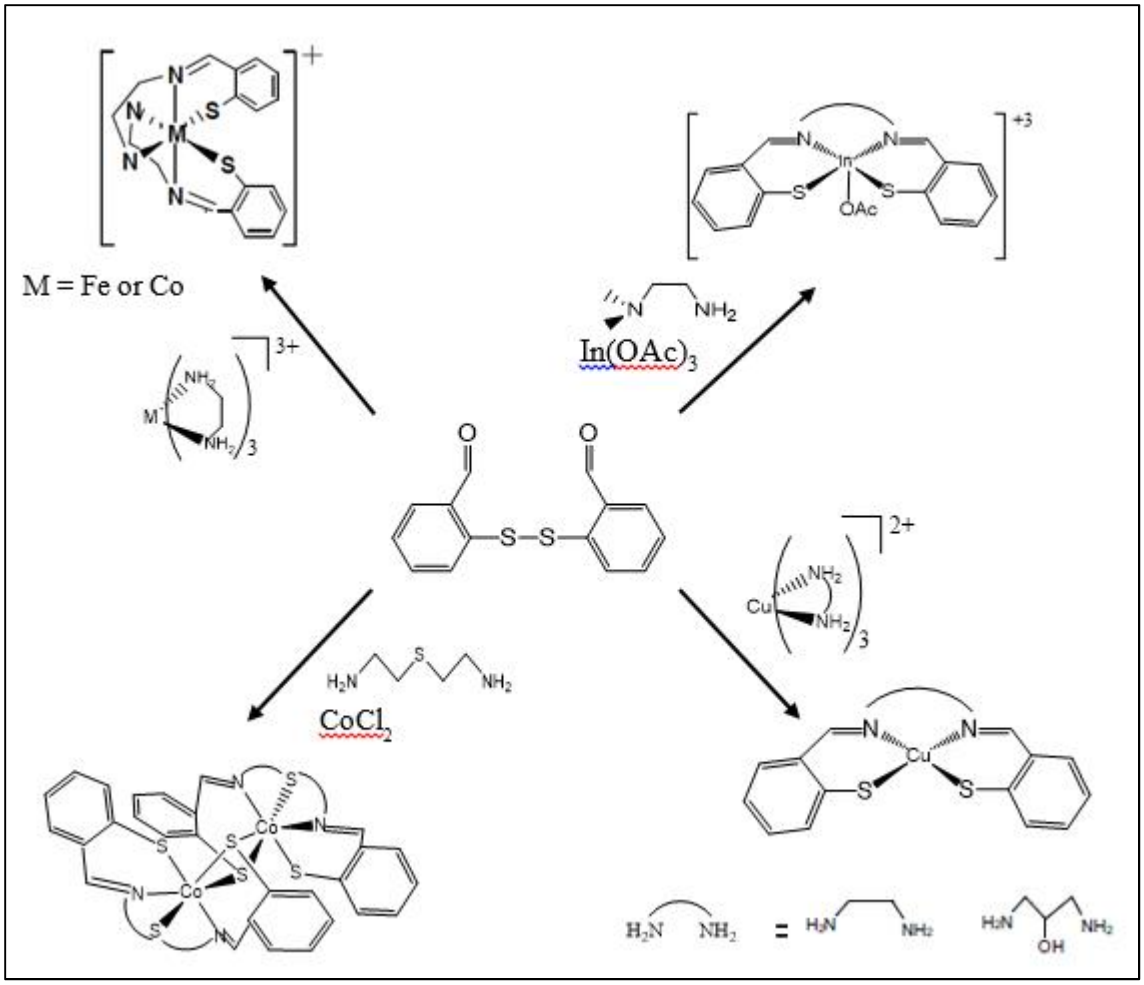

Figure 1.6.1.2. Other metal-N/S complexes prepared using DTDB in our research group

1.6.2. Ni complexes related to NiSOD modeling prepared using DTDB

One type of NiSOD models that our group has been making consists of amine/imine/bisthiolate coordination. The use of DTDB in order to get these models has given successful results. Zimmerman was able to make [Ni($N^{amine}N^{imine}S$)X] monomer where X is an anionic ligand. This complex was successfully used to make desired NiN_2S_2 complexes by replacing X ligand with thiolates. Tom Mwania has continued this work and made three NiSOD model complexes which contain the general formula [Ni(NNS)SR]. The use of DTDB for this work is summarized in Figure 1.6.2.1.

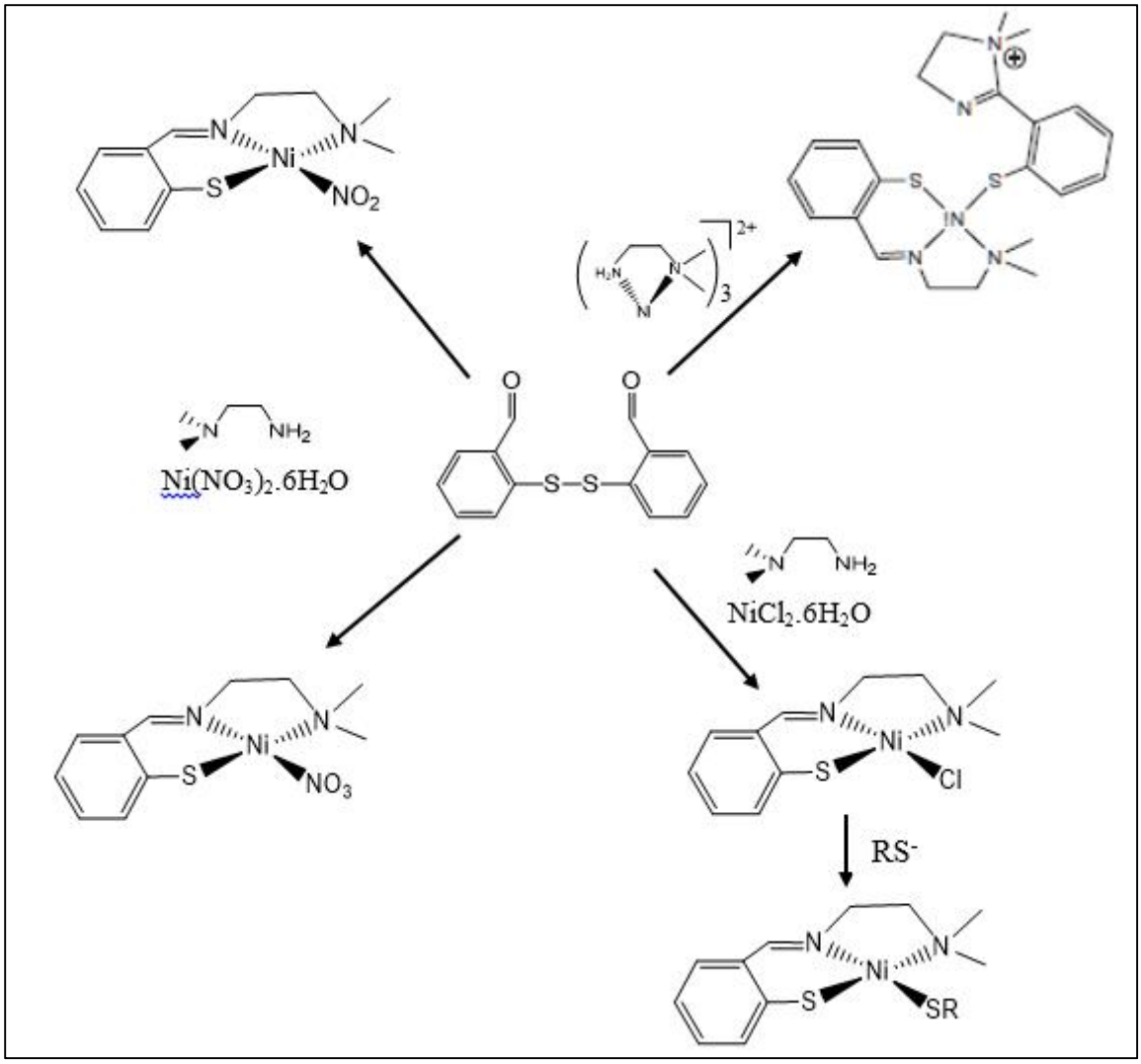

Figure 1.6.2.1. Use of DTDB in preparing previous NiSOD model complexes by our research group[85]

1.7. Goals of the current research

The overall goal of this research is to synthesize and characterize nickel-thiolate complexes which reproduce the coordination sphere of NiSOD as synthetic models of NiSOD. In particularly, the main focus is given to understand the role of one coordination unit, the unusual amide N coordination in NiSOD. This is done by comparing models containing amide N coordination with analogous molecules containing imine N coordination. For this comparison a series of NiN_2S_2

complexes containing amine/amide /bisthiolate coordination and the analogous complexes with amine/imine/bisthiolate coordination are synthesized. All these complexes are structurally characterized using single crystal X-ray crystallography and the electronic properties are studied by electronic spectroscopy and electrochemistry. The effect of the electron-donating nature of the thiolates on the redox properties of the Ni center is also studied by changing the second thiolate coordination site with different thiolate groups. In addition attempts are made to synthesize five coordinated NiN_3S_2 complexes to model the fifth coordination site that NiSOD utilizes in its catalytic mechanism. The ability of all these complexes to perform SOD catalysis is studied using an NBT/formazan assay.

This research allows us to understand the precise role and importance of amide N coordination over the more common imine coordination in metalloenzymes. Based on the properties of the model complexes, necessary modifications can be made to reach an efficient synthetic SOD catalyst.

CHAPTER 2: IMINE COMPLEXES AS MODELS FOR $NiSOD_{red}$

2.1. Introduction

The primary coordination sphere of the $NiSOD_{red}$ active site consists of amine/amide/bisthiolate coordination. Substitution of one moiety around Ni allows us to understand the contribution of one particular feature in the active site towards NiSOD activity. As mentioned is Chapter 1, the NiSOD is one of very few metalloenzymes with amide coordination to the active site metal and that the normal type of N atom to be used in coordinating metals in metalloenzymes is the imidazole N from Histidine. In this chapter we will discuss imine-containing compounds as models for the NiSOD active site if it were to have an imidazole donor, with the imine N serving as a model for an imidazole N. These models will be used as comparisons for the amide-containing molecules to be introduced in chapter 3.

This chapter discusses our efforts to synthesize NiN_2S_2 complexes with amine/imine/bisthiolate coordination as models for $NiSOD_{red}$. Our research group has reported the synthesis of a nickel monomer [Ni($NN^{im}S$)Cl] (Figure 2.1.1, left)[85] by reacting DTDB, dmen and $NiCl_2.6H_2O$ in methanol where $NN^{im}S$ ligand and Cl coordinated to Ni to give a square planar geometry. This chapter reports on expanding the work of Mwania by incrporting a wider range of thiolates in the [Ni(NNimS)SR] framework and exploring their structural and electronic properties. Because of the success achieved by our research group for the synthesis of Schiff-base metal complexes starting from DTDB, to get the desired [Ni($NN^{im}S$)SR] (Figure 2.1.1, right) coordination, [Ni($NN^{im}S$)Cl] was successfully used by substituting Cl with different thiolates.

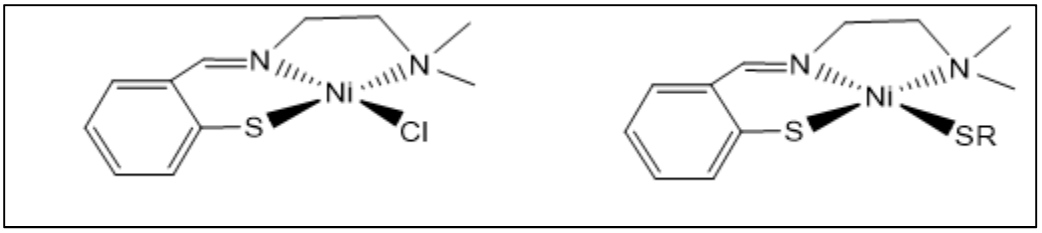

Figure 2.1.1. Structure of [Ni(NN^{im}S)Cl] (left) and the general structure of [Ni(NN^{im}S)SR] (right).

2.2. Nickel Imine Complexes

2.2.1. [Ni(NN^{im}S)SR] Monomers

[Ni(NN^{im}S)Cl] , synthesized as previously described,[85] serves as a precursor to complexes of the formula [Ni(NN^{im}S)SR] and a series of Ni-imine monomer complexes were synthesized. Addition of two molar equivalents of the Na^+ salt of each thiolate to [Ni(NN^{im}S)Cl] in methanol resulted in the isolation of model complexes **1-6** (Figure 2.2.1.1). Each complex has similar N_2S_2 coordination geometry and they enabled us to focus on the effects of the electron donating nature of the thiolates on the properties of $NiSOD_{red}$ models with amine/imine bisthiolate coordination.

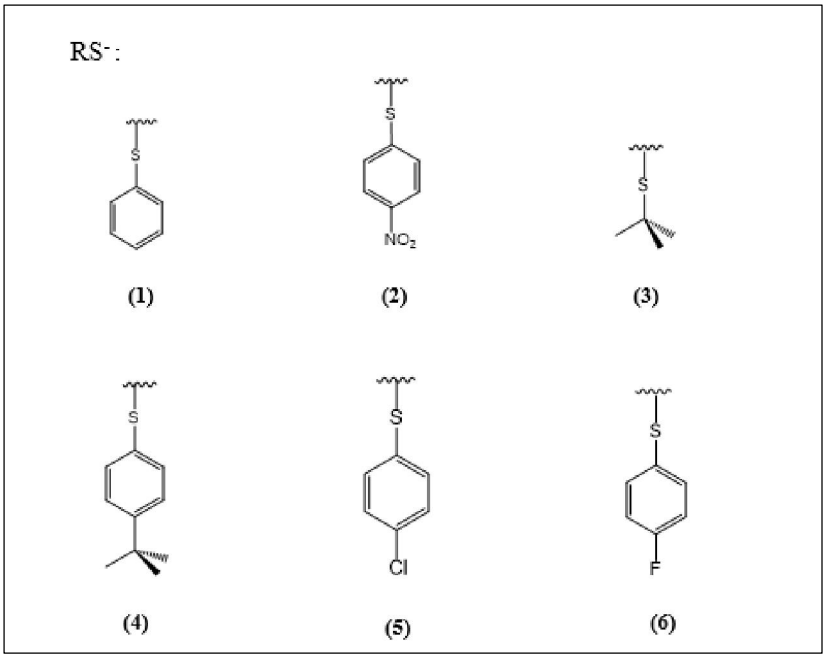

Figure: 2.2.1.1. The RS^- groups used to make different [Ni(NN^{im}S)SR] complexes (**1-6**)

The reaction of [Ni($NN^{im}S$)Cl] with the sodium salt of benzenethiolate in methanol resulted in [Ni($NN^{im}S$)SPh] (**1**). Similar reactions with 4-nitrothiophenolate, *tert*-butyl thiolate, 4-*tert*-butyl benzenethiolate, 4-chlorothiophenolate, 4-fluorothiophenolate in methanol afforded complexes (**2**) - (**6**) respectively. Complexes (**1**)**,** (**2**) and (**3**) were first synthesized by Tom Mwania of our research group; these syntheses were optimized and repeated in order to obtain samples for further studies. X-ray quality crystals of (**1**) were grown by slow evaporation of the compound dissolved in CH_2Cl_2. X-ray quality crystals of (**2**) and (**4**) were formed by vapor diffusion of hexanes into a CH_2Cl_2 solution, (**3**) was crystallized by vapor diffusion of diethyl ether into CH_2Cl_2 under N_2 environment. Crystals of (**5**) and (**6**) were grown by slow evaporation of 1:1 CH_2Cl_2/MeOH solutions under N_2 environment.

2.2.2. Structure & Properties

Complexes **1-6** were structurally characterized by X-ray crystallography (see Figures 2.2.2.1-2.2.2.3 for thermal ellipsoid plots). All six complexes have similar structures with N_2S_2 coordination to Ni. The $NN^{im}S$ ligand provides three coordination sites to Ni and the fourth coordination site is given by the monodentate thiolate (*trans* to the imine N donor). All six complexes crystallize on general positions in their respective space groups. **1** and **5** are essentially isostructural, with similar unit cell dimensions in $P2_1/n$, while **2, 3, 4,** and **6** crystallize in Cc, Iba2, Pbca and P-1 respectively. Selected bond distances and angles are given in Table 2.2.2.1. The coordination spheres do not deviate significantly from square-planar, with dihedral angles between the planes defined by N-Ni-N and S-Ni-S ranging from 1.59° for **1** to 7.97° for **2.** The $NN^{im}S$ ligand is essentially coplanar with the coordination sphere. The thiolate substituents all protrude from the coordination plane, due to the angle about the S atom, with Ni-S-C angles ranging from 103.4° for **4** to 113.0° for **3**. Ni-N_{imine} bond length is somewhat affected by the trans effect of the

thiolate group. Complex **3** which has a stronger aliphatic thiolate has a Ni-N_{imine} bond approximately 0.1 Å longer Ni-N_{imine} bond relative to others which contain aromatic thiolates. Bonds to the amine N atoms are approximately 0.1 Å longer than those to the imine N atoms, while the Ni-S bond to the $NN^{im}S$ ligand thiolate is also consistently on the order of 0.1 Å shorter than that to the monodentate thiolate S. The angle between the NNSS coordination plane and the phenyl ring plane in aromatic thiolates was measured. In complex **2** and **4**, the phenyl ring is closely perpendicular to the coordination plane having angles of 83.23° and 81.37° respectively. The other three complexes show a significant rotation of the phenyl ring with respect to the Ni-S bond with the angles between planes of 73.43°, 73.94°, and 69.39° for **1**, **5**, and **6**, respectively. The only significant difference in the structures can be seen in the five complexes with substituted phenyl thiolates. In two of them (**2** and **4**) the phenyl ring is parallel to the Ni-S bond, as defined by the Ni-S-C-C torsional angles of 3.1° and 7.6° respectively. The other three complexes show torsional angles of 23.0°, 26.5°, and 30.7° for **1**, **5**, and **6** respectively.

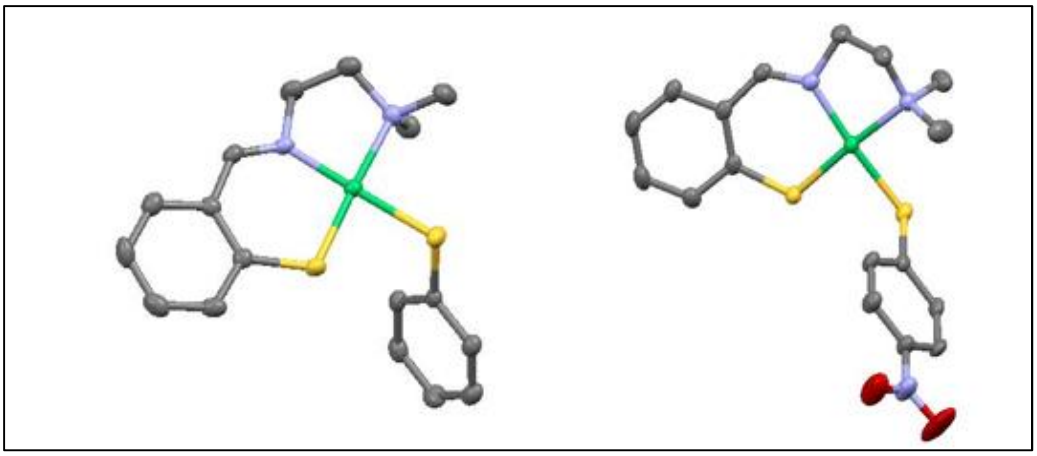

Figure 2.2.2.1. Mercury diagrams of [Ni($NN^{im}S$)SPh](**1**) (left) and [Ni($NN^{im}S$)(4-NO_2PhS)] (**2**) (right) showing 50% thermal ellipsoids for all non-hydrogen atoms.

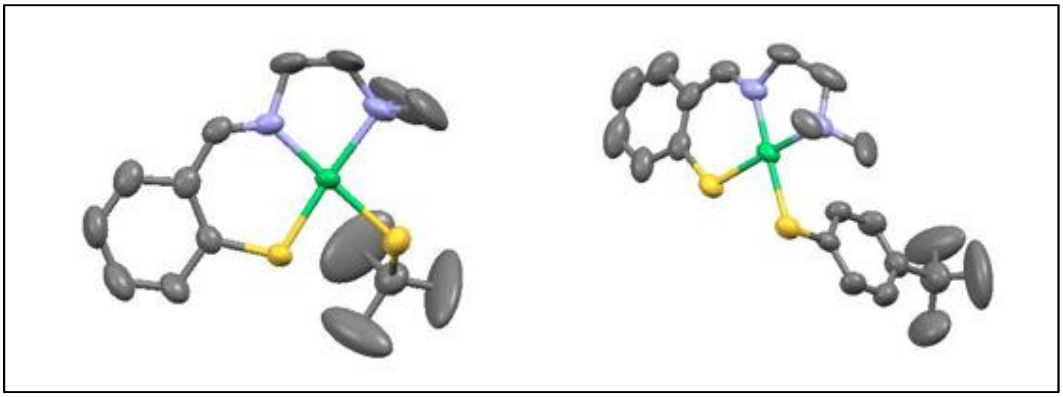

Figure 2.2.2.2. Mercury diagrams of [Ni(NN^{im}S)S^{t}Bu](**3**) (left) and [Ni(NN^{im}S)(4-^{t}BuPhS)] (**4**) (right) showing 50% thermal ellipsoids for all non-hydrogen atoms.

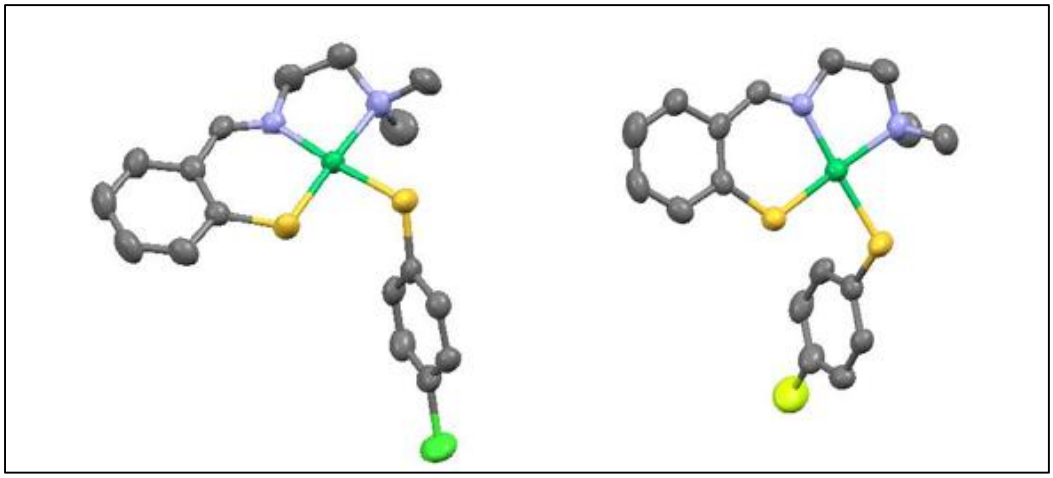

Figure 2.2.2.3. Mercury diagrams of [Ni(NN^{im}S)(4-ClPhS)](**5**) (left) and [Ni(NN^{im}S)(4-FPhS)] (**6**) (right) showing 50% thermal ellipsoids for all non-hydrogen atoms.

Table 2.2.2.1. Selected Bond Distances (Å) and Angles (deg) for complexes (**1-6**).

	1	**2**	**3**	**4**	**5**	**6**
Ni-N(amine)	2.015(3)	1.989(2)	2.022(6)	1.924(3)	2.014(3)	2.019(5)
Ni-N(imine)	1.884(3)	1.889(2)	1.910(6)	1.808(3)	1.888(2)	1.891(5)
Ni-S(NNS)	2.141(9)	2.132(7)	2.119(19)	2.044(10)	2.139(9)	2.141(19)
Ni-S(RS)	2.219(10)	2.220(7)	2.219(2)	2.144(10)	2.209(9)	2.219(19)
Coord'n plane dihedral	1.59	7.97	4.74	5.54	4.67	2.09
Ni-S(RS)-C	108.36(11)	110.53(9)	113.0(3)	103.4(2)	111.76(10)	110.7(2)
NNSS/ Ph(SR) angle	73.43	83.23	N/A	81.37	73.94	69.39

Table 2.2.2.2. Electronic absorption spectral properties of complexes **1**-**6** in CH_3CN at 298 K

Complex	λ_{max} (nm)	ε ($M^{-1}cm^{-1}$)
1	255, 304,424	1007,647,74
2	253, 295, 423	1265, 665, 667
3	253, 300, 456	879,376,65
4	256, 304,405	1165, 745, 102
5	255, 304, 410	2428, 1848, 247
6	256, 304, 403	3574, 2150, 415

Table 2.2.2.3. Oxidation potentials (mV) of complexes **1**-**6** in CH_3CN at 298 K (Reported vs Ag/AgCl)

Complex	**Potential 1**	**Potential 2**	**Potential 3**
1	535	906	1253
2	715	983	1289
3	485	931	1338
4	528	1030	1385
5	512	820	1188
6	492	874	1301

The $\nu_{C=N}$ band in the IR spectra of complex **1**-**6** has shifted from 1602 cm^{-1} in [Ni($NN^{im}S$)Cl] to higher energy by about 4-14 cm^{-1}. These complexes are soluble in polar aprotic solvents such as MeCN and, DMF and in non-polar solvents like CH_2Cl_2. As shown in Table 2.2.2.2 UV-Vis absorption spectra of all six complexes in MeCN show strong absorption bands in the region of 250-305 nm assigned to RS^- to Ni^{+2} LMCT transitions compared to similar NiN_2S_2 complexes.[87,76] Low intensity bands in the visible region arise due to ligand field d-d-transitions with a minor charge transfer contribution. These absorption bands are not very sensitive to the type of exogenously added thiolate. In the mass spectrometry, all six complexes show a common peak at

m/z 265 which corresponds to the $[Ni(NN^{im}S)]^+$ moiety; the parent ion is not seen. The cyclic voltammetry measurements of **1-6** in CH_3CN revealed irreversible oxidation peaks. This indicates either the instability of Ni^{+3} species or S based oxidation. As given in Table 2.2.2.3 each complex shows three oxidation events. The first peak of each complex occurs in between 450 and 750 mV and indicates the dependence of oxidation potential on electron donating nature of the S_{exo} ligand, and this first redox event could be associated with the metal based oxidation. The higher the electron donating nature of S_{exo} ligand, the easier it is to oxidize the metal center and thereby the more positive redox potential. This correlation has been reported in similar NiN_2S_2 complexes as well.[88]

2.3. Conclusions

$[Ni(NN^{im}S)Cl]$ was synthesized as per previous research[85] starting from DTDB. This work again shows the successful use of DTDB to make metal-imine complexes as reported in previous research of our group.[83,89,85] By substituting Cl in $[Ni(NN^{im}S)Cl]$ with different thiolates we have been able to isolate complexes **1-6** having NiN_2S_2 coordination. All six complexes are structurally very similar and they have square planar amine/imine/bisthiolate coordination to Ni, rendering them reasonable models for the $NiSOD_{red}$ active site with the amide N atom replaced by a histidine imidazole donor. Crystals of all six complexes are dark red-black in color and they have similar solubility properties and UV-Vis absorption properties by comparison to similar complexes reported.[85] Cyclic voltammetry measurements reveal the dependence of redox potentials on the electron donating nature of the S_{exo} ligand.

2.4. Experimental

2.4.1. General Experimental

All reagents were purchased from commercial suppliers (Acros, Aldrich, Fisher Scientific, and TCI) and used as received unless otherwise noted. 2,2'-dithiodibenzaldehyde (DTDB) and [Ni(NN^{im}S)Cl] were synthesized by literature methods.[90] Acetonitrile (MeCN), dimethylformamide (DMF), methanol (MeOH), methylene chloride (CH_2Cl_2), tetrahydrofuran (THF), diethyl ether (Et_2O) were purified using Securall pure-solv solvent purification system. All reactions were performed under an inert atmosphere of N_2 using standard Schlenk line techniques or in a Nexus One dry box. UV-Vis data was collected on a Shimadzu UV-1650 PC UV-Vis spectrophotometer and FTIR spectra were collected on a Thermo Nicolet Avatar 360 spectrophotometer running the OMNIC software, either as a KBr disk (where noted) or as neat powders with an ATR attachment. Low resolution ESI-MS data were collected using a Varian 1200L quadrupole mass spectrometer and high resolution ESI-MS data were collected using an Agilent 6230 ToF. NMR spectra were recorded in the listed deuterated solvent on a 400MHz Varian Inova NMR spectrometer. Elemental analyses were obtained from M-H-W Laboratories of Phoenix, AZ and Columbia Analytical services, Tucson, AZ.

2.4.2. Crystallographic Experimental

The crystals were affixed to a nylon cryoloop using oil (Paraton-n,Exxon) and mounted in the cold stream of a Bruker Kappa-Apex-II area-detector diffractometer. The temperature at the crystal was maintained at 150 K using a Cryostream 700EX cooler (Oxford Cryosystems). Initial unit cels were determined from the setting angles of 36 frames of data; final unit cells were determined from the setting angles of subset of the final dataset. Data were measured using a CCD detector at a distance of 50 mm from the crystal with a combination of phi and omega scans. A scan width of

0.5 degrees and scan time of 10, 15, or 30 seconds were employed along with graphite mono-chromated molybdenum Kα radiation (λ=0.71073 Å) that was collimated to a 0.6 mm diameter. Data collection, reduction, structure solution and refinement were performed using the Bruker Apex 2 suite (v2013.4-1).[91] All available reflections to $2\theta_{max}$ = 52 were harvested and corrected for Lorentz and polarization factors with Bruker SAINT (v6.45).[92] Reflections were then corrected for absorption, interframe scaling and other systematic errors with SADABS 2012/1. The structures were solved using SHELXT[93] (direct methods) and refined (full matrix least squares against F^2) with Bruker SHELXL (v6.14-1) within the Olex2[94] package. All non-hydrogen atoms were refined using anisotropic thermal parameters. All hydrogen atoms were included at idealized positions; hydrogen atoms were not refined. Cyclic voltammetry was performed on a Princeton Applied Research potentiostat model 263A at room temperature and the potentials reported vs Ag/AgCl.

2.4.3. Synthesis of [Ni(NN^{im}S)SPh] (1)

Under nitrogen, a solution of sodium thiophenolate (0.020 g, 0.15 mmol) in 10 mL of methanol was added dropwise to a solution of [Ni(NN^{im}S)Cl] (0.045 g, 0.15 mmol) in 10 mL of methanol. After stirring for 24 h the solution was filtered, leaving a black-red precipitate which was washed with methanol and diethyl ether and dried to yield **1** as a dark black-red powder (0.034g, 0.09 mmol, 61%). X-ray quality crystals were grown by slow evaporation of CH_2Cl_2 solution. Elemental Anal. Calc. for $C_{17}H_{20}N_2S_2Ni$: C, 54.44; H, 5.37; N, 7.47. Found: C, 53.81; H, 5.81; N, 7.44 IR (cm^{-1}) 3046, 2920, 2850, 1609, 1588, 1570, 1529, 1459, 1403, 1219, 1024, 947, 733. ^{1}H NMR (400 MHz, CD_3CN, δ): 8.25 (S, 1H, NH), 7.98-6.91 (m, 9H, Ar-H), 3.79 (t, 2H, NCH_2), 2.61 (S, 6H, N(CH_3)$_2$), 2.48 (t, 2H, N(CH_3)$_2$CH_2). ESI-MS (positive mode, methanol, m/z): 397 [Ni(NN^{im}S)SPh + Na]$^+$, 265 [Ni(NN^{im}S)]$^+$. UV-Vis (acetonitrile); λ_{max} = 255, 304,424 nm.

2.4.4. Synthesis of [Ni(NN^{im}S)(4-NO$_2$PhS], (2)

Under nitrogen, NaOH (0.0070 g, 0.17 mmol) was added to a solution of 4-nitrothiophenol (0.026 g, 0.17 mmol) in 10 mL methanol. After stirring for 5 min, the resulting orange Na(4-NO$_2$PhS) solution was added to a solution of [Ni(NN^{im}S)Cl] (0.050 g, 0.17 mmol) in 10 mL of methanol. While stirring for 24 h, a red precipitate separated which was isolated by filtration, washed with methanol and diethyl ether, and dried to give **2** as a red powder (0.058 g, 0.14 mmol, 84%). X-ray quality crystals were formed by vapor diffusion of hexanes into a CH_2Cl_2 solution. Elemental Anal. Calc. for $C_{17}H_{19}N_3S_2O_2Ni$: C, 48.56; H, 4.56; N, 10.0. Found: C, 48.74; H, 5.18; N, 10.18. IR (KBr pellet, cm^{-1}): 3096, 2545, 2175, 2111, 1922, 1574, 1497, 1476, 1329, 1179, 1115, 1089, 960, 928, 834, 738. ^{1}H NMR (400 MHz, CD_3COCD_3, δ): 8.44 (S, 1H, NH), 8.32-6.99 (m, 8H, Ar-H), 4.02 (t, 2H, NC*H*$_2$), 2.81 (S, 6H, N(C*H*$_3$)$_2$), 2.67 (t, 2H, N(CH$_3$)$_2$C*H*$_2$). ESI-MS (positive mode, methanol, m/z): 684 [(Ni(NN^{im}S))$_2$NO$_2$PhS]$^+$, 265 [Ni(NN^{im}S)]$^+$. UV-Vis (acetonitrile); λ_{max} = 253, 295, 423 nm.

2.4.5. Synthesis of [Ni(NN^{im}S)(S^{t}Bu)], (3)

Under nitrogen, a solution of sodium 2-methyl-2-propanethiolate (0.018 g, 0.16 mmol) in 10 mL methanol was added dropwise to a solution of [Ni(NN^{im}S)Cl] (0.045 g, 0.15 mmol) in 10 mL of methanol. After stirring for 24 h, the resulting black solution was filtered and the solvent removed under reduced pressure to give a black solid. Extraction with CH_2Cl_2, filtration and removal of the solvent under reduced pressure gave **3** as a black powder (0.020 g, 0.0060 mmol, 38%). X-ray quality crystals were formed by vapor diffusion of diethyl ether into a CH_2Cl_2 solution under a nitrogen environment. Elemental Anal. Calc. for $C_{15}H_{24}N_2S_2Ni$: C, 50.72; H, 6.81; N, 7.89. Found: C, 49.40; H, 6.70; N, 7.46. IR (KBr pellet, cm^{-1}): 2960, 2922, 1602, 1588, 1530, 1512, 1456, 1362, 1218, 1158, 1069, 1007, 869, 784, 749, 720, 702. ^{1}H NMR (400 MHz, CD_3CN, δ): 8.23 (S, 1H,

NH), 7.94-6.94 (m, 4H, Ar-H), 3.70 (t, 2H, NCH_2), 2.63 (S, 6H, N(CH_3)$_2$), 2.40 (t, 2H, N(CH$_3$)$_2$CH_2), 1.53 (S, 9H, S(CH$_3$)$_3$). ESI-MS (positive mode, methanol, m/z): 355 [Ni(NN^{im}S)S^{t}Bu+H]$^+$, 265 [Ni(NN^{im}S)]$^+$, 619 [(Ni(NN^{im}S))$_2$S^{t}Bu]$^+$. UV-Vis (acetonitrile); λ_{max} = 253, 300, 456 nm.

2.4.6. Synthesis of [Ni(NN^{im}S)(4-^{t}BuPhS)], (4)

Under nitrogen, NaOH (0.027 g, 0.67 mmol) was added to a solution of 4-*tert*-butylphenylthiol (0.11 g, 0.66 mmol) in 10 mL of methanol. After stirring for 5 min, the resulting Na(4-^{t}BuPhS) solution was added dropwise to a solution of [Ni(NN^{im}S)Cl] (0.20 g, 0.66 mmol). After stirring for 24 h the resulting dark red solution was filtered, yielding a black-red precipitate which was washed with diethyl ether and dried to give **4** as a dark black-red powder (0.22 g, 0.51 mmol, 77%). X-ray quality crystals were formed by slow evaporation of a 1:1 CH_2Cl_2/methanol solution under nitrogen environment. Elemental Anal. Calc. for $C_{21}H_{28}N_2S_2Ni$: C, 58.48; H, 6.54; N, 6.50. Found: C, 58.25; H, 6.76; N, 6.45. IR (cm^{-1}): 3075, 3040, 2949, 2896, 1606, 1588, 1532, 1477, 1458, 1431, 1405, 1266, 1244, 1118, 1024, 949, 817,744. ^{1}H NMR (400 MHz, CD_3CN, δ): 8.25 (S, 1H, NH), 7.89-6.94 (m, 8H, Ar-H), 3.79 (t, 2H, NCH_2), 2.66 (S, 6H, N(CH_3)$_2$), 2.49 (t, 2H, N(CH$_3$)$_2$CH_2), (S, 9H, Ph(CH_3)$_3$). ESI-MS (positive mode, CH_2Cl_2, m/z): 265 [Ni(NN^{im}S)]$^+$, 531 [Ni(NN^{im}S)$_2$+H]$^+$. UV-Vis (acetonitrile); λ_{max} = 256, 304, 405 nm.

2.4.7. Synthesis of [Ni(NN^{im}S)(4-ClPhS)], (5)

Under nitrogen, NaOH (0.044 g, 1.1mmol) was added to a solution of 4-chlorothiophenol (0.16 g, 1.1 mmol) in 15 mL of methanol. After stirring for 5 min, the resulting Na(4-ClPhS) solution was added dropwise to a solution of [Ni(NN^{im}S)Cl] (0.34 g, 1.1 mmol) in 15 mL of methanol. After stirring for 24 h the solution was filtered to give a black-red precipitate which was extracted into

CH_2Cl_2. The solution was filtered, washed with diethyl ether and dried to give **5** as a dark red powder (0.41g, 1.0 mmol, 89%). X-ray quality crystals were formed by slow evaporation of a 1:1 CH_2Cl_2/methanol solution under a nitrogen environment. Elemental Anal. Calc. for $C_{17}H_{19}N_2S_2ClNi$: C, 49.83; H, 4.69; N, 6.84. Found: C, 50.0; H, 4.80; N, 6.75. IR (cm^{-1}): 3065, 3047, 2985, 2918, 1611, 1589, 1532, 1220, 1087, 1009, 949, 813, 751. ^{1}H NMR (400 MHz, CD_3COCD_3, δ): 8.39 (S, 1H, NH), 7.97-6.92 (m, 8H, Ar-H), 3.95 (t, 2H, NCH_2), 2.71 (S, 6H, N(CH_3)$_2$), 2.60 (t, 2H, N(CH$_3$)$_2$CH_2). ESI-MS (positive mode, CH_2Cl_2, m/z): 409 [Ni(NN^{im}S)(4-ClPhS)+H]$^+$, 431 [Ni(NN^{im}S)(4-ClPhS)+Na]$^+$, UV-Vis (acetonitrile); λ_{max} = 255, 304, 410 nm.

2.4.8. Synthesis of [Ni(NN^{im}S)(4-FPhS)], (6)

Under nitrogen, sodium hydroxide NaOH (0.004 g, 0.1 mmol) was added to a solution of 4-fluorothiophenol (0.013 g, 0.10 mmol) in 10 mL of methanol. After stirring for 5 min, the resulting Na(4-FPhS) solution was added dropwise to a solution of [Ni(NN^{im}S)Cl] (0.03 g.0.1 mmol) in 10 mL of methanol. After stirring for 24 h, a dark red precipitate was isolated, washed with methanol and diethyl ether, and dried to give **6** as a dark red powder (0.037 g, 0.094 mmol, 94%). X-ray quality crystals were formed by slow evaporation of a 1:1 CH_2Cl_2/methanol solution under a nitrogen environment. Elemental Anal. Calc. for $C_{17}H_{19}N_2S_2FNi\cdot H_2O$: C, 50.27; H, 5.19; N, 6.77. Found: C, 49.66; H, 5.15; N, 6.81. IR (cm^{-1}): 3065, 2920, 1616, 1588, 1476, 1203, 1081, 1027, 903, 783, 752. ^{1}H NMR (400 MHz, CD_3CN, δ): 8.23 (S, 1H, NH), 7.88-6.78 (m, 8H, Ar-H), 3.78 (t, 2H, NCH_2), 2.65 (S, 6H, N(CH_3)$_2$), 2.50 (t, 2H, N(CH$_3$)$_2$CH_2). ESI-MS (positive mode, CH_2Cl_2, m/z): 659 [{Ni(NN^{im}S)}$_2$(4-FPhS)]$^+$, 265 [Ni(NN^{im}S)]$^+$. UV-Vis (acetonitrile); λ_{max} = 256, 304, 403 nm.

CHAPTER 3: AMIDE COMPLEXES AS MODELS OF $NiSOD_{RED}$

3.1. Introduction

The unique coordination environment of the NiSOD active site provides motivation to study the contribution of each donor towards the optimal catalytic activity of the enzyme. The active site consists of amine/amide bisthiolate coordination to Ni and the presence of both amine and amide N donation to the metal is uncommon in metalloenzymes. It is clear that each component plays a vital role towards the activity by tuning the Ni center and this work gives attention to the contribution of one particular component. We have focused on understanding the role of the carboxamido N by comparing it with imine N. The NiSOD models described in Chapter 2 contain imine N coordination, which is a reasonable electronic model for the histidine imidazole usually found as the N donor to the active sites of metalloenzymes. This chapter will discuss our efforts to synthesize the analogous amide N coordinated complexes as models for $NiSOD_{red.}$ Comparison of these two types of structures allow us to understand specifically, the role of the unusual carboxamido N donor in NiSOD.

3.2. Nickel-amide complexes

By analogy with the synthesis of imine-containing ligands using DTDB, replacement of the aldehydes in DTDB with acid chlorides would be expected to yield amide-containing ligands. We were aiming to synthesize two types of amide containing models, (Figure 3.2.1) by reacting DTSACl with dmen and with dmap respectively. The only difference between the two models is that the first one has an ethyl bridge between two nitrogens, and forms a five-membered metallocycle after coordinating to Ni, as opposed to a propyl bridge in the second one which forms a 6 membered metallocycle. The two types of ligands are referred to as $NN^{am}S$ and $NN^{am}S$' hereafter.

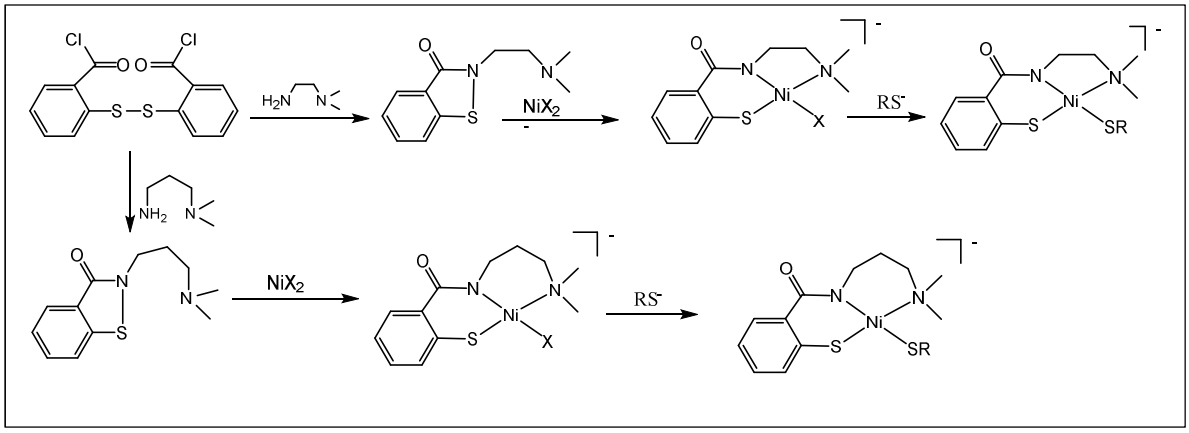

Figure 3.2.1. Synthesis of $[Ni(NN^{am}S)SR]^-$ (top) and $[Ni(NN^{am}S')SR]^-$ (bottom) complexes.

3.2.1. DTSACl

To get the desired amide N instead of imine N, a reaction between acid chloride and amine was used. The acid chloride of 2,2'-dithiodisalicylic acid (DTSA) was easily synthesized by reacting DTSA with thionyl chloride using the methodology in previous research.[95] The previous research reported the synthesis in CH_2Cl_2, whereas we performed it in CH_3CN since isolation of the product is easy as it is not soluble in CH_3CN. The reaction mixture was refluxed for 3h and then allowed to cool, upon which DTSACl is separated as a light brown powder. IR and NMR spectra confirm the formation of the product. As showed in Figure 3.2.1, DTSACl was used to make both $NN^{am}S$ and $NN^{am}S$' ligands successfully.

3.2.2. $NN^{am}S$ Ligand (7)

The $NN^{am}S$ ligand acts as a very important intermediate to get the $NiSOD_{red}$ models by providing three coordination sites including amide N. DTSACl was reacted with dmen in the presence of excess triethylamine (TEA). After refluxing 3h and removing the solvent, a yellow frothy product was isolated which was identified as $NN^{am}S$ [Figure 3.2.1]. ESI/MS in CH_2Cl_2 solution shows the product with a peak at 223 m/z which corresponds to $[NN^{am}S+H]^+$. We were able to isolate crystals

of $NN^{am}S$ as a monomer as well as a dimer. Treatment with $AgPF_6$ gave rise to crystals of the monomer as the HPF_6 salt (Figure 3.2.2.1) (**7**) by vapor diffusion of diethyl ether into a CH_2Cl_2 solution, while slow evaporation of the CH_2Cl_2 solution resulted in crystals of the dimer $(NN^{am}S)_2$ as the bis(HCl) salt (Figure 3.2.2.2) (**8**). X-ray crystallography confirmed the structures and selected bond distances and angles are listed in Table 3.2.2.1.

The $NN^{am}S$ (**7**) crystallizes with two molecules in the asymmetric unit in the monoclinic space group $P2_1/n$. The two independent molecules interact through a hydrogen bond connecting the protonated tertiary amine of one molecule with the carbonyl O atom of the other molecule. In addition, π-stacking is observed between the two molecules. The resulting dimer then interacts in a similar fashion with neighboring dimers, forming stacks of molecules running parallel to the crystallographic *a*-axis. **8** crystallizes on a two-fold axis with two molecules of CH_2Cl_2 in the monoclinic space group C2/c. The Cl^- ions engage in hydrogen bonds with the protonated tertiary amines. The two halves of **8** are approximately perpendicular to each other, with a dihedral angle between the planes of the phenyl rings of 74.69. As a result, the amide O atoms and disulfide S atoms are all approximately in a straight line.

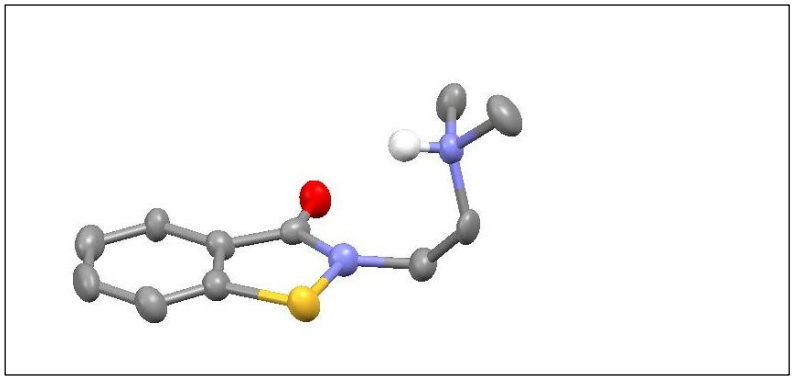

Figure 3.2.2.1. Mercury diagram of $NN^{am}S$ (**7**) showing 50% thermal ellipsoids for all non-hydrogen atoms.

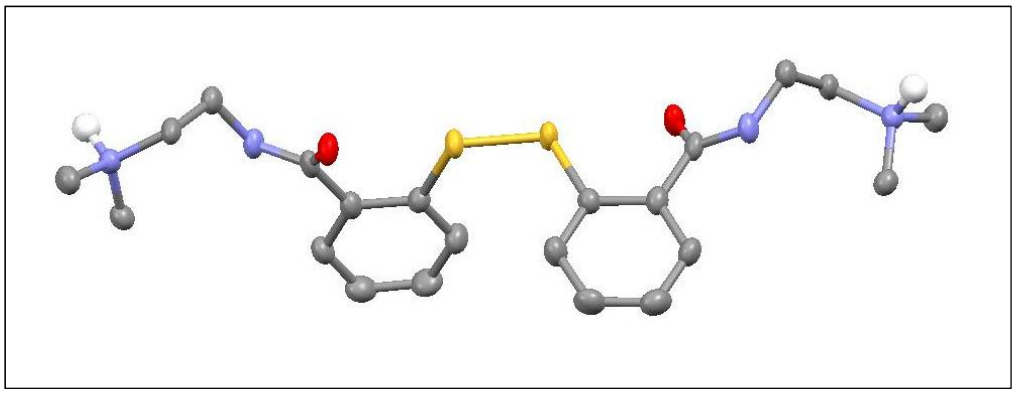

Figure 3.2.2.2. Mercury diagram of $(NN^{am}S)_2$ (**8**) showing 50% thermal ellipsoids for all non-hydrogen atoms

Table 3.2.2.1. Selected Bond Distances (Å) and Angles (°) of complexes **7** and **8.**

7			**8**	
C-O	1.233(10)	1.225(10)	C-O	1.242(7)
C-S	1.745(8)	1.747(9)	C-S	1.790(5)
N-S	1.712(7)	1.716(8)	S-S	2.028(2)
N …O	2.752(10)		N…Cl	3.075(5)
O…N		2.808(10)	N-C(O)	1.340(9)
C-S-N	90.8(4)	90.9(4)	N-C(O)-C	115.9(5)
C(O)-N-S	115.7(5)	115.0(6)	Ph/Ph dihedral	74.69
N-C(O)-C	108.8(7)	109.1(7)		

3.2.3. $(Et_4N)[Ni(NN^{am}S)Cl]$ (9) and $(Et_4N)[Ni(NN^{am}S)OAc]$ (10)

$NN^{am}S$ was reacted with Ni salts in order to get amide N coordinated $[Ni(NN^{am}S)X]$ complexes. Addition of 1 mol equiv of either $NiCl_2{\cdot}6H_2O$ or $Ni(OAc)_2{\cdot}4H_2O$ with Et_4NCl in to $NN^{am}S$ in DMF and refluxing overnight under N_2 afforded $[Ni(NNamS)Cl]^-$ (**9**) and $[Ni(NN^{am}S)OAc]^-$ (**10**) (Figure 3.2.3.1). Products **9** and **10** are monoanionic complexes and both of them were synthesized as salts of Et_4N^+.Their formation was confirmed by mass spectrometry which shows their parent peaks. Both of them are readily soluble in polar protic solvents and our attempts at crystallization

were not successful. The same synthetic procedure was followed with $Ni(NO_3)_2.6H_2O$ and no evidences was observed for the formation of the analogous $[Ni(NN^{am}S)NO_3]^-$.

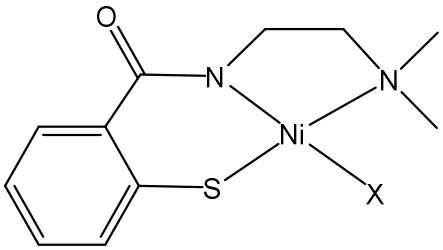

(**9**) X = Cl

(**10**) X = $OC(O)CH_3$

Figure 3.2.3.1. Structure of $[Ni(NN^{am}S)X]^-$

In further attempts at crystallization, complexes **9** and **10** were synthesized incorporating different polyatomic cations Me_4N^+, Et_4N^+, Bu_4N^+, TPP^+, PPN^+ and Ph_4As^+ as well as with monoatomic cations Na^+ and K^+. But none of them gave the desired crystals. Instead a very interesting byproduct was crystallized (Figure 3.2.3.2) (**11**) having the formula $[\{Ni(H_2NN^{am}S)_2(OMe)_2\}_2(NiCl_2)]$. In complex **11**, four protonated $NN^{am}S$ ligands have coordinated to three Ni atoms via S to give a trinuclear species. Each Ni has octahedral coordination geometry and they are coplanar. Each peripheral Ni atom is coordinated by the thiolate S and amide O atoms of two $H_2NN^{am}S$ ligands and complete their octahedral by coordinating to two OMe groups. Each S atom bridges to the central Ni atom, whose octahedral coordination is completed by two axial Cl atoms. The Cl atoms show intramolecular hydrogen-bonding interactions with the protonated amine nitrogens.

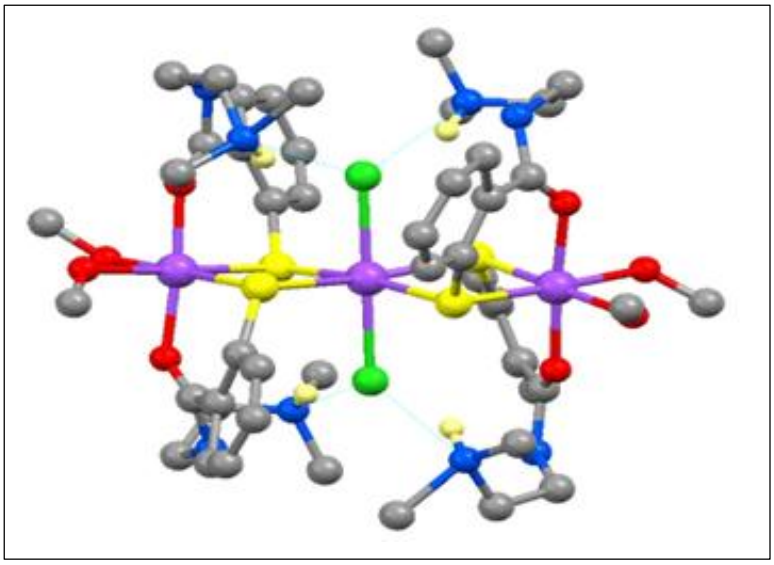

Figure 3.2.3.2. Crystal structure of [{Ni($H_2NN^{am}S$)$_2$(OMe)$_2$}$_2$($NiCl_2$)] (**11**)

3.2.4. [Ni_3(NNS)$_2$(SR)$_2$] Trimers

Our goal was to synthesize a series of [Ni($NN^{am}S$)SR] monomeric complexes analogous to [Ni($NN^{im}S$)SR] complexes as reported in chapter 2, using the same methodology used to make [Ni($NN^{im}S$)SR] complexes. [Ni($NN^{am}S$)Cl]$^-$ and [Ni($NN^{am}S$)OAc]$^-$ complexes were reacted with the thiolates which were used to get Ni-imine complexes. All these reactions were performed in glove box. While the reactions with the imine-containing ligands in Chapter 2 easily produced the desired monomeric species, the only species initially isolated from analogous reactions with $NN^{am}S$ were trimeric. Addition of 2 molar equivalents of the sodium salts of t-butylthiolate and 4-fluorothiophenolate to [Ni($NN^{am}S$)Cl] in MeOH and in DMF respectively afforded trimeric species **12** and **13** of the form [{Ni($NN^{am}S$)(SR)}$_2$Ni] as shown in figure 3.2.4.1.

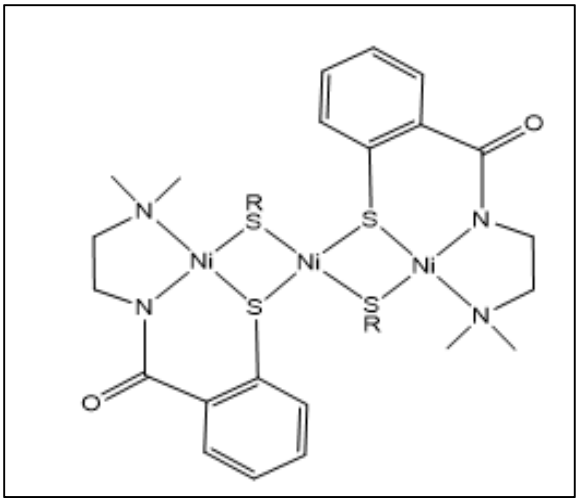

Figure 3.2.4.1. General structure of trinuclear species **12-14**.

X ray quality crystals of $[Ni_3(NN^{am}S)_2(^tBuS)_2]$ (**12**) and $[Ni_3(NN^{am}S)_2(4\text{-}FPhS)_2]$ (**13**) were grown by vapor diffusion of hexane into CH_2Cl_2 solution and slow evaporation of MeOH solution in N_2 environment respectively. The thermal ellipsoid drawings of **12** and **13** are shown in Figure 3.2.4.2 and 3.2.4.3. From the reaction between the sodium salt of benzenethiolate and (**10**) in MeOH, a black-red precipitate was formed leaving a red-green filtrate. The trimeric species $[Ni_3(NN^{am}S)_2(PhS)_2]$ (**14**), which is similar to Figure 3.2.4.1 formula was crystallized by slow evaporation of a MeOH solution of the red-green solid which was isolated by evaporating the filtrate at RT in N_2 environment. Figure 3.2.4.4 shows the thermal ellipsoid drawing of **14.** Attempts of cleaving the trimers to get the monomers by reacting with excess $NN^{am}S$ ligand were not successful.

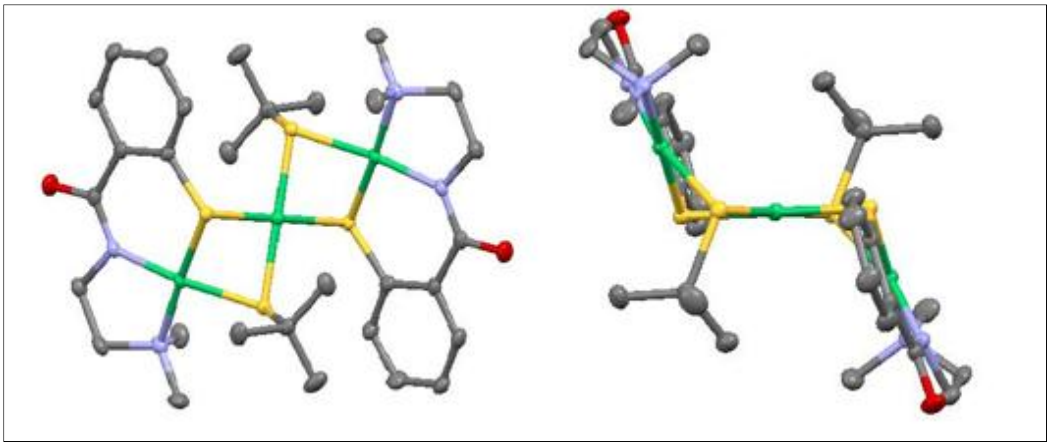

Figure 3.2.4.2. Mercury diagram of the trinuclear complex **12** (left) and its side view (right) showing 50% thermal ellipsoids for all non-hydrogen atoms.

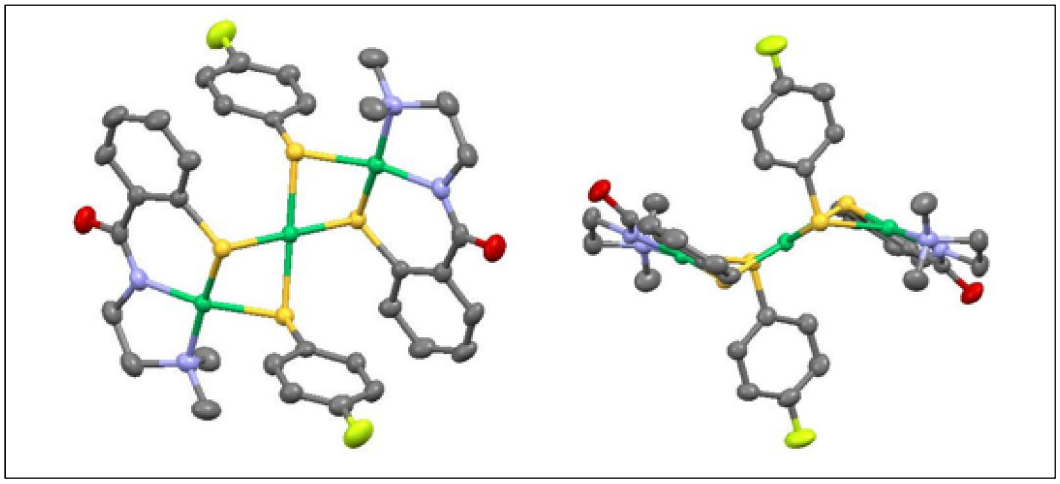

Figure 3.2.4.3. Mercury diagram of the trinuclear complex **13** (left) and its side view (right) showing 50% thermal ellipsoids for all non-hydrogen atoms.

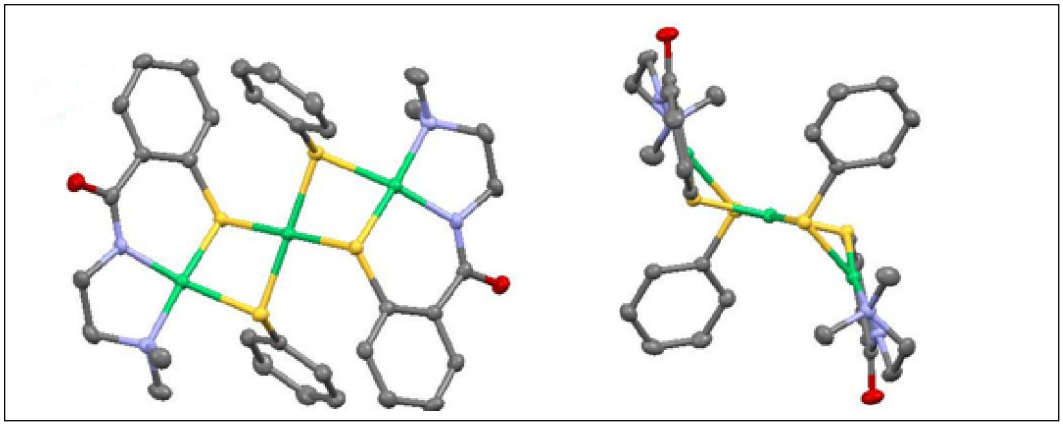

Figure 3.2.4.4. Mercury diagram of the trinuclear complex **14** (left) and its side view (right) showing 50% thermal ellipsoids for all non-hydrogen atoms

Table 3.2.4.1. Comparison of **s**elected Bond Distances (Å) and Angles (°) of complexes **12**, **13** and **14**.

	12	**13**	**14**
Ni1-N(amine)	1.9817(19)	1.973(2)	1.972(3)
Ni1-N(amide)	1.8904(19)	1.875(2)	1.877(3)
Ni1-S(NNS)	2.1323(8)	2.1336(9)	2.1339(10)
Ni1-S(RS)	2.2151(9)	2.2032(9)	2.2023(12)
Ni2-S(NNS)	2.2045(7)	2.1975(8)	2.2050(11)
Ni2-S(RS)	2.1938(8)	2.220(8)	2.2213(10)
Ni1…Ni2	2.8545(9)	2.9791(5)	3.036
NNSS/SSSS dihedral	63.7	53.5	49.5

Table 3.2.4.2. Electronic absorption spectral properties and IR stretching frequencies of $\nu_{C=O}$ of complexes **12**, **13** and **14**.

	12	**13**	**14**
λ (nm)	269, 318, 405	-	288, 423
ϵ ($M^{-1}cm^{-1}$)	1221,875,366	-	1790,422
$\nu_{C=O}$ (cm^{-1})	1572	1570	1571

3.2.5. Properties of Trimers

All these three trimers **12**, **13, 14** were confirmed by X-ray crystallography. They are structurally very similar and crystallize with the central Ni atom on a crystallographic inversion center. Two monomers in each type have coordinated to a central Ni atom and each monomer acts as a bidentate ligand. As shown in the Table 3.2.4.1, bond lengths are comparable except the distance between the central and peripheral Ni atoms. This distance is longer in **13** and **14** by about 0.1 Å than in **12**. This may be due to the bulkiness of the exogenous thiolate ligands of **13** to **14**. Trimeric molecules such as these have been previously reported by a number of groups. [76,87,96] In all cases the 4 donor atoms around the peripheral Ni are either part of a tetradentate N_2S_2 ligand or of two bidentate NS ligands. These trimers, like most of the previously reported species in this class, feature a "stair-step" structure in which the terminal N_2S_2 planes are parallel to each other.

Complexes **12** and **14** are soluble in polar solvents such as MeOH, DMF, and CH_3CN but unstable in aerobic environment, they can be handled without significant decomposition for about 5h before the color begins to fade. Complex **13** is insoluble in both polar and non-polar solvents and therefore it was unable to be characterized using MS and UV-Vis spectroscopy. ESI-MS of **12** and **14** in MeOH show peaks corresponding to $[Ni(NNS)SR]^-$, $[\{Ni_3(NNS)_2(SR)_2\}+H]^+$ and $[\{Ni_3(NNS)_2(SR)_2\}+Na]^+$ ions. FTIR spectra of **12-14** support the metal coordinated nature of the carboxamido N group as the $\nu_{C=O}$ band shifted from 1632 cm^{-1} from NNS ligand to lower frequencies by 60, 62 and 61 cm^{-1} for **12-14** respectively (Table 3.2.4.2).

3.2.6. $[Ni(NN^{am}S)SR]^-$ Monomers

The facile isolation of trimeric species with the amide-containing ligands, in contrast to the isolation of monomeric species with the imine-containing ligands, can possibly be explained by the more electron-donating nature of the amide-ligand, which creates a thiolate atom that is more likely to bridge. In addition, the monomers with the imine-containing ligand are neutral, while the monomers with the amide-containing ligands would be anionic. Therefore, we explored different cations in order to isolate monomeric species with the amide-containing ligand.

The black-red precipitate resulting from the reaction between the sodium salt of benzenethiolate and complex **10** afforded monomeric $(Ph_4As)[Ni(NN^{am}S)SPh]$ (**15**) at -20 ºC by vapor diffusion of diethyl ether in to $MeOH/CH_2Cl_2$ 1:1 solution in which excess tetraphenylarsonium chloride was dissolved. Another desired monomeric species $(Ph_4As)[Ni(NN^{am}S)(4\text{-}NO_2PhS)]$ (**16**) was obtained from the reaction between **9** and 4-nitrophenylthiolate in MeOH. This complex was also crystallized as a salt of Ph_4As^+ from a CH_2Cl_2 solution in which excess Ph_4AsCl was added and layered with diethyl ether at -20 ºC. Compared to previously reported low molecular weight

models of NiSOD, $[Ni^{II}(BEAAM)]^{-1}$ and $(Ni^{II}(HL2))^{-1}$ [where BEAAM = N-{2-[benzyl(2-mercapto-2-methylpropyl)amino]ethyl-2-mercapto-2-methylpropionamide) and HL2= N-(2"-mercaptoethyl)-2-((2'-mercaptoethyl)amino)acetamide] (Figure 3.2.6.1)[75-76] containing amine/amide/bisthiolate coordination, model **15** and **16** are the very first Ni complexes to completely reproduce the amine/amide/bisthiolate coordination found in $NiSOD_{red}$. Figure 3.2.6.2 shows the thermal ellipsoid drawings of **15** and **16**.

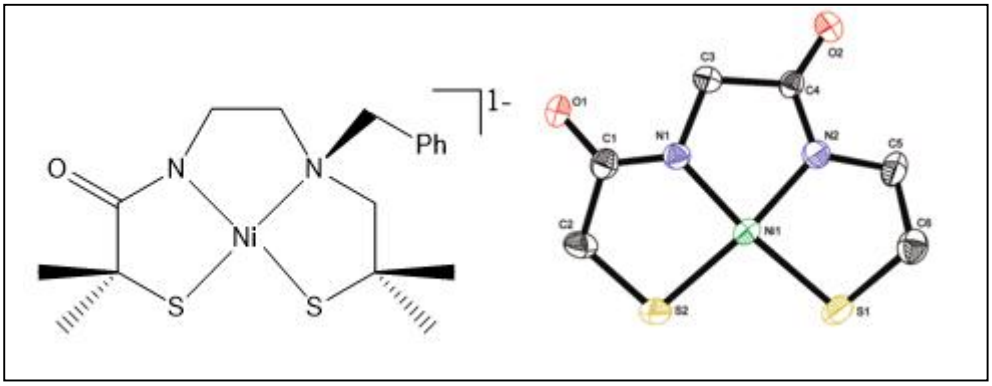

Figure 3.2.6.1. Previously reported NiSOD models with amine/amide/bisthiolate coordination.[75-76]

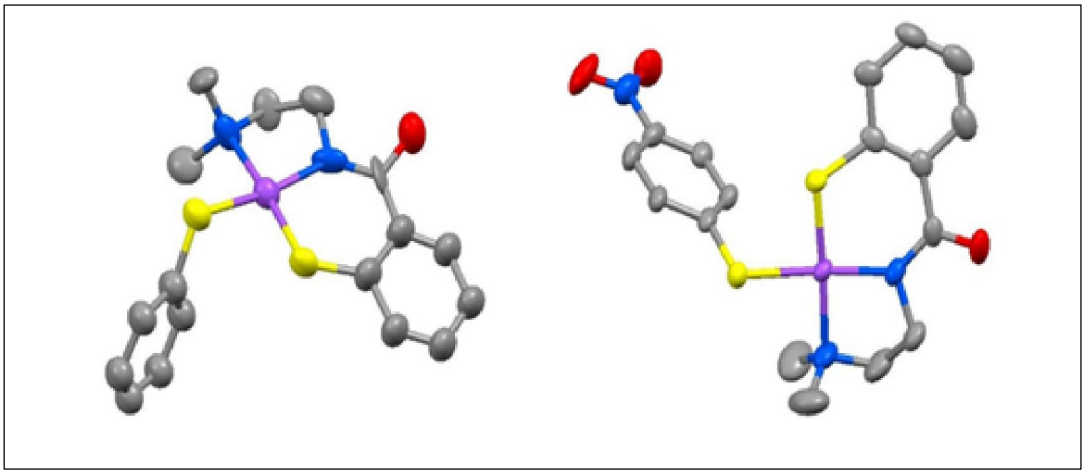

Figure 3.2.6.2. Mercury drawings of the anions in 1**5** (left) and **16** (right) showing the 50% thermal ellipsoids. H atoms and the Ph_4As cations have been omitted for clarity.

The reactions of 2-molar equivalents of the sodium salt of 4-chlorothiophenolate with **9** and **10** in DMF show the formation of the monomer product in mass spectroscopy giving a peak at 423 m/z in negative mode corresponding to $[NiNN^{am}S(4\text{-}Cl)SPh]^-$. Figure 3.2.6.3 shows the mass spectrum of the product which we have been unable to crystallize so far. No evidence was obtained for the formation of $[Ni(NN^{am}S)SR]$ product from the reactions of **9** and **10** with 4-*tert*-butylphenylthiolate which were performed in MeOH and in DMF.

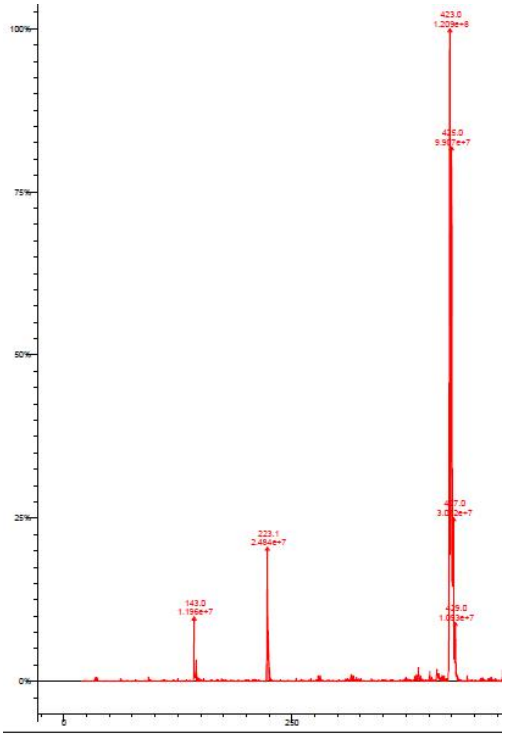

Figure 3.2.6.3. ESI-MS (negative mode) of the reaction mixture of **9** and 4-chlorothiophenolate in MeOH displaying the peaks corresponding to the formation of $[NiNN^{am}S(4\text{-}Cl)SPh]^-$.

Table 3.2.6.1. Comparison of Bond Distances (Å) and Angles (°) of complexes **15** and **16** with $NiSOD_{red}$

	15	**16**	**NiSOD**[3]	
N_{amide}-Ni-N_{amine}	87.9(4)	87.4(2)	N_{His1}-Ni-N_{Cys2}	83.6(1.6)
N_{amine}-Ni-S_{RS}	92.6(3)	91.98(18)	N_{Cys2}-Ni-N_{Cys2}	88.2(0.7)
N_{amide}-Ni-S_{NNS}	95.4(3)	95.42(16)	N_{His1}-Ni-S_{Cys6}	93.3(1.3)
S-Ni-S	85.31(14)	85.08(6)	S_{Cys2}-Ni-S_{Cys6}	95.0(0.6)
Ni-N_{amine}	2.017(9)	1.998(5)	Ni-N_{Cys2}	2.16(0.02)
Ni-N_{amide}	1.966(9)	1.889(5)	Ni-N_{His1}	1.87(0.06)
Ni-S_{NNS}	2.126(4)	2.1261(16)	Ni-S_{Cys2}	2.16(0.02)
Ni-S_{RS}	2.243(3)	2.2278(17)	Ni-S_{Cys6}	2.19(0.02)
Coord'n plane dihedral	13.19	7.52	_	_
Ni-S(RS)-C	109.89	110.38	_	_
NNSS/Ph(SR) angle	87.79	79.14	_	_

Table 3.2.6.2. Electronic absorption spectral properties and IR stretching frequencies of $\nu_{C=O}$ of complexes **15** and **16.**

	15	**16**
λ (nm)	265, 271, 461	266, 271, 452
ε ($M^{-1}cm^{-1}$)	1037,1056,84	1048,1117,149
$\nu_{C=O}$ (cm^{-1})	1575	1559

3.2.7. Properties of $[Ni(NN^{am}S)SR]^-$ Monomers

Both monomer complexes **15** and **16** were characterized by X-ray crystallography and they crystallized as Ph_4As^+ salts. Even though complex **15** crystalizes as a tetraphenylphosphonium salt, due to poor quality of the crystals it was not possible to get a fully refined structure with X-ray diffraction. **15** and **16** crystallizes on general positions in $P2_1/c$ and $P2_12_12_1$ respectively. The asymmetric unit of 1**5** contains one molecule of the anionic Ni complex, two Ph_4As cations, and

one chloride ion, whereas the asymmetric unit of **16** contains the anionic Ni complex, the Ph_4As cation, and two molecules of CH_2Cl_2. The coordination plane of these two structures are somewhat distorted and the phenyl group of the $NN^{am}S$ ligand is not coplanar with the coordination plane. These deviations are caused primarily by a rotation around the phenyl-amide C bond, yielding torsion angles involving the α and β phenyl C atoms and the amide C and N atoms of 20.5° and 22.0° for 1**5** and **16**, respectively. As shown in Table 5, the plane of the phenyl ring in the exogenous thiolate of **15** is closely perpendicular to the coordination plane with an angle of 87.79^0 and the angle is smaller in **16** (79.14^o). This may be related to the degree of freedom of the thiolate group. The $Ni\text{-}S_{thiolate}$ bond length is somewhat sensitive to the electron donating strength of the exogenous thiolate. It is contracted by about 0.1 Å in **16** which contains a less strongly donating thiolate group relative to **15**. Proportionately, the length of the $Ni\text{-}N_{amide}$ bond, which is *trans* to the exogenous thiolate, is longer in **15** by about 0.1 Å relative to **16**. The strong σ donating character of the anionic amide N is reflected by the $Ni\text{-}N_{amide}$ bond lengths of **15** and **16** which are shorter than $Ni\text{-}N_{amine}$ bonds by 0.1 Å. Similar $Ni(II)N_2S_2$ complexes with amide/amine mixed N donors reported $Ni\text{-}N_{amide}$ and $Ni\text{-}N_{amine}$ bond distances comparable to **15** and **16.**[78,95,97,98]. Bond length and angles of these two complexes are comparable to those in NiSOD as shown in Table 3.2.6.1.

Both **15** and **16** are soluble in polar solvents like MeOH, MeCN, DMF, H_2O and in nonpolar solvents like CH_2Cl_2 giving red-orange solutions. But they are stable in those solvents only about 2h as confirmed by UV-Vis spectra before the color begins to fade. As shown in Table 3.2.6.2, **15** and **16** show visible absorption bands at 499 nm and 452 nm, respectively, compared to 450 nm in native $NiSOD_{red}$.[3] These are believed to be d-d transition bands with a minor charge transfer contribution as reported for similar complexes.[99,76] The high energy spectral bands arise due to

LMCT from S^- in thiolate ligands to the Ni center. The absorption band in **15** has shifted to low energy relative to **16** which may due to the higher donor strength of the exogenous thiolate in **15** with respect to the one in **16**. This nature has been observed in previously reported amine-amide coordinated Ni(II)N_2S_2 complexes as well.[78,100]

3.2.8. $NN^{am}S$' ligand (17)

As shown in Figure 3.2.1, in order to give a strong NNS coordination environment with two 6-membered chelate rings, the $NN^{am}S$' ligand which contains a propyl bridge between two N atoms as opposed to the ethyl bridge in the $NN^{am}S$ ligand was made. Similar to the synthetic strategy applied to make the $NN^{am}S$ ligand acid chloride –amine reaction was used. DTSACl was reacted with dmap in MeCN in the same manner as explained in section 3.2.2 for the $NN^{am}S$ ligand. The product was confirmed by mass spectrometry and X-ray crystallography. ESI/MS shows peaks at 237 m/z and 475 m/z corresponding to $[(NN^{am}S')+H]^+$ and $[(NN^{am}S')_2+H]^+$ions and X-ray quality crystals were obtained from the slow evaporation of a CH_2Cl_2 solution. A thermal ellipsoid drawing of **17** is shown in Figure 3.2.8.1.

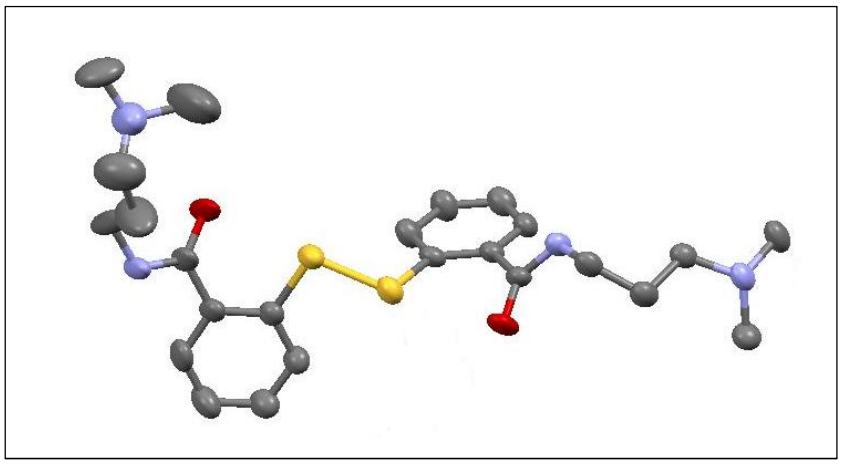

Figure 3.2.8.1. Mercury diagram of $NN^{am}S$' (**17**) showing 50% thermal ellipsoids for all non-hydrogen atoms

3.2.9. $(Et_4N)[Ni(NN^{am}S')Cl]$ (18) and $(Et_4N)[Ni(NN^{am}S')OAc]$ (19)

Analogous to complexes **9** and **10,** complexes **18** and **19** were synthesized by reacting $NN^{am}S'$ with $NiCl_2{\cdot}6H_2O$ and $Ni(OAc)_2{\cdot}4H_2O$ respectively following the same reaction pathway as shown in Figure 3.2.1 aiming to get $[Ni(NN^{am}S')SR]^-$ complexes by substituting Cl and OAc with different thiolates. Mass spectrometry confirms the formation of the products **18** and **19**, giving their parent peaks at m/z 329 and 353 in negative mode corresponding to $[Ni(NN^{am}S')Cl]^-$ and $[Ni(NN^{am}S')OAc]^-$, respectively. Attempts at crystallization by incorporating different cations were not successful.

3.2.10. Reactions of $(Et_4N)[Ni(NN^{am}S')Cl]$ (18) and $(Et_4N)[Ni(NN^{am}S')OAc]$ (19) with thiolates

Complexes **18** and **19** were reacted with all the thiolates which were reacted with $[Ni(NN^{im}S)Cl]$ and $[Ni(NN^{am}S)Cl]^-$ following the same reaction procedures. The reactions were performed in MeOH and DMF in N_2 environment and none of these reactions showed any evidence for the formation of any $[Ni(NN^{am}S')SR]^-$ products under the conditions applied.

3.3. Conclusions

Novel model complexes having amine/amide bisthiolate coordination to resemble the $NiSOD_{red}$ active site have been synthesized successfully using the acid chloride analogue of DTDB. Two monomer complexes the first complexes to exactly reproduce the coordination environment of the $NiSOD_{red}$ active site and three trinuclear complexes resulted. A tridentate ligand, $NN^{am}S$ was incorporated to provide amine, amide and one thiolate donor to Ni and the fourth thiolate donation is given by an external thiolate ligand. Two identical monomers have coordinated to an extra central Ni atom to give the trinuclear complexes. The monomer complexes are not stable for more

than about 2h under ambient conditions in all the solvents in which they are soluble and the trimers are stable for up to about 6h.

3.4. Experimental Section

3.4.1. General Experimental

See Chapter 2, section 2.4 for information regarding reagents, solvents and analytical instrumentation.

3.4.2. Synthesis of $NN^{am}S$ (7)

To a refluxing solution of DTSACl (3.0 g, 8.75 mmol) in 70 mL CH_3CN in a 250 mL round-bottom flask under N_2 was added *N,N*-dimethylethylenediamine (1.93 mL,17.5 mmol) dropwise and then was added triethylamine (7.31mL, 52.5 mmol) dropwise with stirring. After 3h of reflux the resulting orange-yellow color solution was filtered and the solvent was removed by rotary evaporation. The resulting sticky yellow solid was dissolved in CH_2Cl_2 (20 mL) and washed with saturated sodium bicarbonate, brine; the organic layer was separated, dried (Na_2SO_4), filtered and the solvent removed under reduced pressure yielding a yellow solid (2.49 g, 11.2 mmol, 64%). Colorless needle-shaped crystals suitable for X-ray diffraction were obtained by vapor diffusion of diethyl ether into CH_2Cl_2. IR (cm^{-1}) 3349, 3036, 2960, 2922, 2853, 1632, 1585, 1520, 1488, 1460, 1432, 1302, 1275, 1038, 1018, 926, 727. ESI-MS (positive mode, MeOH, m/z): 223 $[NNS+H]^+$, 447 $[(NNS)_2+H]^+$

3.4.3. Synthesis of $(Et_4N)[Ni(NN^{am}S)Cl]$ (9)

Under N_2, to a solution of of $NN^{am}S$ ligand (2.05 g, 9.23 mmol) in 10 mL DMF was added tetraethylammonium chloride (1.53 g, 9.23 mmol) and heated to reflux in a 250 mL two-neck flask. To the refluxing solution was added dropwise a solution of $NiCl_2{\cdot}6H_2O$ (2.2 g, 9.25 mmol) in 20

mL DMF resulting a dark brownish green solution. After refluxing overnight it was filtered and the solvent was removed under reduced pressure resulting a dark brownish green solid. IR (cm^{-1}) 3046, 2977, 1643, 1532, 1458, 1392, 1182, 1033, 731. ESI-MS (negative mode, MeOH, m/z): 315 $[Ni(NNS)Cl)]^-$

3.4.4. Synthesis of $(Et_4N)[Ni(NN^{am}S)OAc]$ (10)

Under N_2, to a solution of $NN^{am}S$ (3.2g, 14 mmol) in 20 mL DMF was added tetraethylammonium chloride (2.32g, 14 mmol) and heated to reflux in a 250 mL two-neck flask. To the refluxing solution was added dropwise a solution of $Ni(OAc)_2{\cdot}4H_2O$ (3.48 g, 14 mmol) in 30 mL DMF with stirring. Heating at reflux overnight resulted dark brownish green solution which was filtered and the solvent was evaporated under reduced pressure resulting a dark brownish green solid. The solid was washed with CH_2Cl_2 and dried to get fairly pure $Ni(NN^{am}S)OAc$ as a light brown powder (2.9 g, 10 mmol, 59 %). IR (cm^{-1}) 3056, 2984, 1630, 1586, 1536, 1392, 1172, 746. ESI-MS (negative mode, MeOH, m/z): 339 $[Ni(NN^{am}S)OAc]^-$.

3.4.5. Synthesis of $[Ni_3(NN^{am}S)_2(S^tBu)_2]$ (12)

Under N_2, to a solution of $[Ni(NN^{am}S)Cl]^-$ (0.365 g, 1.15 mmol) in 20 mL MeOH was added dropwise a solution of sodium 2-methyl-2-propanethiolate (0.130 g, 1.15 mmol) in 10 mL MeOH. The solution turned black-red. While stirring for 24 h a black precipitate deposited which was filtered, washed with diethyl ether and dried to get a black powder as the product (0.12 g, 0.33 mmol, 13%). Vapor diffusion of hexanes into a CH_2Cl_2 solution in N_2 environment yielded dark red crystals which were suitable for X-ray diffraction.

Elemental Anal. Calc. for $C_{30}H_{46}N_4O_2S_4Ni_3$: C, 45.10; H, 5.76; N, 7.01. Found: C, 44.63; H, 5.90; N, 6.87. IR (cm^{-1}) 3059, 2970, 2886, 1650, 1572, 1527, 1455, 1147, 1004, 749. ESI-MS (negative

mode, MeOH, m/z): 369 $[Ni(NN^{am}S)StBu]^-$, (positive mode) 799 $[\{Ni_3(NN^{am}S)_2(S^tBu)_2\}+H]^+$, 821 $[\{Ni_3(NN^{am}S)_2(S^tBu)_2\}+Na]^+$. UV-Vis (methanol); λ = 269 nm, 405 nm.

3.4.6. Synthesis of $[Ni_3(NN^{am}S)_2S(4\text{-}F)Ph]$ (13)

Under N_2, sodium hydride (00.020g, 0.83 mmol) was added to a solution of 4-fluorothiophenol (0.044 g, 0.37 mmol) in 10 mL DMF and the solution was stirred for 5 min. The solution was added dropwise to $[Ni(NN^{am}S)Cl]^-$ (0.12 g, 0.37 mmol) in 10 mL DMF with stirring. After stirring 24h, a dark brown-red solution resulted, which was filtered and the solvent was removed by rotary evaporation, yielding a dark brown-red solid. X-ray quality dark red crystals were grown by slow evaporation of a MeOH solution in N_2 environment (0.042 g, 0.10 mmol, 28%). Elemental Anal. Calc. for $C_{34}H_{36}N_4O_2S_4F_2Ni_3$: C, 46.67; H, 4.15; N, 6.40. Found: C, 46.58; H, 4.72; N, 6.33. IR (cm^{-1}) 3081, 2897, 1650, 1570, 1530, 1456, 1353, 1220, 1154, 996.

3.4.7. Synthesis of $[Ni_3(NN^{am}S)_2(SPh)_2]$ (14) and $(Ph_4As)[Ni(NN^{am}S)SPh]$ (15)

Under N_2, sodium thiophenolate (0.31 g, 2.35 mmol) in 10 mL MeOH was added dropwise into a stirring solution of $[Ni(NN^{am}S)OAc]^-$ (0.40 g, 1.18 mmol) in 10 mL MeOH. The solution turned dark red quickly and a dark red-black precipitate separated while stirring for 24h.The solution was filtered to get a black-red precipitate and reddish green filtrate. The filtrate was evaporated to get a reddish green solid, X-ray quality crystals of the trinuclear complex, **14**, were grown using the crude product by slow evaporation of a MeOH solution under N_2 environment (0.18g, 0.21 mmol, 54% based on Ni, 36% based on ligand). Elemental Anal. Calc. for $C_{34}H_{38}N_4O_2S_4Ni_3.H_2O$: C, 47.65; H, 4.7, N, 6.54. Found: C, 47.80; H, 5.33; N, 6.23. IR (cm^{-1}) 3059, 2970, 2898, 1571, 1521, 1459, 1374, 1355, 1042, 905,750. ESI-MS (positive mode, MeOH, m/z): 859

[{$Ni_3(NN^{am}S)_2(SPh)_2$}+Na]$^+$, 839 [{$Ni_3(NN^{am}S)_2(SPh)_2$}+H]$^+$, UV-Vis (acetonitrile); λ_{max} = 288, 423 nm.

The precipitate was dissolved in CH_2Cl_2, filtered and the solvent was removed by rotary evaporation to get [$Ni(NN^{am}S)SPh$]$^-$ as a black-red solid (0.31 g, 0.27 mmol, 23%; yield based on the additional Ph_4AsCl found in the crystal structure). X-ray quality crystals of the mononuclear complex **15** were grown at -20 ºC from the precipitate by vapor diffusion of diethyl ether into CH_2Cl_2/MeOH (1:1) solution in which excess tetraphenylarsonium chloride was dissolved. IR (cm^{-1}) 3046, 2920, 2854, 1628, 1560, 1508,1467,1434,1364, 1105, 995, 720. ESI-MS (negative mode, MeOH, m/z): 109 [SPh]$^-$, 389 [$Ni(NN^{am}S)SPh$]$^-$, 315 [$Ni(NN^{am}S)Cl$]$^-$. UV-Vis (acetonitrile); λ_{max} = 265, 271, 304, 461 nm. Elemental Anal.: Calc. for $C_{17}H_{19}N_2S_2ONi \cdot 2(C_{24}H_{20}As) \cdot Cl \cdot 0.5\ CH_2Cl_2$**:** C, 63.51; H, 4.88; N, 2.26. Found: C, 63.11; H, 5.51; N, 2.26.

3.4.8. Synthesis of (Ph_4As)[$Ni(NN^{am}S)S(4\text{-}NO_2)Ph$] (16)

Under N_2, to a solution of 4-nitrothiophenol (0.390 g, 2.52 mmol) in 15 mL MeOH was added sodium hydroxide (0.10 g , 2.5 mmol) and the solution was stirred for 5 minutes and was added dropwise to a solution of [$Ni(NN^{am}S)Cl$]$^-$ (0.800 g, 2.52 mmol) in 15 mL MeOH. After 24 h stirring a red-orange solution resulted; the solution was filtered and the solvent was removed under reduced pressure. The resulting red solid was extracted into CH_2Cl_2 and the solvent was condensed to 20 mL. Addition of excess diethyl ether resulted in deposition of the product as a red solid, which was isolated and dried (0.33 g, 0.76 mmol, 48%). To get X-ray quality crystals, a slight excess of tertraphenylarsonium chloride was added to a CH_2Cl_2 solution of the product which was stirred for 10 minutes and filtered. Layering with diethyl ether at -20 ºC produced dark red crystals. Elemental Anal. Calc. for $C_{41}H_{38}N_3O_3S_2NiAs$: C, 60.16; H, 4.68; N, 5.13. Found: C, 59.95; H, 5.01; N, 4.82. IR (cm^{-1}) 3056, 2863, 1641, 1559, 1513, 1436, 1300, 1070, 996, 737. ^{1}H NMR (400

MHz, CD_3COCD_3, δ): 8.46-6.69 (m, 28H, Ar-H), 3.39 (t, 2H, NC*H*$_2$), 2.48 (S, 6H, N(C*H*$_3$)$_2$), 2.29 (t, 2H, N$(CH_3)_2$C*H*$_2$).

ESI-MS (negative mode, MeOH, m/z): 154 $[SPhNO_2]^-$, 434 $[Ni(NN^{am}S)SPhNO_2]^-$. UV-Vis (acetonitrile); λ_{max} = 266, 271, 452 nm.

3.4.9. Reaction of 4-chlorothiophenol with $[Ni(NN^{am}S)Cl]^-$ and $[Ni(NN^{am}S)OAc]^-$

Under N_2, sodium hydride (0.05 g, 2.07 mmol) was added to a solution of 4-chlorothiophenol (0.30 g, 2.1 mmol) in 10mL of DMF and the solution was stirred for 20 min. It was filtered and added dropwise to a solution of $(Et_4N)[Ni(NN^{am}S)Cl]$ (0.460 g, 1.04 mmol) in 20 mL DMF and stirred for 2 days. A dark red solution resulted; the solvent was removed under reduced pressure to get a dark red solid which shows a 423(-) m/z peak in ESI/MS corresponding to the expected $[Ni(NN^{am}S)(4\text{-}Cl)SPh]^-$. Attempts at crystallization were not successful.

When the reaction is performed in MeOH with $(Et_4N)[Ni(NN^{am}S)Cl]$ and $(Et_4N)[Ni(NN^{am}S)OAc]$ a dark red precipitate is formed which is insoluble in all solvents. No evidence is seen the mass spec for the formation of product.

3.4.10. Synthesis of $NN^{am}S$' (17)

To a refluxing solution of DTSACl (3.00 g,8.75 mmol) in 70 mL CH_3CN in 250 mL round-bottom flask under N_2 was added dropwise *N,N*-dimethylethylenediamine (2.20 mL,17.5 mmol) and then was added triethylamine (7.31mL, 52.5 mmol) dropwise with stirring. After 3h of reflux the resulting orange-yellow solution was filtered and the solvent was removed by rotary evaporation. The resulting sticky yellow solid was dissolved in CH_2Cl_2 (20 mL) and washed with saturated sodium bicarbonate and brine. The organic layer was separated, dried (Na_2SO_4), filtered and the solvent was removed under reduced pressure, yielding a yellow solid (2.15 g, 9.10 mmol, 52%).

Colorless needle-shaped crystals suitable for X-ray diffraction were obtained by slow evaporation of a CH_2Cl_2 solution IR (cm^{-1}) 3059, 2936, 2860, 1629, 1536, 1485, 1445, 1307, 1257, 1159, 740. ESI-MS (positive mode, MeOH, m/z): 237 $[NNS'+H]^+$, 475 $[(NNS')_2+H]^+$.

3.4.11. Synthesis of $(Et_4N)[Ni(NN^{am}S')Cl]$ (18) and $(Et_4N)[Ni(NN^{am}S')OAc]$ (19)

Under N_2, tetraethylammonium chloride (0.70 g, 4.23 mmol) was added to a solution of of $NN^{am}S'$ (2.00 g, 8.47 mmol) in 10 mL DMF and the solution was heated to reflux in a 250 mL two-neck flask. To the refluxing solution was added dropwise a solution of $NiCl_2 \cdot 6H_2O$ (1.0 g, 4.23 mmol) in 20 mL DMF resulting in a dark brownish green solution. After refluxing overnight it was filtered and the solvent was removed under reduced pressure resulting in **18** as a dark brownish green solid. IR (cm^{-1}) 3050, 2978, 2678, 1635, 1585, 1537, 1459, 1391, 1311, 1258, 1173, 1034, 745. ESI-MS (negative mode, MeOH, m/z): 329 $[Ni(NN^{am}S')Cl)]^-$. The same procedure was followed to synthesize **19** using $Ni(OAc)_2 \cdot 4H2O$ as the Ni salt. A dark brown solid was obtained after removing the solvent under reduced pressure. IR (cm^{-1}) 3040, 2935, 1638, 1560, 1385, 1340, 1312, 1256, 1164, 1092, 1034, 745. ESI-MS (negative- mode, MeOH, m/z): 353 $[Ni(NN^{am}S')OAc)]^-$.

CHAPTER 4: ATTEMPTS TO INTRODUCE 5TH COORDINATION OF NiSOD$_{OX}$ ACTIVE SITE

4.1. Introduction

As discussed in Chapter 1, the Ni center of NiSOD toggles between +2 and +3 oxidation states in its catalytic cycle during which the coordination environment about Ni is changed from four to five coordinate, respectively.

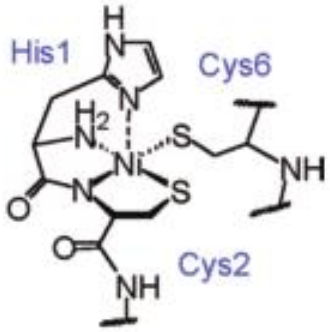

Figure 4.1.1. Active site of NiSOD$_{ox}$[73]

The axial Ni-N interaction with the histidine imidazole N in the oxidized state plays a major role in tuning the reduction potential of the catalytic Ni center to perform superoxide dismutation. Therefore modeling this feature is crucial during modeling of the enzyme active site.

Chapters 2 and 3 discussed the syntheses of four coordinate Ni-N_2S_2 complexes having amine/imine and amine/amide bisthiolate coordination as NiSOD$_{red}$ models. This chapter discusses our attempts at synthesizing five coordinate N_3S_2 complexes to model the coordination found in NiSOD$_{ox}$ by introducing an extra N donor in the [Ni(NNS)Cl] and [Ni(NNS)OAc] complexes, discussed in chapter 2 and 3. Our aim of this work was to model the fifth Ni-N axial coordination to get closer models of NiSOD.

4.2. Synthetic strategy for introducing 5th N coordination

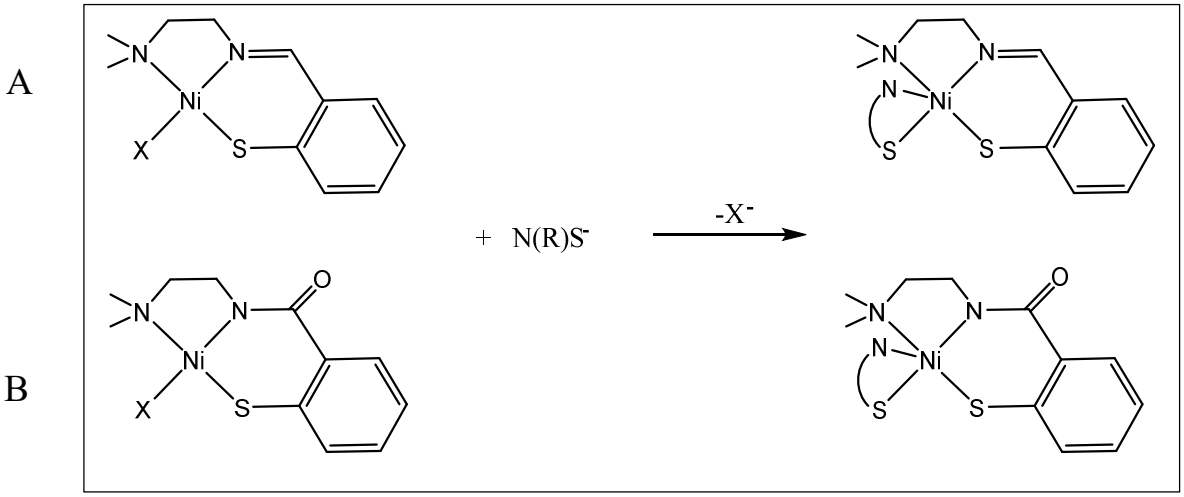

Figure 4.2.1. Schematic representation of the synthesis of (A) - [Ni(NN^{im}S)NRS] and (B) - [Ni(NN^{am}S)NRS]$^{-}$ complexes.

As shown in Figure 4.2.1, in order to get NiN_3S_2 complexes analogous to both imine and amide containing [Ni(NNS)X] complexes, [Ni(NN^{im}S)Cl], [Ni(NN^{am}S)Cl]$^{-}$ and [Ni(NN^{am}S)OAc]$^{-}$ were reacted with different thiolate compounds containing an extra N donor in addition to the S (Figure 4.2.2). All (**a**)-(**h**) compounds are available commercially and some modifications were done for some compounds to improve the reactivity. All these thiols are expected to make 5-membered chelate rings with the central nickel atom.

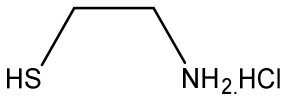

(a)

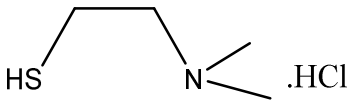

(b)

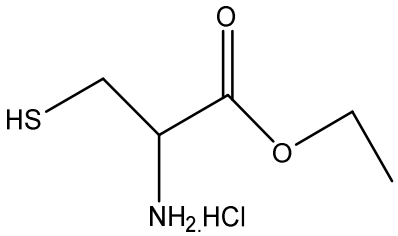

(c)

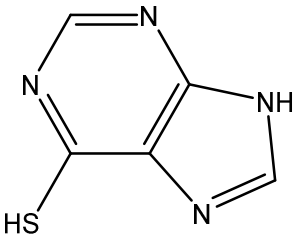

(d)

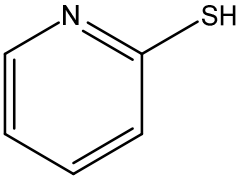

(e)

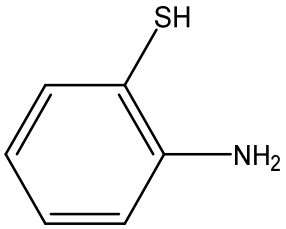

(f)

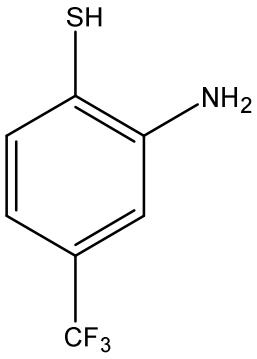

(g)

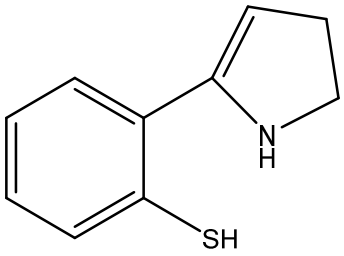

(h)

Figure 4.2.2. Structures of N(R)S thiols with S and N donor sites reacted with [Ni(NNS)X] complexes to get N_3S_2 coordination.

4.3 Reactions with [Ni(NNS)X]

4.3.1 With [Ni(NN^{im}S)Cl]

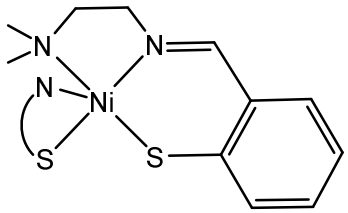

Figure 4.3.1.1. Structure of [Ni(NN^{im}S)S(R)N]

With the aim of getting complexes as shown in Figure 4.3.1.1, the aforementioned thiolates were reacted with [Ni(NN^{im}S)Cl]. The sodium salt of 2-aminoethanethiol was made by reacting the hydrochloride salt with 2 molar equivalents of NaOH in MeOH and then was added dropwise to [Ni(NN^{im}S)Cl] in MeOH and stirred for 24 h under N_2. No evidence was observed for the formation of the desired N_3S_2 coordinated product and the only crystals isolated were identified as [Ni(SN^{im}S)]$_2$ by X-ray crystallography, which has been reported before by our research group as well as other groups (Figure 4.3.1.2).[89,101,102]

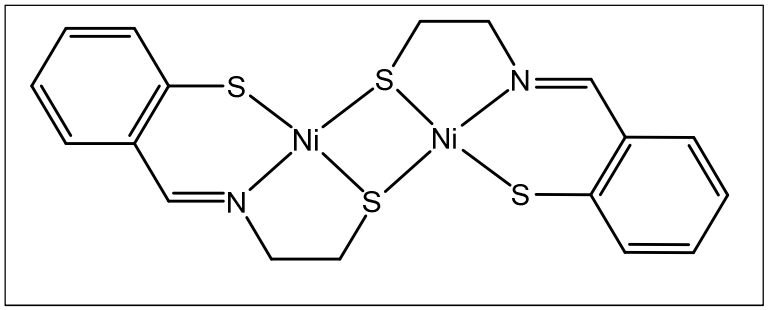

Figure 4.3.1.2. Structure of [Ni(SN^{im}S)]$_2$ obtained from the reaction of [Ni(NN^{im}S)Cl] and 2-aminoethanethiolate(**a**).

In our previous research this dimer resulted from the Schiff-base condensation between DTDB and Ni(2-aminoethanethiolate)$_2$. In the current system, one explanation for its formation could be

reaction with DTDB left over from the synthesis of [Ni(NN^{im}S)Cl]. In order to prevent this Schiff-base condensation the tertiary amine reagent N,N-dimethylaminoethane thiolate (**b**) was used. The sodium salt of (**b**) was obtained by reacting 2 molar equivalents of NaOH with hydrochloride salt in MeOH. After stirring for 10 min, it was added to a solution of [Ni(NN^{im}S)Cl] in MeOH and stirred for 24 h in the glove box. After removing the solvent a red solid was obtained and the mass spectrum of the solid (Figure 4.3.1.3) indicates the formation of the [Ni(NNS)S(R)N] complex, as evidenced by the peak at 370 m/z corresponding to [[Ni(NN^{im}S)SCH$_2$CH$_2$N(CH$_3$)$_2$]+H]$^+$. Attempts at crystallization of the desired product were not successful and the only crystals which could be isolated were identified as [Ni(NN^{im}S)Cl] and [Ni(SCH$_2$CH$_2$N(CH$_3$)$_2$]$_2$ by X-ray crystallography.

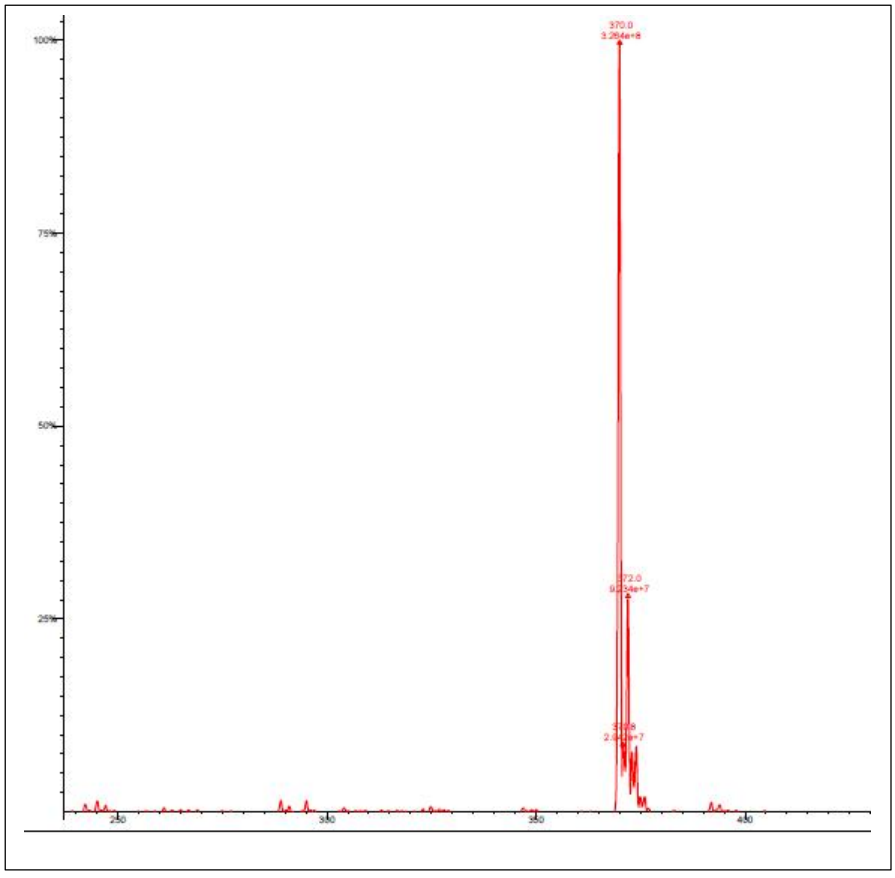

Figure: 4.3.1.3. ESI-MS (positive mode) of the reaction mixture of [Ni(NN^{im}S)Cl] and the sodium salt of (**b)** in MeOH displaying the peak corresponding to the formation of [[Ni(NN^{im}S)SCH$_2$CH$_2$N(CH$_3$)$_2$].

Since the desired NiN_3S_2 product was not isolated even with **(b),** thiol (**a)** was modified to get a secondary amine (Figure 4.3.1.4) by benzylation of the amine group.[103]

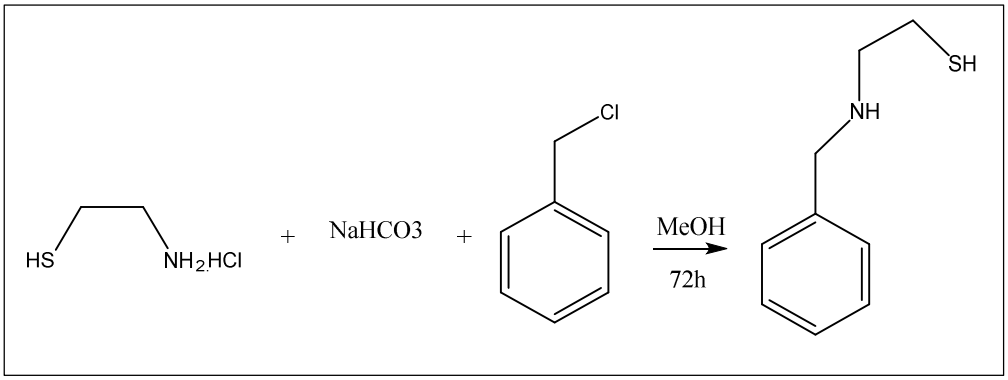

Figure 4.3.1.4. Benzylation of (**a**)

The sodium salt of benzylated (**a**) was made with NaOH and then it was reacted with [Ni(NN^{im}S)Cl] in MeOH. The solvent was evaporated and the resulting red solid was extracted into CH_2Cl_2. No evidence was observed in the mass spectrum for the formation of the product and no crystals were isolated. Similar to (**a**) and (**b**) the sodium salt of (**c**) was made by reacting cysteine ethyl ester hydrochloride with NaOH. It was added slowly to [Ni(NN^{im}S)Cl] in MeOH in 2:1 ratio and allowed to stir for 2 days. A red-brown precipitate was separated with time which is soluble in CH_2Cl_2. No evidence was obtained in the mass spectrum for the formation of the product and no crystals could be isolated from the precipitate or from the filtrate.

Another interested thiol compound that we used was 6-mercaptopurine (**d**). As in the previously mentioned procedures, the sodium salt was made with NaOH and then it was reacted with [Ni(NN^{im}S)Cl] in MeOH for 2 days. The resulting red-brown solution shows the formation of the product in ESI/MS giving a peak at 415 m/z in negative mode corresponding to [[Ni(NN^{im}S)S(R)N]-H]$^-$. A monomeric species (**17**) was, in fact, isolated (Figure 4.3.1.5) from the crystallization of the product by vapor diffusion of diethyl ether into MeOH solution at -20 ^{o}C.

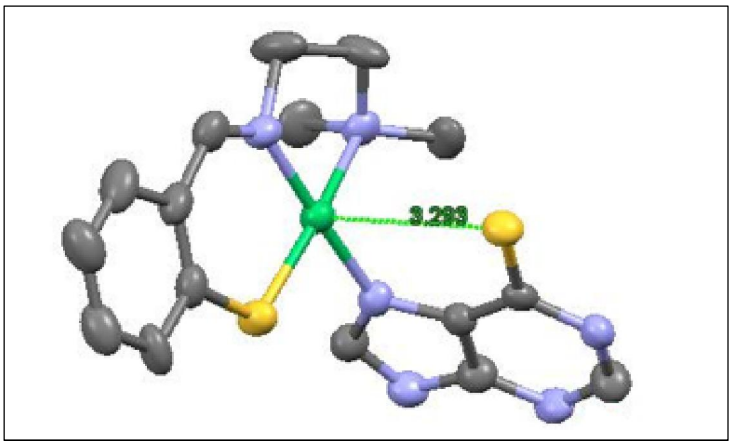

Figure 4.3.1.5. Mercury diagram of complex **17** showing 50% thermal ellipsoids for all non-hydrogen atoms.

Table 4.3.1.1. Selected Bond Distances (Å) and Angles (deg) for **17**

	17
Ni-N_{amine}	2.003(8)
Ni-N_{imine}	1.881(8)
Ni-S_{NNS}	2.143(3)
N_{imine}-Ni-N_{amine}	86.3(3)
N_{imine}-Ni-S_{NNS}	96.8(3)
S_{NNS}-Ni-N_{RS}	86.0(2)
Coord'n plane dihedral	10.03
NNSS/Ph_{SR} angle	80.02

Complex **17** has been structurally characterized by X-ray crystallography and the structure has not been satisfactorily refined due to the crystal quality is not good enough (see Table 4.3.1.1 for bond lengths and angles). It crystallizes on a general position in the P-1 space group and bond lengths are comparable to other monomeric structures **1-6**. ESI/MS shows a peak at 415 m/z in negative mode corresponds to $[M-H]^+$ (Figure 4.3.1.6). The interesting feature of this monomer is the exogenous thiolate is bonded to the Ni via N giving a four-coordinate N_3S coordination and leaving

S unbound. The thiolate ring plane forms an angle of 80.02° with the coordination plane so that Ni-S_{exo} distance is 3.293 Å (Figure 4.3.1.5) which is too long to be considered bonding with the Ni. In order to facilitate the formation of Ni-S_{exo} bond, this product was chemically oxidized with $(NH_4)_2Ce(NO_3)_6$. It was deprotonated with trimethylamine in MeOH and after removing excess Et_3N it was treated with $(NH_4)_2Ce(NO_3)_6$ in MeOH. Immediately after adding the oxidizing agent, a yellow precipitate separated, which is soluble only in DMF and DMSO and shows peaks characteristic of aromatic rings of the 6-mercaptopurine only (6-8 δ region) in the ^{1}H-NMR.This suggests the precipitate is not the desired NiN_3S_2 product. Evidence was not seen in the mass spectrum of the filtrate for the formation of the product and none of the products could be isolated from crystallization except some colorless crystals which show a unit cell volume of only 131 $Å^3$.

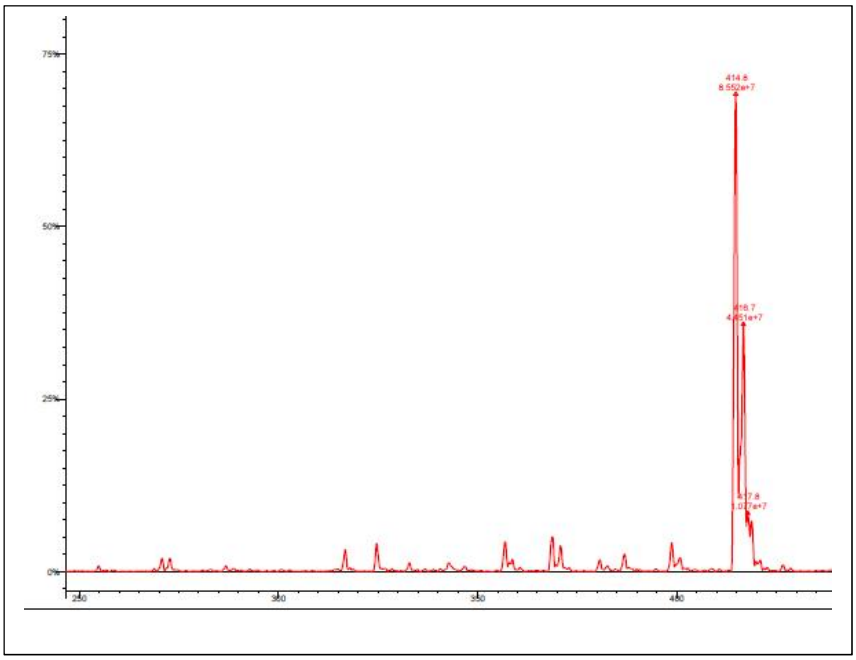

Figure 4.3.1.6. ESI-MS (negative mode) of **17** showing peak at 415 corresponding to $[M-H]^+$.

Reaction between the sodium salt of (2-mercaptopyridine) (**e**) and [Ni($NN^{im}S$)Cl] in MeOH was not successful. Even after several attempts, no evidence was observed for the formation of the

product. One of the reasons for this may be that this thiolate would make a 4-membered chelate ring with Ni which is not a stable as 5 and 6-membered rings due to high ring strain.

From the reaction of the sodium salt of (2-aminothiophenol) (**f**) with [Ni(NN^{im}S)Cl] in MeOH, a dark red solution was obtained. Upon crystallization, dark red crystals were isolated and identified as the [Ni(SN^{im}S)]$_2$ dimer from X-ray crystallography (Figure 4.3.1.7), which has been reported before by our group as well as others.[102,84] Similar to the crystals isolated from the reaction between (**a**) and [Ni(NN^{im}S)Cl], this product may also have been formed from the Schiff-base reaction between a trace amount of DTDB present in the reaction mixture and thiolate. To avoid this Schiff-base reaction, [Ni(NN^{im}S)Cl] was recrystallized and the crystals were reacted with (**f**), but no evidence was obtained for the formation of the desired NiN_3S_2 product.

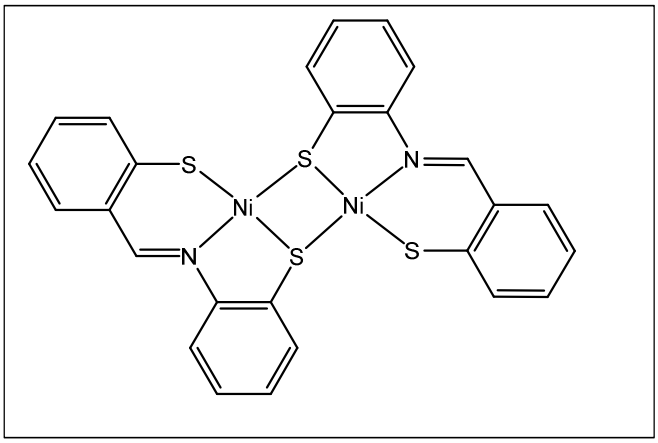

Figure 4.3.1.7. Structure of [Ni(SN^{im}S)]$_2$ obtained from the reaction of [Ni(NN^{im}S)Cl] and 2-aminothiophenol (**f**).

In order to lower the donor strength of S in (**f**) which should support coordination to Ni, thiolate (**g**) was selected. The sodium salt of (**g**) was made and reacted with [Ni(NN^{im}S)Cl] in MeOH but no evidence was observed for the formation of the product.

4.3.2. With [Ni(NN^{am}S)Cl]$^-$ (9) and [Ni(NN^{am}S)OAc]$^-$ (10)

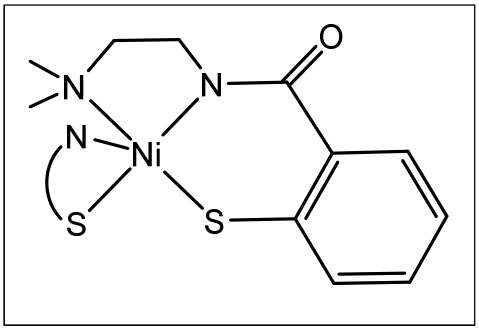

Figure 4.3.2.1. Structure of [Ni(NN^{am}S)S(R)N]

As shown in Figure 4.2.1, complexes **9** and **10** were reacted with all the thiolates shown in Figure 4.2.2 aiming to make amide-containing NiN_3S_2 complexes (Figure 4.3.2.1) to resemble $NiSOD_{ox}$. The sodium salts of each thiolate were made as described in reactions in 4.3.1, by reacting with NaOH. All reactions were carried out in the glove box under N_2. When **9** is reacted with the sodium salt of (**a**) in MeOH, a green precipitate is separated which is soluble only in hot DMSO. The IR spectrum of the precipitate does not show the $\nu_{C=O}$ band therefore, it may be a polymeric Ni-thiolate species. Its insolubility in cold DMSO, makes doing NMR impossible. The same product is apparently formed by reaction with **10**. When benzylated (**a**) is reacted with **9** or **10** in DMF, a black-green precipitate is separated which is soluble in MeOH. No evidence was observed in the mass spectrum for the formation of product and attempts at crystallization were not successful. In another attempt, the primary amine group of (**a**) was protected with a boc group (Figure 4.3.2.2) and the resulting product reacted with **9** and **10** in MeOH after deprotonation with Et_3N. A dark red solution resulted and the ESI/MS of the solution shows a peak at 456 m/z (<5%) in negative mode which corresponds to [Ni(NN^{am}S)S$(CH_2)_2$(boc)N]$^-$. Our aim was to isolate this product and deprotect the amine group to get the desired NiN_3S_2 product but attempts at purification and isolation of the product by crystallization have been unsuccessful.

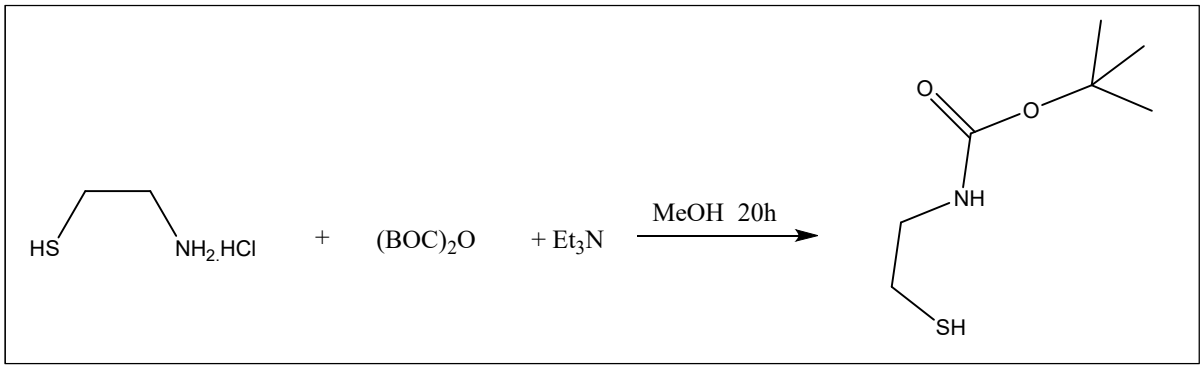

Figure 4.3.2.2. BOC protection of (**a**)[103]

The reaction of complex **9** and the sodium salt of (**b**) in MeOH resulted in a red solution. ESI/MS of this solution showed a strong peak at 384 m/z in negative mode which is consistent with the $[Ni(NN^{am}S)S(CH_2)_2N(CH_3)_2]^-$ monomer and a peak at 827 m/z in positive mode corresponding to the $[Ni_3(NN^{am}S)_2(S(CH_2)_2N(CH_3))_2 +H]^+$ trimer. Dark red crystals were formed by slow evaporation of this solution in the glove box and they were identified as the trinuclear species (**20**) (Figure 4.3.2.3). The bond distances and angles are listed in Table 4.3.2.1.

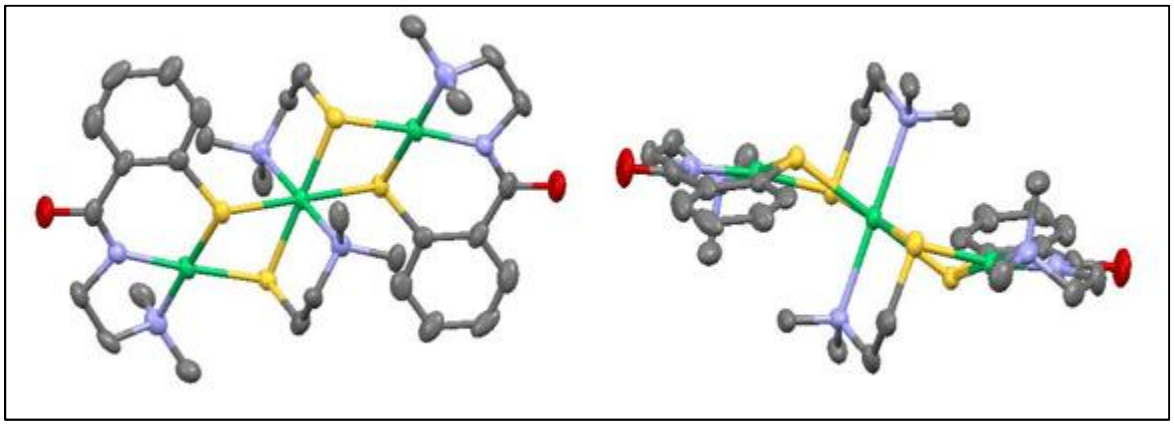

Figure 4.3.2.3. Mercury diagram of the trinuclear complex **20** (left) and its side view (right) showing 50% thermal ellipsoids for all non-hydrogen atoms

Unlike the other trimers (**12-14**) discussed in chapter 3, the central Ni atom of this structure has octahedral coordination geometry resulting from the coordination of both pendant N groups and S

of the thiolate. This flattens out the trimer reducing the dihedral angle between the coordination planes of the terminal and central Ni atoms to 26.6° (see Table 4.3.2.1). Similar to other trimers **12-14,** this trimer also has a "stair-step" structure. Mascharak and coworkers reported a similar structure with an octahedral central Ni atom.[104]

Table 4.3.2.1. Selected Bond Distances (Å) and Angles (deg) for **20**

	20
Ni1-N(amine)	1.982(6)
Ni1-N(amide)	1.894(6)
Ni1-S(NNS)	2.131(2)
Ni1-S(RS)	2.222(2)
Ni2-S(NNS)	2.488
Ni2-S(RS)	2.341
Ni1…Ni2	3.4284
NNSS/SSSS dihedral	26.6

Bond lengths from the terminal Ni atom (Ni1) are comparable to those in trimers **12-14** whereas Ni2-S bond lengths and Ni1-Ni2 distance are longer than in the other trimers. The IR spectrum of **20** shows the $\nu_{C=O}$ band at 1566 cm^{-1} similar to other trimers and λ_{max} at 253 and 453 nm in CH_3CN.

Efforts were made to cleave this trimer to get the anticipated NiN_3S_2 monomer. To a solution of **20** in CH_3CN was added $NN^{am}S$ ligand and the sodium salt of the thiolate in 1:1:1 ratio and stirred for 1h. The resulted dark red solution shows the 384 m/z monomer peak in ESI/MS, but upon crystallization the same trimer **20** was obtained, as identified by X-ray diffraction. The reaction was repeated with increasing the reaction time to 3h, but the same product was crystallized.

The reactions of **9** and **10** with the sodium salt of (**c**) were performed in MeOH and in DMF for 1-3 days reaction times. When 2 molar equivalents of the thiolate was reacted with **10** in MeOH a

yellow-green precipitate was separated which is soluble in DMF. This precipitate shows a band at 1712 cm^{-1} in IR which is consistent for a (C=O) bond. Upon crystallization of this product by vapor diffusion of diethyl ether into a DMF solution in which a few drops of MeOH and CH_2Cl_2 was added light green crystals were formed at -20 ^oC and they were identified as Ni(cysteine methylester)$_2$ **(21)** (Figure 4.3.2.4) by X-ray crystallography, although the structure has not been satisfactorily refined. The interesting feature of this product is that the $–OCH_2CH_3$ group of the thiolate has been replaced by $–OCH_3$ group, likely due to a transesterification reaction with the methanol solvent. The desired NiN_3S_2 product, however was not resulted from the above reactions.

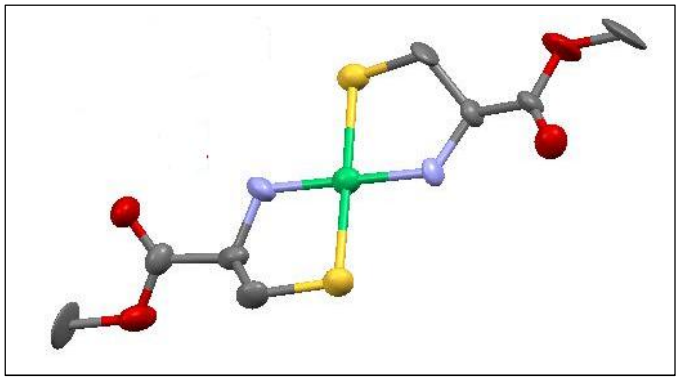

Figure 4.3.2.4. Mercury diagram of **21** showing 50% thermal ellipsoids for all non-hydrogen atoms

Sodium thiolates of (**d**), (**e**), (**f**) and (**g**) were reacted with **9** and **10** in MeOH and in DMF with reaction times varying from 1-3 days. The thiolate (**h**) was reacted only with **9** and ESI/MS shows a peak at 456(-) m/z (<1%) corresponding to the formation of [Ni($NN^{am}S$)SR]. Purification and crystallization attempts of the product have not been successful yet. None of the other reactions showed evidences in ESI/MS for the formation of expected products and attempts at crystallization failed to produce any desired complexes.

4.4. Conclusions

In order to get NiN_3S_2 complexes as NiSOD models containing all appropriate ligands in the accurate arrangement, a series of thiolates (**a**)-(**h**) which contain an additional N donor were reacted with the imine and amide N containing [Ni($NN^{im}S$)Cl], [Ni($NN^{am}S$)Cl]$^-$ (**9**) and [Ni($NN^{am}S$)OAc]$^-$ (**10**) complexes. The [Ni($NN^{im}S$)Cl] forms an interesting NiN_3S complex with (**d**) via coordinating the thiolate through N which was characterized by x-ray crystallography and (**a**) and (**f**) form dinuclear species in the form of [Ni($SN^{im}S$)]$_2$ which have been reported before.[84] Reaction with the thiolate (**b**) shows an ESI/MS peak corresponding to the desired NiN_3S_2 complex, which we have been unable to crystallize and the other thiolates (**c**), (**e**), (**g**) did not produced any evidence for the formation of desired products.

Amide N containing complexes **9** and **10** produce a trinuclear complex **20** with (**b**) through the coordination of two N_2S_2 monomers to a central Ni atom, via pendant N groups and S_{exo}; attempts at cleaving the trimer in order to make the monomer have been unsuccessful. Boc-protection and benzylation of amine N of the thiolate (**a**) did not help to produce any desired products. From the reactions with the thiolate (**c**), a byproduct [Ni(cysteine methylester)$_2$] (**21**) could be isolated and none of the products were isolated from the reactions with the other thiolates (**d**) - (**h**).

4.5. Experimental Section

4.5.1. General Experimental

See chapter 2, section 2.4 for information regarding reagents, solvents and analytical instrumentation.

4.5.2. Synthesis of [Ni(NN^{im}S)(with 6-mercaptopurine)] (17)

Under N_2, to a solution of 6-mercaptopurine (0.30 g, 1.97 mmol) in 15 mL MeOH was added sodium hydroxide (0.16 g, 3.94 mmol). After stirring for 10 minutes the solution was added dropwise to a solution of [Ni(NN^{im}S)Cl] (0.30 g, 1.0 mmol) in 15 mL MeOH. After 48 h of stirring a dark red solution resulted; the solution was filtered and the solvent was removed under reduced pressure. The resulting red-brown solid (yield 68%) was washed with CH_2Cl_2. ESI-MS (MeOH, m/z): 265 [Ni(NN^{im}S)]$^+$, 415 [[Ni(NN^{im}S)SR]-H]$^-$. IR (cm^{-1}): 3366, 3018, 2900, 1585, 1561, 1533, 1461, 1375. 1336, 1205, 1009, 861, 782. X-ray quality red-orange crystals were made by vapor diffusion of diethyl ether into a MeOH solution at -20 ºC.

4.5.3. Reaction of [Ni(NN^{im}S)Cl] with 2-aminoethanethiol

Under N_2, to a solution of 2-aminoethanethiol hydrochloride (0.20 g, 1.76 mmol) in 10 mL MeOH was added sodium hydroxide (0.14 g, 3.52 mmol). After stirring for 10 minutes the solution was added dropwise to a solution of [Ni(NN^{im}S)Cl] (0.26 g, 0.88mmol) in 15 mL MeOH. After 24 h stirring a dark red solution resulted; the solution was filtered and a dark-red solid was isolated after removing the solvent by rotary evaporation. ESI/MS (MeOH, m/z) 265 [Ni(NN^{im}S)]$^+$. Upon crystallizing by slow evaporation of a MeOH solution under N_2, dark red crystals formed which were identified as the [Ni(SN^{im}S)]$_2$ dimer.

4.5.4. Reaction of [Ni(NN^{im}S)Cl] with benzylated 2-aminoethanethiol

Under N_2, to a solution of benzylated 2-aminoethanethiol (0.050 g, 0.30 mmol) in 10 mL MeOH was added sodium hydroxide (0.012 g, 0.30 mmol). After stirring for 10 minutes the solution was added dropwise to a solution of [Ni(NN^{im}S)Cl] (0.045 g, 0.15 mmol) in 10 mL MeOH. After stirring for 24 h a dark red solution formed; the solution was filtered and a dark-red solid was

isolated after removing the solvent by rotary evaporation. The resulting solid was extracted into CH_2Cl_2. Upon crystallizing the product by vapor diffusion of diethyl ether in to a CH_2Cl_2 solution a dark red crystals were obtained which were identified as $[Ni(dmen)_2(H_2O)_2]\cdot 2Cl$ by X-ray crystallography.

4.5.5. Reaction of [Ni(NN^{im}S)Cl] with BOC Protected 2-aminoethanethiol

Under N_2, to a solution of boc-protected 2-Aminoethanethiol (0.10 g, 0.56 mmol) in 10 mL CH_2Cl_2 was added triethylamine (0.16 mL, 1.12 mmol). After stirring for 30 minutes the solution was added dropwise to [Ni(NN^{im}S)Cl] (0.08 g, 0.28 mmol) in 10 mL MeOH. After stirring for 24 h a red-brown solution formed. ESI-MS (MeOH, negative mode): 456 to $[Ni(NN^{im}S)S(CH_2)_2N(boc)]^-$.

4.5.6. Reaction of [Ni(NN^{im}S)Cl] with N'N-dimethylaminoethanethiol

Under N_2, to a solution of N'N-dimethylaminoethanethiol hydrochloride (0.28 g, 2.00 mmol) in 15 mL MeOH was added sodium hydroxide (0.16 g, 4.00 mmol). After stirring for 10 minutes the solution was added dropwise to [Ni(NN^{im}S)Cl] (0.30 g, 1.00 mmol) in 15 mL MeOH. After 48 h of stirring a dark red-brown solution and a dark brown precipitate resulted, the solution was filtered and the precipitate was isolated. Upon crystallization of the precipitate by slow evaporation of a CH_2Cl_2 solution dark brown crystals formed which were identified as [Ni(NN^{im}S)Cl]. ESI/MS of the filtrate shows a peak at 370 m/z corresponding to $[[Ni(NN^{im}S)SCH_2CH_2N(CH_3)_2]+H]^+$.

4.5.7. Reaction of [Ni(NN^{im}S)Cl] with 2-mercaptopyridine

Under N_2, to a solution of 2-mercaptopyridine (0.15 g, 1.35 mmol) in 10 mL DMF was added sodium hydride (0.03 g, 1.35 mmol). After stirring for 10 minutes the solution was added dropwise to [Ni(NN^{im}S)Cl] (0.20 g, 0.675 mmol) in 10 mL DMF. After 48 h stirring a dark red solution

resulted; the solution was filtered and a dark-red solid was isolated after removing the solvent by rotary evaporation. A sample in MeOH was used for mass spectrometry.

4.5.8. Reaction of [Ni(NN^{im}S)Cl] with 2-aminothiophenol

Under N_2, to a solution of 2-aminothiophenol (0.15 mL, 1.36 mmol) in 10 mL MeOH was added sodium hydroxide (0.15 g, 3.69 mmol). After stirring for 10 minutes the resulted solution was added dropwise to [Ni(NN^{im}S)Cl] (0.20 g, 0.68 mmol) in 10 mL MeOH. After 24 h stirring a dark purple color solution resulted, the solvent was evaporated by rotary evaporation and a sample in MeOH was used for mass spectrometry. Dark red crystals were obtained by slow evaporation of MeOH solution and they were identified as [Ni(SN^{im}S)]$_2$ dimer.

4.5.9. Reaction of [Ni(NN^{im}S)Cl] with 2-amino-4-(trifluoromethyl)benzenethiol

Under N_2, to a solution of 2-Amino-4-(trifluoromethyl)benzenethiol hydrochloride (0.15g, 0.66 mmol) in 10 mL MeOH was added sodium hydroxide (0.05 g, 1.32 mmol). After stirring for 10 minutes the solution was added dropwise and to [Ni(NN^{im}S)Cl] (0.10 g, 0.33 mmol) in 10 mL MeOH. After 24 h stirring a dark red solution resulted, the solvent was evaporated by rotary evaporation and a sample in MeOH was used for mass spectrometry.

4.5.10. Synthesis of [Ni$_3$(NN^{am}S)$_2$(SCH$_2$CH$_2$N(CH3)$_2$)$_2$] trimer

Under N_2, to a solution of N'N-(dimethylamino)ethanethiol hydrochloride (0.640 g, 4.50 mmol) in 30 mL MeOH was added sodium hydride (0.360 g, 9.00 mmol). After stirring for 20 min the solution was added dropwise to (Et$_4$N)[Ni(NN^{am}S)Cl] (1.00 g, 2.25 mmol) in 10 mL MeOH. After stirred 24h, a dark brown-red solution resulted. It was filtered and the solvent was removed by rotary evaporation yielding a dark brown-red solid. X-ray quality dark red crystals were grown by slow evaporation of a MeOH solution in N_2 environment. Elemental Anal. Calc. for

$C_{30}H_{48}N_6O_2S_4Ni_3.3H_2O$: C, 40.92; H, 6.40; N, 9.46. Found: C, 40.78; H, 6.18; N, 9.52 IR (cm^{-1}) 3046, 2998, 2890, 1583, 1566, 1511, 1455, 1367, 1293, 1069. ESI-MS (negative mode, MeOH, m/z): 384 $[Ni(NN^{am}S)SCH_2CH_2(CH_3)_2N]^-$, 827 $[\{Ni_3(NNS)_2(SCH_2CH_2(CH_3)_2N)_2\}+H]^+$, UV-Vis (acetonitrile); λ_{max} = 253, 453 nm.

4.5.11. Reaction of $[Ni(NN^{am}S)Cl]^-$ / $[Ni(NN^{am}S)OAc]^-$ with 2-aminoethanethiol

Under N_2, to a solution of 2-aminoethanethiol hydrochloride (0.150 g, 1.35 mmol) in 10 mL MeOH was added sodium hydroxide (0.110 g, 2.70 mmol). After stirring for 10 min the solution was added dropwise to $(Et_4N)[Ni(NN^{am}S)Cl]$ (0.30 g, 0.67 mmol) in 20 mL MeOH. After stirring for 48 h the solution was filtered, a yellow-green solution and a light green precipitate was resulted which is only soluble in hot DMSO. Mass spectrum of the filtrate in MeOH does not give peaks corresponds to the expected product.

Same reaction procedure was followed with $[Ni(NN^{am}S)OAc]^-$ and no evidence was obtained for the formation of the expected product.

4.5.12. Reaction of $[Ni(NN^{am}S)Cl]^-$ / $[Ni(NN^{am}S)OAc]^-$ with benzylated 2-aminoethanethiol

Under N_2, to a solution of benzylated 2-aminoethanethiol (0.26 g, 1.56 mmol) in 10 mL MeOH was added sodium hydroxide (0.12 g, 3.12 mmol). After stirring for 10 min the solution was added dropwise to $(Et_4N)[Ni(NN^{am}S)Cl]$ (0.35 g, 0.78 mmol) in 20 mL MeOH. After stirred for 24 h a dark brown solution was obtained. Solvent was removed by rotary evaporation and extracted into CH_2Cl_2. Mass spectrum was taken in MeOH. In addition to [Ni(NNS)Cl] peak no peaks observed relevant to $[Ni(NN^{am}S)SR]$. Reaction was done in DMF and the same result observed. No positive results obtained from the reaction with $[Ni(NN^{am}S)OAc]^-$.

4.5.13. Reaction of $[Ni(NN^{am}S)OAc]^-$ with BOC protected 2-aminoethanethiol

Under N_2, to a solution of boc-protected 2-aminoethanethiol (0.16 g, 0.90 mmol) in 10 mL CH_2Cl_2 was added triethylamine (0.13 mL, 0.90 mmol). After stirring for 10 min the solution was added dropwise to $(Et_4N)[Ni(NN^{am}S)OAc]$ (0.21 g, 0.45 mmol) in 20 mL MeOH. After stirred for 24 a red-brown solution was obtained and solvent was removed by rotary evaporation. Mass spectrum was taken in CH_2Cl_2 which shows 456 m/z in negative mode corresponding to $[Ni(NN^{am}S)SRN]^-$. Abundance of the peak was <1% and attempts at purification were not successful.

4.5.14. Reaction of $[Ni(NN^{am}S)Cl]^-$ / $[Ni(NN^{am}S)OAc]^-$ with cysteine ethyl ester

Under N_2, to a solution of cysteine ethylester hydrochloride (1.15 g, 6.19 mmol) in 20 mL MeOH was added sodium hydroxide (0.50 mL, 12.4 mmol). After stirring for 30 min the solution was added dropwise to $(Et_4N)[Ni(NN^{am}S)OAc]$ (1.45 g, 3.10 mmol) in 20 mL MeOH. With stirring for 24 a light green precipitate separated which is soluble in DMF and resulted a red-brown solution. Upon crystallizing the precipitate by vapor diffusion of diethyl ether into a DMF solution in which few drops of MeOH and CH_2Cl_2 added, green crystals formed. They were identified as $[Ni(cysteine\ methylester)_2]$ by X-ray crystallography. No evidence was obtained from the mass spectrum of the red-brown solution for the formation of expected product. The same reaction was repeated with $(Et_4N)[Ni(NN^{am}S)Cl]$ and the same precipitate was resulted.

4.5.15. Reaction of $[Ni(NN^{am}S)Cl]^-$ / $[Ni(NN^{am}S)OAc]^-$ with 6-mercaptopurine

Under N_2, to a solution of 6-mercaptopurine (0.290 g, 1.91 mmol) in 10 mL MeOH was added sodium hydroxide (0.15 g, 3.82 mmol). After stirring 10 min the solution was added dropwise to $(Et_4N)[Ni(NN^{am}S)Cl]$ (0.43 g, 0.96 mmol) in 20 mL MeOH. After stirred for 24 h a light yellow solution and an orange precipitate were obtained. The precipitate is only soluble in DMSO and no responsible peaks were observed from the mass spec of the filtrate. The same result was obtained with $(Et_4N)[Ni(NN^{am}S)OAc]$.

4.5.16. Reaction of $[Ni(NN^{am}S)Cl]^-$ / $[Ni(NN^{am}S)OAc]^-$ with 2-mercapopyridine

Under N_2, to a solution of 2-mercaptopyridine (0.11 g, 0.99 mmol) in 10 mL DMF was added sodium hydride (0.02 g, 0.99 mmol). After stirring for 10 min the solution was added dropwise to $(Et_4N)[Ni(NN^{am}S)Cl]$ (0.22 g, 0.50 mmol) in 20 mL MeOH. After stirring for 24 h a dark green-red solution was obtained. Solvent was evaporated by rotary evaporation and the resulted solid was extracted into MeOH. The mass spectrum in MeOH shows a relatively small peak (<10%) at 391 m/z corresponding to $[Ni(NN^{am}S)SR]$. Attempts at purification and crystallization were not successful.

4.5.17. Reaction of $[Ni(NN^{am}S)Cl]^-$ / $[Ni(NN^{am}S)OAc]^-$ with 2-aminothiophenol

Under N_2, to a solution of 2-aminothiophenol (0.20 mL, 1.84 mmol) in 10 mL MeOH was added sodium hydroxide (0.15 g, 3.68 mmol) and stirred for 20 minutes and it was added to $(Et_4N)[Ni(NN^{am}S)Cl]$ (0.41 g, 0.92 mmol) dropwise in 20 mL MeOH. A light yellow precipitate is separated quickly leaving a light yellow solution. No change was observed in the reaction after 24 h stirring. The precipitate is only soluble in hot DMSO and no $\nu_{C=O}$ peak observed in the IR spectrum. The reaction was done in DMF using NaH as the base, after refluxing overnight a relatively small amount of precipitate and a light-red solution was resulted. No evidence in ESI/MS was observed for the formation of the product.

The same result was obtained from the reaction with $(Et_4N)[Ni(NN^{am}S)OAc]$.

4.5.18. Reaction of $[Ni(NN^{am}S)Cl]^-$ with 2-amino-4-(trifluoromethyl)thiophenol

Under N_2, to a solution of 2-amino-4-(trifluoromethyl) thiophenol hydrochloride (0.21 g, 0.91 mmol) in 10 mL MeOH was added sodium hydroxide (0.07 g, 1.83 mmol). After stirring for 20 minutes the solution was added dropwise to a solution of $(Et_4N)[Ni(NN^{am}S)Cl]$ (0.20 g, 0.45 mmol) in 10 mL MeOH. With stirring a light yellow precipitate is separated from a red solution.

After 24 h stirring the solution was filtered and the precipitate was isolated which is soluble in DMF. IR spectrum of the precipitate has no peaks for $\nu_{C=O}$ or for aliphatic $\nu_{C-H.}$ No peaks in ESI/MS of the filtrate are relevant to expected products.

The reaction was done in DMF using NaH as the base. A dark-red solution was obtained and no evidence was observed from mass spectrometry for the formation of the product.

4.5.19. Reaction of $[Ni(NN^{am}S)Cl]^-$ with 2-(4,5-dihydro-1H-pyrrol-2-yl)benzenethiol

Under N_2, to a solution of 2-(4,5-dihydro-1H-pyrrol-2-yl)benzenethiol (0.10 g, 0.56 mmol) in 10 mL MeOH was added sodium hydroxide (0.02 g, 0.56 mmol). After atirring for 10 minutes the solution was added dropwise to $(Et_4N)[Ni(NN^{am}S)Cl]$ (0.12 g, 0.28 mmol) in 10 mL MeOH. With stirring a light yellow precipitate separated. After 24 h stirring a brown-green precipitate and a brown solution was obtained. The precipitate was isolated by filtering the solution which is only partially soluble in CH_3CH_2OH. IR spectrum of the precipitate shows peaks relevant to ν_{N-H} and aromatic ν_{C-H}. ESI/MS of the brown color filtrate in MeOH shows a peak at 456(-) <1% corresponding to the $[Ni(NN^{am}S)SR]^-$. Attempts at purification and crystallization were not successful.

CHAPTER 5: COMPARISON OF [Ni(NN^{am}S)SR]$^{-}$ & [Ni(NN^{im}S)SR] COMPLEXES

5.1. Introduction

As discussed in the previous chapters NiSOD has unique structural and functional properties that distinguishes it from other enzymes in the SOD family. The unprecedented coordination framework of NiSOD is crucial to give it those properties and therefore understanding the role of each component of the active site towards optimal catalytic activity is a very important subject to be addressed using synthetic models of NiSOD. This research is mainly focused on identifying the significance of the unusual amide N coordination in NiSOD by comparing models with and without amide N coordination.

This chapter presents the comparison of two model complexes [Ni(NN^{am}S)SPh]$^{-}$ (**15**) and [Ni(NN^{am}S)(4-NO$_2$PhS]$^{-}$ (**16**) which contain amine/amide/bisthiolate coordination and were discussed in chapter 3 (Figure 3.2.6.1) with the analogous model complexes [Ni(NN^{im}S)SPh] (**1**) and [Ni(NN^{im}S)(4-NO$_2$PhS] (**2**) containing amine/imine bisthiolate coordination and discussed in chapter 2 (Figure 2.2.2.1). These two types of model complexes are structurally similar except for the amide and imine coordination groups. Comparison of structural, electronic and activity properties of these complexes afforded insight to the importance of amide N coordination in NiSOD.

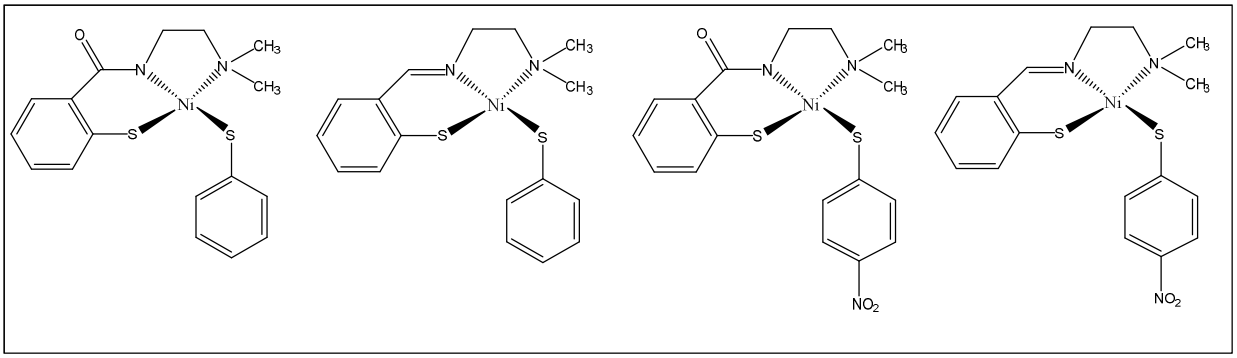

Figure 5.1.1. The two pairs of $[Ni(NN^{am}S)SR]^-$ & $[Ni(NN^{im}S)SR]$ complexes compared. (Left to right (**15**) (**1**) (**16**) and (**2**)).

5.2.1. Comparison of structures of analogous $[Ni(NN^{am}S)SR]^-$ and $[Ni(NN^{im}S)SR]$ complexes

The structures of the four mentioned complexes (Figure 5.1.1) were confirmed by X-ray crystallography (See Figures 2.2.2.1 and 3.2.6.1). Selected bond lengths and angles are compared in Table 5.2.1.1.

Table 5.2.1.1. Comparison of selected bond angles (º) and bond lengths (Å) of $[Ni(NN^{am}S)SR]^-$ and analogous $[Ni(NN^{im}S)SR]$ complexes

	15	**1**	**16**	**2**
$N_{amide/imine}$-Ni-N_{amine}	87.9(4)	86.21(11)	87.40(2)	86.44(9)
N_{amine}-Ni-S_{RS}	92.6(3)	92.13(8)	91.98(18)	91.96(7)
N_{amine}-Ni-S_{NNS}	95.4(3)	96.29(9)	95.42(16)	96.86(7)
S-Ni-S	85.31(14)	85.39(4)	85.08(6)	84.97(3)
Ni-N_{amine}	2.017(9)	2.015(3)	1.998(5)	1.989(2)
Ni-$N_{amide/imine}$	1.896(9)	1.884(3)	1.889(5)	1.889(2)
Ni-S_{NNS}	2.126(4)	2.141(9)	2.1261(16)	2.132(7)
Ni-S_{RS}	2.243(3)	2.219(10)	2.2278(17)	2.220(7)
Ni-S(RS)-C	111.8(5)	108.36(11)	110.4(2)	110.53(9)

Comparison of complex **15**, $[Ni(NN^{am}S)SPh]^-$ with complex **1**, $[Ni(NN^{im}S)SPh]$ clearly indicates that the bond angles in NiN_2S_2 coordination sphere in both complexes slightly deviate from the ideal square planar geometry. By comparison it is clear that there are no significant differences in bond lengths between the amide and imine containing complexes. The slight difference in $Ni\text{-}S_{NNS}$ distance between two complexes are apparently due to the phenyl ring of NNS ligand is not coplanar with the coordination plane.

Similar to complex **15** and **1**, comparison of complex **16**, $[Ni(NN^{am}S)(4\text{-}NO_2PhS]^-$ and **2**, $[Ni(NN^{im}S)(4\text{-}NO_2PhS]$ reveal the presence of slightly deviated coordination sphere from identical square planar geometry. The $Ni\text{-}N_{amide}$ distance in **16** and $Ni\text{-}N_{imine}$ distance in **2** are similar. This could be associated with less electron donating nature of S_{exo}. Similar to **15** and **1**, $Ni\text{-}N_{NNS}$ distance is slightly shorter (0.006 Å) in **16** and $Ni\text{-}S_{exo}$ is elongated by 0.007 Å. The thiolate substituent in **16** protrude more from the coordination plane than **2**. Altogether the structural parameters of these four complexes do not deviate significantly from each other.

5.2.2. Comparison of electronic properties of analogous $[Ni(NN^{am}S)SR]^-$ and $[Ni(NN^{im}S)SR]$ complexes

The UV-Vis spectra of complex **15**,**16**,**1** and **2** were collected in CH_3CN using a Shimadzu UV-1650 PC UV-Vis spectrophotometer. Comparison is reported in Table 5.2.2.1.

Table 5.2.2.1. Comparison of electronic absorption spectral properties of complexes **15, 1** and complex **16, 2**

Complex	**UV-Vis absorption spectral properties**		
	λ_1, nm (ε, $M^{-1}cm^{-1}$)	**λ_2, nm (ε, $M^{-1}cm^{-1}$)**	**λ_3, nm (ε, $M^{-1}cm^{-1}$)**
15	271 (1037)	304 (1056)	461 (84)
1	255 (1007)	304 (647)	424 (74)
16	266 (1048)	271 (1117)	452 (149)
2	253 (1265)	295 (665)	423 (667)

UV-Vis spectra of complexes **15** and **1** and complex **16** and **2** are very similar. The high energy spectral bands arise due to LMCT from S to Ni as reported for similar square planer $Ni^{+2}N_2S_2$ complexes.[99,76,88,75,105] Low intensity bands in the visible region are considered due to d-d transitions with a minor charge-transfer contribution.[88] Compared to amine/imine containing complexes **1** and **2**, the ligand field bands in amine/amide containing complexes **15** and **16** have shifted to higher energy. This could be due to the weaker ligand field in former complexes that may result decreased energy of the d-d transitions.

5.2.3. Comparison of electrochemistry of analogous $[Ni(NN^{am}S)SR]^-$ and $[Ni(NN^{im}S)SR]$ complexes

The electrochemistry of complex **15** and **1**, **16** and **2** studied by cyclic voltammetry was compared. Cyclic voltammetry was performed in CH_3CN on a PAR potentiostat model 263A at room temperature and the potentials are reported vs Ag/AgCl.

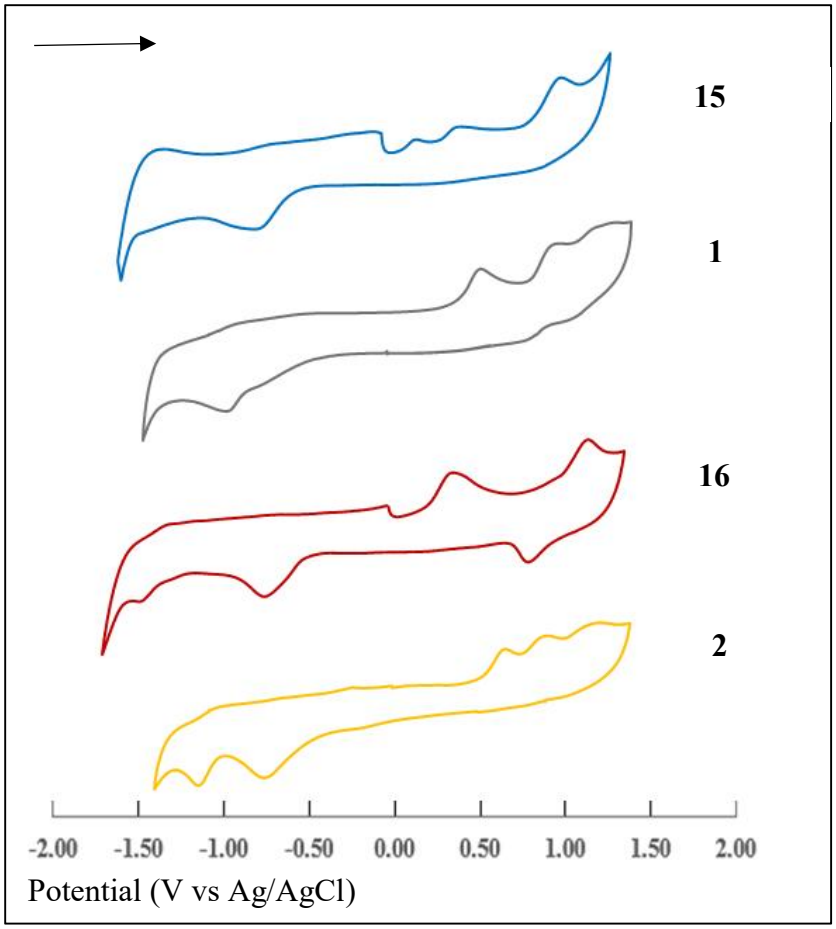

Figure 5.2.3.1. Cyclic voltagramms of **15**, **1**, **16**, **2** (top to bottom) (vs Ag/AgCl in CH_3CN, 0.1M Et_4NClO_4 supporting electrolyte, glassy carbon working electrode, scan rate 100 mV/S, arrow indicates the direction of scan).

Table 5.2.3.1. Comparison of oxidation potentials of complexes **15**, **1** and **16**, **2** (vs Ag/AgCl) in CH_3CN.

Complex	**15**	**1**	**16**	**2**
E^{ox}_1 (mV vs. Ag/AgCl)	228	536	436	715
E^{ox}_2 (mV vs. Ag/AgCl)	523	939	_	983
E^{ox}_3 (mV vs. Ag/AgCl)	1174	1301	1271	1317

As seen in the Figure 5.2.3.1 cyclic voltammetry reveals irreversible/quasi reversible oxidation events for all four complexes (vs Ag/AgCl) in CH_3CN. This has been reported in many Ni(II)N_2S_2

complexes.[88,76,58,] According to E^{ox} peaks as shown in the Table 5.2.3.1 it is clear that the coordination environment plays an important role in determining E^{ox} values. First, comparison between complexes **15** and **16** and between complexes **1** and **2** reveals that there is a correlation between the donor strength of the monodentate thiolate and the E^{ox} values. The complexes with the more electron-donating SPh ligand (**15** and **1**) display less positive oxidation potentials than the analogous complexes with the less electron-withdrawing $SPhNO_2$ ligand (**16** and **2**). Comparing the amide-containing complexes **15** and **16** with the analogous imine-containing complexes **1** and **2** shows that the E^{ox} for complex **15** and **16** are less positive compared to those in **1** and **2** respectively, indicating oxidation of the Ni center in amine/amide complexes are easier than in corresponding amine/imine complexes. This effect is related to that observed in $[Ni(nmp)SR]^-$ complexes reported by Harrop and co-workers,[88] in which diamide/dithiolate complexes were compared to diimine/dithiolate complexes.[88] Our results are important, in that they are the first comparison of amide/amine/dithiolate complexes with their imine/amine/dithiolate analogues. These results confirm that incorporation of the amide ligand is likely very important in tuning the nickel center of NiSOD to lower potential.

5.2.4. Comparison of reactivity of analogous $[Ni(NN^{am}S)SR]^-$ and $[Ni(NN^{im}S)SR]$ complexes

The ability for superoxide reactivity of all above mentioned four complexes was studied via nitroblue tetrazolium (NBT) assay.[73] Since amide containing complexes are not air stable and undergo color bleach with time, NBT assay of all four complexes was performed in glove box under N_2 environment. UV-Vis absorption properties were also monitored under N_2 environment using EPP2000 StellarNet Inc spectrophotometer housed in glove box. In the presence of superoxide NBT forms a deep blue color formazan which shows maximum absorbance at 580 nm. As the four Ni complexes are not sufficiently soluble and stable in water, a DMF/MeOH (1:1)

mixture was used to carry out the study. 100 equivalents of KO_2 were exposed to NBT (36 µM) in the absence and presence of Ni complexes **15**,**16**,**1** and **2** (40 µM) and the absorption at 580 nm was monitored. The differential absorptions at 580 nm between a run in which no Ni complex was added and a run in which the Ni complex was added (corrected for the absorption of the pure Ni complex) were plotted vs time (Figure 5.2.4.1).

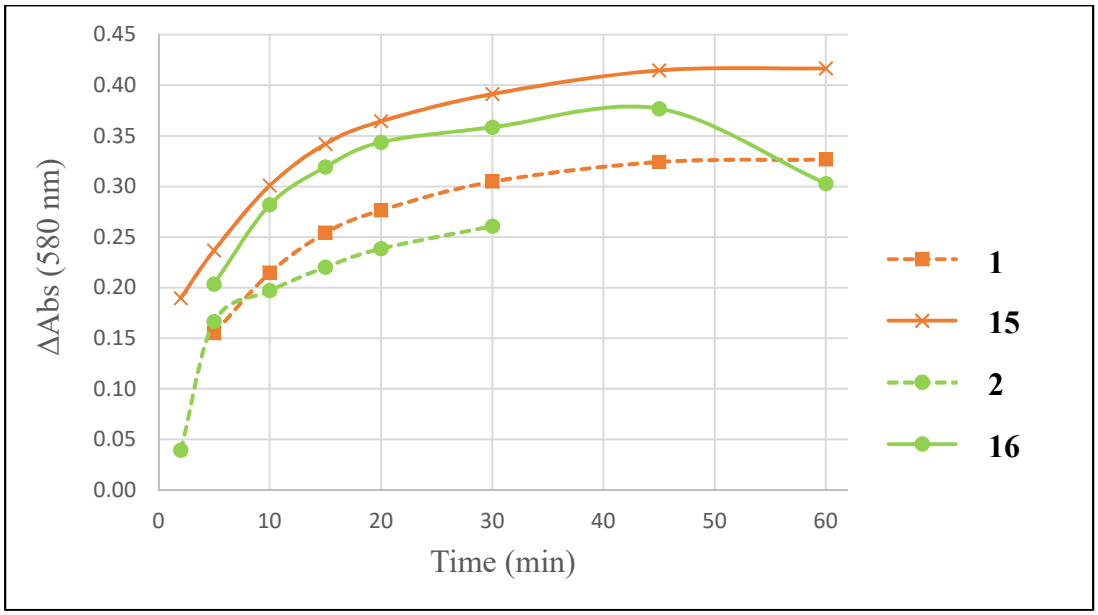

Figure 5.2.4.1. Differential absorption at 580 nm of complexes **1**, **15**, **2** and **16** obtained from NBT assay.

If the Ni complex is able to catalyze the decomposition of O_2^-, it is expected that the runs with the Ni complex to show a lower absorption and therefore result in a positive differential. As shown in the Figure 5.2.4.1 it is appeared to be true for all four complexes. This clearly indicates that the two complexes with amide-donor ligands show a large differential than those with imine-donor ligands, suggesting that amide-donor complexes have increased ability to catalyze O_2^- disproportionation.

5.3. Conclusions

The structure, electronic properties and reactivity of two complexes **15** and **16** with amine/amide/bisthiolate coordination were compared with the two analogous amine/imine/bisthiolate complexes **1** and **2**. Structurally both types of complexes share slightly deviated square-planar geometry around Ni and there are no considerable differences in bond lengths and angles. The comparison of UV-Vis spectral properties shows the two complexes with amide-donor ligands have low energy ligand filed bands in visible region compared to those with imine-donor containing complexes. This could be due to the weaker ligand field in imine-donor containing complexes. The cyclic voltammetry measurements show both ligand based and Ni based oxidation events and the comparison reveals that the redox potentials of amide-containing complexes are less positive compared to imine-containing complexes, and high electron donor strength of monodentate thiolates lead to lower the redox potentials and thereby make easier to oxidize the Ni center.

CHAPTER 6: CONCLUSIONS

The uniqueness of the NiSOD enzyme among other metalloenzymes attracts scientists and motivates them to understand the structure-function relationship of the enzyme. The model approach, which is the design, synthesis and study of small molecules that mimic an active site of an enzyme is a popular method among scientists to unveil the chemistry of enzymes. This approach has been used for more than a decade in the Eichhorn group to study metalloenzymes including NiSOD. In the work described in this dissertation, we have successfully synthesized and studied six mononuclear Ni(II) complexes with amine/imine/bisthiolate coordination of the form [Ni($NN^{im}S$)SR] and two analogous complexes with amine/amide/bisthiolate coordination, [Ni($NN^{am}S$)SR]. The first group of complexes incorporate a tridentate $NN^{im}S$ ligand with one amine, one imine, and one thiolate donor and a monodentate thiolate ligand, while the second group of complexes incorporate a tridentate $NN^{am}S$ ligand with one amine, one amide, and one thiolate donor as the models of the NiSOD active site. A number of related trinuclear species have also been synthesized and characterized. Structures of all these complexes were confirmed by X-ray crystallography. Different thiolate ligands with varying electron donating nature were utilized and the comparison of structural, spectroscopic and reactivity properties of the two types of complexes allowed us to understand the importance of the presence of amide N coordination in NiSOD.

The success gained in this work of synthesizing imine containing Ni-N/S complexes using DTDB, again demonstrates the suitability of DTDB as a starting material to make metal imine complexes with thiolate coordination. The complexes with amide N coordination were successfully made by using the bis(acid chloride) analogue of DTDB namely, 2'2-dithiosalicylyl chloride (DTSACl). The [Ni($Ni^{amine}N^{amide}S$)SR] complexes are monoanionic and the two complexes made were

crystallized with non-coordinating complex cations, tetraphenylarsonium (Ph_4As^+) and tetraphenylphosponium (TPP^+). Trinuclear species of the form [{Ni($NN^{am}S$)(SR)}$_2$Ni] resulted only from the amide containing NNS ligand. The stronger amide donor may promote bridging through the thiolates of two anionic monomers to a central Ni atom to give neutral trimeric complexes.

The stronger donor ability of the amide N compare to the imine N make the amide containing models less stable in air. This highlights the role of the protein network of NiSOD towards the stability of the enzyme. In addition to the NiN_2S_2 four coordinate models to mimic the NiSOD reduced state, we attempted to make five coordinate NiN_3S_2 models to mimic the oxidized NiSOD state. The thiolates utilized contain both N and S donor sites and were expected to coordinate through both sites to the Ni atom in the Ni(NNS) moiety to give five coordinate complexes. None of these attempts were successful and ended up with the formation of dimer/trimer/polymer materials.

The two types of [Ni(NNS)SR] models show very similar structural properties and electronic absorption properties as evidenced by X-ray crystallography and UV-Vis spectroscopy. This reveals that the nature of the thiolate ligands has very little influence on the structural and electronic properties of these complexes. Cyclic voltammetry measurements showed two distinct trends. The redox potentials of the [Ni(NNS)SR] models shifted to less positive values as the electron donor strength of the exogenous thiolate increases and, compared to imine containing models the analogous amide containing models showed less positive redox potentials. These results demonstrate the role the amide donor plays in tuning the redox potential of NiSOD. Even though these models are still missing one of the major features present in the enzyme, the fifth N donor, we studied their ability to perform the superoxide disproportionation. None of the

complexes showed reactivity consistent with an effective catalyst, but the results suggest that the optimization of amide containing models may have more promised reactivity compared to imine containing models.

In summary, we have been able to synthesize and study a series of Ni(II)N_2S_2 complexes as models for the reduced state of the NiSOD and further understand the importance of the presence of an amide ligand over an imine ligand in NiSOD, towards superoxide disproportionation activity. Even though we were not successful at synthesizing Ni(III)N_3S_2 complexes to mimic the oxidized state of NiSOD, this work would give one a solid foundation to make an efficient synthetic catalysts for NiSOD in the future.

REFERENCES

LIST OF REFERENCES

(1) Sigel Helmut, S. A. *Metal Ions in Biological Systems*; New York : M. Dekker, c1983.

(2) Landis, G. N.; Tower, J. *Mech. Ageing Dev.* **2005**, *126* (8), 907–908.

(3) Barondeau, D. P.; Kassmann, C. J.; Bruns, C. K.; Tainer, J. A.; Getzoff, E. D. *Biochemistry* **2004**, *43* (25), 8038–8047.

(4) Noor, R.; Mittal, S.; Iqbal, J. *Med Sci Monit*. **2002**, *8* (9), 210–216.

(5) Fukai, T.; Ushio-Fukai, M. *Antioxid. Redox Signal.* **2011**, *15* (6), 1583–1606.

(6) *Nickel and its surprising impact in nature vol 2, 2007, Astrid Sigel, Helmut Sigel, Roland K. O. Sigel page 418-422*; **2007**; Vol. 2.

(7) Hunter, T.; Ikebukuro, K.; Bannister, W. H.; Bannister, J. V.; Hunter, G. J. *Biochemistry* **1997**, *36* (16), 4925–4933.

(8) Eldik, R. van.; Hubbard, C. D. *Advances in inorganic chemistry*; Orlando : Academic Press, **1987**.

(9) Hearn, A. S.; Stroupe, M. E.; Cabelli, D. E.; Ramilo, C. A.; Luba, J. P.; Tainer, J. A.; Nick, H. S.; Silverman, D. N. *Biochemistry* **2003**, *42* (10), 2781–2789.

(10) Whittaker, J. W. *Biochem. Soc. Trans.* **2003**, *31* (Pt 6), 1318–1321.

(11) Perry, J. J. P.; Hearn, A. S.; Cabelli, D. E.; Nick, H. S.; Tainer, J. A.; Silverman, D. N. *Biochemistry* **2009**, *48* (15), 3417–3424.

(12) Hearn, A.S., Stroupe, M.E., Ramilo, C.A., Luba, J.P., Cabelli, D.E., Tainer, J.A., Silverman, D. N. **2002**, 2002.

(13) Atzenhofer, W.; Regelsberger, G.; Jacob, U.; Peschek, G. A.; Furtmüller, P. G.; Huber, R.; Obinger, C. *J. Mol. Biol.* **2002**, *321* (3), 479–489.

(14) Vance, C. K.; Miller, A. F. *Biochemistry* **1998**, *37* (16), 5518–5527.

(15) Stoddard, B. L.; Howell, P. L.; Ringe, D.; Petskos, G. A. *Biochemistry* **1990**, *29* (38), 8885–8893.

(16) Abreu, I. A.; Cabelli, D. E. *Biochim. Biophys. Acta - Proteins Proteomics* **2010**, *1804* (2), 263–274.

(17) Chalovich, J. M.; Eisenberg, E. *Biophys. Chem.* **2005**, *257* (5), 2432–2437.

(18) Zheng, J.; Domsic, J. F.; Cabelli, D.; McKenna, R.; Silverman, D. N. *Biochemistry* **2007**, *46* (51), 14830–14837.

(19) Leitch, J. M.; Li, C. X.; Baron, J. a; Matthews, L. M.; Cao, X.; Hart, P. J.; Culotta, V. C. *Biochemistry* **2012**, *51* (2), 677–685.

(20) Carloni, P.; Bloechl, P.; Parrinello, M. *J. Phys. Chem.* **1995**, *99* (January), 1338–1348.

(21) Tainer, John A. Getzoff D. Elizabeth, Richardson S. Jane, R. C. D. *Nature* **1983**, *306* (November), 1983.

(22) Branco, R. J. F.; Fernandes, P. A.; Ramos, M. J. *J. Phys. Chem. B* **2006**, *110* (33), 16754–16762.

(23) Jefferson Lab., http://education.jlab.org/itselemental/ele028.html (accessed Oct 3, 2017).

(24) Ragsdale, S. W. *Encycl. Inorg. Chem.* **2006**, *1* (i), 1–16.

(25) Zamble, D. B. *Metallomics* **2015**, *7* (4), 588–589.

(26) Holm, R. H.; Kennepohl, P.; Solomon, E. I. *Chem. Rev.* **1996**, *96* (7), 2239–2314.

(27) Halcrow, M.; Christou, G. *Biomimetic Chemistry of Nickel*; 1994; Vol. 94.

(28) Murray, C. K.; Margerum, D. W. *Inorg. Chem.* **1982**, *21* (9), 3501–3506.

(29) Shearer, J. *Acc. Chem. Res.* **2014**, *47* (8), 2332–2341.

(30) Ragsdale, S. W. *J. Biol. Chem.* **2009**, *284* (28), 18571–18575.

(31) Mcmaster, M. L.; Kristinsson, S. Y.; Turesson, I.; Bjorkholm, M.; Landgren, O. *Clin. Lymphoma* **2010**, *9* (1), 19–22.

(32) Mulrooney, S. B.; Hausinger, R. P. *FEMS Microbiol. Rev.* **2003**, *27* (2–3), 239–261.

(33) Maroney, M. J.; Ciurli, S. *Chem. Rev.* **2014**, *114* (8), 4206–4228.

(34) Hegg, E. L. *Acc. Chem. Res.* **2004**, *37* (10), 775–783.

(35) Harrop, T. C.; Olmstead, M. M.; Mascharak, P. K. *Inorg. Chem.* **2006**, *45* (8), 3424–3436.

(36) Ito, M.; Kotera, M.; Song, Y.; Matsumoto, T.; Tatsumi, K. *Inorg. Chem.* **2009**, *48* (3), 1250–1256.

(37) Ragsdale, S. W. *J. Inorg. Biochem.* **2007**, *101* (11–12), 1657–1666.

(38) Can, M.; Armstrong, F. A.; Ragsdale, S. W. *Chem. Rev.* **2014**, *114* (8), 4149–4174.

(39) Lacasse, M. J.; Zamble, D. B. *Biochemistry* **2016**, *55* (12), 1689–1701.

(40) Kaliakin, D. S.; Zaari, R. R.; Varganov, S. A. *J. Phys. Chem. A* **2015**, *119* (6), 1066–1073.

(41) Volbeda, A.; Garcin, E.; Piras, C.; De Lacey, A. L.; Fernandez, V. M.; Hatchikian, E. C.; Frey, M.; Fontecilla-Camps, J. C. *J. Am. Chem. Soc.* **1996**, *118* (51), 12989–12996.

(42) Fichtner, C.; Laurich, C.; Bothe, E.; Lubitz, W. *Biochemistry* **2006**, *45* (32), 9706–9716.

(43) Vardar-Schara, G.; Maeda, T.; Wood, T. K. *Microb. Biotechnol.* **2008**, *1* (2), 107–125.

(44) De Gioia, L.; Fantucci, P.; Guigliarelli, B.; Bertrand, P. *Inorg. Chem.* **1999**, *38* (11), 2658–2662.

(45) Nishigaki, J. I.; Matsumoto, T.; Tatsumi, K. *Inorg. Chem.* **2012**, *51* (6), 3690–3697.

(46) Ebner, S.; Jaun, B.; Goenrich, M.; Thauer, R. K.; Harmer, J. *J. Am. Chem. Soc.* **2010**, *132* (2), 567–575.

(47) Wongnate, T.; Ragsdale, S. W. *J. Biol. Chem.* **2015**, *290* (15), 9322–9334.

(48) Harmer, J.; Finazzo, C.; Piskorski, R.; Ebner, S.; Duin, E. C.; Goenrich, M.; Thauer, R. K.; Reiher, M.; Schweiger, A.; Hinderberger, D.; Jaun, B. *J. Am. Chem. Soc.* **2008**, *130* (33), 10907–10920.

(49) Sarangi, R.; Dey, M.; Ragsdale, S. W. *Biochemistry* **2009**, *48* (14), 3146–3156.

(50) Sheng, Y.; Abreu, I. A.; Cabelli, D. E.; Maroney, M. J.; Miller, A. F.; Teixeira, M.; Valentine, J. S. *Chem. Rev.* **2014**, *114* (7), 3854–3918.

(51) Eitinger, T. *J. Bacteriol.* **2004**, *186* (22), 7821–7825.

(52) Broering, E. P.; Truong, P. T.; Gale, E. M.; Harrop, T. C. *Biochemistry* **2013**, *52* (1), 4–18.

(53) Shearer, J.; Long, L. M. *Inorg. Chem.* **2006**, *45* (6), 2358–2360.

(54) Ryan, K. C.; Guce, A. I.; Johnson, O. E.; Brunold, T. C.; Cabelli, D. E.; Garman, S. C.; Maroney, M. J. *Biochemistry* **2015**, *54* (4), 1016–1027.

(55) Zahn, S.; Schmidt, M.; Zahn, S.; Carella, M.; Ohlenschläger, O. *ChemBioChem*. **2017**, 9, 2135-2146.

(56) Lee, W. Z.; Chiang, C. W.; Lin, T. H.; Kuo, T. S. *Chem. - A Eur. J.* **2012**, *18* (1), 50–53.

(57) Pelmenschikov, V.; Siegbahn, P. E. *J Am Chem Soc* **2006**, *128* (23), 7466–7475.

(58) Broering, E. P.; Dillon, S.; Gale, E. M.; Steiner, R. A.; Telser, J.; Brunold, T. C.; Harrop, T. C. *Inorg. Chem.* **2015**, *54* (8), 3815–3828.

(59) Herbst, R. W.; Guce, A.; Bryngelson, P. A.; Higgins, K. A.; Ryan, K. C.; Cabelli, D. E.; Garman, S. C.; Maroney, M. J. *Biochemistry* **2009**, *48* (15), 3354–3369.

(60) Gale, E. M.; Simmonett, A. C.; Telser, J.; Schaefer, H. F.; Harrop, T. C. *Inorg. Chem.* **2011**, *50* (19), 9216–9218.

(61) Ryan, K. C.; Johnson, O. E.; Cabelli, D. E.; Brunold, T. C.; Maroney, M. J. *J. Biol. Inorg. Chem.* **2010**, *15* (5), 795–807.

(62) Youn, H.-D.; Kim, E.-J.; Roe, J.-H.; Hah, Y. C.; Kang, S.-O. *Biochem. J.* **1996**, *318*, 889–896.

(63) Mullins, C. S.; Grapperhaus, C. A.; Frye, B. C.; Wood, L. H.; Hay, A. J.; Buchanan, R. M.; Mashuta, M. S. *Inorg. Chem.* **2009**, *48* (21), 9974–9976.

(64) Fiedler, A. T.; Bryngelson, P. A.; Maroney, M. J.; Brunold, T. C. *J. Am. Chem. Soc.* **2005**, *127* (15), 5449–5462.

(65) Fiedler, A. T.; Bryngelson, P. A.; Maroney, M. J.; Brunold, T. C. *J. Am. Chem. Soc.* **2005**, *127* (15), 5449–5462.

(66) Miller, A. F. *Curr. Opin. Chem. Biol.* **2004**, *8* (2), 162–168.

(67) Choudhury, S. B.; Lee, J. W.; Davidson, G.; Yim, Y. I.; Bose, K.; Sharma, M. L.; Kang, S. O.; Cabelli, D. E.; Maroney, M. J. *Biochemistry* **1999**, *38* (12), 3744–3752.

(68) Tietze, D.; Voigt, S.; Mollenhauer, D.; Tischler, M.; Imhof, D.; Gutmann, T.; González, L.; Ohlenschläger, O.; Breitzke, H.; Görlach, M.; Buntkowsky, G. *Angew. Chemie - Int. Ed.* **2011**, *50* (13), 2946–2950.

(69) Szilagyi, R. K.; Bryngelson, P. a.; Maroney, M. J.; Hedman, B.; Hodgson, K. O.; Solomon, E. I. *J. Am. Chem. Soc.* **2004**, *126* (10), 3018–3019.

(70) Shearer, J.; Long, L. M. *Inorg. Chem.* **2006**, *45* (6), 2358–2360.

(71) Shearer, J.; Neupane, K. P.; Callan, P. E. *Inorg. Chem.* **2009**, *48* (22), 10560–10571.

(72) Neupane, K. P.; Gearty, K.; Francis, A.; Shearer, J. *J. Am. Chem. Soc.* **2007**, *129* (47), 14605–14618.

(73) Jenkins, R. M.; Singleton, M. L.; Almaraz, E.; Reibenspies, J. H.; Darensbourg, M. Y. *Inorg. Chem.* **2009**, *48* (15), 7280–7293.

(74) Fiedler, A. T.; Brunold, T. C. *Inorg. Chem.* **2007**, *46* (21), 8511–8523.

(75) Shearer, J.; Zhao, N. Inorg. Chem. **2006**, *45* (24), 9637–9639.

(76) Mathrubootham, V.; Thomas, J.; Staples, R.; McCraken, J.; Shearer, J.; Hegg, E. L. *Inorg. Chem.* **2010**, *49* (12), 5393–5406.

(77) Grapperhaus, C. A.; Mullins, C. S.; Kozlowski, P. M.; Mashuta, M. S. *Inorg. Chem.* **2004**, *43* (9), 2859–2866.

(78) Gale, E. M.; Patra, A. K.; Harrop, T. C. *Inorg. Chem.* **2009**, *48* (13), 5620–5622.

(79) Gale, E. M.; Narendrapurapu, B. S.; Simmonett, A. C.; Schaefer, H. F.; Harrop, T. C. *Inorg. Chem.* **2010**, *49* (15), 7080–7096.

(80) Ma, H.; Chattopadhyay, S.; Petersen, J. L.; Jensen, M. P. *Inorg. Chem.* **2008**, *47* (18), 7966–7968.

(81) Steiner, R. A.; Dzul, S. P.; Stemmler, T. L.; Harrop, T. C. *Inorg. Chem.* **2017**, *56* (5), 2849–2862.

(82) Smucker, B. W.; VanStipdonk, M. J.; Eichhorn, D. M. *J. Inorg. Biochem.* **2007**, *101* (10), 1537–1542.

(83) Eichhorn, D. M.; Goswami, N. *Comments Inorg. Chem.* **2003**, *24* (March 2014), 1–13.

(84) Goswami, N.; Eichhorn, D. M. *Inorg. Chem.* **1999**, *38*, 4329–4333.

(85) Zimmerman, J. R.; Smucker, B. W.; Dain, R. P.; Van Stipdonk, M. J.; Eichhorn, D. M. *Inorganica Chim. Acta* **2011**, *373* (1), 54–61.

(86) Sullivan, M. T.; Senaratne, N. K.; Eichhorn, D. M. *Polyhedron* **2016**, *114*, 152–155.

(87) Hatlevik, yvind; Blanksma, M. C.; Mathrubootham, V.; Arif, A. M.; Hegg, E. L. *J. Biol. Inorg. Chem.* **2004**, *9* (2), 238–246.

(88) Gale, E. M.; Cowart, D. M.; Scott, R. A.; Harrop, T. C. *Inorg. Chem.* **2011**, *50* (20), 10460–10471.

(89) Goswami, N. and Eichhorn, D.M. *Inorg. Chim. Acta* **2000**, *303*, 271

(90) Zimmerman, J. R.; Smucker, B. W.; Dain, R. P.; Van Stipdonk, M. J.; Eichhorn, D. M. *Inorganica Chim. Acta* **2011**, *373* (1), 54–61.

(91) Bruker (2007). APEX. Bruker AXS Inc., Madison, WI, USA.

(92) Bruker (2007). SAINT. Bruker AXS Inc., Madison, WI, USA.

(93) V2014/4, George M. Sheldrick 2010-2014.

(94) Dolomanov, O. V.; Bourhis, L. J.; Glidea, R. J.; Howard, J. A. K.; Puschmann, H. *J. Appl. Crystallogr.* **2009**, *42*, 339–34

(95) Moore, Curtis.E., 2007, Modeling the active sites of metalloenzymes with thiolate coordination, Retrieved from httt://soar.wichita.edu/handle/10057/1492

(96) Denny, J. A.; Darensbourg, M. Y. *Chem. Rev.* **2015**, *115* (11), 5248–5273.

(97) Shearer, J.; Dehestani, A.; Abanda, F. *Inorg. Chem.* **2008**, *47* (7), 2649–2660.

(98) Nakane, D.; Wasada-Tsutsui, Y.; Funahashi, Y.; Hatanaka, T.; Ozawa, T.; Masuda, H. *Inorg. Chem.* **2014**, *53* (13), 6512–6523.

(99) Fritz, T.; Steinfeld, G.; Kersting, B. *Zeitschrift fur Naturforsch. - Sect. B J. Chem. Sci.* **2007**, *62* (4), 508–518.

(100) Neupane, K. P.; Shearer, J. *Inorg. Chem.* **2006**, *45* (26), 10552–10566.

(101) Tobergte, D. R.; Curtis, S. *J. Chem. Inf. Model.* **2013**, *53* (9), 1689–1699.

(102) Bouwman, E.; Henderson, R. K.; Powell, A. K.; Reedijk, J.; Smeets, W. J. J.; Spek, A. L.; Veldman, N.; Wocadlo, S. *J. Chem. Soc., Dalt. Trans.* **1998**, No. 20, 3495–3500.

(103) El-Gendy, B. E. D. M.; Ghazvini Zadeh, E. H.; Sotuyo, A. C.; Pillai, G. G.; Katritzky, A. R. *Chem. Biol. Drug Des.* **2013**, *81* (5), 577–582.

(104) Harrop, T. C.; Olmstead, M. M.; Mascharak, P. K. *Chem. Commun.* **2004**, *2410* (15), 1744–1745.

(105) Tamayo, A.; Casab, J.; Escriche, L.; Lodeiro, C.; Covelo, B.; Brondino, C. D.; Kiveks, R.; Sillamp, R. *Inorg. Chem.* **2006**, *45* (3), 1140–1149.

APPENDIX (Crystallographic Tables)

Table A: Crystallographic Data

Compound	[Ni(NN^{im}S)SPh]	[Ni(NN^{im}S)(4-NO$_2$PhS)]
Empirical formula	$C_{17}H_{20}N_2S_2Ni$	$C_{17}H_{19}N_3NiO_2S_2$
Formula weight	375.18	420.18
Temperature/K	150	150
Crystal system	monoclinic	monoclinic
Space group	$P2_1/n$	Cc
a/Å	8.3054(4)	10.8613(8)
b/Å	18.2939(9)	18.6949(15)
c/Å	10.8345(5)	9.0507(7)
α/°	90	90
β/°	98.592(3)	92.178(4)
γ/°	90	90
Volume/Å^3	1627.70(14)	1836.4(2)
Z	4	4
ρ_{calc}g/cm^3	1.531	1.520
μ/mm^{-1}	1.445	1.299
F(000)	784.0	872.0
Crystal size/mm^3	0.401 × 0.217 × 0.099	0.565 × 0.246 × 0.081
Radiation	MoKα (λ = 0.71073)	MoKα (λ = 0.71073)
2Θ range for data collection/°	5.438 to 51.998	7.51 to 54.81
Index ranges	$-10 \le h \le 10$ $-22 \le k \le 22$ $-13 \le l \le 13$	$-13 \le h \le 14$ $-24 \le k \le 23$ $-11 \le l \le 11$
Reflections collected	19495	17141
Independent reflections	3194 [R_{int} = 0.0771, R_{sigma} = 0.0568]	3792 [R_{int} = 0.0215, R_{sigma} = 0.0294]
Data/restraints/parameters	3194/0/201	3792/2/229
Goodness-of-fit on F^2	1.040	1.028
Final R indexes [I>=2σ (I)]	R_1 = 0.0386, wR_2 = 0.0882	R_1 = 0.0205, wR_2 = 0.0450
Final R indexes [all data]	R_1 = 0.0647, wR_2 = 0.1001	R_1 = 0.0225, wR_2 = 0.0456
Largest diff. peak/hole / e Å^{-3}	0.47/-0.42	0.24/-0.17

Table A: Crystallographic Data (cont.)

Compound	[Ni(NN^{im}S)(4-^{t}BuPhS)]
Empirical formula	$C_{21}H_{28}N_2NiS_2$
Formula weight	431.28
Temperature/K	150
Crystal system	orthorhombic
Space group	Pbca
a/Å	14.9466(19)
b/Å	10.8127(15)
c/Å	27.158(4)
α/°	90
β/°	90
γ/°	90
Volume/Å^3	4389.2(10)
Z	8
ρ_{calc}g/cm^3	1.305
μ/mm^{-1}	1.081
F(000)	1824.0
Crystal size/mm^3	0.602 × 0.268 × 0.242
Radiation	MoKα (λ = 0.71073)
2Θ range for data collection/°	7.276 to 54.356
Index ranges	-19 ≤ h ≤ 19 -13 ≤ k ≤ 13 -34 ≤ l ≤ 34
Reflections collected	133002
Independent reflections	4844 [R_{int} = 0.0609, R_{sigma} = 0.0250]
Data/restraints/parameters	4844/0/240
Goodness-of-fit on F^2	1.039
Final R indexes [I>=2σ (I)]	R_1 = 0.0420, wR_2 = 0.1084
Final R indexes [all data]	R_1 = 0.0717, wR_2 = 0.1268
Largest diff. peak/hole / e Å^{-3}	0.44/-0.39

Table A: Crystallographic Data (cont.)

Compound	Ni(NN^{im}S)(4-ClPhS)]	Ni(NN^{im}S)(4-FPhS)
Empirical formula	$C_{17}H_{19}ClN_2NiS_2$	$C_{17}H_{19}N_2FS_2Ni$
Formula weight	409.62	393.17
Temperature/K	150	150
Crystal system	monoclinic	monoclinic
Space group	$P2_1/n$	$P2_1/n$
a/Å	8.9086(12)	8.558(5)
b/Å	17.699(2)	18.001(11)
c/Å	11.2809(15)	11.153(7)
α/°	90	90
β/°	93.964(7)	97.64(2)
γ/°	90	90
Volume/Å^3	1774.4(4)	1703.0(18)
Z	4	4
ρ_{calc}g/cm^3	1.533	1.533
μ/mm^{-1}	1.478	1.393
F(000)	848.0	816.0
Crystal size/mm^3	0.464 × 0.178 × 0.171	0.425 × 0.151 × 0.126
Radiation	MoKα (λ = 0.71073)	MoKα (λ = 0.71073)
2Θ range for data collection/°	7.242 to 54.212	6.6 to 53.778
Index ranges	$-11 \le h \le 11$ $-22 \le k \le 22$ $-14 \le l \le 14$	$-10 \le h \le 10$ $-22 \le k \le 22$ $-14 \le l \le 13$
Reflections collected	55176	29964
Independent reflections	3891 [R_{int} = 0.0498, R_{sigma} = 0.0318]	3613 [R_{int} = 0.1148, R_{sigma} = 0.0831]
Data/restraints/parameters	3891/0/210	3613/0/210
Goodness-of-fit on F^2	0.959	0.947
Final R indexes [I>=2σ (I)]	R_1 = 0.0430, wR_2 = 0.1327	R_1 = 0.0703, wR_2 = 0.1819
Final R indexes [all data]	R_1 = 0.0649, wR_2 = 0.1569	R_1 = 0.1211, wR_2 = 0.2221
Largest diff. peak/hole / e Å^{-3}	0.50/-0.64	0.61/-1.49

Table A: Crystallographic Data (cont.)

Compound	$NN^{am}S$	$(NN^{am}S)_2$
Empirical formula	$C_{11}H_{15}N_2OSPF_6$	$C_{24}H_{36}Cl_6N_4O_2S_2$
Formula weight	368.28	689.39
Temperature/K	150.15	150
Crystal system	monoclinic	monoclinic
Space group	$P2_1/n$	C2/c
a/Å	7.1349(6)	31.780(4)
b/Å	20.2169(16)	10.1128(12)
c/Å	20.8974(17)	10.4558(14)
α/°	90	90
β/°	97.275(6)	100.484(9)
γ/°	90	90
Volume/$Å^3$	2990.1(4)	3304.2(8)
Z	8	4
$\rho_{calc}g/cm^3$	1.636	1.386
μ/mm^{-1}	0.390	0.675
F(000)	1504.0	1432.0
Crystal size/mm^3	0.332 × 0.171 × 0.094	0.287 × 0.254 × 0.134
Radiation	MoKα (λ = 0.71073)	MoKα (λ = 0.71073)
2Θ range for data collection/°	3.93 to 51.988	4.234 to 54.332
Index ranges	$-8 \leq h \leq 8$ $-24 \leq k \leq 24$ $-25 \leq l \leq 25$	$-40 \leq h \leq 40$ $-12 \leq k \leq 12$ $-13 \leq l \leq 13$
Reflections collected	49156	32064
Independent reflections	5871 [R_{int} = 0.2033, R_{sigma} = 0.1389]	3625 [R_{int} = 0.0563, R_{sigma} = 0.0549]
Data/restraints/parameters	5871/0/402	3625/0/184
Goodness-of-fit on F^2	1.021	1.111
Final R indexes [I>=2σ (I)]	R_1 = 0.1007, wR_2 = 0.2510	R_1 = 0.0900, wR_2 = 0.2748
Final R indexes [all data]	R_1 = 0.2076, wR_2 = 0.3258	R_1 = 0.1260, wR_2 = 0.3004
Largest diff. peak/hole / e $Å^{-3}$	2.23/-1.13	0.90/-0.99

Table A: Crystallographic Data (cont.)

Compound	$[Ni_3(NN^{am}S)_2(S^tBu)_2]$	$[Ni_3(NN^{am}S)_2S(4\text{-}F)Ph]$
Empirical formula	$C_{30}H_{46}N_4Ni_3O_2S_4$	$C_{34}H_{36}F_2N_4Ni_3O_2S_4$
Formula weight	799.08	875.04
Temperature/K	150	150
Crystal system	Monoclinic	triclinic
Space group	C2/c	P-1
a/Å	21.289(7)	8.3177(13)
b/Å	8.128(3)	9.8644(14)
c/Å	19.730(6)	12.3810(19)
α/°	90	108.837(9)
β/°	91.331(19)	91.865(10)
γ/°	90	113.830(8)
Volume/$Å^3$	3413(2)	863.7(2)
Z	4	1
$\rho_{calc}g/cm^3$	1.555	1.682
μ/mm^{-1}	1.917	1.910
F(000)	1672.0	450.0
Crystal size/mm^3	0.581 × 0.179 × 0.106	0.312 × 0.21 × 0.181
Radiation	MoKα (λ = 0.71073)	MoKα (λ = 0.71073)
2Θ range for data collection/°	5.366 to 54.624	8.318 to 54.34
Index ranges	$-27 \le h \le 25$ $-10 \le k \le 10$ $-25 \le l \le 25$	$-10 \le h \le 10$ $-12 \le k \le 12$ $-15 \le l \le 15$
Reflections collected	36097	32582
Independent reflections	3788 [R_{int} = 0.0740, R_{sigma} = 0.0384]	3764 [R_{int} = 0.0690, R_{sigma} = 0.0461]
Data/restraints/parameters	3788/0/201	3764/0/225
Goodness-of-fit on F^2	1.029	1.053
Final R indexes [I>=2σ (I)]	R_1 = 0.0276, wR_2 = 0.0604	R_1 = 0.0364, wR_2 = 0.0765
Final R indexes [all data]	R_1 = 0.0437, wR_2 = 0.0661	R_1 = 0.0586, wR_2 = 0.0857
Largest diff. peak/hole / e $Å^{-3}$	0.40/-0.38	0.53/-4.40

Table A: Crystallographic Data (cont.)

Compound	$[Ni_3(NN^{am}S)_2(SPh)_2]$	$[Ni(NN^{im}S)S^tBu]$
Empirical formula	$C_{35}H_{42}N_4Ni_3O_3S_4$	$C_{15}H_{24}N_2S_2Ni$
Formula weight	871.09	355.19
Temperature/K	150	150.15
Crystal system	triclinic	orthorhombic
Space group	P-1	Iba2
a/Å	8.273(2)	14.303(3)
b/Å	9.902(2)	30.539(7)
c/Å	12.824(3)	7.6973(19)
α/°	81.623(15)	90
β/°	87.592(15)	90
γ/°	65.612(13)	90
Volume/Å^3	946.4(4)	3362.2(14)
Z	1	8
ρ_{calc}g/cm^3	1.528	1.403
μ/mm^{-1}	1.737	1.394
F(000)	452.0	1504.0
Crystal size/mm^3	0.649 × 0.192 × 0.14	0.784 × 0.307 × 0.119
Radiation	MoKα (λ = 0.71073)	MoKα (λ = 0.71073)
2Θ range for data collection/°	5.408 to 53.912	6.29 to 54.36
Index ranges	$-10 \le h \le 10$ $-11 \le k \le 12$ $-16 \le l \le 16$	$-17 \le h \le 18$, $-38 \le k \le 38$, $-9 \le l \le 9$
Reflections collected	9634	20565
Independent reflections	3840 [R_{int} = 0.0376, R_{sigma} = 0.0635]	3682 [R_{int} = 0.0376, R_{sigma} = 0.0314]
Data/restraints/parameters	3840/0/236	3682/1/186
Goodness-of-fit on F^2	1.029	1.061
Final R indexes [I>=2σ (I)]	R_1 = 0.0414, wR_2 = 0.0791	R_1 = 0.0515, wR_2 = 0.1343
Final R indexes [all data]	R_1 = 0.0666, wR_2 = 0.0897	R_1 = 0.0604, wR_2 = 0.1411
Largest diff. peak/hole / e Å^{-3}	0.53/-0.70	1.12/-0.60

Table A: Crystallographic Data (cont.)

Compound	$(Ph_4As)[Ni(NN^{am}S)SPh]$	$(Ph_4As)[Ni(NN^{am}S)(4\text{-}NO_2PhS]$
Empirical formula	$C_{137}H_{146}As_4Cl_2N_4Ni_2O_9S_4$	$C_{43}H_{42}AsCl_4N_3NiO_3S_2$
Formula weight	2608.81	988.34
Temperature/K	150	150
Crystal system	triclinic	orthorhombic
Space group	P-1	$P2_12_12_1$
a/Å	9.758(7)	10.737(2)
b/Å	13.980(10)	13.839(3)
c/Å	52.73(3)	30.052(6)
α/°	90.56(5)	90
β/°	90.55(5)	90
γ/°	104.41(5)	90
Volume/$Å^3$	6966(9)	4465.2(15)
Z	2	4
$\rho_{calc}g/cm^3$	1.244	1.470
μ/mm^{-1}	1.365	1.545
F(000)	2708.0	2024.0
Crystal size/mm^3	0.607 × 0.225 × 0.111	0.53 × 0.502 × 0.428
Radiation	MoKα (λ = 0.71073)	MoKα (λ = 0.71073)
2Θ range for data collection/°	3.1 to 55	4.802 to 52
Index ranges	$-11 \le h \le 12$ $-17 \le k \le 14$ $-62 \le l \le 66$	$-12 \le h \le 13$ $-17 \le k \le 17$, $-37 \le l \le 36$
Reflections collected	43499	56766
Independent reflections	18139 [R_{int} = 0.1614, R_{sigma} = 0.3359]	8756 [R_{int} = 0.0395, R_{sigma} = 0.0354]
Data/restraints/parameters	18139/0/863	8756/0/517
Goodness-of-fit on F^2	0.969	1.080
Final R indexes [I>=2σ (I)]	R_1 = 0.1388, wR_2 = 0.3270	R_1 = 0.0442, wR_2 = 0.1227
Final R indexes [all data]	R_1 = 0.2499, wR_2 = 0.3923	R_1 = 0.0503, wR_2 = 0.1274
Largest diff. peak/hole / e $Å^{-3}$	1.30/-0.92	1.23/-0.81

Table A: Crystallographic Data (cont.)

Compound	$NN^{am}S$'	$[Ni_3(NN^{am}S)_2(SC_2H_5(CH_3)_2N)_2]$
Empirical formula	$C_{12}H_{16}N_2OSCl_2$	$C_{15.5}H_{24}N_3Ni_{1.5}O_3S_2$
Formula weight	307.23	452.56
Temperature/K	150	150
Crystal system	orthorhombic	monoclinic
Space group	Iba2	$P2_1/c$
a/Å	13.639(13)	8.0470(11)
b/Å	45.74(4)	19.952(3)
c/Å	9.753(10)	12.5583(17)
α/°	90	90
β/°	90	102.106(7)
γ/°	90	90
Volume/$Å^3$	6085(11)	1971.5(5)
Z	16	4
$\rho_{calc}g/cm^3$	1.341	1.525
μ/mm^{-1}	0.554	1.678
F(000)	2560.0	944.0
Crystal size/mm^3	0.535 × 0.516 × 0.244	0.338 × 0.24 × 0.24
Radiation	MoKα (λ = 0.71073)	MoKα (λ = 0.71073)
2Θ range for data collection/°	4.006 to 54.714	5.178 to 51.996
Index ranges	$-17 \le h \le 17$ $-58 \le k \le 59$ $-11 \le l \le 12$	$-9 \le h \le 9$ $-24 \le k \le 24$ $-15 \le l \le 15$
Reflections collected	39096	61092
Independent reflections	6488 [R_{int} = 0.0606, R_{sigma} = 0.0598]	3878 [R_{int} = 0.0454, R_{sigma} = 0.0254]
Data/restraints/parameters	6488/1/329	3878/0/245
Goodness-of-fit on F^2	1.090	1.109
Final R indexes [I>=2σ (I)]	R_1 = 0.0812 wR_2 = 0.2220	R_1 = 0.0357, wR_2 = 0.0856
Final R indexes [all data]	R_1 = 0.1233 wR_2 = 0.2619	R_1 = 0.0496 wR_2 = 0.0925
Largest diff. peak/hole / e $Å^{-3}$	1.06/-0.99	0.73/-0.39

Table A: Crystallographic Data (cont.)

Compound	Ni(Cysteine-methylester)$_2$	[{Ni($H_2NN^{am}S$)$_2$(OMe)$_2$}$_2$(NiCl$_2$)]
Empirical formula	$C_8H_{16}N_2O_4S_2Ni$	$C_{48}H_{68}N_8O_8S_4Cl_2Ni_3$
Formula weight	327.06	1260.37
Temperature/K	150	296.15
Crystal system	triclinic	triclinic
Space group	P1	P-1
a/Å	5.044(3)	11.740(3)
b/Å	10.484(6)	13.624(4)
c/Å	13.403(6)	25.033(7)
α/°	79.34(4)	79.769(15)
β/°	89.97(4)	79.879(16)
γ/°	89.70(4)	77.470(15)
Volume/Å^3	696.5(6)	3807.0(19)
Z	1	4
ρ_{calc}g/cm^3	0.780	2.199
μ/mm^{-1}	0.848	1.913
F(000)	170.0	2632.0
Crystal size/mm^3	0.759 × 0.193 × 0.13	0.164 × 0.349 × 0.397
Radiation	MoKα (λ = 0.71073)	MoKα (λ = 0.71073)
2Θ range for data collection/°	3.092 to 54.482	3.34 to 54.442
Index ranges	$-6 \le h \le 6$, $-13 \le k \le 13$, $-17 \le l \le 17$	$-15 \le h \le 12$, $-17 \le k \le 16$, $-31 \le l \le 26$
Reflections collected	10535	42156
Independent reflections	4456 [R_{int} = 0.0881, R_{sigma} = 0.1345]	12754 [R_{int} = 0.0505, R_{sigma} = 0.0741]
Data/restraints/parameters	4456/3/311	12754/12/806
Goodness-of-fit on F^2	0.927	1.019
Final R indexes [I>=2σ (I)]	R_1 = 0.0601, wR_2 = 0.1385	R_1 = 0.0884, wR_2 = 0.2751
Final R indexes [all data]	R_1 = 0.1328, wR_2 = 0.1787	R_1 = 0.1290, wR_2 = 0.3149
Largest diff. peak/hole / e Å^{-3}	0.90/-1.05	3.33/-2.12

Table A: Crystallographic Data (cont.)

Compound	Ni(6-mercaptopurine)
Empirical formula	$C_{16}H_{19}N_6S_2NiO_{0.25}$
Formula weight	484.51
Temperature/K	296.15
Crystal system	triclinic
Space group	P-1
a/Å	7.156(3)
b/Å	10.050(4)
c/Å	31.039(12)
α/°	90
β/°	90
γ/°	99.87(3)
Volume/Å^3	2199.1(14)
Z	4
ρ_{calc}g/cm^3	1.4633
μ/mm^{-1}	1.218
F(000)	963.3
Crystal size/mm^3	106 × 159 × 198
Radiation	Mo Kα (λ = 0.71073)
2Θ range for data collection/°	3.94 to 54.9
Index ranges	$-9 \leq h \leq 9$, $-12 \leq k \leq 12$, $-39 \leq l \leq 39$
Reflections collected	81114
Independent reflections	9696 [R_{int} = 0.5770, R_{sigma} = 0.3444]
Data/restraints/parameters	9696/0/531
Goodness-of-fit on F^2	1.507
Final R indexes [I>=2σ (I)]	R_1 = 0.1384, wR_2 = 0.3378
Final R indexes [all data]	R_1 = 0.2990, wR_2 = 0.4312
Largest diff. peak/hole / e Å^{-3}	8.81/-2.70

Table B1: Fractional Atomic Coordinates ($\times 10^4$) and Equivalent Isotropic Displacement Parameters ($Å^2 \times 10^3$) for [Ni(NN^{im}S)SPh]. U_{eq} is defined as 1/3 of of the trace of the orthogonalised U_{IJ} tensor.

Atom	*x*	*y*	*z*	U(eq)
C1	10163(4)	1703.6(17)	5941(3)	20.8(7)
C2	10674(4)	1027.8(18)	5543(3)	23.5(7)
C3	10398(4)	1842.3(19)	7231(3)	24.8(7)
C4	11082(4)	1316(2)	8070(3)	30.3(8)
C5	11547(4)	639(2)	7646(3)	31.8(9)
C6	11345(4)	506.2(19)	6384(3)	29.0(8)
C7	5157(4)	867.3(17)	3169(3)	21.9(7)
C8	3980(4)	502.2(19)	3750(3)	28.6(8)
C9	2747(5)	108(2)	3076(4)	34.1(9)
C10	2601(5)	71(2)	1780(4)	35.2(9)
C11	3718(4)	418.7(19)	1192(3)	30.6(8)
C12	5041(4)	806.6(17)	1865(3)	22.1(7)
C13	6231(4)	1087.4(18)	1152(3)	25.0(8)
C14	8641(5)	1585(2)	621(3)	33.7(9)
C15	9284(5)	2339(2)	841(3)	33.7(9)
C16	10124(5)	3215.5(19)	2426(4)	35.1(9)
C17	11537(4)	2055(2)	2508(4)	32.9(9)
N1	7541(3)	1448.2(14)	1551(2)	22.1(6)
N2	9921(4)	2414.6(15)	2195(3)	25.2(7)
Ni1	8326.6(5)	1881.5(2)	3101.7(4)	20.87(14)
S2	6640.4(11)	1358.3(5)	4129.7(7)	25.0(2)
S1	9330.2(12)	2396.2(5)	4908.3(8)	28.8(2)

Table B2: Anisotropic Displacement Parameters ($Å^2 \times 10^3$) for [Ni(NN^{im}S)SPh]. The Anisotropic displacement factor exponent takes the form: $-2\pi^2[h^2a^{*2}U_{11}+2hka^*b^*U_{12}+\ldots]$.

Atom	**U_{11}**	**U_{22}**	**U_{33}**	**U_{23}**	**U_{13}**	**U_{12}**
C1	17.6(18)	24.2(18)	20.5(17)	-2.4(13)	2.4(14)	-4.4(13)
C2	20.7(19)	26.2(18)	23.0(17)	-4.5(14)	1.5(15)	-2.8(14)
C3	21.6(19)	29.7(18)	23.0(17)	-4.0(15)	2.9(15)	0.7(15)
C4	25(2)	43(2)	22.1(18)	-2.5(16)	2.2(16)	-3.1(17)
C5	25(2)	35(2)	33(2)	8.4(16)	-4.1(17)	1.5(16)
C6	22(2)	26.3(18)	38(2)	-5.0(16)	3.4(16)	-2.3(15)
C7	19.5(18)	22.7(17)	23.7(17)	0.7(14)	3.8(15)	5.0(14)
C8	26(2)	35(2)	25.7(19)	6.3(15)	9.2(16)	5.8(16)

C9	26(2)	33(2)	45(2)	8.6(17)	11.9(18)	0.2(16)
C10	26(2)	30(2)	50(2)	-11.4(17)	4.4(18)	-6.3(17)
C11	31(2)	33(2)	26.3(19)	-4.2(15)	0.5(16)	2.9(17)
C12	21.4(19)	20.4(17)	24.7(17)	2.1(14)	4.3(15)	2.9(14)
C13	28(2)	28.5(18)	17.8(17)	-0.8(14)	1.8(15)	1.8(16)
C14	33(2)	47(2)	23.4(19)	-1.7(16)	9.6(17)	-5.3(18)
C15	38(2)	39(2)	25.6(19)	2.5(16)	11.1(17)	-4.0(18)
C16	46(3)	27(2)	34(2)	1.3(16)	13.2(19)	-5.8(17)
C17	26(2)	36(2)	38(2)	2.0(17)	11.8(18)	1.8(16)
N1	24.1(17)	26.4(15)	16.4(14)	1.4(12)	4.7(12)	1.2(13)
N2	23.4(17)	27.6(15)	25.4(15)	-0.5(12)	5.7(13)	-2.0(12)
Ni1	23.3(3)	22.3(2)	17.2(2)	0.23(17)	3.47(17)	-0.02(18)
S2	28.1(5)	28.8(5)	18.7(4)	0.9(3)	6.0(4)	-1.1(4)
S1	40.0(6)	23.3(4)	21.6(4)	-1.9(3)	0.0(4)	-0.7(4)

Table B3: Bond Lengths for [Ni(NN^{im}S)SPh].

Atom	**Atom**	**Length/Å**	**Atom**	**Atom**	**Length/Å**
C1	C2	1.396(5)	C11	C12	1.415(5)
C1	C3	1.406(4)	C12	C13	1.438(5)
C1	S1	1.762(3)	C13	N1	1.291(4)
C2	C6	1.378(5)	C14	C15	1.486(5)
C3	C4	1.387(5)	C14	N1	1.479(4)
C4	C5	1.395(5)	C15	N2	1.489(5)
C5	C6	1.374(5)	C16	N2	1.492(4)
C7	C8	1.407(5)	C17	N2	1.488(5)
C7	C12	1.406(5)	N1	Ni1	1.884(3)
C7	S2	1.739(3)	N2	Ni1	2.015(3)
C8	C9	1.371(5)	Ni1	S2	2.1410(9)
C9	C10	1.393(5)	Ni1	S1	2.2192(10)
C10	C11	1.359(5)			

Table B4: Bond Angles for [Ni(NN^{im}S)SPh].

Atom	Atom	Atom	Angle/°	Atom	Atom	Atom	Angle/°
C2	C1	C3	117.6(3)	N1	C14	C15	106.9(3)
C2	C1	S1	123.3(3)	C14	C15	N2	108.1(3)
C3	C1	S1	119.0(2)	C13	N1	C14	115.7(3)
C6	C2	C1	121.4(3)	C13	N1	Ni1	132.6(2)
C4	C3	C1	120.6(3)	C14	N1	Ni1	111.7(2)
C3	C4	C5	120.5(3)	C15	N2	C16	105.7(3)
C6	C5	C4	119.1(3)	C15	N2	Ni1	105.8(2)
C5	C6	C2	120.9(3)	C16	N2	Ni1	117.4(2)
C8	C7	S2	117.1(3)	C17	N2	C15	111.0(3)
C12	C7	C8	117.6(3)	C17	N2	C16	108.7(3)
C12	C7	S2	125.3(3)	C17	N2	Ni1	108.1(2)
C9	C8	C7	121.7(3)	N1	Ni1	N2	86.21(11)
C8	C9	C10	120.5(3)	N1	Ni1	S2	96.29(9)
C11	C10	C9	119.1(4)	N1	Ni1	S1	178.14(9)
C10	C11	C12	121.7(3)	N2	Ni1	S2	177.19(8)
C7	C12	C11	119.3(3)	N2	Ni1	S1	92.13(8)
C7	C12	C13	124.2(3)	S2	Ni1	S1	85.39(4)
C11	C12	C13	116.5(3)	C7	S2	Ni1	112.30(11)
N1	C13	C12	128.0(3)	C1	S1	Ni1	108.36(11)

Table B5: Torsion Angles for [Ni(NN^{im}S)SPh].

A	B	C	D	Angle/°	A	B	C	D	Angle/°
C1	C2	C6	C5	-0.7(5)	C12	C7	S2	Ni1	0.1(3)
C1	C3	C4	C5	-0.1(5)	C12	C13	N1	C14	172.5(3)
C2	C1	C3	C4	-1.3(5)	C12	C13	N1	Ni1	-10.4(5)
C2	C1	S1	Ni1	23.0(3)	C13	N1	Ni1	N2	-165.4(3)
C3	C1	C2	C6	1.7(5)	C13	N1	Ni1	S2	13.3(3)
C3	C1	S1	Ni1	-159.8(2)	C14	C15	N2	C16	-165.0(3)
C3	C4	C5	C6	1.1(6)	C14	C15	N2	C17	77.3(4)
C4	C5	C6	C2	-0.8(6)	C14	C15	N2	Ni1	-39.8(3)
C7	C8	C9	C10	-1.6(6)	C14	N1	Ni1	N2	11.8(2)
C7	C12	C13	N1	-2.1(6)	C14	N1	Ni1	S2	-169.5(2)
C8	C7	C12	C11	3.2(5)	C15	C14	N1	C13	140.7(3)
C8	C7	C12	C13	-173.8(3)	C15	C14	N1	Ni1	-37.0(3)
C8	C7	S2	Ni1	-179.(2)	N1	C14	C15	N2	50.2(4)
C8	C9	C10	C11	1.5(6)	S2	C7	C8	C9	179.2(3)

C9	C10	C11	C12	1.0(6)	S2	C7	C12	C11	-176.8(3)
C10	C11	C12	C7	-3.4(5)	S2	C7	C12	C13	6.2(5)
C10	C11	C12	C13	173.8(3)	S1	C1	C2	C6	178.9(3)
C11	C12	C13	N1	-179.2(3)	S1	C1	C3	C4	-178.7(3)
C12	C7	C8	C9	-0.8(5)					

Table B6: Hydrogen Atom Coordinates (Å×10^4) and Isotropic Displacement Parameters (Å^2×10^3) for [Ni(NN^{im}S)SPh].

Atom	***x***	***y***	***z***	**U(eq)**
H2	10557	925	4675	28
H3	10084	2301	7531	30
H4	11234	1416	8940	36
H5	11998	275	8222	38
H6	11671	49	6088	35
H8	4042	530	4631	34
H9	1987	-143	3496	41
H10	1731	-193	1312	42
H11	3608	401	307	37
H13	6029	996	279	30
H14A	8038	1539	-236	40
H14B	9545	1227	723	40
H15A	8407	2700	593	40
H15B	10167	2428	338	40
H16A	10517	3301	3313	53
H16B	9074	3461	2193	53
H16C	10913	3411	1924	53
H17A	12299	2266	1997	49
H17B	11424	1529	2339	49
H17C	11952	2132	3393	49

Table C1: Fractional Atomic Coordinates ($\times 10^4$) and Equivalent Isotropic Displacement Parameters ($Å^2 \times 10^3$) for [Ni(NN^{im}S)(4-NO_2PhS)]. U_{eq} is defined as 1/3 of of the trace of the orthogonalised U_{IJ} tensor.

Atom	*x*	*y*	*z*	U(eq)
Ni1	2785.7(3)	3093.9(2)	5125.3(3)	20.57(9)
S2	4616.6(6)	2694.3(4)	4489.7(7)	26.47(15)
S1	3748.5(5)	3488.7(4)	7054.0(7)	24.99(15)
N1	1180.1(19)	3303.0(12)	5733(2)	23.5(5)
C1	2775(2)	3937.1(13)	8228(3)	22.9(5)
C7	777(2)	3628.5(14)	6882(3)	24.6(5)
C5	802(3)	4339.4(14)	9115(3)	30.9(6)
C9	729(2)	3055.9(15)	3185(3)	30.1(6)
C2	3342(3)	4313.3(14)	9406(3)	30.0(6)
C15	6867(3)	4392.1(16)	2264(3)	34.8(7)
C8	219(2)	3014.2(16)	4692(3)	32.3(7)
C12	5450(2)	3374.8(15)	3650(3)	24.6(5)
C13	6606(2)	3196.2(15)	3092(3)	29.0(6)
C6	1479(2)	3959.1(13)	8067(3)	24.0(5)
C4	1377(3)	4701.7(15)	10246(4)	39.0(7)
N3	7616(3)	4931.5(16)	1571(4)	51.0(8)
C14	7305(2)	3694.4(16)	2409(3)	34.3(7)
C17	5038(3)	4077.8(15)	3480(3)	30.6(6)
C16	5738(3)	4583.7(16)	2800(3)	35.5(7)
C3	2652(3)	4694.2(15)	10392(3)	37.3(7)
O1	7298(3)	5551.0(14)	1566(3)	72.4(9)
N2	1983.4(19)	2736.4(12)	3256(2)	26.0(5)
O2	8575(3)	4735.7(15)	1024(5)	99.4(13)
C11	1912(3)	1946.5(15)	3314(4)	42.6(8)
C10	2587(3)	2937(2)	1863(3)	46.9(8)

Table C2: Anisotropic Displacement Parameters ($Å^2 \times 10^3$) for [Ni(NN^{im}S)(4-NO_2PhS)]. The Anisotropic displacement factor exponent takes the form: $-2\pi^2[h^2a^{*2}U_{11}+2hka^*b^*U_{12}+\ldots]$.

Atom	U_{11}	U_{22}	U_{33}	U_{23}	U_{13}	U_{12}
Ni1	18.75(14)	23.47(16)	19.64(15)	-1.58(14)	2.74(11)	1.26(14)
S2	23.4(3)	30.2(4)	26.1(4)	-2.2(3)	4.2(3)	5.2(3)
S1	21.4(3)	30.9(4)	22.8(3)	-4.0(3)	2.1(3)	1.2(3)
N1	21.4(10)	25.5(11)	23.8(12)	1.8(9)	2.7(9)	-0.3(9)
C1	29.5(13)	17.5(12)	22.4(14)	2.3(10)	7.8(11)	-1.8(10)
C7	22.6(12)	24.7(13)	27.1(15)	4.7(11)	6.6(10)	3.0(11)

C5	33.6(15)	28.1(15)	31.7(16)	-1.3(12)	12.8(12)	1.1(12)
C9	26.6(14)	35.6(16)	27.7(16)	-3.3(12)	-3.5(11)	3.1(11)
C2	32.2(14)	31.3(15)	26.8(15)	-1.3(12)	5.6(12)	-9.6(12)
C15	27.8(14)	35.5(16)	42.0(18)	-11.4(13)	13.9(13)	-4.6(12)
C8	20.8(13)	44.7(18)	31.4(16)	-6.1(12)	-0.5(12)	0.4(12)
C12	20.1(12)	32.7(14)	20.9(14)	-7.4(11)	-0.1(10)	0.1(11)
C13	23.3(13)	31.4(15)	32.3(16)	-11.2(12)	2.3(11)	6.4(11)
C6	29.1(13)	18.0(12)	25.3(14)	2.6(10)	8.1(11)	0.9(11)
C4	47.6(18)	31.5(16)	39.0(19)	-12.7(13)	17.7(14)	-0.4(14)
N3	40.5(15)	45.7(17)	69(2)	-13.3(15)	28.9(14)	-7.9(13)
C14	18.1(13)	43.6(18)	41.9(18)	-14.3(14)	10.5(12)	1.5(12)
C17	24.1(13)	34.3(16)	34.1(16)	-6.6(13)	11.2(11)	4.0(12)
C16	30.3(15)	29.8(15)	47.2(19)	-5.2(13)	12.8(13)	1.8(12)
C3	47.7(18)	31.8(15)	33.0(19)	-12.1(13)	10.0(14)	-10.9(14)
O1	72.9(19)	36.2(13)	112(2)	-7.6(15)	52.8(18)	-6.6(13)
N2	23.9(11)	32.7(13)	21.4(12)	-4.2(10)	2.5(9)	-1.6(9)
O2	73(2)	60.4(18)	171(4)	-2(2)	90(2)	-2.3(16)
C11	31.8(15)	34.7(17)	61(2)	-17.2(15)	-5.5(14)	3.2(12)
C10	35.8(16)	82(2)	23.4(17)	-0.9(16)	3.0(13)	-7.6(17)

Table C3: Bond Lengths for [Ni($NN^{im}S$)(4-NO_2PhS)].

Atom	**Atom**	**Length/Å**	**Atom**	**Atom**	**Length/Å**
Ni1	S2	2.2205(7)	C9	N2	1.486(3)
Ni1	S1	2.1323(7)	C2	C3	1.385(4)
Ni1	N1	1.889(2)	C15	N3	1.453(4)
Ni1	N2	1.989(2)	C15	C14	1.393(4)
S2	C12	1.751(3)	C15	C16	1.382(4)
S1	C1	1.742(3)	C12	C13	1.411(4)
N1	C7	1.295(3)	C12	C17	1.395(4)
N1	C8	1.482(3)	C13	C14	1.365(4)
C1	C2	1.400(4)	C4	C3	1.386(4)
C1	C6	1.411(4)	N3	O1	1.208(4)
C7	C6	1.432(4)	N3	O2	1.227(4)
C5	C6	1.414(4)	C17	C16	1.374(4)
C5	C4	1.360(4)	N2	C11	1.480(4)
C9	C8	1.494(4)	N2	C10	1.491(4)

Table C4: Bond Angles for [Ni(NN^{im}S)(4-NO$_2$PhS)].

Atom	Atom	Atom	Angle/°	Atom	Atom	Atom	Angle/°
S1	Ni1	S2	84.97(3)	C13	C12	S2	117.7(2)
N1	Ni1	S2	172.17(7)	C17	C12	S2	124.3(2)
N1	Ni1	S1	96.86(7)	C17	C12	C13	118.0(3)
N1	Ni1	N2	86.44(9)	C14	C13	C12	121.2(3)
N2	Ni1	S2	91.96(7)	C1	C6	C7	124.4(2)
N2	Ni1	S1	176.38(7)	C1	C6	C5	119.2(3)
C12	S2	Ni1	110.53(9)	C5	C6	C7	116.3(2)
C1	S1	Ni1	112.07(9)	C5	C4	C3	119.7(3)
C7	N1	Ni1	132.43(19)	O1	N3	C15	120.2(3)
C7	N1	C8	115.5(2)	O1	N3	O2	122.1(3)
C8	N1	Ni1	112.04(18)	O2	N3	C15	117.7(3)
C2	C1	S1	116.5(2)	C13	C14	C15	119.2(2)
C2	C1	C6	118.2(2)	C16	C17	C12	121.1(3)
C6	C1	S1	125.3(2)	C17	C16	C15	119.5(3)
N1	C7	C6	128.1(2)	C2	C3	C4	120.5(3)
C4	C5	C6	121.3(3)	C9	N2	Ni1	105.83(16)
N2	C9	C8	108.1(2)	C9	N2	C10	107.1(2)
C3	C2	C1	121.1(3)	C11	N2	Ni1	109.09(18)
C14	C15	N3	119.7(2)	C11	N2	C9	110.7(2)
C16	C15	N3	119.3(3)	C11	N2	C10	107.9(3)
C16	C15	C14	120.9(3)	C10	N2	Ni1	116.23(18)
N1	C8	C9	106.6(2)				

Table C5: Torsion Angles for [Ni(NN^{im}S)(4-NO$_2$PhS)].

A	B	C	D	Angle/°	A	B	C	D	Angle/°
Ni1	S2	C12	C13	-176.01(17)	C8	C9	N2	C11	75.9(3)
Ni1	S2	C12	C17	3.1(2)	C8	C9	N2	C10	-166.7(2)
Ni1	S1	C1	C2	-170.25(17)	C12	C13	C14	C15	0.1(4)
Ni1	S1	C1	C6	8.6(3)	C12	C17	C16	C15	0.5(4)
Ni1	N1	C7	C6	2.0(4)	C13	C12	C17	C16	-0.4(4)
Ni1	N1	C8	C9	-33.5(3)	C6	C1	C2	C3	0.3(4)
S2	C12	C13	C14	179.3(2)	C6	C5	C4	C3	-0.7(4)
S2	C12	C17	C16	-179.5(2)	C4	C5	C6	C1	2.0(4)
S1	Ni1	N1	C7	4.8(3)	C4	C5	C6	C7	-176.9(3)
S1	Ni1	N1	C8	-173.27(17)	N3	C15	C14	C13	178.5(3)
S1	C1	C2	C3	179.2(2)	N3	C15	C16	C17	-178.8(3)

S1	C1	C6	C7	-1.8(4)	C14	C15	N3	O1	-172.9(3)
S1	C1	C6	C5	179.36(19)	C14	C15	N3	O2	6.0(5)
N1	C7	C6	C1	-4.9(4)	C14	C15	C16	C17	-0.2(4)
N1	C7	C6	C5	174.0(3)	C17	C12	C13	C14	0.1(4)
C1	C2	C3	C4	1.0(4)	C16	C15	N3	O1	5.7(5)
C7	N1	C8	C9	148.1(2)	C16	C15	N3	O2	-175.5(3)
C5	C4	C3	C2	-0.9(5)	C16	C15	C14	C13	-0.1(4)
C2	C1	C6	C7	177.1(2)	N2	Ni1	N1	C7	-173.7(3)
C2	C1	C6	C5	-1.8(4)	N2	Ni1	N1	C8	8.24(18)
C8	N1	C7	C6	-180.0(2)	N2	C9	C8	N1	49.5(3)
C8	C9	N2	Ni1	-42.1(2)					

Table C6: Hydrogen Atom Coordinates (Å×10^4) and Isotropic Displacement Parameters (Å^2×10^3) for [Ni(NN^{im}S)(4-NO_2PhS)].

Atom	***x***	***y***	***z***	**U(eq)**
H7	-93	3651	6947	30
H5	-72	4342	9027	37
H9A	192	2791	2467	36
H9B	771	3561	2861	36
H2	4215	4307	9530	36
H8A	-545	3301	4735	39
H8B	26	2512	4944	39
H13	6904	2720	3195	35
H4	908	4959	10934	47
H14	8081	3567	2037	41
H17	4260	4209	3842	37
H16	5449	5061	2698	43
H3	3055	4952	11174	45
H11A	2746	1746	3379	64
H11B	1479	1769	2417	64
H11C	1462	1801	4183	64
H10A	2691	3458	1826	70
H10B	2072	2780	1011	70
H10C	3396	2706	1836	70

Table D1: Fractional Atomic Coordinates ($\times 10^4$) and Equivalent Isotropic Displacement Parameters ($Å^2 \times 10^3$) for [Ni(NN^{im}S)(4-^{t}BuPhS)]. U_{eq} is defined as 1/3 of of the trace of the orthogonalised U_{IJ} tensor.

Atom	*x*	*y*	*z*	U(eq)
Ni1	2320.1(2)	1843.5(3)	7949.7(2)	45.92(14)
S2	2993.7(5)	527.4(6)	7440.1(3)	54.7(2)
S1	3605.8(5)	1924.1(7)	8287.9(3)	57.7(2)
N2	1113.4(15)	1585(2)	7643.8(10)	58.4(7)
N1	1753.7(16)	3008(2)	8357.6(10)	58.1(6)
C12	3217.0(17)	1425(3)	6915.1(11)	49.9(7)
C1	3669(2)	3088(3)	8727.6(11)	58.8(8)
C13	3529(2)	865(3)	6486.9(12)	63.4(8)
C15	3535(2)	2804(3)	6038.9(13)	69.2(9)
C17	3088(2)	2698(3)	6891.7(12)	59.4(8)
C14	3683(2)	1539(3)	6065.7(13)	71.9(9)
C2	4504(3)	3251(4)	8956.5(13)	76.7(10)
C16	3236(2)	3351(3)	6465.5(13)	68.5(9)
C10	742(2)	443(3)	7861.6(16)	79.2(11)
C6	2970(2)	3896(3)	8851.8(11)	65.9(9)
C9	580(2)	2671(4)	7758.5(19)	88.6(13)
C7	2066(2)	3786(3)	8672.6(13)	68.8(9)
C8	768(2)	3060(4)	8272.7(17)	89.6(13)
C3	4646(4)	4207(5)	9285.3(15)	101.2(15)
C5	3137(3)	4870(4)	9184.2(15)	96.0(13)
C18	3675(4)	3504(5)	5552.1(17)	103.4(14)
C4	3961(5)	5024(5)	9392.4(18)	115.1(17)
C11	1054(3)	1454(6)	7095.7(15)	120.7(19)
C20	4576(5)	3196(6)	5331(2)	161(3)
C19	3629(7)	4876(5)	5624(3)	229(5)
C21	2970(7)	3060(9)	5192(3)	250(6)

Table D2: Anisotropic Displacement Parameters ($Å^2 \times 10^3$) for [Ni(NN^{im}S)(4-^{t}BuPhS)]. The Anisotropic displacement factor exponent takes the form: $-2\pi^2[h^2a^{*2}U_{11}+2hka^*b^*U_{12}+\ldots]$.

Atom	U_{11}	U_{22}	U_{33}	U_{23}	U_{13}	U_{12}
Ni1	31.5(2)	43.5(2)	62.7(3)	0.97(16)	1.68(14)	0.53(14)
S2	50.3(4)	43.0(4)	70.6(5)	-5.2(3)	-2.5(3)	4.5(3)
S1	37.8(3)	63.6(5)	71.7(5)	-7.1(4)	-3.9(3)	-0.5(3)
N2	35.8(11)	54.1(15)	85(2)	4.6(13)	-4.4(12)	-1.5(10)
N1	46.9(13)	52.7(15)	74.7(18)	-1.0(13)	11.7(12)	4.6(11)

C12	38.4(13)	48.8(15)	62.5(18)	-11.1(14)	-3.7(12)	5.5(12)
C1	63.7(18)	64.4(19)	48.2(17)	5.8(14)	2.1(14)	-18.5(15)
C13	66.1(19)	51.5(17)	72(2)	-13.8(16)	-0.9(16)	10.6(15)
C15	66(2)	73(2)	69(2)	5.3(18)	0.6(17)	13.2(17)
C17	61.4(18)	49.9(17)	67(2)	-9.4(15)	8.1(16)	6.6(14)
C14	73(2)	81(2)	62(2)	-14.6(18)	4.9(17)	15.1(18)
C2	77(2)	93(3)	60(2)	10.1(19)	-9.5(17)	-26.8(19)
C16	77(2)	47.4(18)	81(2)	1.1(17)	9.4(18)	10.3(15)
C10	46.6(16)	55.8(19)	135(3)	11(2)	-7.0(19)	-10.3(15)
C6	81(2)	65(2)	51.5(19)	-3.7(15)	9.2(16)	-12.7(18)
C9	42.9(17)	61(2)	161(4)	-1(2)	-7(2)	4.4(16)
C7	69(2)	62(2)	76(2)	-4.3(18)	25.0(18)	3.7(17)
C8	48.2(18)	100(3)	121(3)	-22(3)	16(2)	21.9(19)
C3	116(4)	117(4)	70(3)	2(3)	-18(2)	-52(3)
C5	125(4)	87(3)	76(3)	-24(2)	12(3)	-21(3)
C18	117(4)	110(3)	83(3)	28(3)	13(3)	27(3)
C4	163(5)	105(4)	77(3)	-26(3)	-3(3)	-42(4)
C11	51(2)	222(6)	90(3)	7(3)	-22(2)	5(3)
C20	204(7)	168(6)	113(4)	34(4)	76(5)	37(5)
C19	395(13)	105(5)	187(7)	76(5)	169(8)	82(7)
C21	241(10)	342(15)	168(7)	140(8)	-98(7)	-51(9)

Table D3: Bond Lengths for [Ni(NN^{im}S)(4-^{t}BuPhS)].

Atom	**Atom**	**Length/Å**	**Atom**	**Atom**	**Length/Å**
Ni1	S2	2.2258(8)	C13	C14	1.376(5)
Ni1	S1	2.1317(8)	C15	C14	1.387(5)
Ni1	N2	2.005(2)	C15	C16	1.375(5)
Ni1	N1	1.879(2)	C15	C18	1.538(5)
S2	C12	1.757(3)	C17	C16	1.374(4)
S1	C1	1.738(3)	C2	C3	1.383(6)
N2	C10	1.478(4)	C6	C7	1.441(5)
N2	C9	1.453(4)	C6	C5	1.409(5)
N2	C11	1.498(5)	C9	C8	1.485(6)
N1	C7	1.287(4)	C3	C4	1.383(7)
N1	C8	1.492(4)	C5	C4	1.365(7)
C12	C13	1.391(4)	C18	C20	1.511(7)
C12	C17	1.392(4)	C18	C19	1.498(7)
C1	C2	1.405(5)	C18	C21	1.515(9)
C1	C6	1.403(5)			

Table D4: Bond Angles for [Ni(NN^{im}S)(4-^{t}BuPhS)].

Atom	Atom	Atom	Angle/°	Atom	Atom	Atom	Angle/°
S1	Ni1	S2	83.47(3)	C14	C13	C12	121.4(3)
N2	Ni1	S2	93.44(8)	C14	C15	C18	120.6(4)
N2	Ni1	S1	174.26(8)	C16	C15	C14	115.6(3)
N1	Ni1	S2	177.44(8)	C16	C15	C18	123.8(3)
N1	Ni1	S1	97.17(9)	C16	C17	C12	121.6(3)
N1	Ni1	N2	86.14(11)	C13	C14	C15	122.6(3)
C12	S2	Ni1	103.74(9)	C3	C2	C1	121.1(4)
C1	S1	Ni1	111.98(12)	C17	C16	C15	122.7(3)
C10	N2	Ni1	106.8(2)	C1	C6	C7	124.4(3)
C10	N2	C11	107.2(3)	C1	C6	C5	119.2(4)
C9	N2	Ni1	107.0(2)	C5	C6	C7	116.4(4)
C9	N2	C10	112.5(3)	N2	C9	C8	109.1(3)
C9	N2	C11	104.9(3)	N1	C7	C6	128.2(3)
C11	N2	Ni1	118.6(2)	C9	C8	N1	108.8(3)
C7	N1	Ni1	131.8(2)	C2	C3	C4	120.0(4)
C7	N1	C8	115.9(3)	C4	C5	C6	121.1(5)
C8	N1	Ni1	112.2(2)	C20	C18	C15	110.7(4)
C13	C12	S2	120.1(2)	C20	C18	C21	107.1(6)
C13	C12	C17	116.0(3)	C19	C18	C15	111.7(4)
C17	C12	S2	123.9(2)	C19	C18	C20	108.1(5)
C2	C1	S1	116.3(3)	C19	C18	C21	111.5(6)
C6	C1	S1	125.2(3)	C21	C18	C15	107.7(5)
C6	C1	C2	118.5(3)	C5	C4	C3	120.2(4)

Table D5: Hydrogen Atom Coordinates (Å×10^4) and Isotropic Displacement Parameters (Å^2×10^3) for [Ni(NN^{im}S)(4-^{t}BuPhS)].

Atom	*x*	*y*	*z*	U(eq)
H13	3637	0	6485	76
H17	2892	3126	7177	71
H14	3900	1122	5782	86
H2	4978	2695	8884	92
H16	3128	4217	6465	82
H10A	1097	-269	7754	119
H10B	121	337	7753	119
H10C	760	503	8222	119
H9A	-64	2476	7721	106

H9B	731	3350	7529	106
H7	1648	4360	8803	83
H8A	458	2502	8506	108
H8B	547	3912	8327	108
H3	5214	4303	9438	121
H5	2668	5428	9265	115
H4	4064	5694	9611	138
H11A	1286	2203	6939	181
H11B	428	1333	7000	181
H11C	1408	739	6990	181
H20A	5046	3633	5513	242
H20B	4587	3452	4985	242
H20C	4678	2302	5353	242
H19A	3047	5096	5766	343
H19B	3702	5291	5306	343
H19C	4107	5137	5848	343
H21A	2971	2154	5183	375
H21B	3102	3385	4864	375
H21C	2380	3353	5298	375

Table E1: Fractional Atomic Coordinates ($\times 10^4$) and Equivalent Isotropic Displacement Parameters ($Å^2 \times 10^3$) for [Ni(NN^{im}S)(4-^{t}BuS)]. U_{eq} is defined as 1/3 of of the trace of the orthogonalised U_{IJ} tensor.

Atom	*x*	*y*	*z*	U(eq)
Ni1	6598.0(5)	3756.6(2)	4880.3(14)	37.9(2)
S1	6775.9(12)	3384.0(5)	7179(2)	42.1(4)
S2	7198.5(16)	4303.8(6)	6414(3)	56.8(5)
C2	6672(5)	2562(3)	8321(12)	53.9(19)
N1	6116(4)	3290(2)	3489(7)	41.3(12)
C6	6131(5)	2647(2)	5356(10)	46.9(17)
N2	6363(5)	4155(2)	2827(8)	57.0(17)
C1	6506(4)	2829(2)	6887(9)	40.8(15)
C7	5967(5)	2883(2)	3803(10)	45.5(16)
C5	5940(6)	2187(3)	5376(13)	62(2)
C3	6480(6)	2122(3)	8246(16)	72(3)
C4	6106(7)	1933(3)	6792(15)	74(3)
C13	8487(6)	4250(3)	6757(14)	66(2)
C8	5913(7)	3438(3)	1710(9)	68(2)
C11	5804(11)	4537(4)	3171(19)	120(5)
C9	5850(20)	3885(5)	1649(18)	221(15)
C14	8949(12)	4657(5)	6760(40)	234(16)
C12	8976(11)	3971(9)	5450(40)	233(15)
C15	8731(11)	3982(9)	8300(30)	192(12)
C10	7188(11)	4294(6)	2020(20)	152(8)

Table E2: Anisotropic Displacement Parameters ($Å^2 \times 10^3$) for [Ni(NN^{im}S)(4-^{t}BuS)]. The Anisotropic displacement factor exponent takes the form: $-2\pi^2[h^2a^{*2}U_{11}+2hka^*b^*U_{12}+\ldots]$.

Atom	U_{11}	U_{22}	U_{33}	U_{23}	U_{13}	U_{12}
Ni1	46.0(4)	42.2(4)	25.6(4)	1.7(4)	-3.0(4)	0.5(3)
S1	52.0(9)	44.8(8)	29.7(7)	2.5(7)	-5.5(7)	0.3(7)
S2	69.8(13)	48.8(9)	51.8(10)	-8.2(8)	-5.9(10)	1.1(9)
C2	45(4)	57(4)	60(5)	12(4)	-9(3)	10(3)
N1	37(3)	60(3)	27(3)	-5(2)	0(2)	-3(2)
C6	34(3)	50(4)	56(5)	-6(3)	8(3)	5(3)
N2	66(4)	70(4)	35(3)	18(3)	-6(3)	10(3)
C1	32(3)	44(3)	47(4)	6(3)	4(3)	4(2)
C7	34(3)	59(4)	44(4)	-14(3)	2(3)	-3(3)
C5	47(4)	58(4)	81(7)	-13(4)	5(4)	-5(3)
C3	55(5)	64(5)	97(8)	30(5)	-11(5)	6(4)

C4	71(6)	41(4)	109(9)	7(5)	1(6)	-1(4)
C13	52(5)	77(6)	68(6)	-8(4)	-2(4)	-13(4)
C8	84(6)	92(6)	27(4)	-3(3)	-7(4)	-25(5)
C11	152(12)	113(9)	94(9)	51(8)	4(9)	60(9)
C9	490(40)	99(9)	71(9)	42(7)	-143(17)	-74(17)
C14	135(14)	91(9)	470(50)	-34(18)	-130(20)	-36(9)
C12	80(10)	350(30)	270(30)	-160(30)	81(15)	-20(15)
C15	74(8)	330(30)	172(18)	150(20)	-39(11)	-52(14)
C10	120(12)	219(18)	116(13)	121(13)	14(10)	-14(11)

Table E3: Bond Lengths for [Ni(NN^{im}S)(4-^{t}BuS)].

Atom	**Atom**	**Length/Å**	**Atom**	**Atom**	**Length/Å**
Ni1	S1	2.1188(19)	C6	C7	1.415(11)
Ni1	S2	2.219(2)	C6	C5	1.433(11)
Ni1	N1	1.910(6)	N2	C11	1.440(14)
Ni1	N2	2.022(6)	N2	C9	1.431(16)
S1	C1	1.752(7)	N2	C10	1.397(15)
S2	C13	1.869(9)	C5	C4	1.358(14)
C2	C1	1.392(11)	C3	C4	1.369(15)
C2	C3	1.373(12)	C13	C14	1.410(16)
N1	C7	1.284(9)	C13	C12	1.49(2)
N1	C8	1.471(9)	C13	C15	1.484(19)
C6	C1	1.409(10)	C8	C9	1.367(17)

Table E4: Bond Angles for [Ni(NN^{im}S)(4-^{t}BuS)].

Atom	**Atom**	**Atom**	**Angle/°**	**Atom**	**Atom**	**Atom**	**Angle/°**
S1	Ni1	S2	85.06(9)	C10	N2	Ni1	112.8(7)
N1	Ni1	S1	96.37(18)	C10	N2	C11	107.7(11)
N1	Ni1	S2	177.72(18)	C10	N2	C9	109.3(14)
N1	Ni1	N2	87.2(3)	C2	C1	S1	115.3(6)
N2	Ni1	S1	174.5(2)	C2	C1	C6	119.8(7)
N2	Ni1	S2	91.6(2)	C6	C1	S1	124.9(5)
C1	S1	Ni1	112.7(3)	N1	C7	C6	128.6(7)
C13	S2	Ni1	113.0(3)	C4	C5	C6	122.3(8)
C3	C2	C1	120.4(9)	C4	C3	C2	121.7(9)
C7	N1	Ni1	132.5(5)	C5	C4	C3	119.0(8)
C7	N1	C8	116.1(6)	C14	C13	S2	112.6(10)

C8	N1	Ni1	111.3(5)	C14	C13	C12	106.5(16)
C1	C6	C7	124.6(6)	C14	C13	C15	112.0(15)
C1	C6	C5	116.8(7)	C12	C13	S2	114.7(10)
C7	C6	C5	118.5(7)	C15	C13	S2	113.2(8)
C11	N2	Ni1	115.9(7)	C15	C13	C12	96.8(17)
C9	N2	Ni1	103.6(6)	C9	C8	N1	110.6(7)
C9	N2	C11	107.3(14)	C8	C9	N2	121.1(13)

Table E5: Hydrogen Atom Coordinates (Å×10^4) and Isotropic Displacement Parameters (Å^2×10^3) for [Ni(NN^{im}S)(4-^{t}BuS)].

Atom	***x***	***y***	***z***	**U(eq)**
H2	6920	2686	9356	65
H7	5714	2718	2868	55
H5	5688	2054	4362	75
H3	6611	1945	9229	86
H4	5964	1629	6775	89
H8A	6417	3339	920	81
H8B	5319	3307	1310	81
H11A	5228	4451	3768	180
H11B	5647	4682	2072	180
H11C	6157	4740	3907	180
H9A	5178	3959	1797	265
H9B	6024	3976	459	265
H14A	8795	4817	5693	350
H14B	9626	4610	6818	350
H14C	8747	4828	7770	350
H12A	8918	3663	5777	349
H12B	9638	4053	5402	349
H12C	8692	4016	4303	349
H15A	8638	4157	9357	289
H15B	9386	3891	8227	289
H15C	8329	3723	8344	289
H10A	7512	4502	2781	227
H10B	7037	4436	917	227
H10C	7592	4040	1810	227

Table F1: Fractional Atomic Coordinates ($\times 10^4$) and Equivalent Isotropic Displacement Parameters ($Å^2 \times 10^3$) for [Ni(NN^{im}S)(4-ClPhS)]. U_{eq} is defined as 1/3 of of the trace of the orthogonalised U_{IJ} tensor.

Atom	*x*	*y*	*z*	U(eq)
Ni1	6929.7(4)	1945.2(2)	2204.6(3)	37.87(18)
S1	8370.4(9)	1344.2(5)	1093.4(7)	47.7(2)
S2	5992.1(11)	2504.7(5)	566.3(8)	56.3(3)
Cl1	3422.0(14)	286.1(6)	-3401.9(11)	89.1(4)
N1	7766(3)	1551.9(13)	3660(2)	39.4(6)
C6	9984(3)	826.6(16)	3146(3)	40.8(7)
N2	5487(3)	2502.6(15)	3190(2)	48.1(6)
C15	4125(3)	890.8(18)	-2272(3)	50.0(8)
C13	5282(4)	2056.2(17)	-1695(3)	45.2(8)
C12	5312(3)	1844.4(17)	-508(3)	41.5(7)
C8	6876(4)	1754(2)	4667(3)	59.6(9)
C16	4113(4)	670.5(19)	-1116(3)	56.5(9)
C14	4674(4)	1586.2(18)	-2584(3)	47.4(7)
C1	9807(3)	868.0(16)	1902(3)	40.2(7)
C17	4705(4)	1147.3(18)	-237(3)	47.2(7)
C7	8950(3)	1151.2(16)	3928(3)	43.0(7)
C2	10889(4)	500.5(19)	1257(3)	54.0(8)
C9	6209(4)	2505(2)	4428(3)	59.3(9)
C5	11211(4)	433.9(19)	3692(3)	54.1(8)
C4	12238(4)	73(2)	3037(4)	65.2(10)
C11	4068(5)	2070(3)	3124(5)	87.0(14)
C3	12062(4)	107(2)	1807(4)	61.6(10)
C10	5139(5)	3297(2)	2909(4)	71.6(11)

Table F2: Anisotropic Displacement Parameters ($Å^2 \times 10^3$) for [Ni(NN^{im}S)(4-ClPhS)]. The Anisotropic displacement factor exponent takes the form: $-2\pi^2[h^2a^{*2}U_{11}+2hka^*b^*U_{12}+\ldots]$.

Atom	U_{11}	U_{22}	U_{33}	U_{23}	U_{13}	U_{12}
Ni1	38.4(3)	42.6(3)	32.5(3)	-0.66(15)	1.91(17)	1.91(14)
S1	52.3(5)	58.6(5)	32.4(5)	-0.4(3)	5.3(3)	10.5(4)
S2	78.9(6)	45.8(5)	41.8(5)	-1.9(3)	-12.1(4)	11.6(4)
Cl1	93.7(8)	77.6(7)	90.8(9)	-23.7(6)	-31.0(6)	-13.3(6)
N1	37.2(13)	46.4(14)	34.9(14)	-3.2(11)	3.5(10)	-3.4(10)
C6	40.1(16)	39.4(15)	43.2(18)	0.8(13)	4.8(13)	-2.0(12)
N2	40.2(14)	58.7(17)	45.9(16)	-0.1(12)	6.7(12)	6.2(11)
C15	37.9(16)	52.6(19)	58(2)	-7.0(15)	-9.1(14)	1.7(13)

C13	43.8(18)	46.7(17)	45.6(19)	4.1(14)	7.5(14)	0.5(13)
C12	38.4(16)	47.7(17)	37.7(17)	2.9(13)	-1.9(13)	10.1(12)
C8	60(2)	83(3)	38(2)	1.1(17)	12.6(16)	13.5(19)
C16	49.0(19)	46.9(19)	72(3)	12.7(18)	-5.1(17)	-0.8(14)
C14	51.0(18)	53.4(18)	37.3(18)	-0.8(14)	0.1(14)	2.7(15)
C1	42.7(16)	40.0(16)	38.7(17)	0.6(12)	7.6(13)	-2.0(12)
C17	48.2(18)	50.5(17)	42.1(18)	9.0(15)	-2.6(14)	5.3(14)
C7	47.2(17)	44.2(16)	36.4(17)	1.5(13)	-5.6(13)	-5.6(13)
C2	57(2)	52.8(19)	54(2)	-3.2(16)	15.9(17)	4.1(16)
C9	60(2)	71(2)	47(2)	-8.2(16)	7.2(17)	7.8(17)
C5	46.9(18)	60(2)	54(2)	7.1(16)	-3.3(16)	4.2(15)
C4	44.6(19)	65(2)	86(3)	12(2)	5.3(19)	11.2(16)
C11	47(2)	107(4)	109(4)	-21(3)	20(2)	-11(2)
C3	50(2)	54(2)	83(3)	-2(2)	20.3(19)	11.7(16)
C10	93(3)	60(2)	62(3)	-10.4(19)	9(2)	24(2)

Table F3: Bond Lengths for [Ni(NN^{im}S)(4-ClPhS)].

Atom	**Atom**	**Length/Å**	**Atom**	**Atom**	**Length/Å**
Ni1	S1	2.1384(9)	N2	C11	1.475(5)
Ni1	S2	2.2092(9)	N2	C10	1.470(5)
Ni1	N1	1.888(2)	C15	C16	1.362(5)
Ni1	N2	2.014(3)	C15	C14	1.379(5)
S1	C1	1.737(3)	C13	C12	1.389(4)
S2	C12	1.761(3)	C13	C14	1.383(4)
Cl1	C15	1.747(3)	C12	C17	1.390(4)
N1	C8	1.474(4)	C8	C9	1.474(5)
N1	C7	1.290(4)	C16	C17	1.379(5)
C6	C1	1.403(4)	C1	C2	1.407(4)
C6	C7	1.438(4)	C2	C3	1.369(5)
C6	C5	1.402(4)	C5	C4	1.372(5)
N2	C9	1.497(4)	C4	C3	1.388(5)

Table F4: Bond Angles for [Ni(NN^{im}S)(4-ClPhS)].

Atom	Atom	Atom	Angle/°	Atom	Atom	Atom	Angle/°
S1	Ni1	S2	86.56(3)	C16	C15	Cl1	119.8(3)
N1	Ni1	S1	96.29(8)	C16	C15	C14	121.7(3)
N1	Ni1	S2	175.00(8)	C14	C15	Cl1	118.5(3)
N1	Ni1	N2	85.95(11)	C14	C13	C12	121.1(3)
N2	Ni1	S1	177.13(8)	C13	C12	S2	117.9(2)
N2	Ni1	S2	91.33(8)	C13	C12	C17	118.1(3)
C1	S1	Ni1	112.55(10)	C17	C12	S2	123.9(2)
C12	S2	Ni1	111.76(10)	C9	C8	N1	108.0(3)
C8	N1	Ni1	112.3(2)	C15	C16	C17	119.1(3)
C7	N1	Ni1	132.3(2)	C15	C14	C13	118.7(3)
C7	N1	C8	115.3(3)	C6	C1	S1	125.3(2)
C1	C6	C7	124.0(3)	C6	C1	C2	117.4(3)
C5	C6	C1	119.7(3)	C2	C1	S1	117.3(2)
C5	C6	C7	116.2(3)	C16	C17	C12	121.3(3)
C9	N2	Ni1	105.46(19)	N1	C7	C6	128.6(3)
C11	N2	Ni1	107.2(2)	C3	C2	C1	122.0(3)
C11	N2	C9	111.1(3)	C8	C9	N2	108.1(3)
C10	N2	Ni1	118.8(2)	C4	C5	C6	121.5(3)
C10	N2	C9	105.6(3)	C5	C4	C3	119.0(3)
C10	N2	C11	108.6(3)	C2	C3	C4	120.4(3)

Table F5: Torsion Angles for [Ni(NN^{im}S)(4-ClPhS)].

A	B	C	D	Angle/°	A	B	C	D	Angle/°
Ni1	S1	C1	C6	4.0(3)	C12	C13	C14	C15	-1.5(5)
Ni1	S1	C1	C2	-175.3(2)	C8	N1	C7	C6	175.6(3)
Ni1	S2	C12	C13	-153.6(2)	C16	C15	C14	C13	2.6(5)
Ni1	S2	C12	C17	31.2(3)	C14	C15	C16	C17	-1.9(5)
Ni1	N1	C8	C9	-32.8(4)	C14	C13	C12	S2	-175.8(2)
Ni1	N1	C7	C6	-4.8(5)	C14	C13	C12	C17	-0.4(4)
Ni1	N2	C9	C8	-41.3(3)	C1	C6	C7	N1	-3.5(5)
S1	Ni1	N1	C8	-170.8(2)	C1	C6	C5	C4	-1.3(5)
S1	Ni1	N1	C7	9.6(3)	C1	C2	C3	C4	-1.4(5)
S1	C1	C2	C3	-179.7(3)	C7	N1	C8	C9	146.8(3)
S2	C12	C17	C16	176.3(2)	C7	C6	C1	S1	2.7(4)
Cl1	C15	C16	C17	178.5(2)	C7	C6	C1	C2	-178.0(3)
Cl1	C15	C14	C13	-177.7(2)	C7	C6	C5	C4	177.2(3)

N1	C8	C9	N2	48.7(4)	C5	C6	C1	S1	-178.9(2)
C6	C1	C2	C3	0.9(5)	C5	C6	C1	C2	0.4(4)
C6	C5	C4	C3	0.8(5)	C5	C6	C7	N1	178.0(3)
N2	Ni1	N1	C8	7.4(2)	C5	C4	C3	C2	0.6(5)
N2	Ni1	N1	C7	-172.2(3)	C11	N2	C9	C8	74.5(4)
C15	C16	C17	C12	0.0(5)	C10	N2	C9	C8	-168.0(3)
C13	C12	C17	C16	1.1(4)					

Table F6: Hydrogen Atom Coordinates (Å×10^4) and Isotropic Displacement Parameters (Å^2×10^3) for [Ni(NN^{im}S)(4-ClPhS)].

Atom	***x***	***y***	***z***	**U(eq)**
H13	5685	2532	-1901	54
H8A	6073	1375	4755	72
H8B	7530	1765	5413	72
H16	3702	195	-918	68
H14	4636	1740	-3392	57
H17	4699	996	571	57
H7	9169	1058	4751	52
H2	10802	526	413	65
H9A	6999	2899	4507	71
H9B	5449	2616	5004	71
H5	11335	417	4535	65
H4	13057	-196	3421	78
H11A	3620	2076	2306	131
H11B	3368	2300	3652	131
H11C	4273	1547	3371	131
H3	12760	-144	1344	74
H10A	6011	3613	3152	107
H10B	4272	3458	3335	107
H10C	4904	3351	2051	107

Table G1: Fractional Atomic Coordinates ($\times 10^4$) and Equivalent Isotropic Displacement Parameters ($Å^2 \times 10^3$) for [Ni(NN^{im}S)(4-FPhS)]. U_{eq} is defined as 1/3 of of the trace of the orthogonalised U_{IJ} tensor.

Atom	***x***	***y***	***z***	**U(eq)**
Ni1	8371.7(8)	6904.4(4)	3096.4(6)	40.9(3)
S1	6784.0(18)	6367.3(8)	4150.4(13)	48.9(4)
S2	9428(2)	7438.1(9)	4807.4(15)	59.8(5)
F1	11731(5)	5272(2)	8597(4)	92.5(14)
N2	9854(5)	7461(2)	2153(4)	45.1(11)
N1	7551(5)	6470(2)	1600(4)	41.9(11)
C13	10244(6)	6965(3)	7112(5)	44.4(14)
C12	10114(6)	6757(3)	5903(5)	45.5(14)
C17	10591(6)	6048(3)	5630(6)	50.9(15)
C1	5274(6)	5894(3)	3258(5)	42.5(13)
C6	5139(6)	5818(3)	1990(5)	44.3(13)
C2	4108(7)	5559(3)	3856(6)	52.7(15)
C5	3850(7)	5425(3)	1388(6)	54.6(16)
C16	11123(7)	5550(3)	6511(6)	56.8(17)
C14	10824(7)	6470(3)	8020(6)	51.0(15)
C3	2902(7)	5167(4)	3248(6)	61.2(18)
C7	6283(7)	6088(3)	1263(5)	44.8(14)
C15	11216(7)	5764(3)	7692(6)	57.4(17)
C4	2754(8)	5097(4)	1991(7)	68(2)
C9	9172(8)	7380(4)	852(5)	57.1(16)
C11	10046(9)	8265(3)	2385(7)	65.2(19)
C8	8553(8)	6613(4)	657(6)	59.9(17)
C10	11447(8)	7103(4)	2362(7)	73(2)

Table G2: Anisotropic Displacement Parameters ($Å^2 \times 10^3$) for [Ni(NN^{im}S)(4-FPhS)]. The Anisotropic displacement factor exponent takes the form: $-2\pi^2[h^2a^{*2}U_{11}+2hka^*b^*U_{12}+\ldots]$.

Atom	**U_{11}**	**U_{22}**	**U_{33}**	**U_{23}**	**U_{13}**	**U_{12}**
Ni1	43.3(5)	40.5(5)	38.1(5)	0.4(3)	1.9(3)	-1.6(3)
S1	53.9(9)	51.2(9)	41.1(9)	0.4(7)	4.6(6)	-5.1(7)
S2	84.4(12)	46.5(9)	44.1(10)	-0.6(7)	-7.6(8)	-11.6(8)
F1	114(4)	67(3)	85(3)	19(2)	-26(3)	15(2)
N2	42(3)	41(3)	53(3)	-5(2)	6(2)	-2(2)
N1	44(3)	44(3)	38(3)	1(2)	8(2)	-3(2)
C13	44(3)	44(3)	46(4)	-7(3)	6(3)	-2(2)
C12	40(3)	49(4)	47(4)	1(3)	4(2)	-5(2)

C17	43(3)	58(4)	51(4)	-15(3)	3(3)	-7(3)
C1	40(3)	39(3)	49(4)	7(3)	7(2)	3(2)
C6	49(3)	31(3)	52(4)	-3(3)	2(3)	1(2)
C2	51(4)	58(4)	51(4)	8(3)	13(3)	4(3)
C5	60(4)	50(4)	52(4)	-4(3)	0(3)	-6(3)
C16	44(3)	45(4)	77(5)	-8(3)	-7(3)	2(3)
C14	50(3)	62(4)	41(4)	0(3)	3(3)	-5(3)
C3	50(4)	51(4)	84(5)	15(3)	14(3)	-6(3)
C7	54(4)	37(3)	42(3)	-3(3)	0(3)	2(3)
C15	56(4)	49(4)	62(4)	5(3)	-13(3)	1(3)
C4	45(4)	60(4)	100(6)	-11(4)	10(4)	-8(3)
C9	57(4)	70(4)	44(4)	8(3)	7(3)	-4(3)
C11	82(5)	49(4)	65(5)	6(3)	12(4)	-11(3)
C8	63(4)	69(4)	50(4)	-6(3)	13(3)	-16(3)
C10	47(4)	82(5)	91(6)	6(4)	12(4)	3(3)

Table G3: Bond Lengths for [Ni(NN^{im}S)(4-FPhS)].

Atom	**Atom**	**Length/Å**	**Atom**	**Atom**	**Length/Å**
Ni1	S1	2.1418(19)	C13	C14	1.391(8)
Ni1	S2	2.2189(19)	C12	C17	1.387(8)
Ni1	N2	2.019(5)	C17	C16	1.363(8)
Ni1	N1	1.891(5)	C1	C6	1.411(8)
S1	C1	1.745(6)	C1	C2	1.408(8)
S2	C12	1.775(6)	C6	C5	1.404(8)
F1	C15	1.371(7)	C6	C7	1.436(8)
N2	C9	1.497(8)	C2	C3	1.355(8)
N2	C11	1.475(8)	C5	C4	1.360(9)
N2	C10	1.498(8)	C16	C15	1.364(9)
N1	C7	1.298(7)	C14	C15	1.376(8)
N1	C8	1.465(7)	C3	C4	1.396(9)
C13	C12	1.389(8)	C9	C8	1.484(9)

Table G4: Bond Angles for [Ni(NN^{im}S)(4-FPhS)].

Atom	Atom	Atom	Angle/°	Atom	Atom	Atom	Angle/°
S1	Ni1	S2	86.51(8)	C17	C12	C13	118.3(5)
N2	Ni1	S1	176.91(14)	C16	C17	C12	121.8(6)
N2	Ni1	S2	91.18(15)	C6	C1	S1	125.1(4)
N1	Ni1	S1	96.28(15)	C2	C1	S1	117.2(5)
N1	Ni1	S2	177.20(15)	C2	C1	C6	117.7(5)
N1	Ni1	N2	86.04(19)	C1	C6	C7	124.2(5)
C1	S1	Ni1	112.5(2)	C5	C6	C1	118.9(5)
C12	S2	Ni1	110.7(2)	C5	C6	C7	116.9(5)
C9	N2	Ni1	105.4(3)	C3	C2	C1	121.8(6)
C9	N2	C10	109.8(5)	C4	C5	C6	122.2(6)
C11	N2	Ni1	117.3(4)	C17	C16	C15	118.7(6)
C11	N2	C9	106.6(5)	C15	C14	C13	118.3(6)
C11	N2	C10	108.5(5)	C2	C3	C4	120.7(6)
C10	N2	Ni1	109.1(4)	N1	C7	C6	128.5(5)
C7	N1	Ni1	132.3(4)	F1	C15	C14	117.8(6)
C7	N1	C8	115.6(5)	C16	C15	F1	120.0(6)
C8	N1	Ni1	112.1(4)	C16	C15	C14	122.2(6)
C12	C13	C14	120.6(5)	C5	C4	C3	118.7(6)
C13	C12	S2	117.3(4)	C8	C9	N2	108.5(5)
C17	C12	S2	124.4(5)	N1	C8	C9	106.9(5)

Table G5: Torsion Angles for [Ni(NN^{im}S)(4-FPhS)].

A	B	C	D	Angle/°	A	B	C	D	Angle/°
Ni1	S1	C1	C6	4.2(5)	C12	C17	C16	C15	-1.3(9)
Ni1	S1	C1	C2	-176.2(4)	C17	C16	C15	F1	179.3(5)
Ni1	S2	C12	C13	-156.1(4)	C17	C16	C15	C14	-1.5(9)
Ni1	S2	C12	C17	26.9(6)	C1	C6	C5	C4	-2.1(9)
Ni1	N2	C9	C8	-39.3(6)	C1	C6	C7	N1	-4.1(9)
Ni1	N1	C7	C6	-5.9(9)	C1	C2	C3	C4	-1.5(10)
Ni1	N1	C8	C9	-37.2(6)	C6	C1	C2	C3	0.8(8)
S1	Ni1	N1	C7	11.3(5)	C6	C5	C4	C3	1.5(10)
S1	Ni1	N1	C8	-169.9(4)	C2	C1	C6	C5	0.9(8)
S1	C1	C6	C5	-179.5(4)	C2	C1	C6	C7	-176.0(5)
S1	C1	C6	C7	3.6(8)	C2	C3	C4	C5	0.3(10)
S1	C1	C2	C3	-178.8(5)	C5	C6	C7	N1	178.9(5)

S2	C12	C17	C16	179.3(5)	C14	C13	C12	S2	-177.8(4)
N2	Ni1	N1	C7	-166.7(5)	C14	C13	C12	C17	-0.6(8)
N2	Ni1	N1	C8	12.2(4)	C7	N1	C8	C9	141.9(5)
N2	C9	C8	N1	50.2(7)	C7	C6	C5	C4	175.0(6)
C13	C12	C17	C16	2.3(9)	C11	N2	C9	C8	-164.7(5)
C13	C14	C15	F1	-177.6(5)	C8	N1	C7	C6	175.4(5)
C13	C14	C15	C16	3.1(9)	C10	N2	C9	C8	78.0(6)
C12	C13	C14	C15	-2.0(9)					

Table G6: Hydrogen Atom Coordinates (Å×10^4) and Isotropic Displacement Parameters (Å^2×10^3) for [Ni(NN^{im}S)(4-FPhS)].

Atom	***x***	***y***	***z***	**U(eq)**
H13	9933	7450	7320	53
H17	10546	5905	4806	61
H2	4168	5608	4709	63
H5	3739	5388	531	66
H16	11424	5063	6307	68
H14	10946	6615	8847	61
H3	2148	4938	3681	73
H7	6086	5971	426	54
H4	1905	4824	1565	82
H9A	8311	7744	647	68
H9B	9995	7475	325	68
H11A	9037	8517	2148	98
H11B	10838	8464	1913	98
H11C	10389	8348	3249	98
H8A	7932	6568	-154	72
H8B	9432	6252	717	72
H10A	11919	7188	3200	110
H10B	12124	7319	1810	110
H10C	11338	6568	2213	110

Table H1: Fractional Atomic Coordinates ($\times 10^4$) and Equivalent Isotropic Displacement Parameters ($Å^2 \times 10^3$) for $NN^{am}S$. U_{eq} is defined as 1/3 of of the trace of the orthogonalised U_{IJ} tensor.

Atom	*x*	*y*	*z*	U(eq)
C1	9364(12)	8817(4)	574(4)	35(2)
C2	8818(13)	9443(5)	749(5)	38(2)
C3	8735(13)	9596(5)	1393(5)	44(2)
C4	9168(13)	9136(4)	1881(4)	37(2)
C5	9722(12)	8515(4)	1703(4)	30.2(19)
C6	9801(12)	8350(4)	1055(4)	29.4(19)
C7	10415(12)	7669(4)	968(4)	30(2)
C8	11509(13)	6703(4)	1659(4)	34(2)
C9	10186(12)	6242(4)	1966(4)	29.7(19)
C10	8208(14)	5891(5)	966(4)	43(2)
C11	6944(15)	5872(5)	2004(5)	51(3)
C12	4318(13)	8886(5)	853(4)	35(2)
C13	3786(14)	9478(5)	1093(4)	40(2)
C14	3817(13)	9521(5)	1766(5)	45(3)
C15	4373(13)	8987(5)	2165(4)	44(3)
C16	4899(12)	8398(5)	1908(4)	32(2)
C17	4853(12)	8344(4)	1247(4)	30(2)
C18	5385(11)	7768(5)	899(4)	28.5(19)
C19	5772(13)	7471(5)	-245(4)	41(2)
C20	4201(13)	7278(5)	-782(4)	36(2)
C21	3079(14)	6375(5)	-98(4)	43(2)
C22	1246(16)	6708(5)	-1117(5)	52(3)
F1	8692(7)	9045(2)	7931(2)	39.8(13)
F2	7004(9)	8327(4)	8450(3)	73(2)
F3	9635(8)	8019(3)	9098(2)	45.7(14)
F4	11343(8)	8721(3)	8567(3)	57.4(16)
F5	9511(10)	7976(3)	7999(3)	67(2)
F6	8821(10)	9094(3)	9016(2)	60.1(18)
F7	1629(11)	9927(4)	3102(4)	91(2)
F8	-230(10)	9556(3)	3740(4)	83(2)
F9	1803(12)	8878(4)	3461(4)	96(3)
F10	4001(11)	9587(3)	3718(4)	87(2)
F11	2221(15)	9282(10)	4483(6)	57(5)
F12	1969(10)	10342(3)	4043(4)	85(2)
F11A	2180(20)	8971(15)	4346(9)	49(7)
N1	10731(10)	7364(3)	1569(3)	29.1(16)
N2	8240(10)	6211(4)	1610(3)	30.5(17)

N3	5141(10)	7905(4)	241(3)	33.8(17)
N4	2571(10)	6951(3)	-552(3)	31.0(17)
O1	10649(9)	7383(3)	463(3)	37.0(15)
O2	5950(9)	7230(3)	1114(3)	37.7(15)
P1	9158(4)	8536.4(12)	8512.8(10)	36.1(7)
P2	1936(4)	9609.8(15)	3848.0(19)	66.8(10)
S1	10399(3)	7851.8(12)	2214.7(10)	36.6(6)
S2	4370(4)	8692.2(12)	40.6(11)	40.1(7)

Table H2: Anisotropic Displacement Parameters ($Å^2 \times 10^3$) for $NN^{am}S$. The Anisotropic displacement factor exponent takes the form: $-2\pi^2[h^2a^{*2}U_{11}+2hka^*b^*U_{12}+\ldots]$.

Atom	**U_{11}**	**U_{22}**	**U_{33}**	**U_{23}**	**U_{13}**	**U_{12}**
C1	38(5)	35(5)	29(5)	2(4)	-5(4)	-3(4)
C2	36(5)	36(5)	40(5)	5(4)	-6(4)	2(4)
C3	43(6)	37(6)	52(6)	-11(5)	8(5)	-2(5)
C4	47(6)	32(5)	32(5)	-8(4)	5(4)	-4(4)
C5	32(5)	35(5)	23(4)	1(4)	3(4)	-4(4)
C6	32(5)	29(5)	26(4)	-2(4)	-2(4)	-2(4)
C7	33(5)	34(5)	21(4)	0(4)	-2(4)	-2(4)
C8	42(6)	32(5)	28(4)	0(4)	5(4)	-1(4)
C9	33(5)	30(5)	23(4)	7(4)	-6(4)	-3(4)
C10	47(6)	52(6)	26(5)	-14(4)	-6(4)	9(5)
C11	61(7)	49(6)	45(6)	0(5)	14(5)	-11(5)
C12	36(5)	40(5)	26(4)	-4(4)	1(4)	-5(4)
C13	46(6)	36(6)	37(5)	-4(4)	-6(4)	1(4)
C14	41(6)	42(6)	52(6)	-20(5)	7(5)	4(5)
C15	41(6)	63(7)	27(5)	-11(5)	0(4)	-6(5)
C16	38(5)	37(5)	22(4)	-4(4)	2(4)	2(4)
C17	33(5)	31(5)	23(4)	-1(4)	-5(4)	-4(4)
C18	26(5)	41(5)	17(4)	5(4)	-3(3)	-7(4)
C19	42(6)	48(6)	34(5)	-10(4)	9(4)	-5(5)
C20	51(6)	43(6)	15(4)	-4(4)	7(4)	0(4)
C21	55(6)	45(6)	31(5)	1(4)	10(4)	11(5)
C22	60(7)	44(6)	47(6)	-12(5)	-12(5)	-5(5)
F1	53(3)	39(3)	26(3)	6(2)	-2(2)	5(2)
F2	51(4)	98(5)	66(4)	37(4)	-8(3)	-19(4)
F3	72(4)	40(3)	24(3)	8(2)	0(3)	4(3)
F4	51(4)	69(4)	49(3)	19(3)	-5(3)	2(3)
F5	128(6)	41(3)	29(3)	-7(3)	1(3)	18(4)

F6	107(5)	45(4)	27(3)	6(3)	5(3)	23(3)
F7	105(6)	95(6)	75(5)	10(4)	20(4)	-4(5)
F8	81(5)	68(5)	90(5)	26(4)	-25(4)	-13(4)
F9	111(7)	71(5)	106(6)	-10(5)	18(5)	-7(5)
F10	105(6)	51(4)	118(6)	12(4)	60(5)	4(4)
F12	67(5)	66(5)	121(6)	-56(5)	5(4)	2(4)
N1	35(4)	31(4)	21(4)	-3(3)	2(3)	0(3)
N2	35(4)	31(4)	24(4)	-1(3)	-3(3)	0(3)
N3	39(4)	36(4)	25(4)	3(3)	-2(3)	1(3)
N4	40(4)	31(4)	22(4)	-3(3)	3(3)	-1(3)
O1	49(4)	40(4)	22(3)	-8(3)	4(3)	4(3)
O2	45(4)	36(4)	30(3)	2(3)	-4(3)	8(3)
P1	51.4(16)	33.7(14)	21.5(11)	2.9(10)	-1.4(10)	2.2(11)
P2	49.1(19)	40.4(17)	114(3)	31.6(18)	23.8(18)	7.6(13)
S1	51.3(15)	37.5(14)	20.2(11)	-2(1)	2(1)	-0.2(11)
S2	54.0(15)	37.6(14)	26.2(11)	2.7(10)	-3.7(10)	-1.7(11)

Table H3: Bond Lengths for $NN^{am}S$.

Atom	**Atom**	**Length/Å**	**Atom**	**Atom**	**Length/Å**
C1	C2	1.387(13)	C17	C18	1.449(12)
C1	C6	1.385(12)	C18	N3	1.393(10)
C2	C3	1.390(13)	C18	O2	1.226(10)
C3	C4	1.386(13)	C19	C20	1.533(12)
C4	C5	1.381(12)	C19	N3	1.456(11)
C5	C6	1.402(11)	C20	N4	1.470(11)
C5	S1	1.744(9)	C21	N4	1.517(11)
C6	C7	1.464(12)	C22	N4	1.498(11)
C7	N1	1.391(10)	F1	P1	1.596(5)
C7	O1	1.233(9)	F2	P1	1.584(6)
C8	C9	1.525(11)	F3	P1	1.611(5)
C8	N1	1.449(11)	F4	P1	1.593(6)
C9	N2	1.491(10)	F5	P1	1.603(6)
C10	N2	1.493(10)	F6	P1	1.581(6)
C11	N2	1.480(11)	F7	P2	1.674(8)
C12	C13	1.371(13)	F8	P2	1.537(8)
C12	C17	1.395(12)	F9	P2	1.683(8)
C12	S2	1.747(9)	F10	P2	1.532(8)
C13	C14	1.406(13)	F11	P2	1.474(11)
C14	C15	1.391(14)	F12	P2	1.534(7)

C15	C16	1.377(13)	N1	S1	1.711(7)
C16	C17	1.381(11)	N3	S2	1.717(7)

Table H4: Bond Angles for $NN^{am}S$.

Atom	Atom	Atom	Angle/°	Atom	Atom	Atom	Angle/°
C6	C1	C2	118.4(8)	C18	N3	S2	114.9(6)
C1	C2	C3	120.4(9)	C19	N3	S2	120.5(6)
C4	C3	C2	122.0(9)	C20	N4	C21	114.4(7)
C5	C4	C3	117.2(8)	C20	N4	C22	109.7(7)
C4	C5	C6	121.6(8)	C22	N4	C21	108.5(7)
C4	C5	S1	126.8(7)	F1	P1	F3	179.6(3)
C6	C5	S1	111.6(6)	F1	P1	F5	88.9(3)
C1	C6	C5	120.4(8)	F2	P1	F1	90.2(3)
C1	C6	C7	126.5(8)	F2	P1	F3	90.0(3)
C5	C6	C7	113.1(7)	F2	P1	F4	177.9(4)
N1	C7	C6	108.8(7)	F2	P1	F5	89.3(4)
O1	C7	C6	128.4(8)	F4	P1	F1	90.6(3)
O1	C7	N1	122.8(8)	F4	P1	F3	89.2(3)
N1	C8	C9	111.8(7)	F4	P1	F5	88.8(4)
N2	C9	C8	113.8(7)	F5	P1	F3	90.8(3)
C13	C12	C17	122.5(8)	F6	P1	F1	90.7(3)
C13	C12	S2	126.4(7)	F6	P1	F2	91.1(4)
C17	C12	S2	111.2(7)	F6	P1	F3	89.6(3)
C12	C13	C14	116.8(9)	F6	P1	F4	90.9(4)
C15	C14	C13	121.2(9)	F6	P1	F5	179.5(4)
C16	C15	C14	120.6(8)	F7	P2	F9	84.1(4)
C15	C16	C17	119.0(9)	F8	P2	F7	83.1(4)
C12	C17	C18	113.8(7)	F8	P2	F9	82.7(4)
C16	C17	C12	119.9(8)	F10	P2	F7	82.1(4)
C16	C17	C18	126.3(8)	F10	P2	F8	160.7(5)
N3	C18	C17	109.1(7)	F10	P2	F9	83.4(4)
O2	C18	C17	128.6(7)	F10	P2	F12	95.3(4)
O2	C18	N3	122.2(8)	F11	P2	F7	175.8(9)
N3	C19	C20	113.7(8)	F11	P2	F8	97.0(5)
N4	C20	C19	114.3(7)	F11	P2	F9	91.8(9)
C7	N1	C8	122.7(7)	F11	P2	F10	96.9(5)
C7	N1	S1	115.7(6)	F11	P2	F12	101.5(10)
C8	N1	S1	121.2(5)	F12	P2	F7	82.7(4)
C9	N2	C10	112.0(7)	F12	P2	F8	95.1(4)

C11	N2	C9	110.5(7)	F12	P2	F9	166.8(5)
C11	N2	C10	111.1(7)	N1	S1	C5	90.9(4)
C18	N3	C19	123.8(8)	N3	S2	C12	90.9(4)

Table H5: Hydrogen Atom Coordinates ($Å \times 10^4$) and Isotropic Displacement Parameters ($Å^2 \times 10^3$) for $NN^{am}S$.

Atom	***x***	***y***	***z***	**U(eq)**
H1	9437	8711	135	42
H2	8498	9769	427	45
H3	8370	10029	1503	52
H4	9088	9243	2319	45
H8A	12738	6726	1937	41
H8B	11737	6522	1235	41
H9A	10733	5791	1989	36
H9B	10109	6391	2413	36
H10A	8856	5463	1016	64
H10B	8851	6176	683	64
H10C	6896	5823	775	64
H11A	7393	5420	2098	76
H11B	5672	5858	1764	76
H11C	6910	6114	2408	76
H13	3414	9842	818	48
H14	3451	9922	1952	54
H15	4390	9029	2618	53
H16	5287	8035	2181	39
H19A	6306	7064	-31	49
H19B	6796	7694	-441	49
H20A	3755	7682	-1023	43
H20B	4736	6978	-1086	43
H21A	3798	6047	-312	65
H21B	1921	6172	17	65
H21C	3848	6535	293	65
H22A	1028	7060	-1440	78
H22B	41	6581	-972	78
H22C	1801	6323	-1307	78
H2A	7780	6676	1538	37
H4A	1886	7288	-318	37

Table H6: Atomic Occupancy for $NN^{am}S$.

Atom	*Occupancy*	Atom	*Occupancy*
F11	0.61(4)	F11A	0.39(4)

Table I1: Fractional Atomic Coordinates ($\times 10^4$) and Equivalent Isotropic Displacement Parameters ($Å^2 \times 10^3$) for $(NN^{am}S)_2$. U_{eq} is defined as 1/3 of of the trace of the orthogonalised U_{IJ} tensor.

Atom	*x*	*y*	*z*	U(eq)
S1	5300.5(5)	4971.1(14)	7300.2(14)	30.0(4)
Cl1	7161.7(5)	2700.5(14)	2545.8(14)	34.2(4)
Cl2	6403.0(12)	-1052(3)	2267(3)	99.2(10)
Cl3B	5892(3)	1083(6)	2980(20)	81(3)
O1	6125.1(13)	4862(4)	6857(4)	33.1(10)
N1	7192.1(16)	4955(4)	4534(5)	28.6(10)
N2	6176.9(16)	4886(5)	4724(5)	31.2(11)
C5	6004.7(18)	5287(6)	5736(6)	29.2(12)
C11	5656(2)	7267(6)	4504(6)	33.6(13)
C3	6953.4(18)	4330(6)	5489(6)	31.7(13)
C1	6992.7(19)	6206(6)	3974(6)	31.9(13)
C4	6508.7(19)	3878(6)	4890(6)	32.8(13)
C8	4969(2)	7138(6)	5789(6)	36.6(14)
C9	4986(2)	8113(7)	4853(6)	41.8(16)
C7	5299.0(18)	6221(5)	6087(5)	28.0(12)
C10	5327(2)	8185(6)	4230(6)	41.6(15)
C6	5648.4(18)	6272(6)	5435(5)	30.3(12)
C2	7647(2)	5156(6)	5150(7)	39.0(15)
C12	6240(3)	600(9)	2033(9)	64(2)
Cl3A	6031(14)	890(30)	3660(40)	98(9)

Table I2: Anisotropic Displacement Parameters ($Å^2 \times 10^3$) for $(NN^{am}S)_2$. The Anisotropic displacement factor exponent takes the form: $-2\pi^2[h^2a^{*2}U_{11}+2hka^*b^*U_{12}+\ldots]$.

Atom	U_{11}	U_{22}	U_{33}	U_{23}	U_{13}	U_{12}
S1	24.8(7)	38.7(8)	29.5(8)	5.2(6)	13.2(6)	3.0(5)
Cl1	43.5(9)	32.4(7)	30.7(7)	-0.1(5)	17.0(6)	6.0(6)
Cl2	139(3)	59.1(14)	101(2)	-10.1(13)	28(2)	25.2(15)
Cl3B	75(4)	53(2)	129(8)	8(3)	54(4)	7(2)
O1	28(2)	49(2)	26(2)	5.0(17)	11.2(18)	5.8(17)
N1	31(3)	29(2)	28(2)	-1.9(18)	11(2)	-0.8(19)
N2	29(3)	43(3)	23(2)	-2(2)	11(2)	1(2)
C5	25(3)	38(3)	28(3)	-3(2)	12(2)	-7(2)
C11	37(3)	37(3)	30(3)	2(2)	15(3)	-6(2)
C3	33(3)	33(3)	34(3)	5(2)	18(3)	5(2)
C1	35(3)	32(3)	31(3)	2(2)	11(3)	-4(2)
C4	34(3)	37(3)	31(3)	1(2)	16(3)	1(2)
C8	39(3)	43(3)	32(3)	4(3)	16(3)	6(3)
C9	49(4)	35(3)	42(4)	7(3)	8(3)	10(3)
C7	28(3)	31(3)	27(3)	-1(2)	8(2)	1(2)
C10	58(4)	33(3)	35(3)	4(3)	12(3)	-1(3)
C6	31(3)	37(3)	25(3)	-3(2)	10(2)	-4(2)
C2	32(3)	39(3)	48(4)	2(3)	14(3)	-1(2)
C12	56(5)	61(5)	72(6)	11(4)	4(4)	-2(4)
Cl3A	140(16)	58(8)	114(16)	-24(9)	72(15)	-47(8)

Table I3: Bond Lengths for $(NN^{am}S)_2$.

Atom	Atom	Length/Å	Atom	Atom	Length/Å
S1	$S1^1$	2.028(3)	C5	C6	1.498(8)
S1	C7	1.790(6)	C11	C10	1.388(9)
Cl2	C12	1.753(9)	C11	C6	1.403(8)
Cl3B	C12	1.684(14)	C3	C4	1.508(9)
O1	C5	1.242(7)	C8	C9	1.398(9)
N1	C3	1.499(7)	C8	C7	1.392(8)
N1	C1	1.487(7)	C9	C10	1.364(9)
N1	C2	1.485(8)	C7	C6	1.406(7)
N2	C5	1.339(7)	C12	Cl3A	1.96(2)
N2	C4	1.454(7)			

Table I4: Bond Angles for $(NN^{am}S)_2$

Atom	Atom	Atom	Angle/°	Atom	Atom	Atom	Angle/°
C7	S1	S1[1]	105.36(19)	C7	C8	C9	120.2(5)
C1	N1	C3	113.0(4)	C10	C9	C8	120.5(6)
C2	N1	C3	109.9(5)	C8	C7	S1	122.2(4)
C2	N1	C1	111.4(4)	C8	C7	C6	119.8(5)
C5	N2	C4	120.6(5)	C6	C7	S1	118.0(4)
O1	C5	N2	122.7(5)	C9	C10	C11	119.9(6)
O1	C5	C6	121.3(5)	C11	C6	C5	121.0(5)
N2	C5	C6	115.9(5)	C11	C6	C7	118.5(5)
C10	C11	C6	121.0(5)	C7	C6	C5	120.5(5)
N1	C3	C4	113.6(5)	Cl2	C12	Cl3A	99.3(13)
N2	C4	C3	116.2(5)	Cl3B	C12	Cl2	113.8(6)

[1]1-X,+Y,3/2-Z

Table I5: Torsion Angles for $(NN^{am}S)_2$.

A	B	C	D	Angle/°	A	B	C	D	Angle/°
S1[1]	S1	C7	C8	13.0(6)	C4	N2	C5	C6	-176.6(5)
S1[1]	S1	C7	C6	-167.8(4)	C8	C9	C10	C11	1.5(11)
S1	C7	C6	C5	1.2(7)	C8	C7	C6	C5	-179.5(6)
S1	C7	C6	C11	-178.5(5)	C8	C7	C6	C11	0.7(9)
O1	C5	C6	C11	144.2(6)	C9	C8	C7	S1	178.7(5)
O1	C5	C6	C7	-35.5(8)	C9	C8	C7	C6	-0.5(10)
N1	C3	C4	N2	-82.4(6)	C7	C8	C9	C10	-0.6(11)
N2	C5	C6	C11	-36.8(8)	C10	C11	C6	C5	-179.6(6)
N2	C5	C6	C7	143.5(5)	C10	C11	C6	C7	0.1(9)
C5	N2	C4	C3	-78.2(6)	C6	C11	C10	C9	-1.2(10)
C1	N1	C3	C4	64.6(6)	C2	N1	C3	C4	-170.3(5)
C4	N2	C5	O1	2.3(9)					

Table I6: Hydrogen Atom Coordinates (Å×10^4) and Isotropic Displacement Parameters (Å^2×10^3) for $(NN^{am}S)_2$

Atom	***x***	***y***	***z***	**U(eq)**
H1	7187	4317	3800	34
H2	6089	5237	3951	37
H11	5890	7313	4054	40
H3A	6933	4974	6188	38
H3B	7119	3560	5894	38
H1A	6713	6014	3438	48
H1B	7178	6621	3436	48
H1C	6956	6808	4680	48
H4A	6520	3491	4027	39
H4B	6424	3164	5440	39
H8	4732	7100	6224	44
H9	4758	8730	4648	50
H10	5340	8864	3610	50
H2A	7661	5620	5979	58
H2B	7790	5686	4572	58
H2C	7789	4296	5304	58
H12A	6496	1176	2212	77
H12B	6105	726	1110	77
H12D	6010	707	1263	77
H12C	6482	1192	1953	77

Table I7: Atomic Occupancy for $(NN^{am}S)_2$.

Atom	***Occupancy***	**Atom**	***Occupancy***	**Atom**	***Occupancy***
Cl3B	0.67(4)	H12A	0.67(4)	H12B	0.67(4)
H12D	0.33(4)	H12C	0.33(4)	Cl3A	0.33(4)

Table J1: Fractional Atomic Coordinates ($\times 10^4$) and Equivalent Isotropic Displacement Parameters ($Å^2 \times 10^3$) for $[Ni_3(NN^{am}S)_2(S^tBu)_2]$. U_{eq} is defined as 1/3 of of the trace of the orthogonalised U_{IJ} tensor.

Atom	*x*	*y*	*z*	U(eq)
Ni1	2165.4(2)	8277.1(3)	1355.6(2)	15.40(8)
Ni2	2500	7500	0	15.12(10)
S2	1613.1(3)	8436.8(7)	392.5(3)	16.66(12)
S1	2889.6(3)	9264.0(7)	747.2(3)	16.02(12)
O1	3525.6(8)	6742(2)	2722.8(8)	26.4(4)
N2	1448.5(9)	7428(2)	1874.7(9)	20.4(4)
C9	1657.0(11)	7683(3)	2595.7(11)	23.7(5)
N1	2685.8(9)	7673(2)	2104.2(9)	17.6(4)
C6	3771.9(11)	7898(3)	1669.4(11)	17.8(5)
C1	3648.6(10)	8731(3)	1058.0(11)	17.3(5)
C2	4145.7(11)	9235(3)	656.3(11)	24.1(5)
C10	1382.4(12)	5659(3)	1722.1(12)	29.4(6)
C7	3302.6(11)	7391(3)	2193.2(11)	18.4(5)
C13	757.7(12)	10556(3)	-127.6(14)	35.0(6)
C8	2327.5(11)	7129(3)	2696.5(11)	22.6(5)
C4	4891.5(12)	8014(3)	1428.8(12)	28.4(6)
C5	4402.7(11)	7539(3)	1830.8(11)	24.5(5)
C12	1460.4(11)	10537(3)	41.4(11)	19.6(5)
C3	4762.6(11)	8886(3)	840.0(12)	30.1(6)
C15	1618.7(12)	11842(3)	563.0(12)	28.0(6)
C14	1830.3(12)	10785(3)	-605.5(11)	28.1(6)
C11	829.1(11)	8234(3)	1772.4(12)	29.5(6)

Table J2: Anisotropic Displacement Parameters ($Å^2 \times 10^3$) for $[Ni_3(NN^{am}S)_2(S^tBu)_2]$. The Anisotropic displacement factor exponent takes the form: $-2\pi^2[h^2a^{*2}U_{11}+2hka^*b^*U_{12}+\ldots]$.

Atom	U_{11}	U_{22}	U_{33}	U_{23}	U_{13}	U_{12}
Ni1	17.19(16)	16.02(14)	13.02(14)	0.79(11)	0.81(11)	-1.07(12)
Ni2	15.1(2)	17.0(2)	13.14(19)	-0.20(16)	-0.67(15)	0.24(16)
S2	15.4(3)	18.7(3)	15.9(3)	-0.4(2)	1.2(2)	-0.9(2)
S1	16.5(3)	17.4(3)	14.1(3)	1.4(2)	-0.5(2)	-1.0(2)
O1	30.5(10)	30.5(9)	18.1(8)	7.9(7)	-3.2(7)	5.1(8)
N2	24.0(11)	20.0(9)	17.2(9)	-0.2(8)	3.6(8)	-3.0(9)
C9	30.6(14)	26.9(12)	14.0(11)	-0.7(10)	6.5(10)	-5.5(11)
N1	21.6(10)	18.2(9)	13.2(9)	1.0(7)	1.7(8)	-1.6(8)
C6	21.2(12)	17.3(11)	14.6(10)	-3.0(8)	-3.1(9)	-0.6(9)

C1	16.4(11)	19.0(11)	16.6(11)	-1.6(9)	-2.1(9)	-1.3(9)
C2	22.1(13)	30.7(13)	19.3(12)	4.1(10)	-3(1)	-4.3(11)
C10	39.5(16)	22.0(12)	26.8(13)	1.2(10)	-0.1(11)	-10.9(12)
C7	24.8(13)	15.1(10)	15.3(11)	-1.9(9)	-3.2(9)	-0.5(10)
C13	23.1(14)	32.4(14)	49.0(17)	1.9(13)	-11.1(12)	4.4(12)
C8	26.7(13)	24.9(12)	16.1(11)	3.0(9)	2(1)	-0.6(10)
C4	19.0(13)	40.1(15)	25.9(13)	0.4(11)	-5.5(10)	-0.9(11)
C5	25.5(13)	28.8(13)	18.9(12)	1.3(10)	-6.9(10)	1.5(11)
C12	19.6(12)	19.1(11)	20.0(11)	-0.1(9)	-3.2(9)	1.2(9)
C3	18.8(13)	43.0(15)	28.4(13)	4.2(12)	0.1(10)	-5.4(12)
C15	36.2(15)	20.8(12)	26.7(13)	-3.3(10)	-4.9(11)	4.5(11)
C14	37.5(15)	26.1(12)	20.6(12)	4.3(10)	1.7(11)	3.3(12)
C11	18.9(13)	43.1(15)	26.8(13)	4.2(12)	6.5(10)	0.9(12)

Table J3: Bond Lengths for $[Ni_3(NN^{am}S)_2(S^tBu)_2]$.

Atom	**Atom**	**Length/Å**	**Atom**	**Atom**	**Length/Å**
Ni1	Ni2	2.8545(9)	N2	C11	1.482(3)
Ni1	S2	2.2151(9)	C9	C8	1.505(3)
Ni1	S1	2.1323(8)	N1	C7	1.340(3)
Ni1	N2	1.9817(19)	N1	C8	1.478(3)
Ni1	N1	1.8904(19)	C6	C1	1.402(3)
Ni2	Ni1[1]	2.8545(9)	C6	C7	1.511(3)
Ni2	S2[1]	2.1938(8)	C6	C5	1.404(3)
Ni2	S2	2.1938(8)	C1	C2	1.398(3)
Ni2	S1	2.2045(7)	C2	C3	1.384(3)
Ni2	S1[1]	2.2046(7)	C13	C12	1.525(3)
S2	C12	1.868(2)	C4	C5	1.378(3)
S1	C1	1.769(2)	C4	C3	1.383(3)
O1	C7	1.254(3)	C12	C15	1.511(3)
N2	C9	1.495(3)	C12	C14	1.529(3)
N2	C10	1.475(3)			

[1]1/2-X,3/2-Y,-Z

Table J4: Bond Angles for $[Ni_3(NN^{am}S)_2(S^tBu)_2]$.

Atom	Atom	Atom	Angle/°	Atom	Atom	Atom	Angle/°
S2	Ni1	Ni2	49.32(2)	C9	N2	Ni1	103.20(14)
S1	Ni1	Ni2	49.94(2)	C10	N2	Ni1	107.76(14)
S1	Ni1	S2	82.61(3)	C10	N2	C9	110.74(18)
N2	Ni1	Ni2	128.25(6)	C10	N2	C11	108.81(19)
N2	Ni1	S2	93.66(6)	C11	N2	Ni1	118.00(14)
N2	Ni1	S1	175.93(6)	C11	N2	C9	108.18(18)
N1	Ni1	Ni2	121.35(6)	N2	C9	C8	110.12(18)
N1	Ni1	S2	167.23(6)	C7	N1	Ni1	134.53(15)
N1	Ni1	S1	96.85(6)	C7	N1	C8	111.54(18)
N1	Ni1	N2	87.15(8)	C8	N1	Ni1	113.05(14)
Ni1	Ni2	Ni1[1]	180.0	C1	C6	C7	127.3(2)
S2[1]	Ni2	Ni1	130.03(2)	C1	C6	C5	117.0(2)
S2	Ni2	Ni1	49.98(2)	C5	C6	C7	115.61(19)
S2	Ni2	Ni1[1]	130.03(2)	C6	C1	S1	124.59(17)
S2[1]	Ni2	Ni1[1]	49.97(2)	C2	C1	S1	115.40(17)
S2	Ni2	S2[1]	180.0	C2	C1	C6	120.0(2)
S2[1]	Ni2	S1	98.53(3)	C3	C2	C1	121.2(2)
S2[1]	Ni2	S1[1]	81.47(3)	O1	C7	N1	122.1(2)
S2	Ni2	S1[1]	98.53(3)	O1	C7	C6	116.2(2)
S2	Ni2	S1	81.47(3)	N1	C7	C6	121.64(19)
S1	Ni2	Ni1[1]	132.24(2)	N1	C8	C9	108.14(18)
S1	Ni2	Ni1	47.76(2)	C5	C4	C3	119.3(2)
S1[1]	Ni2	Ni1	132.24(2)	C4	C5	C6	122.9(2)
S1[1]	Ni2	Ni1[1]	47.76(2)	C13	C12	S2	104.58(16)
S1	Ni2	S1[1]	180.0	C13	C12	C14	109.7(2)
Ni2	S2	Ni1	80.70(3)	C15	C12	S2	110.79(16)
C12	S2	Ni1	117.14(7)	C15	C12	C13	110.1(2)
C12	S2	Ni2	109.27(7)	C15	C12	C14	111.4(2)
Ni1	S1	Ni2	82.31(3)	C14	C12	S2	109.98(15)
C1	S1	Ni1	112.28(8)	C4	C3	C2	119.6(2)
C1	S1	Ni2	113.51(7)				

[1]1/2-X,3/2-Y,-Z

Table J5: Torsion Angles for $[Ni_3(NN^{am}S)_2(S^tBu)_2]$.

B	C	D	Angle/°	A	B	C	D	Angle/°
Ni1	S2	C12	C13	-131.59(14)	N2	Ni1	N1	C8	-7.49(15)
Ni1	S2	C12	C15	-12.98(19)	N2	C9	C8	N1	41.3(2)
Ni1	S2	C12	C14	110.63(15)	C6	C1	C2	C3	1.9(4)
Ni1	S1	C1	C6	-6.1(2)	C1	C6	C7	O1	-175.9(2)
Ni1	S1	C1	C2	175.52(15)	C1	C6	C7	N1	1.9(3)
Ni1	N2	C9	C8	-45.1(2)	C1	C6	C5	C4	2.1(3)
Ni1	N1	C7	O1	-168.19(16)	C1	C2	C3	C4	0.4(4)
Ni1	N1	C7	C6	14.2(3)	C10	N2	C9	C8	70.0(2)
Ni1	N1	C8	C9	-16.3(2)	C7	N1	C8	C9	172.87(19)
Ni2	Ni1	N1	C7	26.5(2)	C7	C6	C1	S1	-3.9(3)
Ni2	Ni1	N1	C8	-141.56(13)	C7	C6	C1	C2	174.5(2)
Ni2	S2	C12	C13	139.16(14)	C7	C6	C5	C4	-175.8(2)
Ni2	S2	C12	C15	-102.23(16)	C8	N1	C7	O1	0.0(3)
Ni2	S2	C12	C14	21.39(17)	C8	N1	C7	C6	-177.63(19)
Ni2	S1	C1	C6	-97.23(19)	C5	C6	C1	S1	178.55(17)
Ni2	S1	C1	C2	84.34(18)	C5	C6	C1	C2	-3.1(3)
S2	Ni1	N1	C7	66.6(4)	C5	C6	C7	O1	1.7(3)
S2	Ni1	N1	C8	-101.5(3)	C5	C6	C7	N1	179.5(2)
S1	Ni1	N1	C7	-20.2(2)	C5	C4	C3	C2	-1.5(4)
S1	Ni1	N1	C8	171.75(14)	C3	C4	C5	C6	0.2(4)
S1	C1	C2	C3	-179.6(2)	C11	N2	C9	C8	-170.85(19)
N2	Ni1	N1	C7	160.5(2)					

Table J6: Hydrogen Atom Coordinates ($Å\times10^4$) and Isotropic Displacement Parameters ($Å^2\times10^3$) for $[Ni_3(NN^{am}S)_2(S^tBu)_2]$.

Atom	*x*	*y*	*z*	U(eq)
H9A	1382	7050	2899	28
H9B	1621	8862	2714	28
H2	4058	9828	250	29
H10A	1243	5519	1249	44
H10B	1072	5172	2021	44
H10C	1788	5111	1795	44
H13A	659	9695	-461	53
H13B	640	11631	-316	53
H13C	523	10354	286	53
H8A	2510	7616	3117	27
H8B	2345	5916	2738	27

H4	5313	7744	1555	34
H5	4497	6943	2235	29
H3	5096	9243	563	36
H15A	1392	11617	979	42
H15B	1495	12924	386	42
H15C	2072	11832	662	42
H14A	2281	10694	-500	42
H14B	1739	11877	-793	42
H14C	1708	9942	-938	42
H11A	874	9423	1839	44
H11B	533	7795	2100	44
H11C	670	8015	1311	44

Table K1: Fractional Atomic Coordinates ($\times 10^4$) and Equivalent Isotropic Displacement Parameters ($Å^2 \times 10^3$) for $[Ni_3(NN^{am}S)_2S(4\text{-}F)Ph]$. U_{eq} is defined as 1/3 of of the trace of the orthogonalised U_{IJ} tensor.

Atom	*x*	*y*	*z*	U(eq)
Ni1	3333.9(5)	6980.1(4)	4553.8(3)	28.26(12)
Ni2	5000	5000	5000	27.71(14)
S1	5923.3(9)	7566.8(9)	5413.4(6)	28.83(17)
S2	3605.5(10)	4890.6(9)	3390.6(6)	31.31(18)
F1	8293(3)	6257(3)	41.5(17)	61.3(6)
O1	2275(3)	9202(3)	7596(2)	49.8(6)
N1	2777(3)	8344(3)	5764(2)	34.4(6)
N2	1175(3)	6576(3)	3547(2)	34.9(6)
C6	5090(4)	9181(3)	7466(3)	31.1(7)
C7	3267(4)	8872(3)	6922(3)	33.4(7)
C2	7977(4)	9117(4)	7545(3)	36.1(7)
C1	6311(4)	8688(3)	6916(2)	27.6(6)
C17	6036(4)	6924(4)	2457(3)	35.7(7)
C13	5314(4)	4140(4)	1601(3)	38.0(7)
C8	1061(4)	8336(4)	5407(3)	44.3(8)
C14	6388(4)	4434(4)	800(3)	42.4(8)
C5	5628(4)	10106(4)	8653(3)	39.9(8)
C16	7096(4)	7222(4)	1642(3)	39.1(7)
C15	7244(4)	5964(4)	843(3)	40.8(8)
C12	5141(4)	5384(4)	2443(2)	31.6(7)
C3	8445(4)	10026(4)	8717(3)	43.7(8)
C4	7257(5)	10528(4)	9282(3)	46.5(9)
C9	829(5)	7982(4)	4130(3)	47.0(9)
C10	-391(4)	5099(4)	3450(3)	50.5(9)
C11	1490(5)	6526(5)	2360(3)	54(1)

Table K2: Anisotropic Displacement Parameters ($Å^2 \times 10^3$) for $[Ni_3(NN^{am}S)_2S(4\text{-}F)Ph]$. The Anisotropic displacement factor exponent takes the form: $-2\pi^2[h^2a^{*2}U_{11}+2hka^*b^*U_{12}+\ldots]$.

Atom	U_{11}	U_{22}	U_{33}	U_{23}	U_{13}	U_{12}
Ni1	27.9(2)	31.1(2)	29.4(2)	11.92(17)	6.14(16)	15.73(17)
Ni2	31.4(3)	28.5(3)	25.3(3)	7.9(2)	4.2(2)	16.8(2)
S1	29.6(4)	29.6(4)	27.4(4)	8.1(3)	5.0(3)	14.8(3)
S2	33.2(4)	32.1(4)	28.9(4)	9.9(3)	3.4(3)	15.8(3)
F1	58.8(13)	71.8(15)	45.4(12)	18.0(11)	26(1)	22.8(11)
O1	47.1(14)	58.5(15)	46.4(14)	9.9(12)	19.1(12)	32.2(12)
N1	33.8(14)	38.4(15)	39.2(16)	14.7(12)	10.7(12)	22.9(12)

N2	33.8(14)	40.8(16)	35.5(15)	18.1(12)	6.4(12)	18.2(12)
C6	33.9(16)	27.9(16)	31.5(16)	11.6(13)	9.1(13)	12.8(13)
C7	36.7(17)	25.3(16)	40.5(19)	11.7(14)	14.7(15)	15.6(14)
C2	33.4(16)	39.4(19)	32.7(17)	13.5(14)	6.8(14)	13.0(14)
C1	31.9(15)	24.6(15)	25.3(15)	9.4(12)	6.2(12)	11.3(13)
C17	36.2(17)	34.1(18)	34.7(18)	8.4(14)	3.7(14)	16.9(15)
C13	44.7(18)	34.9(18)	34.4(18)	9.2(14)	2.9(15)	20.6(15)
C8	42.6(19)	47(2)	50(2)	13.1(17)	7.3(16)	30.4(17)
C14	51(2)	46(2)	29.6(18)	4.8(15)	6.0(16)	27.5(18)
C5	47.0(19)	37.9(19)	29.2(17)	7.1(14)	13.3(15)	17.0(16)
C16	40.2(18)	39.9(19)	34.5(18)	13.6(15)	7.2(15)	14.9(15)
C15	34.0(17)	55(2)	33.8(18)	14.9(16)	7.9(14)	20.4(16)
C12	32.6(16)	39.3(18)	24.8(15)	10.3(13)	-0.1(13)	19.1(14)
C3	40.6(18)	41(2)	34.6(19)	10.3(15)	-1.7(15)	7.5(16)
C4	56(2)	44(2)	25.3(17)	5.6(15)	4.2(16)	13.6(17)
C9	44.7(19)	49(2)	58(2)	23.1(18)	8.0(17)	28.7(18)
C10	34.6(18)	52(2)	61(2)	25.1(19)	0.4(17)	12.1(17)
C11	50(2)	82(3)	43(2)	30(2)	7.4(17)	36(2)

Table K3: Bond Lengths for $[Ni_3(NN^{am}S)_2S(4\text{-}F)Ph]$.

Atom	**Atom**	**Length/Å**	**Atom**	**Atom**	**Length/Å**
Ni1	Ni2	2.9791(5)	N2	C10	1.475(4)
Ni1	S1	2.1336(9)	N2	C11	1.490(4)
Ni1	S2	2.2032(9)	C6	C7	1.507(4)
Ni1	N1	1.875(2)	C6	C1	1.400(4)
Ni1	N2	1.973(2)	C6	C5	1.398(4)
Ni2	Ni1[1]	2.9791(5)	C2	C1	1.396(4)
Ni2	S1[1]	2.1975(8)	C2	C3	1.379(4)
Ni2	S1	2.1975(8)	C17	C16	1.386(4)
Ni2	S2[1]	2.2220(8)	C17	C12	1.389(4)
Ni2	S2	2.2220(8)	C13	C14	1.378(4)
S1	C1	1.770(3)	C13	C12	1.393(4)
S2	C12	1.791(3)	C8	C9	1.492(5)
F1	C15	1.366(4)	C14	C15	1.366(5)
O1	C7	1.252(3)	C5	C4	1.371(5)
N1	C7	1.343(4)	C16	C15	1.369(4)
N1	C8	1.476(4)	C3	C4	1.389(5)
N2	C9	1.488(4)			

[1]1-X,1-Y,1-Z

Table K4: Bond Angles for $[Ni_3(NN^{am}S)_2S(4\text{-}F)Ph]$.

Atom	Atom	Atom	Angle/°	Atom	Atom	Atom	Angle/°
S1	Ni1	Ni2	47.44(2)	C8	N1	Ni1	111.6(2)
S1	Ni1	S2	83.01(3)	C9	N2	Ni1	103.88(19)
S2	Ni1	Ni2	47.95(2)	C9	N2	C11	108.6(2)
N1	Ni1	Ni2	121.46(8)	C10	N2	Ni1	113.04(19)
N1	Ni1	S1	97.44(8)	C10	N2	C9	110.0(3)
N1	Ni1	S2	163.16(8)	C10	N2	C11	109.1(3)
N1	Ni1	N2	87.94(11)	C11	N2	Ni1	112.04(19)
N2	Ni1	Ni2	135.89(7)	C1	C6	C7	127.7(3)
N2	Ni1	S1	169.48(8)	C5	C6	C7	115.5(3)
N2	Ni1	S2	94.46(8)	C5	C6	C1	116.8(3)
Ni1	Ni2	Ni1[1]	180.0	O1	C7	N1	121.8(3)
S1	Ni2	Ni1	45.65(2)	O1	C7	C6	117.2(3)
S1[1]	Ni2	Ni1[1]	45.65(2)	N1	C7	C6	120.9(3)
S1[1]	Ni2	Ni1	134.35(2)	C3	C2	C1	120.6(3)
S1	Ni2	Ni1[1]	134.35(2)	C6	C1	S1	124.0(2)
S1	Ni2	S1[1]	180.0	C2	C1	S1	115.5(2)
S1	Ni2	S2	81.14(3)	C2	C1	C6	120.5(3)
S1[1]	Ni2	S2	98.86(3)	C16	C17	C12	120.4(3)
S1	Ni2	S2[1]	98.86(3)	C14	C13	C12	120.5(3)
S1[1]	Ni2	S2[1]	81.14(3)	N1	C8	C9	107.0(3)
S2[1]	Ni2	Ni1[1]	47.42(2)	C15	C14	C13	118.3(3)
S2[1]	Ni2	Ni1	132.58(2)	C4	C5	C6	123.3(3)
S2	Ni2	Ni1[1]	132.58(2)	C15	C16	C17	118.0(3)
S2	Ni2	Ni1	47.42(2)	F1	C15	C14	118.5(3)
S2	Ni2	S2[1]	180.00(4)	F1	C15	C16	118.1(3)
Ni1	S1	Ni2	86.91(3)	C14	C15	C16	123.4(3)
C1	S1	Ni1	111.87(10)	C17	C12	S2	122.6(2)
C1	S1	Ni2	113.84(9)	C17	C12	C13	119.4(3)
Ni1	S2	Ni2	84.63(3)	C13	C12	S2	117.8(2)
C12	S2	Ni1	112.47(10)	C2	C3	C4	120.0(3)
C12	S2	Ni2	110.56(9)	C5	C4	C3	118.8(3)
C7	N1	Ni1	131.3(2)	N2	C9	C8	109.0(2)
C7	N1	C8	112.8(2)				

[1]1-X,1-Y,1-Z

Table K5: Torsion Angles for $[Ni_3(NN^{am}S)_2S(4\text{-}F)Ph]$.

A	B	C	D	Angle/°	A	B	C	D	Angle/°
Ni1	S1	C1	C6	-2.2(3)	C2	C3	C4	C5	-0.1(5)
Ni1	S1	C1	C2	179.78(19)	C1	C6	C7	O1	169.1(3)
Ni1	S2	C12	C17	-0.3(3)	C1	C6	C7	N1	-14.3(4)
Ni1	S2	C12	C13	-174.79(19)	C1	C6	C5	C4	-0.4(5)
Ni1	N1	C7	O1	-149.8(2)	C1	C2	C3	C4	-0.3(5)
Ni1	N1	C7	C6	33.9(4)	C17	C16	C15	F1	-179.8(3)
Ni1	N1	C8	C9	-29.3(3)	C17	C16	C15	C14	0.7(5)
Ni1	N2	C9	C8	-43.6(3)	C13	C14	C15	F1	-179.2(3)
Ni2	Ni1	N1	C7	13.6(3)	C13	C14	C15	C16	0.3(5)
Ni2	Ni1	N1	C8	-141.06(18)	C8	N1	C7	O1	4.7(4)
Ni2	S1	C1	C6	-98.8(2)	C8	N1	C7	C6	-171.7(3)
Ni2	S1	C1	C2	83.2(2)	C14	C13	C12	S2	175.9(2)
Ni2	S2	C12	C17	-93.0(2)	C14	C13	C12	C17	1.2(4)
Ni2	S2	C12	C13	92.5(2)	C5	C6	C7	O1	-12.7(4)
S1	Ni1	N1	C7	-30.3(3)	C5	C6	C7	N1	163.8(3)
S1	Ni1	N1	C8	175.0(2)	C5	C6	C1	S1	-177.9(2)
S2	Ni1	N1	C7	60.1(4)	C5	C6	C1	C2	0.0(4)
S2	Ni1	N1	C8	-94.6(3)	C16	C17	C12	S2	-174.6(2)
N1	C8	C9	N2	48.5(3)	C16	C17	C12	C13	-0.2(4)
N2	Ni1	N1	C7	158.7(3)	C12	C17	C16	C15	-0.7(5)
N2	Ni1	N1	C8	4.1(2)	C12	C13	C14	C15	-1.3(5)
C6	C5	C4	C3	0.4(5)	C3	C2	C1	S1	178.4(2)
C7	N1	C8	C9	171.1(3)	C3	C2	C1	C6	0.3(4)
C7	C6	C1	S1	0.2(4)	C10	N2	C9	C8	77.7(3)
C7	C6	C1	C2	178.2(3)	C11	N2	C9	C8	-163.0(3)
C7	C6	C5	C4	-178.7(3)					

Table K6: Hydrogen Atom Coordinates ($Å\times10^4$) and Isotropic Displacement Parameters ($Å^2\times10^3$) for $[Ni_3(NN^{am}S)_2S(4\text{-}F)Ph]$.

Atom	*x*	*y*	*z*	U(eq)
H2	8796	8779	7162	43
H17	5920	7777	3028	43
H13	4687	3082	1578	46
H8A	1082	9385	5827	53
H8B	62	7511	5583	53
H14	6531	3593	233	51

H5	4825	10460	9044	48
H16	7703	8269	1639	47
H3	9580	10308	9138	52
H4	7567	11153	10090	56
H9A	-404	7755	3823	56
H9B	1675	8915	3974	56
H10A	-124	4186	3111	76
H10B	-1423	4967	2950	76
H10C	-665	5163	4223	76
H11A	2536	7500	2419	81
H11B	437	6448	1917	81
H11C	1705	5598	1962	81

Table L1: Fractional Atomic Coordinates ($\times 10^4$) and Equivalent Isotropic Displacement Parameters ($Å^2 \times 10^3$) for $[Ni_3(NN^{am}S)_2(SPh)_2]$. U_{eq} is defined as 1/3 of of the trace of the orthogonalised U_{IJ} tensor.

Atom	***x***	***y***	***z***	**U(eq)**
Ni2	0	5000	5000	17.87(16)
Ni1	3777.0(6)	2944.7(5)	4529.7(3)	17.73(13)
S1	1664.3(11)	2577.6(10)	5350.6(7)	18.3(2)
S2	1581.4(12)	4686.9(10)	3541.6(7)	19.6(2)
O1	6716(3)	1576(3)	7204.7(19)	28.1(6)
N2	5652(4)	3105(3)	3585(2)	21.4(7)
N1	5550(4)	1922(3)	5577(2)	20.6(7)
O2	7178(4)	2037(4)	9172(2)	49.7(8)
C2	911(5)	1578(4)	7291(3)	21.8(8)
C1	2211(5)	1873(4)	6702(3)	18.7(8)
C12	771(5)	3888(4)	2628(3)	20.5(8)
C3	1222(5)	971(4)	8349(3)	26.0(9)
C7	5448(5)	1717(4)	6625(3)	21.4(8)
C9	7323(5)	1855(4)	4051(3)	29.0(9)
C6	3874(5)	1543(4)	7157(3)	19.8(8)
C17	1356(5)	2359(4)	2641(3)	23.9(8)
C8	7304(5)	1837(5)	5228(3)	27.4(9)
C11	5424(6)	2879(5)	2489(3)	35.2(10)
C13	-366(5)	4876(4)	1822(3)	26.5(9)
C5	4138(5)	918(4)	8227(3)	26.2(9)
C4	2857(5)	633(4)	8815(3)	28.9(9)
C16	796(5)	1813(5)	1852(3)	30.8(9)
C10	5770(5)	4563(4)	3548(3)	32(1)
C15	-333(5)	2793(5)	1049(3)	32.1(10)
C14	-903(5)	4314(5)	1040(3)	29.6(9)
C18	5680(8)	3189(6)	9477(4)	69.8(17)

Table L2: Anisotropic Displacement Parameters ($Å^2 \times 10^3$) for $[Ni_3(NN^{am}S)_2(SPh)_2]$. The Anisotropic displacement factor exponent takes the form: $-2\pi^2[h^2a^{*2}U_{11}+2hka^*b^*U_{12}+\ldots]$.

Atom	**U_{11}**	**U_{22}**	**U_{33}**	**U_{23}**	**U_{13}**	**U_{12}**
Ni2	17.7(4)	18.8(4)	15.9(4)	-1.7(3)	-0.1(2)	-6.6(3)
Ni1	16.6(3)	18.9(3)	18.2(3)	-3.03(19)	1.26(17)	-7.7(2)
S1	16.4(5)	19.3(5)	18.5(5)	-1.1(4)	-0.2(3)	-7.3(4)
S2	21.5(5)	20.5(5)	17.0(5)	-2.2(4)	0.8(3)	-9.0(4)

O1	21.9(15)	38.7(17)	23.6(15)	2.7(12)	-5.8(11)	-13.9(14)
N2	24.5(18)	23.4(17)	19.2(17)	-7.9(13)	4.4(13)	-11.3(15)
N1	13.5(16)	24.7(17)	23.2(18)	-1.5(14)	-0.8(12)	-8.0(15)
O2	33.6(19)	72(2)	37.3(19)	-16.3(17)	-2.4(14)	-12.5(19)
C2	20(2)	20(2)	26(2)	-4.3(16)	0.3(15)	-8.2(18)
C1	23(2)	15.4(18)	18.0(19)	-4.6(15)	1.0(14)	-7.1(17)
C12	19(2)	24(2)	19(2)	-3.4(16)	3.0(14)	-10.5(18)
C3	27(2)	23(2)	28(2)	-2.4(17)	5.5(16)	-10.9(19)
C7	23(2)	15.7(19)	24(2)	0.4(16)	-4.3(15)	-6.5(18)
C9	21(2)	28(2)	35(2)	-8.9(18)	8.6(16)	-6.6(19)
C6	23(2)	16.5(19)	20(2)	-2.5(15)	2.9(15)	-8.4(17)
C17	22(2)	25(2)	24(2)	-2.6(16)	-0.7(15)	-8.9(18)
C8	17(2)	32(2)	31(2)	0.9(18)	2.6(15)	-10.6(19)
C11	35(2)	53(3)	25(2)	-12(2)	8.7(18)	-24(2)
C13	26(2)	26(2)	25(2)	-6.1(17)	2.0(16)	-7.8(19)
C5	23(2)	28(2)	26(2)	1.5(17)	-5.0(16)	-9.7(19)
C4	35(2)	32(2)	20(2)	3.9(17)	-2.0(16)	-16(2)
C16	30(2)	28(2)	39(3)	-12.3(19)	1.0(18)	-13(2)
C10	35(2)	30(2)	37(3)	-6.5(19)	4.6(18)	-19(2)
C15	30(2)	45(3)	28(2)	-14(2)	0.7(17)	-19(2)
C14	27(2)	38(3)	21(2)	-2.4(18)	-3.1(16)	-11(2)
C18	74(4)	59(4)	55(4)	-25(3)	-14(3)	1(3)

Table L3: Bond Lengths for $[Ni_3(NN^{am}S)_2(SPh)_2]$.

Atom	**Atom**	**Length/Å**	**Atom**	**Atom**	**Length/Å**
Ni2	S1	2.2050(11)	O2	C18	1.383(6)
Ni2	S1[1]	2.2050(11)	C2	C1	1.392(5)
Ni2	S2[1]	2.2213(10)	C2	C3	1.390(5)
Ni2	S2	2.2213(10)	C1	C6	1.408(5)
Ni1	S1	2.1339(10)	C12	C17	1.384(5)
Ni1	S2	2.2023(12)	C12	C13	1.392(5)
Ni1	N2	1.972(3)	C3	C4	1.391(5)
Ni1	N1	1.877(3)	C7	C6	1.505(5)
S1	C1	1.774(4)	C9	C8	1.506(5)
S2	C12	1.795(3)	C6	C5	1.407(5)
O1	C7	1.260(4)	C17	C16	1.391(5)
N2	C9	1.497(5)	C13	C14	1.385(5)
N2	C11	1.487(5)	C5	C4	1.375(5)

N2	C10	1.481(4)	C16	C15	1.384(5)
N1	C7	1.334(4)	C15	C14	1.378(6)
N1	C8	1.473(4)			

[1]-X,1-Y,1-Z

Table L4: Bond Angles for $[Ni_3(NN^{am}S)_2(SPh)_2]$.

Atom	Atom	Atom	Angle/°	Atom	Atom	Atom	Angle/°
S1	Ni2	S1[1]	180.0	C7	N1	C8	112.3(3)
S1	Ni2	S2[1]	99.18(4)	C8	N1	Ni1	112.5(2)
S1[1]	Ni2	S2	99.18(4)	C3	C2	C1	120.5(3)
S1[1]	Ni2	S2[1]	80.82(4)	C2	C1	S1	115.6(3)
S1	Ni2	S2	80.82(4)	C2	C1	C6	121.0(3)
S2	Ni2	S2[1]	180.0	C6	C1	S1	123.3(3)
S1	Ni1	S2	82.84(4)	C17	C12	S2	122.9(3)
N2	Ni1	S1	170.11(8)	C17	C12	C13	119.9(3)
N2	Ni1	S2	94.58(10)	C13	C12	S2	116.9(3)
N1	Ni1	S1	97.61(9)	C2	C3	C4	119.6(3)
N1	Ni1	S2	163.57(9)	O1	C7	N1	120.9(3)
N1	Ni1	N2	87.57(12)	O1	C7	C6	117.6(3)
Ni1	S1	Ni2	88.79(4)	N1	C7	C6	121.4(3)
C1	S1	Ni2	115.57(12)	N2	C9	C8	108.5(3)
C1	S1	Ni1	112.00(12)	C1	C6	C7	127.8(3)
Ni1	S2	Ni2	86.67(4)	C5	C6	C1	116.7(3)
C12	S2	Ni2	111.69(11)	C5	C6	C7	115.5(3)
C12	S2	Ni1	111.21(13)	C12	C17	C16	119.9(4)
C9	N2	Ni1	104.2(2)	N1	C8	C9	106.5(3)
C11	N2	Ni1	113.0(2)	C14	C13	C12	119.4(4)
C11	N2	C9	108.6(3)	C4	C5	C6	122.7(3)
C10	N2	Ni1	112.3(2)	C5	C4	C3	119.5(4)
C10	N2	C9	110.4(3)	C15	C16	C17	120.3(4)
C10	N2	C11	108.4(3)	C14	C15	C16	119.4(4)
C7	N1	Ni1	130.9(2)	C15	C14	C13	121.0(4)

[1]-X,1-Y,1-Z

Table L5: Torsion Angles for $[Ni_3(NN^{am}S)_2(SPh)_2]$.

A	B	C	D	Angle/°	A	B	C	D	Angle/°
Ni2	S1	C1	C2	81.4(3)	N2	C9	C8	N1	48.2(4)
Ni2	S1	C1	C6	-102.1(3)	N1	C7	C6	C1	-14.6(6)
Ni2	S2	C12	C17	-88.8(3)	N1	C7	C6	C5	162.5(3)
Ni2	S2	C12	C13	97.4(3)	C2	C1	C6	C7	176.7(3)
Ni1	S1	C1	C2	-178.9(2)	C2	C1	C6	C5	-0.4(5)
Ni1	S1	C1	C6	-2.4(3)	C2	C3	C4	C5	0.7(6)
Ni1	S2	C12	C17	6.2(3)	C1	C2	C3	C4	-1.1(5)
Ni1	S2	C12	C13	-167.6(2)	C1	C6	C5	C4	0.0(5)
Ni1	N2	C9	C8	-44.1(3)	C12	C17	C16	C15	0.6(6)
Ni1	N1	C7	O1	-150.0(3)	C12	C13	C14	C15	0.1(6)
Ni1	N1	C7	C6	34.1(5)	C3	C2	C1	S1	177.6(3)
Ni1	N1	C8	C9	-28.9(4)	C3	C2	C1	C6	1.0(5)
S1	Ni1	N1	C7	-30.5(3)	C7	N1	C8	C9	171.8(3)
S1	Ni1	N1	C8	175.0(2)	C7	C6	C5	C4	-177.5(4)
S1	C1	C6	C7	0.4(5)	C6	C5	C4	C3	-0.1(6)
S1	C1	C6	C5	-176.8(3)	C17	C12	C13	C14	0.2(5)
S2	Ni1	N1	C7	60.0(5)	C17	C16	C15	C14	-0.3(6)
S2	Ni1	N1	C8	-94.5(4)	C8	N1	C7	O1	4.5(5)
S2	C12	C17	C16	-174.1(3)	C8	N1	C7	C6	-171.4(3)
S2	C12	C13	C14	174.2(3)	C11	N2	C9	C8	-164.7(3)
O1	C7	C6	C1	169.3(3)	C13	C12	C17	C16	-0.5(5)
O1	C7	C6	C5	-13.5(5)	C16	C15	C14	C13	0.0(6)
N2	Ni1	N1	C7	157.9(3)	C10	N2	C9	C8	76.6(4)
N2	Ni1	N1	C8	3.5(2)					

Table L6: Hydrogen Atom Coordinates ($Å \times 10^4$) and Isotropic Displacement Parameters ($Å^2 \times 10^3$) for $[Ni_3(NN^{am}S)_2(SPh)_2]$.

Atom	*x*	*y*	*z*	U(eq)
H2A	7053	1956	8540	75
H2	-197	1794	6967	26
H3	324	789	8750	31
H9A	8369	2008	3754	35
H9B	7397	887	3883	35
H17	2139	1683	3187	29
H8A	8257	904	5574	33
H8B	7490	2702	5408	33

H11A	5260	1951	2502	53
H11B	6481	2811	2085	53
H11C	4380	3727	2156	53
H13	-769	5926	1809	32
H5	5248	683	8556	31
H4	3086	208	9536	35
H16	1189	764	1865	37
H10A	4676	5368	3231	48
H10B	6784	4559	3123	48
H10C	5928	4727	4265	48
H15	-712	2420	508	38
H14	-1677	4987	489	36
H18A	4748	3520	8932	105
H18B	5970	4028	9573	105
H18C	5261	2834	10143	105

Table M1: Fractional Atomic Coordinates ($\times 10^4$) and Equivalent Isotropic Displacement Parameters ($Å^2 \times 10^3$) for (Ph_4As)[Ni($NN^{am}S$)SPh]. U_{eq} is defined as 1/3 of of the trace of the orthogonalised U_{IJ} tensor.

Atom	***x***	***y***	***z***	**U(eq)**
Ni1	847.2(17)	6183.7(3)	4599.2(10)	38.0(5)
S1	1983(4)	5935.6(6)	5810(2)	45.6(9)
S2	1530(4)	6491.8(6)	5740(2)	45.5(9)
O1	1110(11)	5605.0(15)	2830(6)	59(3)
N1	658(10)	5942.9(18)	3610(6)	36(2)
N2	-402(10)	6423.5(18)	3508(6)	41(3)
C1	1845(14)	5615.0(19)	5399(10)	43(3)
C4	1940(20)	5093(3)	5024(14)	88(5)
C2	2243(18)	5428(3)	6165(11)	72(5)
C3	2210(20)	5180(3)	5963(12)	85(6)
C5	1436(17)	5275(2)	4297(9)	62(4)
C6	1439(14)	5531(2)	4411(9)	39(3)
C7	1101(12)	5707(2)	3590(9)	37(3)
C8	173(14)	6079(2)	2667(8)	48(3)
C9	-1089(14)	6261(2)	2614(9)	49(3)
C10	516(14)	6643(2)	3370(9)	51(3)
C11	-1697(15)	6548(2)	3597(9)	58(4)
C12	494(15)	6474(2)	6497(10)	47(3)
C13	1122(18)	6589(2)	7390(9)	63(4)
C14	196(18)	6586(2)	7949(10)	61(4)
C15	-1130(20)	6478(3)	7610(12)	67(4)
C16	-1702(16)	6354(2)	6702(12)	58(4)
C17	-906(16)	6357(2)	6149(10)	51(3)
As2	5100.8(14)	7116.3(2)	5173.7(9)	38.0(4)
C48	4719(13)	6788(2)	4554(8)	39(3)
C53	4572(14)	6578(2)	5057(9)	48(3)
C52	4312(14)	6336(2)	4595(9)	53(3)
C51	4333(15)	6317(2)	3637(9)	57(4)
C50	4540(13)	6527(2)	3173(9)	49(3)
C49	4795(14)	6764(2)	3614(9)	54(4)
C42	7035(13)	7229.2(19)	5289(8)	36(3)
C47	8119(13)	7054(2)	5456(8)	43(3)
C46	9543(14)	7130(2)	5545(8)	47(3)
C45	9823(17)	7386(3)	5390(10)	72(4)
C44	8579(16)	7569(3)	5181(9)	63(4)
C43	7254(15)	7491(2)	5157(9)	54(3)
C60	3492(13)	7346.0(19)	4442(8)	36(3)

C65	2335(16)	7258(2)	3605(10)	62(4)
C64	1063(18)	7430(3)	3080(11)	76(4)
C63	1057(16)	7665(2)	3491(10)	63(4)
C62	2196(18)	7747(3)	4289(11)	75(4)
C61	3418(15)	7586(2)	4820(9)	53(3)
C54	5183(13)	7086.7(19)	6459(8)	36(3)
C59	6521(15)	7000(2)	7235(9)	55(4)
C58	6443(16)	6968(2)	8146(10)	62(4)
C57	5267(15)	7018(2)	8301(10)	53(3)
C56	3966(16)	7094(2)	7576(9)	56(4)
C55	3896(16)	7122(2)	6627(10)	54(4)
As1	2133.6(15)	4377.1(2)	2466.8(9)	40.6(4)
C18	34(13)	4394(2)	1898(8)	37(3)
C19	-749(16)	4629(2)	1538(9)	62(4)
C20	-2304(17)	4635(3)	1149(10)	71(4)
C21	-3078(18)	4425(2)	1076(10)	67(4)
C22	-2449(15)	4202(2)	1401(9)	54(4)
C23	-836(15)	4185(2)	1795(9)	58(4)
C24	3041(13)	4684(2)	2253(8)	39(3)
C25	3160(14)	4893(2)	2798(9)	53(3)
C26	3667(18)	5112(3)	2597(11)	81(5)
C27	4194(17)	5133(3)	1879(11)	77(4)
C28	4122(18)	4920(3)	1363(11)	85(5)
C29	3505(13)	4685(2)	1487(8)	47(3)
C30	2785(14)	4347(2)	3878(9)	45(3)
C31	1791(13)	4298.3(18)	4268(8)	37(3)
C32	2261(15)	4287(2)	5263(9)	51(3)
C33	3718(14)	4316(2)	5853(9)	45(3)
C34	4768(15)	4365(2)	5490(9)	52(3)
C35	4311(15)	4383(2)	4473(9)	52(3)
C36	2751(13)	4101.4(19)	1896(8)	34(3)
C37	4155(13)	3981(2)	2418(9)	40(3)
C38	4615(15)	3784(2)	2049(9)	54(4)
C39	3699(16)	3706(2)	1038(10)	63(4)
C40	2354(16)	3820(2)	535(10)	62(4)
C41	1870(16)	4025(2)	923(10)	62(4)
Cl1	7278(5)	8174.8(7)	5854(3)	75.4(12)

Table M2: Anisotropic Displacement Parameters ($Å^2 \times 10^3$) for (Ph_4As)[Ni($NN^{am}S$)SPh]. The Anisotropic displacement factor exponent takes the form: $-2\pi^2[h^2a^{*2}U_{11}+2hka^*b^*U_{12}+\ldots]$.

Atom	U_{11}	U_{22}	U_{33}	U_{23}	U_{13}	U_{12}
Ni1	32.1(10)	48.8(9)	31.2(10)	-0.2(7)	11.3(8)	-0.3(8)
S1	41(2)	63(2)	28.4(19)	3.2(16)	9.3(17)	0.0(17)
S2	48(2)	54(2)	35(2)	-5.6(15)	18.5(18)	-7.0(17)
O1	79(7)	53(5)	53(6)	4(5)	36(6)	13(5)
N1	22(6)	54(6)	17(6)	-7(5)	-7(5)	1(5)
N2	23(6)	58(6)	29(6)	0(5)	-2(5)	10(5)
C1	43(8)	26(6)	76(10)	21(7)	40(8)	9(6)
C4	134(16)	40(9)	124(16)	-9(10)	89(13)	-2(9)
C2	109(14)	66(10)	73(11)	14(8)	69(10)	16(9)
C3	148(17)	48(10)	89(14)	36(9)	79(12)	41(10)
C5	120(14)	50(9)	34(8)	9(7)	50(9)	14(8)
C6	60(9)	36(7)	33(8)	-8(6)	32(7)	-2(6)
C7	14(7)	65(9)	18(8)	-7(7)	-5(6)	-5(6)
C8	38(9)	70(9)	33(9)	-11(7)	13(7)	-8(7)
C9	42(9)	62(8)	31(8)	-17(7)	3(7)	-2(7)
C10	47(9)	58(8)	54(9)	12(7)	29(8)	7(7)
C11	53(10)	87(10)	42(9)	-3(7)	26(8)	-17(8)
C12	46(9)	54(8)	55(10)	9(7)	34(8)	15(7)
C13	105(13)	71(9)	21(8)	-19(7)	35(9)	-11(9)
C14	68(11)	68(9)	67(10)	-15(8)	48(9)	-26(9)
C15	79(14)	52(9)	74(13)	21(8)	37(10)	16(9)
C16	39(9)	54(9)	78(12)	20(8)	22(9)	8(7)
C17	55(11)	46(8)	52(9)	7(6)	23(8)	1(7)
As2	32.6(8)	49.5(8)	28.6(8)	0.8(6)	9.8(7)	1.8(6)
As1	39.3(9)	45.9(8)	34.4(8)	-1.0(6)	13.5(7)	2.1(6)
Cl1	96(3)	71(2)	46(2)	-3.4(18)	16(2)	-7(2)

Table M3: Bond Lengths for (Ph_4As)[Ni($NN^{am}S$)SPh].

Atom	Atom	Length/Å	Atom	Atom	Length/Å
Ni1	S1	2.126(4)	C44	C43	1.342(17)
Ni1	S2	2.243(3)	C60	C65	1.365(16)
Ni1	N1	1.896(9)	C60	C61	1.399(14)
Ni1	N2	2.017(9)	C65	C64	1.471(18)
S1	C1	1.784(11)	C64	C63	1.384(17)
S2	C12	1.808(12)	C63	C62	1.313(17)

O1	C7	1.260(12)	C62	C61	1.406(17)
N1	C7	1.320(13)	C54	C59	1.408(16)
N1	C8	1.471(13)	C54	C55	1.392(16)
N2	C9	1.486(13)	C59	C58	1.404(16)
N2	C10	1.529(14)	C58	C57	1.289(16)
N2	C11	1.480(15)	C57	C56	1.337(16)
C1	C2	1.433(16)	C56	C55	1.396(16)
C1	C6	1.426(15)	As1	C18	1.861(12)
C4	C3	1.391(19)	As1	C24	1.934(11)
C4	C5	1.375(18)	As1	C30	1.933(12)
C2	C3	1.339(17)	As1	C36	1.906(10)
C5	C6	1.363(15)	C18	C19	1.433(15)
C6	C7	1.460(15)	C18	C23	1.361(15)
C8	C9	1.537(16)	C19	C20	1.378(18)
C12	C13	1.353(16)	C20	C21	1.322(17)
C12	C17	1.386(17)	C21	C22	1.319(16)
C13	C14	1.465(18)	C22	C23	1.433(17)
C14	C15	1.304(18)	C24	C25	1.347(14)
C15	C16	1.391(17)	C24	C29	1.396(15)
C16	C17	1.351(17)	C25	C26	1.338(17)
As2	C48	1.922(11)	C26	C27	1.375(19)
As2	C42	1.917(11)	C27	C28	1.344(17)
As2	C60	1.919(11)	C28	C29	1.423(17)
As2	C54	1.893(11)	C30	C31	1.349(15)
C48	C53	1.382(14)	C30	C35	1.389(16)
C48	C49	1.442(15)	C31	C32	1.358(14)
C53	C52	1.419(15)	C32	C33	1.330(16)
C52	C51	1.442(16)	C33	C34	1.370(16)
C51	C50	1.364(15)	C34	C35	1.395(15)
C50	C49	1.387(15)	C36	C37	1.409(15)
C42	C47	1.348(14)	C36	C41	1.401(15)
C42	C43	1.425(14)	C37	C38	1.339(14)
C47	C46	1.399(16)	C38	C39	1.453(16)
C46	C45	1.413(16)	C39	C40	1.347(17)
C45	C44	1.480(18)	C40	C41	1.398(16)

Table M4: Bond Angles for $(Ph_4As)[Ni(NN^{am}S)SPh]$.

Atom	Atom	Atom	Angle/°	Atom	Atom	Atom	Angle/°
S1	Ni1	S2	85.31(14)	C47	C46	C45	120.9(12)
N1	Ni1	S1	95.4(3)	C46	C45	C44	117.4(13)
N1	Ni1	S2	167.6(3)	C43	C44	C45	120.1(13)
N1	Ni1	N2	87.9(4)	C44	C43	C42	119.4(12)
N2	Ni1	S1	173.8(3)	C65	C60	As2	118.0(9)
N2	Ni1	S2	92.6(3)	C65	C60	C61	120.9(12)
C1	S1	Ni1	110.7(4)	C61	C60	As2	120.6(9)
C12	S2	Ni1	111.8(5)	C60	C65	C64	117.7(12)
C7	N1	Ni1	136.3(8)	C63	C64	C65	118.5(14)
C7	N1	C8	114.5(9)	C62	C63	C64	122.4(15)
C8	N1	Ni1	107.8(7)	C63	C62	C61	120.4(14)
C9	N2	Ni1	104.8(7)	C60	C61	C62	119.6(13)
C9	N2	C10	112.6(9)	C59	C54	As2	119.3(9)
C10	N2	Ni1	113.2(7)	C55	C54	As2	121.0(9)
C11	N2	Ni1	117.1(7)	C55	C54	C59	119.3(11)
C11	N2	C9	104.9(9)	C58	C59	C54	115.2(13)
C11	N2	C10	104.2(9)	C57	C58	C59	124.3(14)
C2	C1	S1	114.9(10)	C58	C57	C56	122.1(14)
C6	C1	S1	126.6(8)	C57	C56	C55	118.4(14)
C6	C1	C2	118.4(10)	C54	C55	C56	120.4(13)
C5	C4	C3	114.7(12)	C18	As1	C24	112.1(5)
C3	C2	C1	121.2(13)	C18	As1	C30	107.2(5)
C2	C3	C4	121.8(13)	C18	As1	C36	109.1(5)
C6	C5	C4	127.7(12)	C30	As1	C24	106.6(5)
C1	C6	C7	122.5(10)	C36	As1	C24	108.2(5)
C5	C6	C1	115.0(10)	C36	As1	C30	113.7(5)
C5	C6	C7	122.5(11)	C19	C18	As1	121.6(9)
O1	C7	N1	123.4(11)	C23	C18	As1	121.8(9)
O1	C7	C6	113.5(11)	C23	C18	C19	116.6(12)
N1	C7	C6	122.6(11)	C20	C19	C18	120.0(12)
N1	C8	C9	106.3(9)	C21	C20	C19	120.2(14)
N2	C9	C8	105.4(9)	C22	C21	C20	123.8(15)
C13	C12	S2	116.8(11)	C21	C22	C23	117.9(13)
C13	C12	C17	122.4(12)	C18	C23	C22	121.4(12)
C17	C12	S2	120.7(10)	C25	C24	As1	121.1(9)
C12	C13	C14	115.0(14)	C25	C24	C29	120.9(11)
C15	C14	C13	122.1(14)	C29	C24	As1	118.0(8)
C14	C15	C16	120.6(14)	C26	C25	C24	121.3(13)
C17	C16	C15	119.4(14)	C25	C26	C27	122.4(15)

C16	C17	C12	120.3(13)	C28	C27	C26	115.8(15)
C42	As2	C48	107.9(5)	C27	C28	C29	125.0(15)
C42	As2	C60	113.2(5)	C24	C29	C28	114.4(11)
C60	As2	C48	110.3(5)	C31	C30	As1	121.3(10)
C54	As2	C48	109.3(4)	C31	C30	C35	121.5(12)
C54	As2	C42	108.4(5)	C35	C30	As1	117.2(9)
C54	As2	C60	107.7(5)	C30	C31	C32	120.5(12)
C53	C48	As2	120.4(8)	C33	C32	C31	119.6(12)
C53	C48	C49	121.1(10)	C32	C33	C34	122.0(13)
C49	C48	As2	118.0(8)	C33	C34	C35	119.6(13)
C48	C53	C52	119.7(11)	C30	C35	C34	116.9(12)
C53	C52	C51	118.1(11)	C37	C36	As1	120.8(8)
C50	C51	C52	120.9(12)	C41	C36	As1	120.8(9)
C51	C50	C49	121.7(12)	C41	C36	C37	118.2(10)
C50	C49	C48	118.1(11)	C38	C37	C36	122.5(12)
C47	C42	As2	118.0(8)	C37	C38	C39	118.7(13)
C47	C42	C43	122.8(11)	C40	C39	C38	118.8(13)
C43	C42	As2	119.2(9)	C39	C40	C41	122.2(14)
C42	C47	C46	119.3(11)	C40	C41	C36	119.1(13)

Table M5: Hydrogen Atom Coordinates (Å×10^4) and Isotropic Displacement Parameters (Å^2×10^3) for (Ph_4As)[Ni($NN^{am}S$)SPh].

Atom	***x***	***y***	***z***	**U(eq)**
H4	2091	4921	4895	105
H2	2399	5479	6790	87
H3	2381	5061	6475	102
H5	1038	5215	3636	74
H8A	-208	5958	2107	57
H8B	1029	6175	2641	57
H9A	-1438	6365	2007	59
H9B	-1960	6165	2617	59
H10A	1045	6723	4010	61
H10B	-146	6754	2884	61
H10C	1255	6564	3154	61
H11A	-2520	6413	3382	70
H11B	-2110	6684	3119	70
H11C	-1407	6583	4291	70
H13	2092	6666	7636	75
H14	573	6665	8578	73
H15	-1707	6484	7986	80
H16	-2645	6269	6473	69

H17	-1307	6278	5518	61
H53	4776	6583	5755	57
H52	4130	6191	4907	64
H51	4201	6156	3324	68
H50	4508	6510	2531	58
H49	5013	6906	3306	65
H47	7918	6879	5514	51
H46	10331	7009	5711	56
H45	10773	7438	5419	86
H44	8717	7742	5064	76
H43	6470	7610	5054	65
H65	2351	7091	3370	74
H64	263	7381	2472	91
H63	199	7772	3185	75
H62	2193	7916	4510	90
H61	4191	7640	5431	64
H59	7413	6966	7148	66
H58	7313	6905	8684	74
H57	5327	7001	8950	63
H56	3109	7129	7703	67
H55	2966	7165	6093	65
H19	-197	4779	1568	74
H20	-2821	4792	933	86
H21	-4150	4434	773	81
H22	-3046	4057	1373	64
H23	-363	4024	1990	70
H25	2880	4886	3334	64
H26	3662	5259	2965	97
H27	4585	5287	1755	93
H28	4512	4928	878	102
H29	3416	4542	1082	56
H31	756	4272	3844	44
H32	1552	4258	5535	61
H33	4041	4302	6547	55
H34	5800	4387	5929	62
H35	5011	4418	4199	63
H37	4799	4043	3056	48
H38	5523	3697	2441	65
H39	4043	3578	736	75
H40	1714	3759	-104	75
H41	957	4110	532	74

Table M6: Solvent masks information for (Ph_4As)[Ni($NN^{am}S$)SPh].

Number	X	Y	Z	Volume	Electron count
1	0.309	0.000	0.500	902.3	390.8
2	-0.230	0.500	1.000	902.3	390.8
3	0.500	0.000	1.000	13.3	0.0
4	0.500	0.500	0.500	13.3	0.0

Table N1: Fractional Atomic Coordinates ($\times 10^4$) and Equivalent Isotropic Displacement Parameters ($Å^2 \times 10^3$) for (Ph_4As)[Ni($NN^{am}S$)(4-NO_2SPh)]. U_{eq} is defined as 1/3 of of the trace of the orthogonalised U_{IJ} tensor.

Atom	***x***	***y***	***z***	**U(eq)**
As1	4368.8(6)	3413.3(4)	1710.6(2)	29.35(16)
C1	3682(7)	6309(4)	2246(2)	40.2(15)
C2	2677(8)	5897(5)	2463(2)	49.7(19)
C3	1504(9)	6042(5)	2307(3)	58(2)
C4	1287(7)	6629(5)	1945(3)	50.4(18)
C5	2297(6)	7082(4)	1721(2)	34.6(13)
C6	3501(6)	6902(4)	1866.1(19)	32.8(13)
C7	1948(6)	7764(4)	1351(2)	35.9(14)
C8	2253(6)	8636(6)	689(2)	46.1(17)
C9	2914(8)	8342(8)	267(3)	67(2)
C11	4814(11)	7713(10)	9(3)	88(4)
C12	8451(6)	6657(5)	1076(2)	37.8(14)
C13	6551(6)	5930(5)	810(2)	34.8(13)
C14	7201(6)	6756(5)	932.9(19)	36.3(14)
C15	7104(6)	5019(5)	820(2)	39.5(15)
C16	8323(6)	4943(5)	963(2)	42.5(16)
C17	9001(6)	5745(5)	1090(2)	42.2(16)
C18	3227(6)	3404(4)	2566(2)	35.0(13)
C19	2227(6)	3361(5)	2859(2)	39.4(14)
C20	1017(6)	3331(5)	2695(2)	41.5(15)
C21	800(6)	3315(5)	2239(2)	44.8(15)
C22	1779(6)	3351(5)	1944(2)	39.2(14)
C23	2989(5)	3408(4)	2112.4(19)	30.8(12)
C24	5549(9)	233(5)	1426(3)	55.3(19)
C25	4471(9)	394(5)	1636(3)	55.7(19)
C26	4078(7)	1355(4)	1728(2)	45.2(16)
C27	4848(6)	2105(4)	1594(2)	34.3(13)
C28	5952(7)	1931(5)	1371(3)	47.0(17)
C29	6280(8)	970(6)	1285(3)	61(2)
C30	5772(6)	4059(4)	1962.9(19)	32.2(12)
C32	6013(6)	5020(4)	1854.0(19)	30.2(12)
C33	6525(6)	3567(5)	2265(2)	42.4(16)
C34	7512(6)	4038(6)	2458(3)	48.8(18)
C35	7761(6)	5008(5)	2360(2)	39.6(15)
C36	7018(6)	5482(5)	2058(2)	38.1(14)
C37	3860(6)	4035(4)	1170(2)	32.6(13)
C38	3180(6)	4900(4)	1199(2)	36.0(14)

C39	2836(7)	5370(5)	814(2)	44.0(16)
C40	3770(9)	4124(6)	384(3)	60(2)
C41	4151(7)	3640(5)	766(2)	43.7(16)
C42	3150(8)	4977(6)	405(3)	52.4(18)
C43	4747(12)	9338(8)	303(3)	90(4)
C47	1194(10)	2442(8)	446(4)	81(3)
C48	4525(10)	5025(8)	8707(3)	85(3)
Cl1	735(5)	3113(3)	-26.5(13)	130.8(16)
Cl2	2215(4)	1526(3)	308.6(15)	125.1(13)
Cl5	4281(2)	4849(2)	9270.4(8)	76.5(6)
Cl6	5273(6)	4027(3)	8452.9(12)	147.9(18)
N1	8900(7)	3986(6)	988(2)	55.7(17)
N2	2776(5)	8009(4)	1043.3(17)	34.3(11)
N3	4286(5)	8379(5)	350.9(17)	47.7(14)
Ni1	4514.7(7)	7876.3(5)	968.8(2)	28.86(18)
O1	838(4)	8059(4)	1352(2)	59.9(15)
O2	9993(6)	3947(5)	1098(2)	78(2)
O3	8264(6)	3281(5)	901(2)	75.0(18)
S3	6581.5(14)	7923.3(12)	906.6(6)	38.0(4)
S4	4858.9(13)	7362.5(11)	1624.1(5)	31.4(3)

Table N2: Anisotropic Displacement Parameters ($Å^2 \times 10^3$) for (Ph_4As)[Ni($NN^{am}S$)(4-NO_2SPh)].The Anisotropic displacement factor exponent takes the form: $-2\pi^2[h^2a^{*2}U_{11}+2hka^*b^*U_{12}+\ldots]$.

Atom	**U_{11}**	**U_{22}**	**U_{33}**	**U_{23}**	**U_{13}**	**U_{12}**
As1	35.8(3)	23.3(3)	29.0(3)	1.4(2)	0.8(3)	2.5(2)
C1	63(4)	23(3)	34(3)	-6(2)	3(3)	1(3)
C2	83(6)	33(3)	34(4)	0(3)	21(4)	-1(3)
C3	79(6)	33(4)	62(5)	-1(4)	31(4)	-2(4)
C4	52(4)	34(3)	65(5)	-11(4)	16(3)	-1(3)
C5	43(3)	24(3)	37(3)	-10(3)	7(3)	0(2)
C6	48(4)	24(3)	26(3)	-11(2)	6(2)	-3(2)
C7	31(3)	26(3)	51(4)	-10(3)	3(3)	-1(2)
C8	37(4)	61(5)	41(4)	2(3)	-11(3)	14(3)
C9	64(5)	83(6)	54(5)	7(5)	-21(4)	25(5)
C11	99(8)	130(9)	36(4)	-4(5)	-4(4)	38(7)
C12	29(3)	52(4)	33(3)	6(3)	-2(2)	9(3)
C13	31(3)	43(3)	30(3)	2(3)	-1(2)	9(3)
C14	33(3)	52(4)	24(3)	3(3)	0(2)	12(3)
C15	42(4)	46(4)	30(3)	0(3)	4(3)	9(3)

C16	47(4)	50(4)	30(3)	5(3)	7(3)	24(3)
C17	32(3)	59(4)	36(3)	0(3)	-1(2)	17(3)
C18	38(3)	32(3)	36(3)	7(3)	-2(3)	0(3)
C19	49(4)	37(3)	32(3)	4(3)	2(3)	4(3)
C20	37(3)	40(3)	47(4)	0(3)	11(3)	-2(3)
C21	33(3)	49(4)	53(4)	0(3)	-1(3)	-7(3)
C22	41(3)	40(3)	37(3)	-4(3)	-3(3)	0(3)
C23	37(3)	21(3)	35(3)	4(2)	1(2)	-1(2)
C24	82(6)	24(3)	60(4)	-7(3)	-9(5)	16(4)
C25	78(5)	21(3)	67(5)	-1(3)	0(5)	1(3)
C26	57(4)	27(3)	52(4)	-5(3)	5(3)	0(3)
C27	44(3)	23(3)	36(3)	4(2)	-1(3)	6(2)
C28	53(4)	32(3)	56(4)	1(3)	9(3)	8(3)
C29	57(5)	64(5)	63(5)	-16(4)	7(4)	28(4)
C30	38(3)	31(3)	28(3)	0(2)	2(2)	1(3)
C32	36(3)	28(3)	27(3)	5(2)	1(2)	1(2)
C33	44(4)	32(3)	51(4)	17(3)	-2(3)	1(3)
C34	34(4)	60(5)	52(4)	21(4)	-1(3)	2(3)
C35	38(3)	49(4)	32(3)	6(3)	-1(3)	-3(3)
C36	45(4)	30(3)	39(3)	3(3)	0(3)	-3(3)
C37	40(3)	26(3)	31(3)	-1(2)	-7(2)	0(2)
C38	50(4)	26(3)	32(3)	-3(2)	0(3)	5(3)
C39	55(4)	36(3)	41(4)	1(3)	-9(3)	11(3)
C40	95(6)	54(4)	32(4)	-6(3)	-1(4)	21(4)
C41	60(5)	42(4)	29(3)	-2(3)	0(3)	13(3)
C42	69(5)	49(4)	39(4)	3(3)	-9(3)	11(4)
C43	122(10)	83(7)	66(6)	38(5)	-15(6)	-4(6)
C47	71(6)	78(7)	95(8)	-10(6)	1(5)	-2(5)
C48	76(6)	105(8)	75(6)	39(6)	-21(5)	-42(6)
Cl1	191(4)	97(2)	105(2)	8.0(18)	-74(3)	-40(2)
Cl2	124(3)	85(2)	166(4)	-11(2)	45(3)	20(2)
Cl5	71.4(15)	89.3(16)	68.8(14)	15.5(12)	0.4(12)	-9.9(13)
Cl6	231(5)	136(3)	76(2)	0(2)	33(3)	38(3)
N1	54(4)	61(4)	52(4)	6(3)	4(3)	27(3)
N2	33(3)	37(3)	33(3)	-8(2)	-6(2)	11(2)
N3	48(3)	65(4)	30(3)	7(3)	-3(2)	20(3)
Ni1	28.7(4)	32.3(4)	25.6(4)	0.5(3)	-3.3(3)	8.3(3)
O1	33(3)	47(3)	100(4)	11(3)	11(3)	13(2)
O2	68(4)	84(5)	81(4)	-3(4)	-21(3)	43(3)
O3	70(4)	48(3)	107(5)	8(3)	16(4)	22(3)
S3	31.5(8)	40.2(9)	42.3(9)	4.2(7)	2.2(6)	5.3(6)
S4	33.7(7)	31.0(7)	29.6(7)	2.2(6)	-7.1(6)	-1.1(5)

Table N3: Bond Lengths for $(Ph_4As)[Ni(NN^{am}S)(4\text{-}NO_2SPh)]$.

Atom	Atom	Length/Å	Atom	Atom	Length/Å
As1	C23	1.911(6)	C22	C23	1.396(9)
As1	C27	1.915(6)	C24	C25	1.336(12)
As1	C30	1.908(6)	C24	C29	1.355(12)
As1	C37	1.917(6)	C25	C26	1.422(9)
C1	C2	1.384(10)	C26	C27	1.386(9)
C1	C6	1.419(9)	C27	C28	1.382(9)
C2	C3	1.359(12)	C28	C29	1.400(11)
C3	C4	1.376(12)	C30	C32	1.395(8)
C4	C5	1.423(9)	C30	C33	1.394(9)
C5	C6	1.387(9)	C32	C36	1.395(9)
C5	C7	1.504(9)	C33	C34	1.372(10)
C6	S4	1.749(6)	C34	C35	1.400(10)
C7	N2	1.328(8)	C35	C36	1.375(9)
C7	O1	1.260(8)	C37	C38	1.405(9)
C8	C9	1.509(11)	C37	C41	1.366(9)
C8	N2	1.483(8)	C38	C39	1.377(9)
C9	N3	1.495(10)	C39	C42	1.385(10)
C11	N3	1.492(11)	C40	C41	1.391(10)
C12	C14	1.416(8)	C40	C42	1.357(11)
C12	C17	1.394(10)	C43	N3	1.423(12)
C13	C14	1.389(10)	C47	Cl1	1.768(12)
C13	C15	1.393(9)	C47	Cl2	1.726(11)
C14	S3	1.749(7)	C48	Cl5	1.731(10)
C15	C16	1.382(10)	C48	Cl6	1.771(14)
C16	C17	1.380(11)	N1	O2	1.221(9)
C16	N1	1.465(9)	N1	O3	1.220(10)
C18	C19	1.390(9)	N2	Ni1	1.889(5)
C18	C23	1.387(9)	N3	Ni1	1.998(5)
C19	C20	1.391(10)	Ni1	S3	2.2278(17)
C20	C21	1.389(10)	Ni1	S4	2.1261(16)
C21	C22	1.376(9)			

Table N4: Bond Angles for $(Ph_4As)[Ni(NN^{am}S)(4\text{-}NO_2SPh)]$.

Atom	Atom	Atom	Angle/°	Atom	Atom	Atom	Angle/°
C23	As1	C27	108.7(3)	C28	C27	As1	118.9(5)
C23	As1	C37	108.4(3)	C28	C27	C26	121.5(6)

C27	As1	C37	110.2(3)	C27	C28	C29	118.1(7)
C30	As1	C23	111.3(3)	C24	C29	C28	120.8(7)
C30	As1	C27	107.7(3)	C32	C30	As1	120.0(4)
C30	As1	C37	110.6(3)	C33	C30	As1	119.2(5)
C2	C1	C6	120.7(7)	C33	C30	C32	120.8(6)
C3	C2	C1	120.0(7)	C30	C32	C36	118.5(6)
C2	C3	C4	121.1(7)	C34	C33	C30	119.4(6)
C3	C4	C5	120.4(8)	C33	C34	C35	120.9(6)
C4	C5	C7	115.9(6)	C36	C35	C34	119.1(6)
C6	C5	C4	118.8(6)	C35	C36	C32	121.3(6)
C6	C5	C7	125.3(5)	C38	C37	As1	118.6(5)
C1	C6	S4	115.5(5)	C41	C37	As1	120.5(5)
C5	C6	C1	119.0(6)	C41	C37	C38	120.9(6)
C5	C6	S4	125.4(5)	C39	C38	C37	119.4(6)
N2	C7	C5	120.6(5)	C38	C39	C42	119.6(6)
O1	C7	C5	115.9(6)	C42	C40	C41	121.6(7)
O1	C7	N2	123.5(6)	C37	C41	C40	118.3(6)
N2	C8	C9	105.5(6)	C40	C42	C39	120.2(7)
N3	C9	C8	108.2(6)	Cl2	C47	Cl1	111.7(7)
C17	C12	C14	119.9(7)	Cl5	C48	Cl6	112.4(6)
C14	C13	C15	121.6(6)	O2	N1	C16	117.5(8)
C12	C14	S3	117.6(6)	O3	N1	C16	118.4(6)
C13	C14	C12	118.5(6)	O3	N1	O2	124.1(7)
C13	C14	S3	123.8(5)	C7	N2	C8	113.4(5)
C16	C15	C13	118.6(7)	C7	N2	Ni1	136.0(4)
C15	C16	N1	119.1(7)	C8	N2	Ni1	110.2(4)
C17	C16	C15	121.6(6)	C9	N3	Ni1	105.4(5)
C17	C16	N1	119.3(6)	C11	N3	C9	103.8(7)
C16	C17	C12	119.7(6)	C11	N3	Ni1	112.1(5)
C23	C18	C19	118.7(6)	C43	N3	C9	111.0(8)
C18	C19	C20	119.9(6)	C43	N3	C11	112.0(8)
C21	C20	C19	120.5(6)	C43	N3	Ni1	112.0(5)
C22	C21	C20	120.5(6)	N2	Ni1	N3	87.4(2)
C21	C22	C23	118.6(6)	N2	Ni1	S3	172.46(17)
C18	C23	As1	118.6(4)	N2	Ni1	S4	95.42(16)
C18	C23	C22	121.8(6)	N3	Ni1	S3	91.98(18)
C22	C23	As1	119.5(5)	N3	Ni1	S4	176.98(19)
C25	C24	C29	121.6(6)	S4	Ni1	S3	85.08(6)
C24	C25	C26	120.3(7)	C14	S3	Ni1	110.4(2)
C27	C26	C25	117.8(7)	C6	S4	Ni1	111.2(2)
C26	C27	As1	119.6(5)				

Table N5: Hydrogen Atom Coordinates (Å×10^4) and Isotropic Displacement Parameters (Å^2×10^3) for (Ph_4As)[Ni($NN^{am}S$)(4-NO_2SPh)].

Atom	*x*	*y*	*z*	U(eq)
H1	4502	6194	2353	48
H2	2807	5514	2721	60
H3	823	5732	2449	70
H4	458	6733	1846	60
H8A	2410	9326	757	55
H8B	1344	8535	661	55
H9A	2664	7680	181	81
H9B	2690	8788	22	81
H11A	4588	7942	-288	133
H11B	4478	7061	55	133
H11C	5723	7696	38	133
H12	8915	7211	1161	45
H13	5708	5987	718	42
H15	6652	4462	730	47
H17	9839	5675	1186	51
H18	4057	3429	2674	42
H19	2370	3352	3171	47
H20	333	3322	2895	50
H21	-30	3279	2130	54
H22	1635	3338	1632	47
H24	5809	-414	1375	66
H25	3965	-135	1724	67
H26	3314	1479	1877	54
H28	6473	2449	1279	56
H29	7024	833	1126	74
H32	5504	5354	1646	36
H33	6357	2911	2337	51
H34	8033	3702	2661	59
H35	8434	5333	2499	47
H36	7192	6137	1986	46
H38	2959	5157	1481	43
H39	2387	5961	829	53
H40	3948	3850	101	72
H41	4602	3051	747	52
H42	2930	5305	139	63
H43A	5631	9354	384	136
H43B	4279	9772	499	136
H43C	4648	9547	-6	136

H47A	1597	2880	664	98
H47B	447	2161	590	98
H48A	5042	5610	8664	102
H48B	3714	5137	8559	102

Table O1: Fractional Atomic Coordinates ($\times 10^4$) and Equivalent Isotropic Displacement Parameters ($Å^2 \times 10^3$) for $(NN^{am}S)'_2$. U_{eq} is defined as 1/3 of of the trace of the orthogonalised U_{IJ} tensor.

Atom	***x***	***y***	***z***	**U(eq)**
Cl01	8569.2(13)	7560.4(5)	7959(2)	45.9(5)
S2	3308.8(16)	6072.4(5)	4313(2)	47.2(5)
S1	2555.4(17)	5687.5(4)	4341(2)	50.4(6)
Cl1	393(4)	6750.9(11)	4629(6)	129.2(17)
Cl2	1209(5)	6759.4(12)	1843(7)	151(2)
O2	4500(5)	6578.4(15)	4537(5)	53.7(16)
N3	5090(5)	6603.9(15)	6730(7)	40.9(15)
N4	6402(5)	7452.7(16)	7844(8)	42.9(15)
C16	2104(6)	6570(2)	8078(10)	49(2)
C20	6092(6)	6683(2)	6312(9)	44.2(19)
C19	4377(6)	6562.9(18)	5813(7)	38.4(18)
O1	1538(8)	5166.0(15)	4416(7)	97(3)
C10	799(7)	5995(2)	1241(10)	52(2)
N2	1586(8)	4953.6(17)	2292(8)	75(3)
C21	6249(6)	7015(2)	6299(9)	49(2)
C22	6055(6)	7147.8(19)	7693(8)	41.3(18)
C14	3385(6)	6487.4(18)	6386(8)	37.9(17)
C18	1899(6)	6202(2)	6317(9)	47(2)
C13	2812(6)	6267.0(18)	5764(7)	38.1(17)
C15	3025(6)	6637.3(19)	7525(8)	43.4(19)
C24	6035(7)	7652(2)	6738(9)	51(2)
C17	1549(7)	6357(2)	7488(10)	52(2)
C7	1242(8)	5469.2(19)	2450(8)	51(2)
C9	387(9)	5746(2)	706(11)	65(3)
C11	1417(6)	5983.8(19)	2352(9)	43.8(19)
C12	1662(6)	5722.7(18)	2952(8)	42.4(18)
C8	621(8)	5491(2)	1317(10)	62(3)
C23	6138(7)	7564(2)	9245(10)	55(2)
N1	3529(12)	4346(3)	4699(13)	108(4)
C6	1477(10)	5185(2)	3116(9)	70(3)
C3	3704(15)	4397(4)	3363(19)	122(6)
C5	1940(20)	4669(3)	2823(12)	131(9)
C2	3777(11)	4059(3)	5239(18)	98(5)
C4	3090(20)	4649(3)	2830(20)	153(10)
C25	1381(13)	6818(4)	3680(20)	114(6)
C1	4110(30)	4560(5)	5610(20)	212(16)

Table O2: Anisotropic Displacement Parameters ($Å^2 \times 10^3$) for $(NN^{am}S)'_2$. The Anisotropic displacement factor exponent takes the form: $-2\pi^2[h^2a^{*2}U_{11}+2hka^*b^*U_{12}+\ldots]$.

Atom	**U_{11}**	**U_{22}**	**U_{33}**	**U_{23}**	**U_{13}**	**U_{12}**
Cl01	29.0(8)	66.6(13)	42(1)	1.6(10)	-2.6(8)	-2.9(8)
S2	53.0(11)	53.4(12)	35.3(9)	-8.3(10)	0.4(10)	-1.8(9)
S1	74.5(15)	41.3(10)	35.5(9)	-1.2(10)	-7.8(11)	0.8(10)
Cl1	134(4)	119(3)	135(4)	27(3)	-12(3)	-18(3)
Cl2	189(6)	96(3)	170(6)	-1(3)	52(4)	-18(3)
O2	60(4)	78(4)	22(3)	6(3)	1(2)	-13(3)
N3	39(4)	57(4)	27(3)	3(3)	4(3)	-12(3)
N4	34(3)	56(4)	38(3)	-7(3)	-1(3)	-10(3)
C16	47(4)	57(5)	44(5)	-8(4)	-1(4)	6(4)
C20	42(4)	61(6)	30(4)	-1(4)	7(3)	-6(4)
C19	49(4)	41(4)	25(4)	4(3)	1(3)	-4(3)
O1	222(11)	49(4)	21(3)	-4(3)	2(5)	-24(5)
C10	59(5)	49(5)	48(5)	-5(4)	-2(4)	11(4)
N2	164(10)	35(4)	27(3)	-3(3)	-13(5)	-7(5)
C21	49(5)	62(6)	37(4)	4(4)	4(4)	-13(4)
C22	34(4)	57(5)	33(4)	3(4)	2(3)	-3(3)
C14	45(4)	41(4)	28(3)	2(3)	-3(3)	-2(3)
C18	40(4)	62(6)	40(4)	-7(4)	-1(4)	-5(4)
C13	41(4)	49(5)	24(3)	2(3)	-1(3)	2(4)
C15	48(5)	49(5)	33(4)	-1(3)	-5(3)	-7(4)
C24	50(5)	54(6)	48(5)	3(4)	-8(4)	0(4)
C17	50(5)	62(6)	44(5)	-14(4)	6(4)	-2(4)
C7	87(7)	41(5)	26(4)	-4(3)	2(4)	-3(4)
C9	80(7)	63(7)	52(5)	-14(5)	-17(5)	6(5)
C11	48(5)	39(4)	44(4)	-5(4)	-1(4)	5(4)
C12	56(5)	41(4)	30(4)	-4(4)	6(4)	-2(3)
C8	89(7)	54(6)	43(5)	-23(5)	4(5)	-18(5)
C23	49(5)	73(6)	42(5)	-15(5)	3(4)	-20(4)
N1	185(14)	66(7)	73(8)	4(6)	-18(8)	-9(7)
C6	141(10)	48(6)	22(4)	-6(4)	5(5)	-17(6)
C3	143(15)	137(15)	87(11)	13(11)	24(10)	39(12)
C5	320(30)	39(6)	36(6)	2(5)	20(11)	-6(11)
C2	116(11)	80(9)	98(10)	45(8)	13(9)	32(8)
C4	260(30)	67(10)	136(18)	7(10)	-90(20)	40(13)
C25	106(12)	75(10)	160(17)	-10(10)	8(11)	-1(8)
C1	410(50)	140(20)	82(14)	-10(13)	-50(20)	10(30)

Table O3: Bond Lengths for $(NN^{am}S)'_2$.

Atom	Atom	Length/Å	Atom	Atom	Length/Å
S2	S1	2.039(3)	N2	C6	1.336(13)
S2	C13	1.804(8)	N2	C5	1.481(18)
S1	C12	1.829(9)	C21	C22	1.512(12)
Cl1	C25	1.66(2)	C14	C13	1.412(11)
Cl2	C25	1.83(2)	C14	C15	1.394(12)
O2	C19	1.258(9)	C18	C13	1.389(12)
N3	C20	1.472(10)	C18	C17	1.428(13)
N3	C19	1.335(10)	C7	C12	1.383(12)
N4	C22	1.480(11)	C7	C8	1.396(14)
N4	C24	1.498(12)	C7	C6	1.489(14)
N4	C23	1.501(12)	C9	C8	1.350(15)
C16	C15	1.402(13)	C11	C12	1.371(12)
C16	C17	1.361(13)	N1	C3	1.34(2)
C20	C21	1.533(13)	N1	C2	1.456(17)
C19	C14	1.504(12)	N1	C1	1.54(3)
O1	C6	1.274(11)	C3	C4	1.52(3)
C10	C9	1.372(14)	C5	C4	1.58(4)
C10	C11	1.374(13)			

Table O4: Bond Angles for $(NN^{am}S)'_2$.

Atom	Atom	Atom	Angle/°	Atom	Atom	Atom	Angle/°
C13	S2	S1	103.1(3)	C14	C15	C16	120.9(8)
C12	S1	S2	104.4(3)	C16	C17	C18	120.6(9)
C19	N3	C20	121.7(7)	C12	C7	C8	118.1(8)
C22	N4	C24	113.3(7)	C12	C7	C6	119.3(9)
C22	N4	C23	109.4(7)	C8	C7	C6	122.6(8)
C24	N4	C23	111.7(7)	C8	C9	C10	116.9(9)
C17	C16	C15	119.5(8)	C12	C11	C10	121.3(8)
N3	C20	C21	112.1(7)	C7	C12	S1	117.7(7)
O2	C19	N3	123.9(8)	C11	C12	S1	123.7(6)
O2	C19	C14	120.1(7)	C11	C12	C7	118.6(8)
N3	C19	C14	116.0(6)	C9	C8	C7	123.7(9)
C9	C10	C11	121.3(9)	C3	N1	C2	117.6(15)
C6	N2	C5	121.4(9)	C3	N1	C1	111.1(18)
C22	C21	C20	111.4(7)	C2	N1	C1	104.1(15)

N4	C22	C21	114.3(7)	O1	C6	N2	122.5(10)
C13	C14	C19	120.1(7)	O1	C6	C7	120.5(9)
C15	C14	C19	120.0(7)	N2	C6	C7	117.0(8)
C15	C14	C13	119.9(7)	N1	C3	C4	111.2(18)
C13	C18	C17	120.2(8)	N2	C5	C4	112.1(15)
C14	C13	S2	118.8(6)	C3	C4	C5	127(2)
C18	C13	S2	122.3(6)	Cl1	C25	Cl2	114.4(11)
C18	C13	C14	118.8(7)				

Table O5: Torsion Angles for $(NN^{am}S)'_2$.

A	**B**	**C**	**D**	**Angle/°**	**A**	**B**	**C**	**D**	**Angle/°**
S2	S1	C12	C7	161.3(6)	C15	C14	C13	C18	-0.7(12)
S2	S1	C12	C11	-16.2(8)	C24	N4	C22	C21	52.7(10)
S1	S2	C13	C14	156.1(6)	C17	C16	C15	C14	-0.5(14)
S1	S2	C13	C18	-21.9(7)	C17	C18	C13	S2	178.4(7)
O2	C19	C14	C13	41.3(12)	C17	C18	C13	C14	0.4(13)
O2	C19	C14	C15	-138.0(9)	C9	C10	C11	C12	1.5(15)
N3	C20	C21	C22	58.5(9)	C11	C10	C9	C8	-0.4(16)
N3	C19	C14	C13	-137.3(8)	C12	C7	C8	C9	-1.8(15)
N3	C19	C14	C15	43.4(11)	C12	C7	C6	O1	40.5(17)
C20	N3	C19	O2	2.4(13)	C12	C7	C6	N2	-141.5(11)
C20	N3	C19	C14	-179.0(7)	C8	C7	C12	S1	-174.9(7)
C20	C21	C22	N4	167.0(7)	C8	C7	C12	C11	2.7(13)
C19	N3	C20	C21	92.7(9)	C8	C7	C6	O1	-140.4(12)
C19	C14	C13	S2	1.9(10)	C8	C7	C6	N2	37.6(17)
C19	C14	C13	C18	180.0(7)	C23	N4	C22	C21	178.0(8)
C19	C14	C15	C16	-179.9(8)	N1	C3	C4	C5	-60(3)
C10	C9	C8	C7	0.6(17)	C6	N2	C5	C4	-86.8(17)
C10	C11	C12	S1	174.8(7)	C6	C7	C12	S1	4.2(12)
C10	C11	C12	C7	-2.6(13)	C6	C7	C12	C11	-178.2(9)
N2	C5	C4	C3	177.3(17)	C6	C7	C8	C9	179.1(11)
C13	C14	C15	C16	0.8(12)	C5	N2	C6	O1	-10(2)
C13	C18	C17	C16	-0.1(15)	C5	N2	C6	C7	172.4(15)
C15	C16	C17	C18	0.1(15)	C2	N1	C3	C4	159.1(17)
C15	C14	C13	S2	-178.8(6)	C1	N1	C3	C4	-81(3)

Table O6: Hydrogen Atom Coordinates (Å×10^4) and Isotropic Displacement Parameters (Å^2×10^3) for $(NN^{am}S)'_2$.

Atom	*x*	*y*	*z*	U(eq)
H3	4957	6583	7607	49
H4	7133	7449	7783	51
H16	1868	6673	8859	59
H20A	6221	6604	5384	53
H20B	6566	6593	6952	53
H10	655	6179	834	63
H2	1445	4971	1415	90
H21A	6932	7058	6021	59
H21B	5805	7105	5616	59
H22A	5340	7142	7871	50
H22B	6378	7026	8399	50
H18	1507	6053	5914	57
H15	3410	6787	7932	52
H24A	6263	7581	5845	76
H24B	6286	7850	6895	76
H24C	5317	7655	6751	76
H17	924	6311	7860	62
H9	-44	5754	-58	78
H11	1679	6160	2713	53
H8	347	5316	956	75
H23A	5424	7583	9317	82
H23B	6444	7755	9392	82
H23C	6374	7426	9940	82
H3A	4153	4288	2820	147
H5A	1672	4510	2246	157
H5B	1689	4641	3768	157
H2A	3510	3908	4634	147
H2B	3496	4037	6159	147
H2C	4491	4039	5289	147
H4A	3300	4679	1872	184
H4B	3320	4823	3347	184
H25A	1921	6690	4003	136
H25B	1585	7023	3833	136
H1A	4805	4552	5364	318
H1B	4029	4504	6574	318
H1C	3863	4759	5471	318

Table P1: Fractional Atomic Coordinates ($\times 10^4$) and Equivalent Isotropic Displacement Parameters ($Å^2 \times 10^3$) for $[Ni_3(NN^{am}S)_2(SCH_2CH_2N(CH3)_2)_2]$. U_{eq} is defined as 1/3 of of the trace of the orthogonalised U_{IJ} tensor.

Atom	*x*	*y*	*z*	U(eq)
C5	8225(4)	7665.7(19)	11834(3)	37.9(9)
C4	7406(4)	7335(2)	12540(3)	41.2(10)
C3	7052(4)	6658(2)	12407(3)	38.4(9)
C2	7537(4)	6319.6(19)	11560(3)	32.3(8)
C1	8408(4)	6647.0(16)	10853(2)	24.9(7)
C6	8766(4)	7333.8(17)	10986(3)	28.4(7)
C9	12412(4)	7635.2(16)	8338(3)	32.5(8)
C8	11674(5)	7959.5(17)	9221(3)	37.2(8)
C7	9738(5)	7744.0(17)	10318(3)	33.0(8)
C11	13314(5)	6608.3(18)	7653(3)	35.9(8)
C10	14420(4)	6903(2)	9528(3)	38.6(9)
C12	10090(4)	5322.4(17)	7530(3)	29.0(7)
C13	8249(4)	5286.6(16)	7612(3)	26.6(7)
C14	7956(4)	4124.0(16)	8031(3)	29.2(7)
C15	6211(4)	4931.4(17)	8656(3)	29.2(7)
N2	12903(3)	6932.2(13)	8635(2)	27.1(6)
N1	10698(3)	7464.1(13)	9698(2)	27.2(6)
N3	7942(3)	4810.8(13)	8462(2)	23.7(6)
Ni1	10992.8(5)	6574.0(2)	9231.4(3)	21.50(12)
Ni2	10000	5000	10000	20.19(14)
O1	9642(4)	8374.4(12)	10426(2)	51.6(8)
S2	11521.3(10)	5520.7(4)	8832.4(6)	22.90(18)
S1	8883.4(9)	6165.3(4)	9791.6(6)	22.99(18)
O3	10790(7)	9524(2)	9805(4)	36.1(12)
C16	12288(17)	9465(4)	10346(8)	64(3)
O2	6219(9)	5968(3)	14833(4)	180(3)
O4	14120(9)	9745(4)	10780(6)	85(2)

Table P2: Anisotropic Displacement Parameters ($Å^2 \times 10^3$) for $[Ni_3(NN^{am}S)_2(SCH_2CH_2N(CH3)_2)_2]$. The Anisotropic displacement factor exponent takes the form: $-2\pi^2[h^2a^{*2}U_{11}+2hka^*b^*U_{12}+\ldots]$.

Atom	U_{11}	U_{22}	U_{33}	U_{23}	U_{13}	U_{12}
C5	29.1(18)	42(2)	39(2)	-16.9(17)	-1.1(16)	8.4(16)
C4	23.8(18)	67(3)	32(2)	-18.9(18)	3.2(15)	12.3(17)
C3	22.7(17)	63(3)	29.7(19)	-6.5(17)	6.5(14)	8.5(17)

C2	23.8(17)	42(2)	31.1(19)	-2.4(15)	4.8(14)	6.2(15)
C1	21.1(15)	29.3(17)	22.1(16)	-3.5(13)	-0.1(12)	7.3(13)
C6	24.6(17)	32.2(18)	24.7(17)	-6.8(14)	-3.4(13)	8.4(14)
C9	32.8(19)	24.7(18)	37(2)	8.9(14)	1.1(15)	-5.0(14)
C8	48(2)	20.8(17)	41(2)	2.0(15)	5.5(17)	-3.4(15)
C7	41(2)	25.2(18)	28.8(18)	-3.0(14)	-2.7(15)	4.4(15)
C11	33.5(19)	38(2)	39(2)	5.3(16)	14.6(16)	-3.1(15)
C10	23.9(18)	47(2)	42(2)	14.3(17)	-1.5(15)	-7.7(16)
C12	36.3(19)	29.6(18)	21.9(16)	-3.0(13)	7.8(14)	-3.9(14)
C13	31.9(17)	25.4(17)	21.1(16)	0.5(13)	2.5(13)	-2.0(14)
C14	30.3(18)	24.3(17)	30.8(18)	-4.9(14)	1.8(14)	-0.6(13)
C15	22.2(16)	31.5(18)	32.7(18)	-0.3(14)	2.8(14)	-0.1(13)
N2	23.1(14)	25.2(14)	31.5(15)	4.9(12)	2.4(11)	-3.0(11)
N1	28.7(14)	20.7(13)	29.7(15)	1.6(11)	0.3(12)	-0.1(11)
N3	24.5(14)	21.8(13)	24.5(14)	-0.9(11)	4.1(11)	-1.5(11)
Ni1	20.5(2)	18.4(2)	25.2(2)	1.51(16)	3.87(16)	-0.04(15)
Ni2	21.5(3)	18.2(3)	22.0(3)	-0.4(2)	7.0(2)	-0.1(2)
O1	84(2)	23.9(14)	46.8(17)	-5.4(12)	14.1(15)	9.5(13)
S2	23.8(4)	21.4(4)	25.3(4)	0.6(3)	9.3(3)	-0.1(3)
S1	23.7(4)	20.9(4)	25.1(4)	-1.6(3)	6.9(3)	0.5(3)
O3	56(3)	26(3)	26(3)	4(2)	9(2)	-17(2)
C16	131(10)	16(4)	61(6)	-6(4)	56(7)	-8(5)
O2	247(7)	191(6)	81(3)	56(4)	-13(4)	-110(6)
O4	71(5)	81(5)	88(6)	-2(4)	-17(4)	5(4)

Table P3: Bond Lengths for $[Ni_3(NN^{am}S)_2(SCH_2CH_2N(CH3)_2)_2]$.

Atom	Atom	Length/Å	Atom	Atom	Length/Å
C5	C4	1.378(6)	C12	S2	1.835(3)
C5	C6	1.399(5)	C13	N3	1.487(4)
C4	C3	1.384(6)	C14	N3	1.475(4)
C3	C2	1.383(5)	C15	N3	1.483(4)
C2	C1	1.403(5)	N2	Ni1	1.979(3)
C1	C6	1.403(5)	N1	Ni1	1.901(3)
C1	S1	1.750(3)	N3	Ni2	2.297(2)
C6	C7	1.503(5)	Ni1	S2	2.2223(9)
C9	C8	1.509(5)	Ni1	S1	2.1313(9)
C9	N2	1.483(4)	Ni2	$N3^1$	2.297(3)
C8	N1	1.467(4)	Ni2	$S2^1$	2.3411(8)
C7	N1	1.329(4)	Ni2	S2	2.3411(8)

C7	O1	1.269(4)	Ni2	$S1^1$	2.4866(8)
C11	N2	1.490(4)	Ni2	S1	2.4866(8)
C10	N2	1.475(4)	O3	C16	1.259(13)
C12	C13	1.508(5)	C16	O4	1.563(14)

Table P4: Bond Angles for $[Ni_3(NN^{am}S)_2(SCH_2CH_2N(CH3)_2)_2]$.

Atom	**Atom**	**Atom**	**Angle/°**	**Atom**	**Atom**	**Atom**	**Angle/°**
C4	C5	C6	122.0(4)	C15	N3	C13	108.5(2)
C5	C4	C3	120.2(3)	C15	N3	Ni2	111.83(19)
C2	C3	C4	119.0(4)	N2	Ni1	S2	93.20(8)
C3	C2	C1	121.2(4)	N2	Ni1	S1	176.98(8)
C2	C1	S1	116.4(3)	N1	Ni1	N2	86.36(12)
C6	C1	C2	119.8(3)	N1	Ni1	S2	174.53(8)
C6	C1	S1	123.7(3)	N1	Ni1	S1	95.51(9)
C5	C6	C1	117.6(3)	S1	Ni1	S2	85.17(3)
C5	C6	C7	116.6(3)	N3	Ni2	$N3^1$	180.00(9)
C1	C6	C7	125.7(3)	N3	Ni2	S2	85.75(7)
N2	C9	C8	110.2(3)	$N3^1$	Ni2	S2	94.25(7)
N1	C8	C9	109.8(3)	N3	Ni2	$S2^1$	94.25(7)
N1	C7	C6	122.1(3)	$N3^1$	Ni2	$S2^1$	85.75(7)
O1	C7	C6	115.4(3)	N3	Ni2	S1	83.35(7)
O1	C7	N1	122.4(3)	$N3^1$	Ni2	$S1^1$	83.35(7)
C13	C12	S2	113.0(2)	N3	Ni2	$S1^1$	96.65(7)
N3	C13	C12	113.1(3)	$N3^1$	Ni2	S1	96.65(7)
C9	N2	C11	107.2(3)	S2	Ni2	$S2^1$	180.00(3)
C9	N2	Ni1	104.5(2)	S2	Ni2	S1	75.17(3)
C11	N2	Ni1	118.8(2)	S2	Ni2	$S1^1$	104.83(3)
C10	N2	C9	111.2(3)	$S2^1$	Ni2	$S1^1$	75.17(3)
C10	N2	C11	108.6(3)	$S2^1$	Ni2	S1	104.83(3)
C10	N2	Ni1	106.4(2)	S1	Ni2	$S1^1$	180.0
C8	N1	Ni1	113.0(2)	C12	S2	Ni1	106.90(11)
C7	N1	C8	112.5(3)	C12	S2	Ni2	98.60(11)
C7	N1	Ni1	134.3(2)	Ni1	S2	Ni2	97.39(3)
C13	N3	Ni2	107.42(18)	C1	S1	Ni1	110.96(12)
C14	N3	C13	108.3(2)	C1	S1	Ni2	124.43(11)
C14	N3	C15	106.9(2)	Ni1	S1	Ni2	95.58(3)
C14	N3	Ni2	113.71(19)	O3	C16	O4	151.8(7)

Table P5: Torsion Angles for $[Ni_3(NN^{am}S)_2(SCH_2CH_2N(CH3)_2)_2]$.

A	B	C	D	Angle/°	A	B	C	D	Angle/°
C5	C4	C3	C2	0.2(5)	C6	C7	N1	Ni1	10.6(5)
C5	C6	C7	N1	161.6(3)	C9	C8	N1	C7	-167.1(3)
C5	C6	C7	O1	-15.2(4)	C9	C8	N1	Ni1	9.7(3)
C4	C5	C6	C1	1.7(5)	C8	C9	N2	C11	169.8(3)
C4	C5	C6	C7	-176.3(3)	C8	C9	N2	C10	-71.6(4)
C4	C3	C2	C1	1.4(5)	C8	C9	N2	Ni1	42.9(3)
C3	C2	C1	C6	-1.5(5)	C12	C13	N3	C14	-77.6(3)
C3	C2	C1	S1	-178.0(3)	C12	C13	N3	C15	166.7(3)
C2	C1	C6	C5	0.0(4)	C12	C13	N3	Ni2	45.6(3)
C2	C1	C6	C7	177.8(3)	C13	C12	S2	Ni1	-68.6(2)
C2	C1	S1	Ni1	-156.4(2)	C13	C12	S2	Ni2	31.9(2)
C2	C1	S1	Ni2	-43.5(3)	N2	C9	C8	N1	-35.4(4)
C1	C6	C7	N1	-16.2(5)	O1	C7	N1	C8	3.1(5)
C1	C6	C7	O1	167.0(3)	O1	C7	N1	Ni1	-172.8(3)
C6	C5	C4	C3	-1.8(5)	S2	C12	C13	N3	-54.8(3)
C6	C1	S1	Ni1	27.2(3)	S1	C1	C6	C5	176.2(2)
C6	C1	S1	Ni2	140.1(2)	S1	C1	C6	C7	-6.0(5)
C6	C7	N1	C8	-173.5(3)					

Table P6: Hydrogen Atom Coordinates ($Å\times10^4$) and Isotropic Displacement Parameters ($Å^2\times10^3$) for $[Ni_3(NN^{am}S)_2(SCH_2CH_2N(CH3)_2)_2]$.

Atom	*x*	*y*	*z*	U(eq)
H5	8428	8133	11925	45
H4	7084	7573	13120	49
H3	6484	6429	12890	46
H2	7275	5857	11456	39
H9A	11562	7643	7643	39
H9B	13422	7890	8236	39
H8A	12602	8141	9793	45
H8B	10925	8336	8911	45
H11A	12291	6592	7072	54
H11B	13727	6152	7835	54
H11C	14196	6868	7407	54
H10A	15363	7138	9307	58
H10B	14735	6434	9692	58
H10C	14169	7119	10178	58

H12A	10218	5669	6989	35
H12B	10428	4887	7264	35
H13A	7866	5739	7779	32
H13B	7558	5148	6899	32
H14A	7046	4077	7380	44
H14B	7775	3802	8585	44
H14C	9055	4036	7839	44
H15A	5382	4904	7964	44
H15B	6162	5378	8973	44
H15C	5945	4592	9159	44

Table P7: Atomic Occupancy for $[Ni_3(NN^{am}S)_2(SCH_2CH_2N(CH3)_2)_2]$.

Atom	**Occupancy**	**Atom**	**Occupancy**	**Atom**	**Occupancy**
O3	0.5	C16	0.5	O4	0.5

Table Q1: Fractional Atomic Coordinates ($\times 10^4$) and Equivalent Isotropic Displacement Parameters ($Å^2 \times 10^3$) for Ni(cysteine methylester)$_2$. U_{eq} is defined as 1/3 of of the trace of the orthogonalised U_{IJ} tensor.

Atom	***x***	***y***	***z***	**U(eq)**
Ni1	6950(6)	7222(3)	2599(2)	33.9(6)
S1	9447(10)	5748(5)	2115(3)	41.4(17)
S2	4519(10)	8703(5)	3122(3)	39.7(16)
O1	4510(40)	2339(15)	3963(10)	75(6)
O2	4070(30)	3754(13)	5003(9)	63(4)
O3	11540(30)	10692(13)	672(9)	47(4)
O4	8460(40)	12095(15)	1002(12)	84(7)
N1	5110(40)	5850(16)	3499(12)	42(5)
N2	8830(30)	8577(17)	1726(10)	40(5)
C1	3850(70)	1300(20)	4802(17)	95(12)
C2	4560(40)	3540(20)	4187(12)	40(7)
C3	5470(30)	4515(17)	3294(11)	33(5)
C4	8360(30)	4352(16)	3048(11)	28(4)
C5	6520(40)	10110(20)	2573(12)	51(7)
C6	7530(30)	9875(17)	1582(11)	30(5)
C7	9360(50)	10950(20)	1019(14)	43(8)
C8	9940(70)	13220(20)	460(20)	105(13)
Ni1A	1948(6)	2272(3)	7628(2)	34.3(6)
S1A	-482(10)	776(5)	7105(3)	41.3(18)
S2A	4466(10)	3755(5)	8105(3)	40.9(17)
O1A	3360(40)	-2582(16)	9230(12)	90(7)
O2A	6520(30)	-1203(14)	9543(9)	52(4)
O3A	-960(30)	5762(13)	5233(8)	62(4)
O4A	-590(30)	7164(16)	6266(10)	62(5)
N1A	3810(30)	926(14)	8510(10)	28(4)
N2A	180(40)	3599(15)	6747(11)	41(5)
C1A	4940(80)	-3670(20)	9780(20)	111(14)
C2A	4350(50)	-1400(20)	9177(13)	37(6)
C3A	2590(40)	-395(17)	8672(12)	32(5)
C4A	1540(40)	-610(17)	7642(12)	39(5)
C5A	3430(40)	5110(18)	7174(12)	41(6)
C6A	510(40)	4963(18)	6916(12)	42(6)
C7A	-430(40)	5990(20)	6038(12)	40(7)
C8A	-1250(60)	8250(30)	5426(15)	93(11)

Table Q2: Anisotropic Displacement Parameters ($Å^2 \times 10^3$) for Ni(cysteine methylester)$_2$. The Anisotropic displacement factor exponent takes the form: $-2\pi^2[h^2a^{*2}U_{11}+2hka^*b^*U_{12}+\ldots]$.

Atom	**U_{11}**	**U_{22}**	**U_{33}**	**U_{23}**	**U_{13}**	**U_{12}**
Ni1	30(1)	37.3(12)	34.9(8)	-7.5(8)	1.3(6)	-6.1(9)
S1	38(4)	42(4)	44(3)	-8(3)	10(3)	-3(3)
S2	35(4)	44(4)	41(2)	-10(2)	3(3)	-8(3)
O1	121(15)	41(11)	63(8)	-7(8)	42(9)	-14(10)
O2	91(12)	51(9)	51(7)	-17(7)	26(7)	-15(9)
O3	36(8)	47(9)	54(7)	-2(6)	7(6)	0(8)
O4	121(16)	16(9)	110(12)	1(8)	76(12)	6(10)
N1	37(12)	35(12)	55(9)	-11(9)	11(9)	5(10)
N2	35(12)	61(14)	29(7)	-19(8)	-1(8)	-12(11)
C1	180(30)	37(19)	69(14)	-2(13)	43(19)	-20(20)
C2	38(15)	46(17)	32(9)	3(10)	-7(10)	-11(14)
C3	28(11)	42(12)	27(7)	-6(8)	-2(7)	-4(10)
C4	21(10)	20(11)	40(9)	-2(8)	-1(7)	20(9)
C5	57(15)	58(15)	39(10)	-13(10)	0(9)	-21(13)
C6	22(10)	29(12)	38(9)	-9(8)	-6(7)	6(9)
C7	46(16)	40(17)	48(11)	-22(12)	11(12)	-13(15)
C8	140(30)	50(20)	130(20)	-25(17)	100(20)	-30(20)
Ni1A	29.8(10)	39.1(12)	34.6(8)	-8.3(8)	2.8(7)	-7.9(9)
S1A	40(4)	44(4)	41(2)	-11(3)	0(3)	-12(3)
S2A	36(4)	42(4)	44(3)	-7(3)	-5(3)	-10(3)
O1A	132(17)	29(11)	108(12)	-6(8)	-48(11)	-28(12)
O2A	46(9)	56(10)	53(7)	-3(7)	-9(6)	-10(8)
O3A	90(12)	48(9)	46(6)	-8(6)	-30(7)	5(9)
O4A	72(11)	52(11)	71(8)	-30(8)	-41(8)	15(9)
N1A	23(10)	23(11)	35(7)	1(7)	-2(7)	8(9)
N2A	56(13)	23(11)	45(8)	-7(8)	-3(9)	-6(10)
C1A	190(40)	12(16)	140(20)	-14(15)	-40(20)	-20(20)
C2A	50(16)	15(13)	46(10)	-4(10)	-8(12)	-2(13)
C3A	35(11)	21(11)	39(9)	0(8)	-6(8)	6(10)
C4A	59(14)	12(10)	48(10)	-9(8)	-3(9)	8(10)
C5A	32(11)	46(13)	46(9)	-9(9)	-5(8)	-16(11)
C6A	53(14)	42(13)	33(8)	-13(8)	-2(8)	-16(11)
C7A	31(14)	52(18)	36(10)	-6(11)	-7(10)	2(13)
C8A	110(30)	100(30)	59(13)	7(14)	-72(16)	30(20)

Table Q3: Bond Lengths for Ni(cysteine methylester)$_2$.

Atom	Atom	Length/Å	Atom	Atom	Length/Å
Ni1	S1	2.178(8)	Ni1A	S1A	2.209(5)
Ni1	S2	2.188(8)	Ni1A	S2A	2.198(5)
Ni1	N1	1.937(15)	Ni1A	N1A	1.908(17)
Ni1	N2	1.920(14)	Ni1A	N2A	1.873(19)
S1	C4	1.827(16)	S1A	C4A	1.81(2)
S2	C5	1.829(17)	S2A	C5A	1.78(2)
O1	C1	1.46(3)	O1A	C1A	1.47(4)
O1	C2	1.34(2)	O1A	C2A	1.33(2)
O2	C2	1.183(19)	O2A	C2A	1.23(2)
O3	C7	1.24(3)	O3A	C7A	1.181(18)
O4	C7	1.28(3)	O4A	C7A	1.32(2)
O4	C8	1.48(2)	O4A	C8A	1.48(3)
N1	C3	1.49(2)	N1A	C3A	1.498(19)
N2	C6	1.49(2)	N2A	C6A	1.50(2)
C2	C3	1.50(2)	C2A	C3A	1.44(3)
C3	C4	1.51(2)	C3A	C4A	1.53(2)
C5	C6	1.48(2)	C5A	C6A	1.53(3)
C6	C7	1.55(2)	C6A	C7A	1.52(3)

Table Q4: Bond Angles for Ni(cysteine methylester)$_2$.

Atom	Atom	Atom	Angle/°	Atom	Atom	Atom	Angle/°
S1	Ni1	S2	178.3(3)	S2A	Ni1A	S1A	178.0(3)
N1	Ni1	S1	88.7(6)	N1A	Ni1A	S1A	89.0(5)
N1	Ni1	S2	91.2(6)	N1A	Ni1A	S2A	91.0(5)
N2	Ni1	S1	91.0(6)	N2A	Ni1A	S1A	91.3(5)
N2	Ni1	S2	89.0(6)	N2A	Ni1A	S2A	88.6(5)
N2	Ni1	N1	178.9(10)	N2A	Ni1A	N1A	178.9(9)
C4	S1	Ni1	98.3(6)	C4A	S1A	Ni1A	97.2(5)
C5	S2	Ni1	97.4(8)	C5A	S2A	Ni1A	98.3(5)
C2	O1	C1	115.6(15)	C2A	O1A	C1A	116.7(19)
C7	O4	C8	119.4(19)	C7A	O4A	C8A	116.8(15)
C3	N1	Ni1	116.4(11)	C3A	N1A	Ni1A	116.4(11)
C6	N2	Ni1	114.8(11)	C6A	N2A	Ni1A	117.8(11)
O1	C2	C3	111.0(15)	O1A	C2A	C3A	112.6(18)
O2	C2	O1	123.3(16)	O2A	C2A	O1A	123(2)
O2	C2	C3	125.6(19)	O2A	C2A	C3A	124.6(17)

N1	C3	C2	110.2(14)	N1A	C3A	C4A	107.4(12)
N1	C3	C4	107.6(13)	C2A	C3A	N1A	112.9(15)
C2	C3	C4	112.7(17)	C2A	C3A	C4A	114.7(15)
C3	C4	S1	109.6(12)	C3A	C4A	S1A	108.2(12)
C6	C5	S2	107.3(11)	C6A	C5A	S2A	109.6(10)
N2	C6	C7	111.7(16)	N2A	C6A	C5A	106.7(17)
C5	C6	N2	109.3(14)	N2A	C6A	C7A	114.1(13)
C5	C6	C7	114.6(13)	C7A	C6A	C5A	112.7(13)
O3	C7	O4	125.2(17)	O3A	C7A	O4A	124(2)
O3	C7	C6	121(2)	O3A	C7A	C6A	123(2)
O4	C7	C6	113.2(19)	O4A	C7A	C6A	113.5(14)

Table Q5: Torsion Angles for Ni(cysteine methylester)$_2$.

A	**B**	**C**	**D**	**Angle/°**	**A**	**B**	**C**	**D**	**Angle/°**
Ni1	S1	C4	C3	33.0(11)	Ni1A	S2A	C5A	C6A	33.0(12)
Ni1	S2	C5	C6	36.7(14)	Ni1A	N1A	C3A	C2A	168.4(12)
Ni1	N1	C3	C2	165.1(13)	Ni1A	N1A	C3A	C4A	41.1(18)
Ni1	N1	C3	C4	42.0(17)	Ni1A	N2A	C6A	C5A	41.1(16)
Ni1	N2	C6	C5	42.7(15)	Ni1A	N2A	C6A	C7A	166.2(14)
Ni1	N2	C6	C7	170.7(10)	S1A	Ni1A	N2A	C6A	165.4(12)
S2	C5	C6	N2	-51.7(17)	S2A	Ni1A	N2A	C6A	-16.6(13)
S2	C5	C6	C7	-178.1(16)	S2A	C5A	C6A	N2A	-47.1(15)
O1	C2	C3	N1	171.2(18)	S2A	C5A	C6A	C7A	-173.1(14)
O1	C2	C3	C4	-69(2)	O1A	C2A	C3A	N1A	-173.8(14)
O2	C2	C3	N1	-13(3)	O1A	C2A	C3A	C4A	-50(2)
O2	C2	C3	C4	108(2)	O2A	C2A	C3A	N1A	8(2)
N1	C3	C4	S1	-47.9(15)	O2A	C2A	C3A	C4A	131.1(18)
N2	C6	C7	O3	6(2)	N1A	C3A	C4A	S1A	-51.0(17)
N2	C6	C7	O4	-171.3(17)	N2A	C6A	C7A	O3A	-12(3)
C1	O1	C2	O2	-1(4)	N2A	C6A	C7A	O4A	168.0(16)
C1	O1	C2	C3	176(2)	C1A	O1A	C2A	O2A	2(3)
C2	C3	C4	S1	-169.6(12)	C1A	O1A	C2A	C3A	-177(2)
C5	C6	C7	O3	130.6(19)	C2A	C3A	C4A	S1A	-177.3(12)
C5	C6	C7	O4	-46(3)	C5A	C6A	C7A	O3A	110(2)
C8	O4	C7	O3	6(4)	C5A	C6A	C7A	O4A	-70(2)
C8	O4	C7	C6	-178(2)	C8A	O4A	C7A	O3A	-6(3)
Ni1A	S1A	C4A	C3A	37.4(11)	C8A	O4A	C7A	C6A	174.4(19)

Table Q6: Hydrogen Atom Coordinates ($Å \times 10^4$) and Isotropic Displacement Parameters ($Å^2 \times 10^3$) for Ni(cysteine methylester)$_2$.

Atom	*x*	*y*	*z*	U(eq)
H1A	5703	5856	4202	51
H1B	3192	6056	3466	51
H2A	10624	8645	2009	48
H2B	9044	8328	1053	48
H1C	4325	459	4623	142
H1D	1943	1317	4938	142
H1E	4835	1409	5409	142
H3	4382	4421	2689	39
H4A	8609	3547	2772	33
H4B	9436	4281	3673	33
H5A	5431	10909	2475	61
H5B	8018	10209	3030	61
H6	5956	9841	1137	36
H8A	9762	13263	-277	157
H8B	11816	13130	646	157
H8C	9225	14019	637	157
H1AA	5618	861	8234	33
H1AB	3998	1187	9179	33
H2AA	765	3569	6046	50
H2AB	-1741	3399	6783	50
H1AC	5511	-3466	10436	167
H1AD	6507	-3805	9381	167
H1AE	3867	-4457	9903	167
H3A	1019	-376	9125	39
H4AA	477	-1413	7732	47
H4AB	3043	-701	7183	47
H5AA	3684	5922	7439	49
H5AB	4525	5160	6554	49
H6A	-557	5058	7527	50
H8AA	-195	8163	4826	140
H8AB	-845	9073	5631	140
H8AC	-3138	8218	5263	140

Table R1: Fractional Atomic Coordinates ($\times 10^4$) and Equivalent Isotropic Displacement Parameters ($Å^2 \times 10^3$) for Ni(6-mercaptopurine). U_{eq} is defined as 1/3 of of the trace of the orthogonalised U_{IJ} tensor**.**

Atom	***x***	***y***	***z***	**U(eq)**
Ni1	4798(3)	8375.7(19)	4246.1(7)	30.4(6)
Ni2	-207(3)	8373.6(19)	753.2(7)	31.6(6)
S3	1224(6)	6533(4)	1523.2(15)	38.1(11)
S4	6236(6)	6537(4)	3475.2(14)	37.3(11)
S5	7235(6)	8662(5)	4659.3(14)	40.4(11)
S6	2234(6)	8660(5)	340.0(14)	41.9(11)
N5	-2513(18)	8450(13)	1111(4)	37(3)
N6	2444(17)	8436(13)	3890(4)	32(3)
N7	3612(19)	10673(13)	2116(4)	40(4)
N8	8632(19)	10655(13)	2879(4)	40(4)
N9	1309(17)	9609(12)	1137(4)	28(3)
N10	8081(18)	8207(12)	2858(4)	35(3)
N11	7520(20)	11609(13)	3536(5)	42(4)
N12	3020(18)	8231(13)	2146(4)	33(3)
N13	6229(18)	9597(12)	3863(4)	34(3)
N14	2600(20)	11599(13)	1460(5)	44(4)
C17	5270(30)	6732(15)	5216(5)	41(4)
C18	2010(20)	9281(14)	1529(5)	31(4)
C19	2810(20)	10570(15)	1723(5)	36(4)
N20	3180(18)	7162(12)	4606(4)	33(3)
C21	-3780(30)	7130(15)	1024(6)	46(5)
C22	6960(20)	7625(16)	5117(6)	42(4)
C23	230(30)	6737(17)	-224(6)	45(5)
N24	-1767(17)	7144(12)	392(4)	34(3)
C26	7040(20)	9308(15)	3467(5)	32(4)
C27	2150(20)	8106(15)	1743(6)	34(4)
C28	7160(20)	8067(14)	3266(5)	29(4)
C29	7790(20)	10554(16)	3283(5)	38(4)
C30	8760(30)	9415(16)	2686(6)	47(5)
C32	1960(30)	7606(15)	-125(6)	41(5)
C33	6630(20)	11019(17)	3883(5)	39(4)
C34	1220(20)	7147(17)	3958(6)	46(5)
C35	3480(30)	6561(18)	4966(6)	47(5)
C36	3560(30)	7661(19)	-402(6)	58(6)
C37	1670(20)	10981(14)	1110(5)	33(4)
C38	3700(30)	9436(16)	2311(6)	45(5)
C39	8350(30)	6863(18)	5747(6)	56(6)

C40	-1510(20)	6551(17)	21(6)	42(4)
C41	8610(30)	7650(18)	5392(5)	49(5)
C42	3380(30)	6868(19)	-770(6)	58(6)
C43	-3300(20)	9599(17)	927(6)	50(5)
C44	1220(20)	6800(20)	4456(7)	54(5)
C45	-2340(20)	8700(20)	1569(6)	50(5)
C46	2610(20)	8691(19)	3426(5)	45(5)
C48	5200(30)	5958(18)	5628(6)	58(6)
C49	1710(30)	9589(17)	4065(6)	51(5)
C50	-3780(20)	6779(18)	548(6)	50(5)
C51	300(40)	5951(18)	-629(7)	68(7)
C52	1750(30)	5962(19)	-887(6)	51(5)
C53	6700(30)	6020(20)	5865(6)	56(5)
O7	3187(17)	12874(11)	2636(4)	59(4)
O8	8128(16)	12895(11)	2349(4)	46(3)
C11	3400(30)	12480(20)	3091(6)	63(6)
C12	8310(30)	12550(20)	1925(6)	79(7)
O1	8659(15)	15977(10)	2390(3)	38(3)
O2	4315(17)	14264(11)	1671(4)	54(3)
C3	5800(11)	14481(7)	2353(3)	-16.3(16)
Cl1	781(10)	14513(6)	2641(2)	96(2)
Cl0a	3699(15)	15974(11)	2596(4)	169(4)

Table R2: Anisotropic Displacement Parameters ($Å^2 \times 10^3$) for Ni(6-mercaptopurine). The Anisotropic displacement factor exponent takes the form: $-2\pi^2[h^2a^{*2}U_{11}+2hka^*b^*U_{12}+\ldots]$.

Atom	**U_{11}**	**U_{22}**	**U_{33}**	**U_{12}**	**U_{13}**	**U_{23}**
Ni1	28.4(12)	28.1(11)	35.2(13)	6.1(9)	0.4(9)	1.5(9)
Ni2	28.7(12)	31.0(11)	35.4(13)	6.0(9)	-1.8(10)	-2.2(9)
S3	38(3)	25(2)	50(3)	2.6(18)	2(2)	-4(2)
S4	38(3)	30(2)	42(3)	-0.1(18)	-3(2)	2.6(19)
S5	35(3)	49(3)	36(3)	2(2)	-3(2)	11(2)
S6	38(3)	50(3)	35(3)	1(2)	1(2)	-10(2)
N5	26(8)	42(8)	43(9)	7(6)	-1(7)	-1(7)
N6	25(7)	39(8)	35(8)	14(6)	7(6)	-2(6)
N7	41(9)	40(8)	40(9)	3(7)	-8(7)	-4(7)
N8	45(9)	35(8)	39(9)	1(6)	-10(7)	17(7)
N9	28(7)	30(7)	27(7)	4(6)	-10(6)	-5(6)
N10	28(8)	32(7)	44(9)	-1(6)	-7(7)	-8(7)
N11	45(9)	29(7)	49(10)	1(7)	0(8)	6(7)

N12	32(8)	47(8)	20(7)	7(6)	-1(6)	-2(6)
N13	38(8)	33(7)	34(8)	13(6)	5(7)	2(6)
N14	46(9)	27(7)	60(10)	6(7)	-7(8)	0(7)
C17	60(13)	27(9)	37(11)	12(9)	5(9)	2(8)
C18	32(9)	23(8)	41(10)	10(7)	1(8)	4(7)
C19	40(10)	29(8)	42(11)	15(7)	-5(9)	-14(8)
N20	29(8)	30(7)	39(9)	2(6)	3(6)	7(6)
C21	65(13)	21(8)	48(12)	-2(8)	14(10)	4(8)
C22	49(12)	38(10)	43(11)	16(8)	1(9)	15(8)
C23	51(12)	40(10)	46(12)	14(9)	-9(9)	-15(9)
N24	26(8)	25(7)	50(9)	4(6)	3(7)	1(7)
C26	40(10)	27(8)	26(9)	-6(7)	1(8)	3(7)
C27	16(8)	28(8)	59(12)	3(6)	16(8)	4(8)
C28	30(9)	26(8)	33(10)	9(7)	-8(7)	-7(7)
C29	55(12)	31(9)	23(9)	-2(8)	-4(8)	5(7)
C30	52(12)	26(9)	61(13)	6(8)	-13(10)	9(9)
C32	52(12)	28(9)	46(11)	14(8)	-23(10)	-2(8)
C33	42(11)	38(9)	38(11)	8(8)	5(8)	-3(8)
C34	44(11)	37(10)	52(12)	-12(8)	-8(9)	3(9)
C35	42(12)	47(11)	54(13)	15(9)	19(10)	-1(10)
C36	75(15)	55(12)	49(13)	28(11)	28(11)	24(10)
C37	40(10)	23(8)	38(10)	11(7)	-4(8)	-10(7)
C38	62(13)	31(9)	44(11)	9(9)	3(10)	0(9)
C39	92(17)	34(10)	46(12)	21(11)	-36(12)	-6(9)
C40	37(11)	44(10)	49(12)	22(8)	5(9)	10(9)
C41	69(14)	56(12)	26(10)	22(10)	-26(9)	-12(9)
C42	103(18)	44(11)	37(12)	41(12)	17(11)	-7(9)
C43	37(11)	48(11)	69(14)	20(9)	1(10)	-2(10)
C44	6(8)	73(13)	81(15)	0(8)	-5(9)	12(11)
C45	34(11)	88(15)	36(11)	32(10)	13(9)	-6(10)
C46	22(9)	86(14)	30(10)	15(9)	-6(8)	12(10)
C48	97(17)	44(11)	36(12)	23(11)	13(11)	28(9)
C49	58(13)	39(10)	63(13)	32(9)	-2(10)	3(9)
C50	26(10)	59(12)	66(14)	7(9)	11(9)	-16(10)
C51	120(20)	37(11)	53(14)	18(12)	-44(14)	-19(10)
C52	55(13)	43(11)	53(13)	5(10)	19(11)	5(10)
C53	61(14)	61(13)	50(13)	21(11)	-26(11)	-1(10)
O7	52(8)	37(7)	82(10)	-6(6)	-4(7)	0(7)
O8	53(8)	40(7)	46(8)	9(6)	0(6)	0(6)
C11	76(15)	78(14)	34(12)	12(12)	-12(11)	27(10)
C12	106(19)	108(19)	25(11)	21(15)	17(12)	-12(12)
O1	39(7)	34(6)	41(7)	10(5)	9(5)	10(5)

O2	56(8)	40(7)	66(9)	15(6)	-10(7)	-3(6)
C3	-22(4)	-19(3)	-9(4)	-6(3)	2(3)	-2(3)
Cl1	92(5)	76(4)	118(6)	4(4)	-4(4)	1(4)
Cl0a	154(9)	147(8)	202(11)	17(7)	9(8)	3(8)

Table R3: Bond Lengths for Ni(6-mercaptopurine).

Atom	**Atom**	**Length/Å**	**Atom**	**Atom**	**Length/Å**
Ni1	S5	2.144(5)	N13	C33	1.41(2)
Ni1	N6	2.025(12)	N14	C19	1.35(2)
Ni1	N13	1.881(13)	N14	C37	1.368(19)
Ni1	N20	1.896(12)	C17	C22	1.41(2)
Ni2	S6	2.146(5)	C17	C35	1.48(2)
Ni2	N5	2.001(13)	C17	C48	1.49(2)
Ni2	N9	1.918(11)	C18	C19	1.45(2)
Ni2	N24	1.886(13)	C18	C27	1.37(2)
S3	C27	1.744(16)	N20	C35	1.31(2)
S4	C28	1.697(16)	N20	C44	1.463(19)
S5	C22	1.752(16)	C21	C50	1.52(2)
S6	C32	1.781(17)	C22	C41	1.46(2)
N5	C21	1.50(2)	C23	C32	1.42(2)
N5	C43	1.48(2)	C23	C40	1.44(2)
N5	C45	1.45(2)	C23	C51	1.49(2)
N6	C34	1.45(2)	N24	C40	1.32(2)
N6	C46	1.464(19)	N24	C50	1.51(2)
N6	C49	1.46(2)	C26	C28	1.41(2)
N7	C19	1.35(2)	C26	C29	1.40(2)
N7	C38	1.39(2)	C32	C36	1.42(2)
N8	C29	1.39(2)	C34	C44	1.59(2)
N8	C30	1.40(2)	C36	C42	1.39(2)
N9	C18	1.377(18)	C39	C41	1.35(2)
N9	C37	1.361(18)	C39	C53	1.38(3)
N10	C28	1.42(2)	C42	C52	1.40(3)
N10	C30	1.34(2)	C48	C53	1.29(2)
N11	C29	1.36(2)	C51	C52	1.31(3)
N11	C33	1.34(2)	O7	C11	1.48(2)
N12	C27	1.39(2)	O8	C12	1.38(2)
N12	C38	1.33(2)	Cl1	Cl0a	2.342(12)
N13	C26	1.409(19)			

Table R4: Bond Angles for Ni(6-mercaptopurine).

Atom	Atom	Atom	Angle/°	Atom	Atom	Atom	Angle/°
N6	Ni1	S5	169.9(4)	C18	C19	N14	110.8(14)
N13	Ni1	S5	87.2(4)	C35	N20	Ni1	132.1(12)
N13	Ni1	N6	89.9(5)	C44	N20	Ni1	115.2(11)
N20	Ni1	S5	97.3(4)	C44	N20	C35	112.7(14)
N20	Ni1	N6	85.5(5)	C50	C21	N5	110.9(14)
N20	Ni1	N13	175.4(5)	C17	C22	S5	123.7(14)
N5	Ni2	S6	169.7(4)	C41	C22	S5	117.1(13)
N9	Ni2	S6	85.9(4)	C41	C22	C17	119.2(16)
N9	Ni2	N5	90.5(5)	C40	C23	C32	127.3(16)
N24	Ni2	S6	96.3(4)	C51	C23	C32	113.9(18)
N24	Ni2	N5	87.4(6)	C51	C23	C40	118.9(17)
N24	Ni2	N9	177.8(6)	C40	N24	Ni2	134.3(12)
C22	S5	Ni1	113.4(6)	C50	N24	Ni2	113.8(11)
C32	S6	Ni2	113.6(6)	C50	N24	C40	111.8(13)
C21	N5	Ni2	104.2(10)	C28	C26	N13	131.2(14)
C43	N5	Ni2	104.1(10)	C29	C26	N13	106.3(13)
C43	N5	C21	111.4(13)	C29	C26	C28	122.5(15)
C45	N5	Ni2	120.3(10)	N12	C27	S3	121.8(12)
C45	N5	C21	110.5(14)	C18	C27	S3	121.4(13)
C45	N5	C43	106.1(13)	C18	C27	N12	116.9(14)
C34	N6	Ni1	105.9(10)	N10	C28	S4	122.2(11)
C46	N6	Ni1	120.0(9)	C26	C28	S4	123.8(13)
C46	N6	C34	108.5(13)	C26	C28	N10	113.9(13)
C49	N6	Ni1	103.6(10)	N11	C29	N8	125.7(14)
C49	N6	C34	114.2(14)	C26	C29	N8	122.0(15)
C49	N6	C46	104.9(13)	C26	C29	N11	112.2(15)
C38	N7	C19	114.2(14)	N10	C30	N8	124.7(17)
C30	N8	C29	114.5(14)	C23	C32	S6	122.5(15)
C18	N9	Ni2	125.7(10)	C36	C32	S6	117.4(14)
C37	N9	Ni2	127.1(10)	C36	C32	C23	120.1(17)
C37	N9	C18	106.6(12)	N13	C33	N11	114.3(14)
C30	N10	C28	122.3(14)	C44	C34	N6	108.3(14)
C33	N11	C29	103.9(13)	N20	C35	C17	127.2(16)
C38	N12	C27	121.2(14)	C42	C36	C32	118.9(19)
C26	N13	Ni1	127.9(10)	N14	C37	N9	113.7(13)
C33	N13	Ni1	128.8(11)	N12	C38	N7	125.3(16)
C33	N13	C26	103.2(12)	C53	C39	C41	126.3(18)
C37	N14	C19	104.1(12)	N24	C40	C23	125.8(16)
C35	C17	C22	125.9(16)	C39	C41	C22	116.2(18)

C48	C17	C22	117.7(17)	C52	C42	C36	124.6(19)
C48	C17	C35	116.2(16)	C34	C44	N20	107.1(13)
C19	C18	N9	104.8(13)	C53	C48	C17	120.8(19)
C27	C18	N9	135.6(15)	N24	C50	C21	107.1(14)
C27	C18	C19	119.6(15)	C52	C51	C23	128(2)
N14	C19	N7	126.4(15)	C51	C52	C42	114.9(19)
C18	C19	N7	122.7(15)	C48	C53	C39	119.6(19)